DNA BARCODING & MULTI-ISOTOPIC FINGERPRINTING: A NOVEL FORENSIC TOOLBOX FOR THE RAPID IDENTIFICATION OF ILLEGAL TRADE IN ENDANGERED WILDLIFE SPECIES

Dissertation

zur Erlangung des Doktorgrades (Dr. rer. nat.)
der
Mathematisch-Naturwissenschaftlichen Fakultät
der
Rheinischen Friedrich-Wilhelms-Universität Bonn

vorgelegt von

Stephanie Juliane Pietsch

aus
Bonn

Bonn, September 2011

Angefertigt mit Genehmigung der Mathematisch-Naturwissenschaftlichen Fakultät der Rheinischen Friedrich-Wilhelms-Universität Bonn.

Die Arbeit wurde am Zoologischen Forschungsmuseum Alexander Koenig in Bonn durchgeführt.

1. Prof. Dr. J.W. Wägele
2. Prof. Dr. K.A. Hobson
Tag der Promotion: 28.10.2011
Erscheinungsjahr: 2012

Der Panther

Im Jardin des Plantes, Paris

Sein Blick ist vom Vorübergehn der Stäbe
so müd geworden, daß er nichts mehr hält.
Ihm ist, als ob es tausend Stäbe gäbe
und hinter tausend Stäben keine Welt.

Der weiche Gang geschmeidig starker Schritte,
der sich im allerkleinsten Kreise dreht,
ist wie ein Tanz von Kraft um eine Mitte,
in der betäubt ein großer Wille steht.

Nur manchmal schiebt der Vorhang der Pupille
sich lautlos auf –. Dann geht ein Bild hinein,
geht durch der Glieder angespannte Stille –
und hört im Herzen auf zu sein.

Rainer Maria Rilke, 1902, Paris

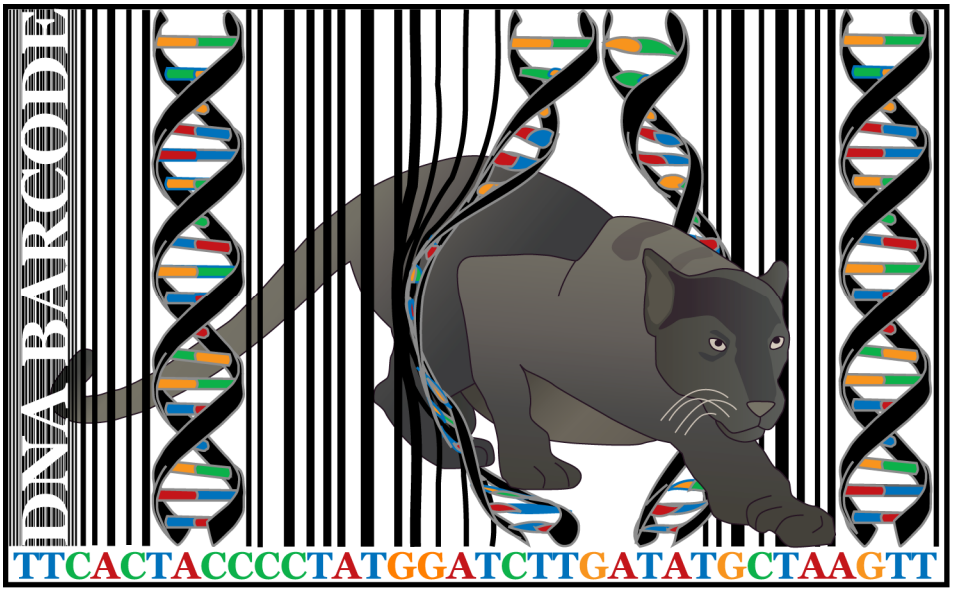

CONTENTS

ABBREVIATIONS AND SYMBOLS

CITES	Convention on International Trade in Endangered Species of Wild Fauna and Flora
IUCN	International Union for Conservation of Nature
COI	Mitochondrial cytochrome c oxidase I gene
ATP6	Mitochondrial ATP synthase F0 subunit 6 gene
mtDNA	Mitochondrial deoxyribonucleic acid
numt	Nuclear mitochondrial DNA
cymt	Cytoplasmic mitochondrial DNA
PCR	Polymerase chain reaction
NCBI	The National Center for Biotechnology Information advances science and health by providing access to biomedical and genomic information.
BOLD	The Barcode of Life Data Systems (BOLD) is an online workbench that aids collection, management, analysis, and use of DNA barcodes.
K2P distance	Kimura two-parameter distance
NJ	Neighbor joining is a bottom-up clustering method for the creation of phenograms
BLAST	Basic Local Alignment Search Tool
δD_h	Hydrogen isotope composition of hair
δD_{riv}	Hydrogen isotope composition of river water
δD_t	Hydrogen isotope composition of animal tissues
δD_{bw}	Hydrogen isotope composition of body water
δD_w	Hydrogen isotope composition of precipitation
$\delta^{18}O_h$	Oxygen isotope composition of hair
$\delta^{18}O_{riv}$	Oxygen isotope composition of river water
$\delta^{18}O_t$	Oxygen isotope composition of animal tissues
$\delta^{18}O_{bw}$	Oxygen isotope composition of body water
$\delta^{18}O_w$	Oxygen isotope composition of precipitation
$\delta^{18}O_p$	Oxygen isotope composition of bone phosphate
$\delta^{18}O_{CO3}$	Oxygen isotope composition of bone carbonate
VSMOW	Vienna Standard Mean Ocean Water is a water standard defining the isotopic composition of water.
IAEA–WMO	International Atomic Energy Agency (IAEA), in cooperation with the World Meteorological Organization
OIPC	Online Isotopes in Precipitation Calculator on http://www.waterisotopes.org
BMR	Basal metabolic rate

SUMMARY

Over-exploitation through illegal wildlife trade is a major threat to a wide range of endangered mammal species around the world, particularly to the Felidae. Illegal trade in wild cats is often in the form of bones, meat, skulls, claws and skins. In many cases, this material lacks detailed morphological features for specific identification and constitutes a significant problem for law enforcement or border control to classify them as endangered, protected or illegal wildlife trade. Moreover, wild cat parts are often traded across multiple international borders and along numerous trade routes, making poaching hotspots and potential trade routes difficult to identify. Successful wildlife forensic casework is thus challenged by unresolved issues such as species identification from animal parts and derivatives and the tracking of their geographic origin.

The specific aims of this thesis are to test the feasibility of rapid, accurate and cost-effective methods for species identification and geographic provenancing of felid species in wildlife forensic investigations. The present study focuses on a comprehensive analysis of all thirty-eight species from the highly endangered Felidae, by applying independent lines of evidence: (a) DNA barcoding and (b) multi-isotopic fingerprinting. For species identification, DNA barcoding of mitochondrial markers was applied because of its effective use in various types of animal tissues (bone, hair, blood, faeces, teeth, skin). To reconstruct the geographic origin of an organism, stable isotope analysis via Isotope Ratio Mass Spectrometry (IRMS) was used as tool for wildlife forensics.

For DNA barcoding a total of 277 tissue samples from 28 felid species were genetically analysed using two different mitochondrial genes (COI and ATP6). Species analysis via barcoding can potentially be compromised by the inadvertent amplification of numts (i.e., nuclear copies of mitochondrial DNA). Thus, reliable identification of felid species via DNA barcoding requires careful examination of numt contaminations and their effect on the results of barcode analyses. Qualitative and quantitative analysis of numts in Felidae revealed that numt contamination does not constitute serious limitations for reliable identification of felid species. The results presented in this thesis demonstrate that DNA barcoding of felid taxa can be reliably performed using species diagnostic authentic mtDNA and numt gene sequences.

Probabilistic provenance determination of felid species based on oxygen and hydrogen stable isotopes has strong potential to be applied to various body tissues as an investigative tool in wildlife forensic science. Both bone and hair tissue samples were isotopically analysed for their potential to record both long- and short-term information of their geographic origin. Understanding the incorporation of hydrogen and oxygen isotopes from the hydrosphere via

diet and drinking water into animal tissues is fundamental for geographic provenancing analysis. For this reason, the concept of geographic source determination based on H/O isotopes using feline carnivore hair and bone requires confirmation from animal tissues of known origin and a detailed understanding of the isotopic routing of dietary nutrients into felid body tissues.

We used coupled hydrogen and oxygen isotope measurements of hair (δD_h, $\delta^{18}O_h$) from the North American bobcat (*Lynx rufus*) and puma (*Puma concolor*) with precipitation-based assignment isoscapes to test the feasibility of isotopic geo-location of Felidae. This study reveals that puma and bobcat hairs do not trace the expected pattern of H and O isotopic variation predicted by precipitation isoscapes for North America. The effective forensic application of water isotopes to trace the provenance of feline carnivores is likely compromised by major controls of their diet, physiology and metabolism on hair $\delta^{18}O$ and δD related to body water budgets.

We further investigated, whether puma and bobcat bone phosphate varied predictably in their oxygen isotopic composition ($\delta^{18}O_p$) among isotopically distinct geographic locations and reflected the spatial pattern of isotopic variation in precipitation ($\delta^{18}O_w$). Previous studies on mammals demonstrated that fractionation between $\delta^{18}O_p$ and $\delta^{18}O_w$ appears to be linear and species-specific but deviations from a constant oxygen fractionation have been documented for some species. Our results show that bobcats and pumas exhibit only a moderate linear relationship of oxygen isotopes in precipitation water ($\delta^{18}O_w$) and bone phosphate ($\delta^{18}O_p$). This finding contrasts with previously published studies on $\delta^{18}O_p$ from omnivores and herbivores. Provenance determination of modern feline carnivores, that is solely based on $\delta^{18}O_p$ (such as for puma and bobcat), therefore lacks the required precision due to the rather weak $\delta^{18}O_p$ - $\delta^{18}O_w$ relationship. Potential explanations causing the deviations from a constant oxygen fractionation between $\delta^{18}O_p$ and $\delta^{18}O_w$ in feline carnivores include climate, diet, animal behaviour, physiology and metabolism.

The results of this thesis demonstrate the species-diagnostic resolution power of DNA barcoding and potential pitfalls in using water isotopic fingerprinting for geographic provenancing of felids in wildlife forensic investigations. In light of evidence presented here, the combination of DNA barcoding and isotope research opens up new avenues of research with relevance and practical applications for wildlife forensics, border control, law enforcement and isotope- and biodiversity research studies.

CHAPTER 1

1. GENERAL INTRODUCTION

1.1. The magnitude of illegal wildlife trade

Over-exploitation through illegal wildlife trade is a major threat to a wide range of endangered mammal species around the world. International and national CITES treaties and laws aim to regulate the international trade in endangered species of wild fauna and flora. The illegal trade, however, continues to boom, worth a ~20 billion US$ a year in protected live animals and animal products [1]. Illegal wildlife trade ranges at the second place right behind illegal drug and arms trade [2]. The European Union (EU) represents one of the three largest markets for wildlife and wildlife products in the world (along with the USA and Japan) [3]. The elimination of internal border controls in the EU has opened up new ways for cross-border wildlife trade crime. Interpol considers illegal wildlife trade as a global phenomenon that has serious implications for biodiversity, ecosystems and economies. Ecosystems worldwide are being disturbed by the removal of predators and other keystone species, causing a loss of biodiversity. Approximately 23% of all mammal species and 27% of all carnivores are at risk with extinction over the next few decades (Appendix S1 and S2).

Today the cat family Felidae are among the most threatened groups of mammals. The IUCN Red List of Threatened Animals 2008 includes almost half (44.4%) of the family Felidae in the top three categories of threat (see Appendix S3 and S4). Market surveys and seizures of poached animals indicate that trade in Felidae continues to impact wild populations. Costumers of felid trophies can still be found all over the world, and valuable material is sold openly, as in some countries, or as hidden merchandise on black markets [4,5]. Each year, millions of endangered animals are illegally killed or captured for private zoo collections, hunting trophies, animal furs and skins for the luxury market, ornamental objects (e.g. skulls, teeth and claws), traditional Asian medicine (e.g. tiger bones and penis), human consumption (e.g. tiger meat) and collectors. Existing laws protecting felids are often difficult to enforce, due to challenges encountered in identifying commercial products containing wild cat parts and derivatives, determining the legality of these products. Moreover, wild cat parts and derivatives (e.g. skull, bones, and skins) are often smuggled across continents and international borders, making poaching hotspots and potential trade routes difficult to identify. The present difficulties to implement CITES laws and regulations have direct consequences for endangered species in view of the enormous market for their products.

Wildlife forensic science is a multi-disciplinary field of research which facilitates the identification of illegal wildlife trade for law enforcement. Scientists in this field currently address two challenging issues: (i) Species identification from problematic biological sources (e.g.: bones, processed meat, faeces, blood, hair, tissue) and (ii) geographic provenancing to

track the origin of an unknown animal sample. These issues are crucial in wildlife crime investigations, food science and in ecological studies. Prior studies presented different techniques to address these topics but have turned out to be either impractical or too time-consuming for applications in mammal forensic case work [6-10]. The need for reliable, rapid and cost-effective tools for the identification of illegal wildlife trade has led to initiate the present study. Felids represent ideal study species to assess the application of (i) DNA barcoding for species identification and (ii) multi-isotopic fingerprinting for geographic provenancing.

1.2. The cat family Felidae

Felids evolved about 35 million years (Ma) ago and are now distributed over all continents, except Antarctica [11]. The cat family Felidae encompasses thirty-eight species [12]. Figure 1 shows the highly resolved molecular phylogeny of all living cat species that was derived from autosomal, X-linked, Y-linked and mitochondrial gene segments [12].

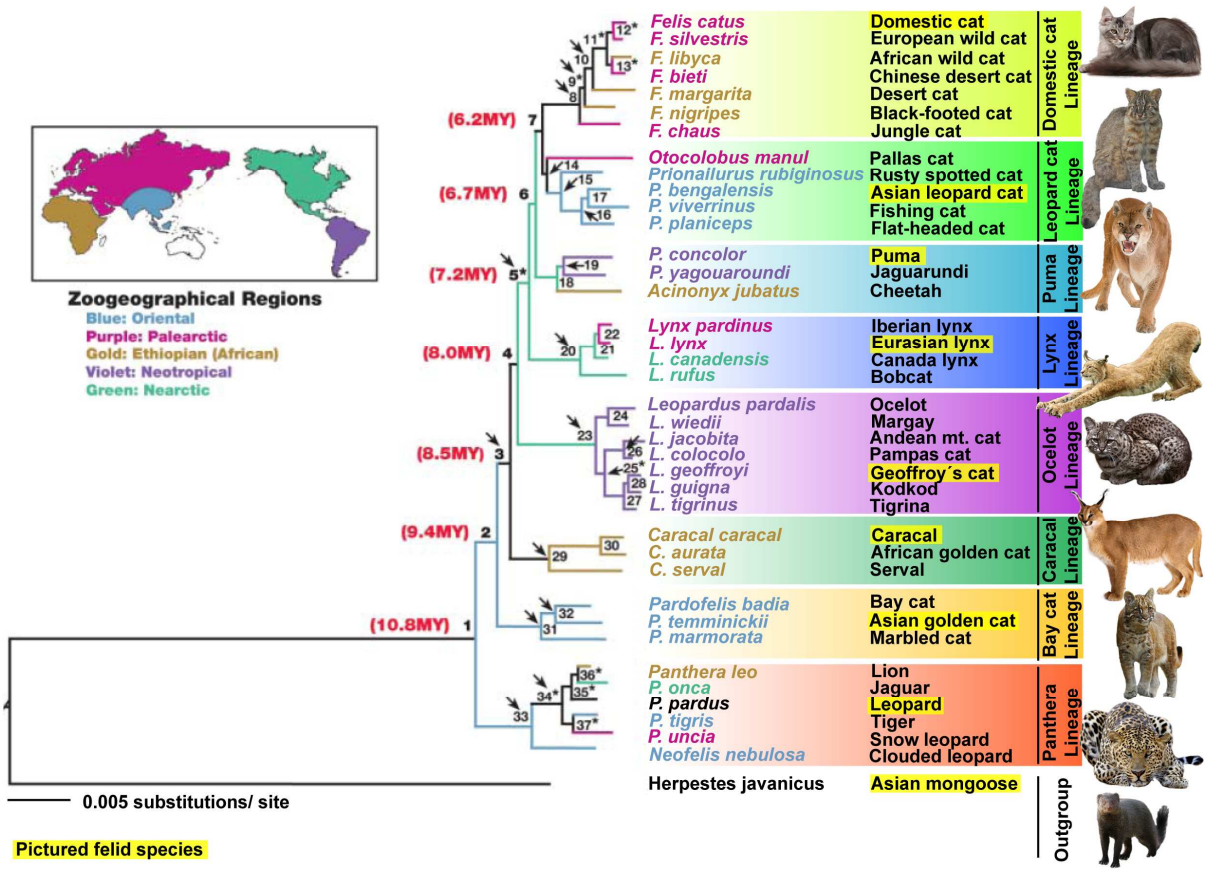

Figure 1. Phylogenetic relations among felids and outgroup taxa depicted in a maximum likelihood tree. Felid species are grouped into 8 major lineages (framed in coloured boxes). Scientific names and branches are colour-coded to depict zoogeographical distribution patterns. Estimated divergence dates of lineage-defining nodes are in red (Modified after [12]).

The taxonomic group of Felidae is ideally suited to test the feasibility of DNA barcoding and multi-isotopic fingerprinting as a novel forensic toolbox for the identification of illegal wildlife trade. The availability of comprehensive sample material from zoos and museums, a well-documented phylogenetic taxonomy (Figure 1) and numts's catalogue of Felidae, and high-resolution precipitation $\delta^{18}O$ and δD isoscapes allowed us to assess the application and efficiency of this forensic toolbox for specific identification and source determination of feline carnivores.

1.3. Aims and scope of the present thesis

The purpose of the present thesis is to test the application and validity of (i) DNA barcoding for species identification and (ii) multi-isotopic fingerprinting for provenance determination of felid species in wildlife forensic investigations.

The thesis is subdivided in four chapters. Each chapter represents an independent study with introduction, materials and methods, results, discussion and conclusions. The chronological order of the chapters reflects the logical sequence of steps from diagnostic identification to provenance determination of felid species in wildlife crime investigations. The specific goals of the chapters are as follows:

Chapter 2 aims to test the validity of DNA barcoding as a forensic tool for the rapid, reliable and cost-effective identification of felid species. Prior studies demonstrate that DNA barcoding can potentially be compromised by the inadvertent amplification of numts (i.e., nuclear copies of mitochondrial DNA). A total of 277 tissue samples (blood, muscle, hair, faeces) was analysed from 28 zoo felid species using two different mtDNA genes (COI and ATP6) to examine the type and extent of numt contaminations and their effect on the barcode results.

Chapter 3 and *4* both focus on the application of stable water isotopes for provenance determination of Felidae using different tissues types, hair and bone, respectively.

Chapter 3 presents the forensic investigation of stable hydrogen and oxygen isotopes in hair (δD_h and $\delta^{18}O_h$) to trace the geographic origin of two endangered felid species. However, reliably predicting the spatial distribution of δD_h and $\delta^{18}O_h$ requires confirmation from animal tissues of known origin and a detailed understanding of the isotopic routing of dietary nutrients into felid hair. A total of 88 hair samples were examined from North American bobcat (*Lynx rufus*) and puma (*Puma concolor*) museum specimens originating from 75 known sites across the United States and Canada. Coupled δD_h and $\delta^{18}O_h$ measurements were compared with precipitation-based assignment isoscapes to assess the control factors of isotopic incorporation into hair and their implications for the feasibility of isotopic geo-location of Felidae.

Chapter 4 explores the oxygen isotope compositions of felid bone phosphate ($\delta^{18}O_p$) as a proxy for felid provenance and migratory patterns in paleontological, archaeological, ecological and wildlife forensics applications. However, previous studies demonstrated that a complex mixture of factors are controlling mammal $\delta^{18}O_p$ and deviations from a constant oxygen fractionation between $\delta^{18}O_p$ and $\delta^{18}O_w$ of ingested precipitation water have been documented for some species. 107 bone samples of puma and bobcat specimens of known origin were analysed to determine whether $\delta^{18}O_p$ varied predictably among isotopically distinct geographic locations and reflected the spatial pattern of $\delta^{18}O_w$. Different factors like diet, physiology, metabolism and climate were identified to potentially contribute to deviations in $\delta^{18}O_p$ of feline carnivores.

CHAPTER 2

2. Taming cat numts:
DNA barcoding of Felidae using mtDNA and numts

Stephanie J. Pietsch

(1) Zoologisches Forschungsmuseum Alexander Koenig, Universität Bonn, Bonn, Germany

* Corresponding author: Stephanie J. Pietsch
E-mail address: feliden.zfmk@googlemail.com

This is the author's version of a work prepared for submission to Biology Letters.

ABSTRACT

Background

Many feline carnivore species are endangered and severely threatened by illegal trade. Genetic species identification is thus essential in wildlife crime investigations to detect illegal trade of protected species and morphologically indistinguishable species` derivatives (e.g. hair, bone powder). As demonstrated for several other species, DNA barcoding has strong potential to be applied to animal tissues as an investigative, rapid, and cost-effective tool in wildlife forensic science. However, DNA barcoding can potentially be compromised by the inadvertent amplification of numts (i.e., nuclear copies of mitochondrial DNA). Thus, reliably identifying feline species via DNA barcoding requires careful examination of numt contaminations and their effect on the results of barcode analyses.

Methodology / Findings

We used two different mtDNA genes (COI and ATP6) to test their validity as barcode markers for the identification of felid species in wildlife forensic investigations. A total of 277 tissue samples (blood, muscle, hair, faeces) were genetically analyzed and originated from 28 felid species held in European zoos. Numt contamination was shown to be present in Felidae and varied among the selected mtDNA markers, tissue types, individuals and species. However, most individual felid taxa are characterized by unique mitochondrial and numt barcode sequences.

Conclusions / Significance

Felid DNA barcoding using the two mitochondrial markers ATP6 and COI is accompanied by numt contaminations. However, with some exceptions, authentic mtDNA as well as numt sequences of the COI and ATP6 gene can be used as species-diagnostic barcode markers applicable for felid forensic investigations. In a few cases numts can potentially impede the species-diagnostic performance of mtDNA barcoding in Felidae. The tissue-specific amplification of ATP6 numts in several felid species and a shared COI numt in domestic and wild cats thus require the analysis of additional tissue materials and nuclear markers.

2.1. INTRODUCTION

Many carnivore species are currently threatened and focus of intense conservation concerns [13]. Forensic species identification is essential in wildlife crime investigations to detect illegal poaching and trade of protected species and species` derivatives [14,15]. Feline carnivores in particular are often involved in the illegal wildlife trade [11,16]. In many cases, traded animal products like bones, meat, skulls, claws and skins lack detailed morphological features for species identification. Such cases require the application of molecular genetic tools based on DNA sequence similarity. BLAST search, the most commonly used tool, enables a researcher to compare an unknown query sequence with a database of authenticated reference DNA sequences (e.g. species barcodes, [17]). DNA barcoding, using the mitochondrial cytochrome c oxidase I (COI) marker [18,19], has strong potential to be applied to animal tissues as an investigative, rapid, and cost-effective tool in wildlife forensic science [17,20-23]. However, DNA barcoding can potentially be compromised by the presence of numts (nuclear mitochondrial DNA: [24,25]). Numts are copies of mitochondrial genes that were trans-located and incorporated into the nuclear genome [24-31]. The inadvertent (and often unnoticed) amplification of numts in addition to, or even instead of, the authentic target cytoplasmic mitochondrial DNA (cymt) sequence represents a substantial source of contamination and a major impediment to DNA barcoding [25]. Methods to detect and avoid numt contamination are often laborious, time-consuming and expensive, and most importantly none of these methods effectively eliminates the problem [24,25,32]. However, numts may not imperil DNA barcoding, if their sequence divergence coincides with species divergence.

Some researchers suppose that numts can be easily identified and removed from data analysis [33] using “anti-numt” quality control strategies as suggested by Song et al. [25]. However, some numts were reported to lack any molecular features for reliable identification and thereby perfectly camouflage the authentic mitochondrial sequences [25]. Failure to differentiate between numts and cymt can lead to an overestimation of the number of species [25], species misidentification [25,34,35], incorrect phylogenetic relationships [24], and thus has important implication for future species conservation strategies (e.g. gorilla: [32,36]).

Hakazani Covo et al. [37] considered numts as “molecular poltergeists” with many facets: they feature different size distributions (<1kb to >2000kb), various degrees of homology with their mitochondrial counterparts, diverse distribution patterns across the nuclear genome, and a positive correlation with genome size [24,37,38]. Richly and Leister et al. [38] documented the widespread occurrence of numts in a large number of eukaryotic clades including plants (e.g. [39]), birds (e.g. [29,40]), reptiles (e.g. [41]), mammals (e.g. [42,43]), and arthropods (e.g. [24,30,44,45]). For Felidae, two well documented cases of

independent numt integrations have been reported to date. The first consisted of the 1.8 MYA old and 7.9 kb long tandemly repeated numt located on the chromosome D2 of the nuclear genome of the domestic cat (*Felis catus*) [28]. The second case described an independent 3.5 MYA old and 12.5 kb long numt insertion located on the chromosome F2 of the tiger (*Panthera tigris* and other *Panthera* species) [46]. Given this widespread occurrence of numts, Moulton et al. [47] postulated that "the more we search for numts, the more common they appear to be [26,38] and their presence may be more of a rule than an exception". In the future, further whole genome sequencing initiatives will continue to elucidate the evolutionary dynamics of numts in other species [38,46].

Various factors were reported to affect numt amplification when using PCR and include: taxon [38], tissue-type [48-50], gene region [51,52], numt age [53], and universal primer use [25]. Hence, a complex molecular toolbox has been developed for the avoidance and detection of numts (for review see: [24,25,54-56]). Methods developed to avoid numt amplification include RT-PCR, long-range PCR, entire mtDNA genome-amplification, specific primer use, mtDNA enrichment, using mtDNA-rich tissue (e.g. muscle), and dilution of DNA extracts. Several post-PCR approaches should help to detect and identify numts like restriction digest, cloning, comparative sequence analysis and translation, checking for stop codons, insertions–deletions (indels), or frame-shift mutations within a coding mtDNA sequence, checking the secondary structure of RNA genes, ambiguity check of the electropherograms, gel-check for the existence of multiple bands.

Here, we provided the first large-scale DNA barcoding analysis of the cat family Felidae using different tissue types (hair, faeces, blood, and muscle) commonly encountered in wildlife forensic investigations. Felids are ideally suited to test the strength of a barcode approach in determining species identity. The availability of comprehensive sample material from captive zoo-felids, a well-established phylogenetic taxonomy of Felidae, and the existence of two well-documented felid-specific numts allowed us to assess the application and efficiency of DNA barcoding for specific identification of feline carnivores in forensic investigations.

Our study was designed to test the effect of numts on DNA barcoding based on barcoding analyses of numt and mtDNA sequences in eight divergent lineages of Felidae. We used two different mtDNA markers: a 658 bp segment of the standard barcode marker COI located within the range of the two reported cat numts, and a 126bp fragment of the ATP6 gene, which was reported to be highly variable in carnivores and located outside the two felid numts. We then assessed the extent of numt contamination and their effect on the results of DNA barcoding analyses.

2.2. MATERIALS AND METHODS

2.2.1. Sampling

A total of 277 tissue samples (blood, muscle, hair, faeces) were genetically analyzed and originated from 28 felid species. Zoos, veterinary pathologies and zoological museums in Europe (see Appendix 1) supported us with sample materials from captive zoo felids. Samples were either non-invasively collected from the enclosure (faeces, hair), during veterinary checkups or from perished animals (muscle, blood, hair). Specimens were initially identified by the mammal curators in the zoos who followed the species nomenclature of Johnson et al. [12]. Each voucher specimen tissue was labelled with the complete scientific species name, sex and full collection record (collectors name, collection date and location). Vouchers will be deposited in the DNA- and tissue bank of the Museum Koenig and data will be accessible via online databases (BOLD in the project Barcoding cats [BACATS]) and NCBI (http://www.ncbi.nlm.nih.gov/)). Tissue samples like blood, muscle and faeces were stored frozen or preserved in 95–99% ethanol; hairs, however, were stored dry in an envelope at room temperature.

2.2.2. DNA extraction, PCR amplification and DNA sequencing

DNA extraction, PCR amplification and DNA sequencing of the COI and ATP6 gene was performed according to the standard laboratory protocols from BOLD and the quality control guidelines suggested by Song et al. [25]. The complete DNA barcode analyses were conducted at the DNA laboratory of the Zoological Museum Alexander Koenig in Bonn/Germany.

Voucher specimens were subsampled and subjected to DNA extraction using 'DNeasy Blood & Tissue Kit' (Qiagen) for muscle, blood and hair, and 'All-tissue DNA-Kit' (Gen-ial) for faeces. Hairs were decontaminated from external sources of contamination prior to DNA extraction using the protocol developed by Gilbert et al. [57]. The hair shafts were manually washed in 0.1x concentration commercial bleach solution (≈0.5% final NaClO concentration; 'DanKlorix') to remove any debris or contaminant DNA that was on the outside of the hair shaft, then rinsed several (2-6 times) in DNA-free H_2O until all traces of the bleach had been removed. Digestion of the hair shafts was performed with 1 M DTT (dithiothreitol) according to the protocol for the 'Isolation of total DNA from hair shafts' (QIAamp DNA Investigator Handbook 12/2007).

PCRs were performed using the QIAGEN Multiplex PCR Kit. The 20 µl PCR reaction mixes included 3.3 µl of ultra pure water, 10 µl of Master Mix (HotStarTaq® DNA Polymerase, Multiplex PCR Buffer*, dNTP Mix), 2 µl Q-Solution, 1.6 µl of each primer (20pmol) and 1.5 µl of extracted DNA. Two different mitochondrial protein coding markers were selected for amplification (Figure 1):

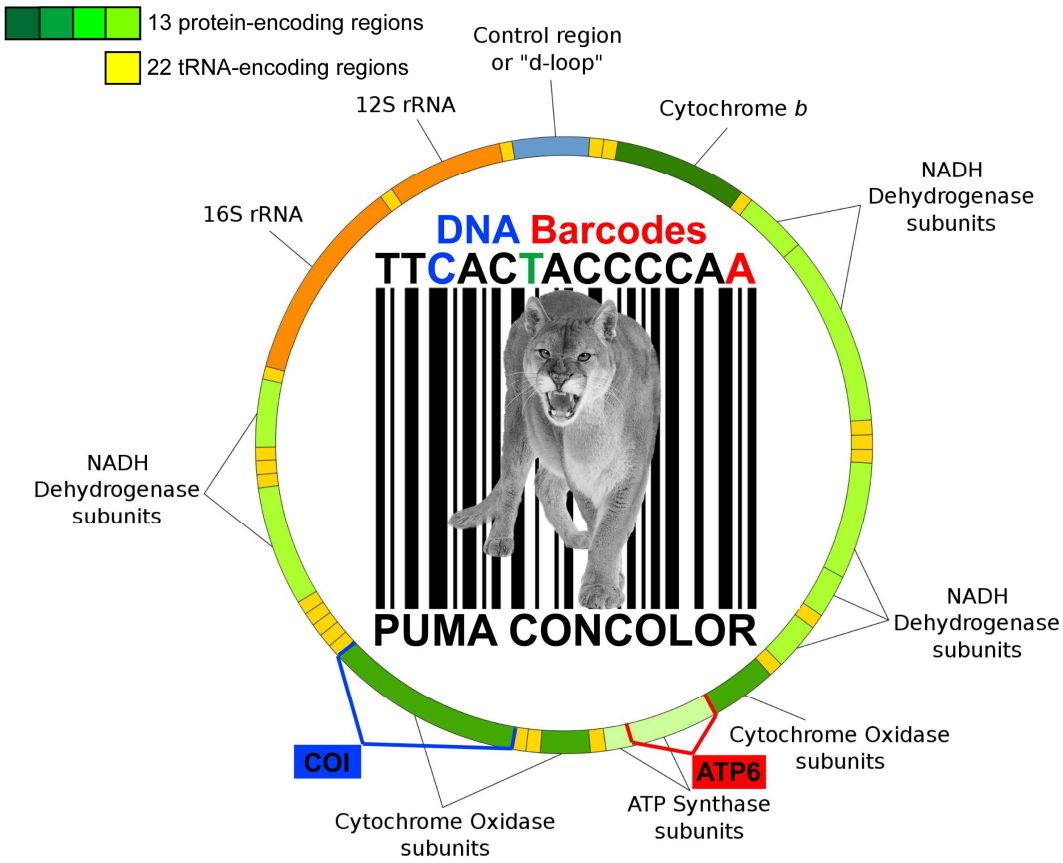

Figure 1. **Mitochondrial barcode markers.** Mitochondrial genome showing the location of the two felid DNA barcode markers, COI and ATP6.

The 658 bp long "Folmer region" at the 5′ end of the mitochondrial cytochrome c oxidase subunit 1 (COI) is the standard barcode region for almost all groups of higher animals [18]. A 216 bp amplicon of the mitochondrial ATP synthase F0 subunit 6 (ATP6) gene was included for DNA barcoding analyses because of three reasons: (i) it was demonstrated to be quite variable in carnivores [58], (ii) it represents a short "mini-barcode" which enables PCR amplification of degraded DNA samples [59], (iii) and it lies outside of the two reported numts in the tiger [46] and the domestic cat [28] genomes (Figure 2). M13-tailed degenerate primers were designed to accommodate variation in mtDNA sequences among feline taxa and to reduce the potential for preferential amplification of nuclear pseudogenes [56]. The following PCR primers were used for this study: ATP6_F (5´-TGTAAAACGACGGCCAGTAACGAAAATCTATTCRCCTCT-3´) and ATP6_R (5´-CAGG AAACAGCTATGACCCAGTATTTGTTTTRAYGTWAGTTG-3´) originally reported by Trigo et al. [58]; and COI_F (5´-TGTAAAACGACGGCCAGTTCTCAACCAACCACAARGAY ATYGG-3´) and COI_R (5´-CAGGAAACAGCTATGACTAGACTTCTGGGTGGCCRAARAA YCA-3´), a standard primer pair for DNA barcoding of mammals developed by Ivanova et al. [60]. In addition, we also tested several primers targeting nuclear genes like the LSU rDNA D1-D2 marker [61] and another 28S marker [48].

PCR thermocycling was performed as a touchdown PCR under the following conditions: 15 min at 95℃; 5 cycles of 35 sec at 94℃, 1.30 min a t 60℃, 1 min at 72℃; 35 cycles of 35 sec at 94℃, 1.30 min at 57℃, 1.30 min at 72℃; 10 min at 72℃; 15 min at 4℃ and held at 12℃. Successful PCR amplification was examined using an agarose gel-check and the most intense products were selected for sequencing. PCR products were cleaned using QIAquick PCR Purification Kit (Qiagen) and submitted for sequencing by an external sequencing service (Macorgen, Korea). Contigs and sequence alignments were generated using Geneious Version 5.1.7 [62].

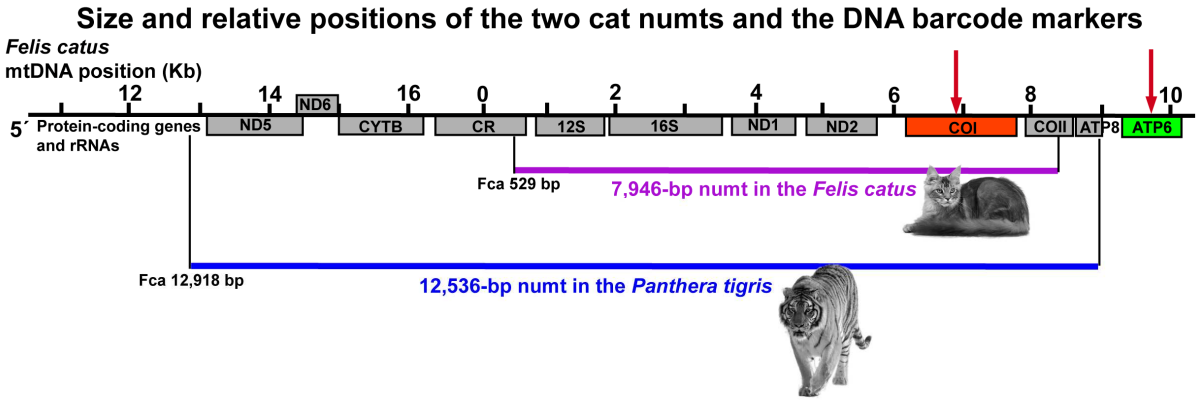

Figure 2. Reported cat numts. Schematic diagram of the relative positions of the *Panthera* and *Felis* numt and the targeted mtDNA barcode markers (ATP6 and COI). The scale bar in Kb corresponds to the domestic cat (*Felis catus*) mtDNA complete sequence [28] aligned with the *Panthera* (blue) [46] and *Felis* (purple) numt [28]. Protein-coding genes and rRNAs are indicated in grey boxes. The red box shows the relative position of the COI barcode marker within the tiger and cat numt region. The ATP6 gene highlighted with a green box is located outside the two reported cat numts. Modified after Kim et al. [46].

2.2.3. Data analysis

2.2.3.1. Identification of numts and tissue-type comparison

Pseudogenes (numts), i.e. mtDNA fragments incorporated in the nuclear genome [24], may represent a source of error since PCR-based analyses will often amplify both the authentic mitochondrial sequence and the pseudogene. We checked protein coding sequences for evidence of frame-shifts, stop codons and divergences in nucleotide composition between sequence types that might indicate that numts are present. We cross-checked clean sequences with COI and ATP6 sequences from published mitochondrial genomes of the most closely-related taxa of the investigated species. A tissue comparison experiment using hair, blood, muscle and faeces of the same individual was performed for several felid species to check, if (i) all tissues yield consistent sequences and (ii) if these match the cymt or numt sequence reported for this species.

2.2.3.2. *Tree building and genetic distance methods*

Pairwise nucleotide sequence divergences were calculated using the Kimura two-parameter (K2P) substitution model [63]. A neighbour-joining (NJ) tree of K2P sequence distances showing intra- and inter-specific variation was created using the 'Taxon ID tree' function of BOLD. K2P sequence divergences for all levels in the taxonomic hierarchy were determined using the 'distance Summary' tool on BOLD. We used the analytical tool 'Nearest Neighbour Summary' on BOLD to calculate nearest neighbour distances.

2.3. RESULTS

2.3.1. COI barcode marker

120 full-length COI sequences were recovered from 23 taxa (61%) of the 38 extant species of Felidae, distributed among 10 genera and 8 felid lineages (Appendix 1 and 2). Individual species were represented by multiple individuals (average = 5.3, range = 1–18) for a total of 106 sequences of a mean length of 658 bp. The original felid dataset consisted of 267 specimens from 28 species. However, we failed to obtain sequences from 30 specimens of 5 species. In addition, we excluded all sequences with >1% ambiguous nucleotides from the analyses (n = 20). Full-length COI barcodes were obtained for about 60% of the specimens. The reasons for our problems with obtaining COI sequences from a number of individuals are unknown, but may partly be due to primer mismatches for the standard COI primers in several felid taxa. Another reason might be the low DNA quality and quantity of some samples (e.g. hair and faeces), which might prevent the recovery of PCR fragments longer than 200 bp, thus impeding full length COI barcode (658 bp) recovery.

2.3.1.1. Putative COI numts

We detected presumptive pseudogenes in 6 (27%) of the 22 species sequenced for COI. Putative numts were recovered from the following felid species: *Panthera tigris*, *Panthera leo*, *Otocolobus manul*, *Felis catus*, *Felis silvestris*, and *Felis libyca.* The putative numts showed evidence of frame shifts, stop codons and nucleotide insertions between sequence types that might indicate that numts are present. The COI sequences obtained from the lion (*Panthera leo*) were classified as putative numts although they lacked any evidence of stop codons. But like others these presumptive numt sequences showed a higher sequence similarity with one of the two published felid numts (*Panthera tigris* numt: [46]; *Felis catus* numt: [28]) versus the authentic cymt sequence from the corresponding species or its sister species. Several different numt haplotypes were discovered for the three species of the *Felis* genus, while *Panthera tigris*, *Panthera leo*, *Otocolobus manul* each exhibited only one numt haplotype (see Table S1).

2.3.1.2. COI tissue-type comparison

COI sequences were derived from different tissue types (hair, blood, muscle, faeces) of a single *Panthera tigris* individual. All tissue types yielded a putative COI numt. The presumptive pseudogene sequence of the tiger showed 99% sequence similarity with the previous reported tiger numt [46]. Figure 3 shows the several nucleotide and amino acid substitutions between the tiger COI cymt and numt sequences.

2.3.1.3. COI-barcode analysis

The NJ tree of sequence divergences (K2P) at the COI region indicated that most genera formed cohesive units (Figure 4). Putative numts are highlighted in grey and cluster separately from the cymt sequences. All species possessed a distinctive set of COI cymt and numt sequences, which showed low intraspecific divergences. The mean K2P sequence distance within species was 0.2%, while the mean divergence between congeners was 28-fold higher at 5.6% (see Table 1, Figure 5). The minimum distances to the nearest neighbour is 0% and thus lower than the maximum intra-specific distance of 2.03% (see Figure 6). *Felis catus* shows a critically low distance of 0% to its nearest neighbour *Felis silvestris*, and *Panthera leo* only differs in 1.14% from its nearest neighbour *Panthera tigris*.

Table 1. Pairwise COI barcode nucleotide divergences for the Felidae using K2P distances (%).

Level	n	Taxa	Number of comparisons	Min. Dist (%)	Mean Dist (%)	Max. Dist (%)	SE Dist (%)
Within Species	104	21	388	0	0.177	2.032	0.021
Within Genus	105	10	653	0	5.643	10.312	0.099
Within Family	105	1	4419	10.306	17.055	39.928	0.091

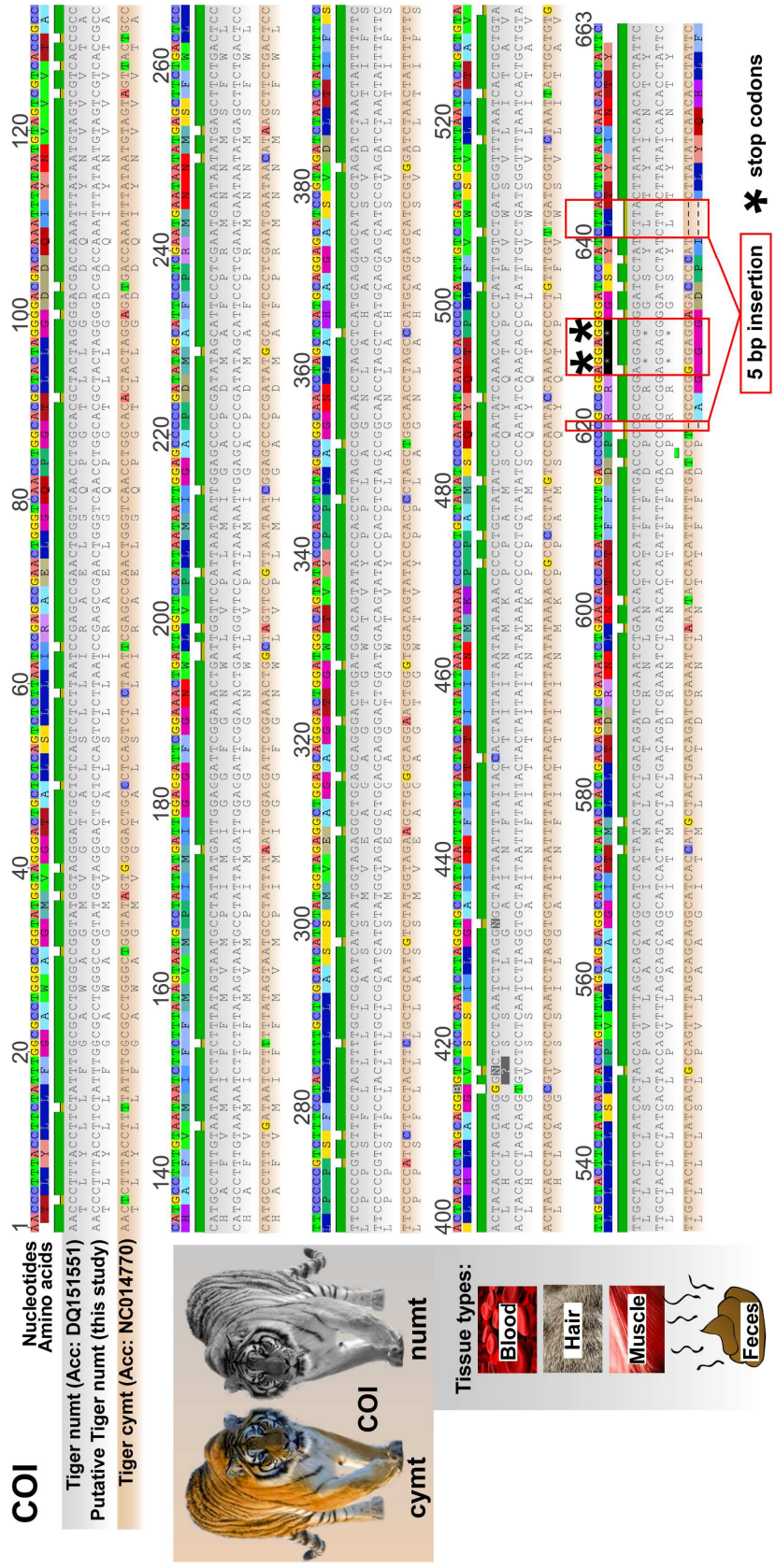

Figure 3. COI numt and cymt sequences of the tiger. Putative COI numt sequences generated from *Panthera tigris* in this study were compared with the corresponding cymt and previous reported numts for the tiger [46]. The putative COI numt sequences were obtained from different tissue types (hair, blood, muscle, faeces) of one individual tiger. Nucleotide and amino acid substitutions between the cymt and numt are highlighted and stop codons marked with an asterisk. The numt and cymt sequences are shaded in grey and brown, respectively.

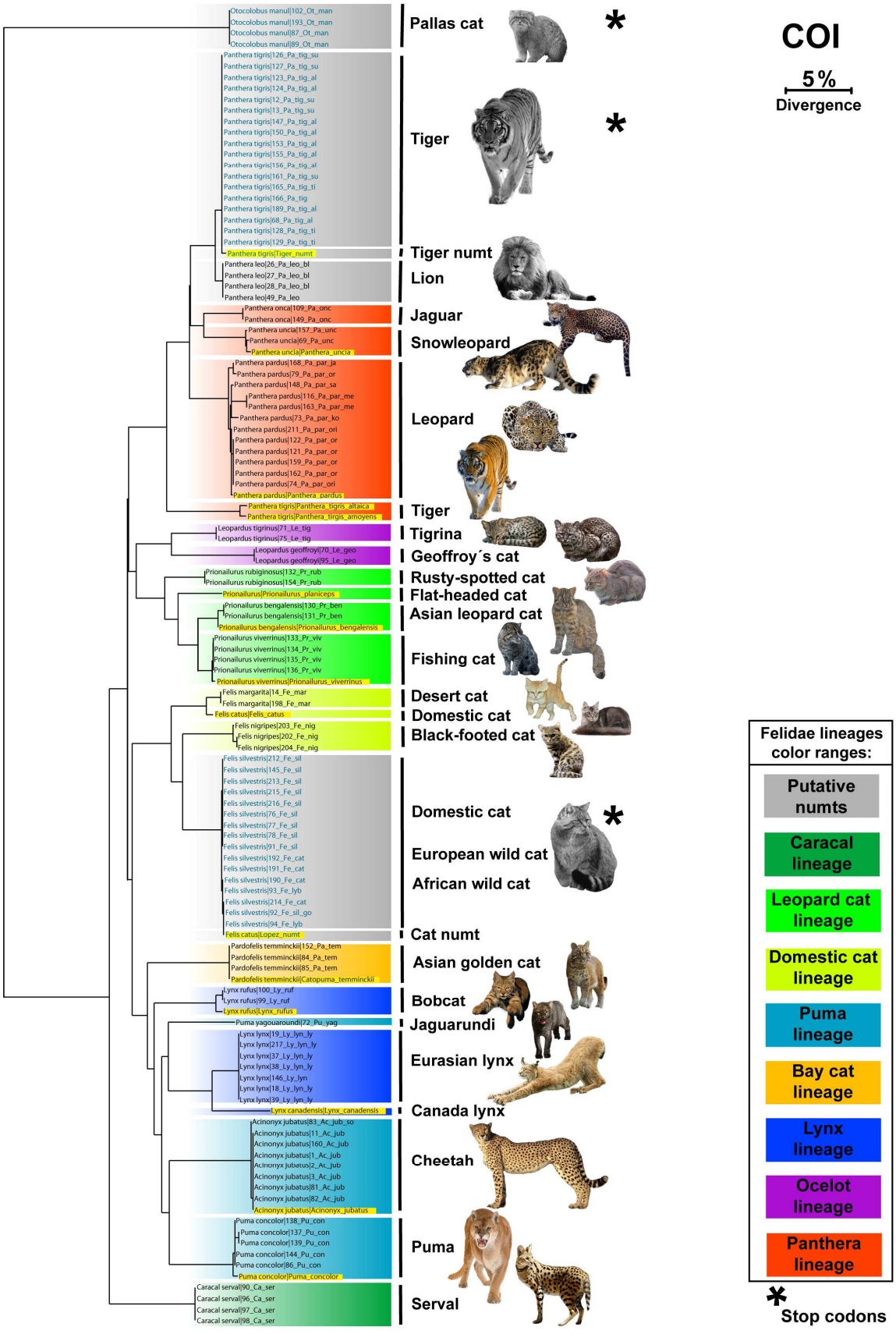

Figure 4: **COI NJ tree of Felidae.** NJ tree of COI sequences from 23 species in the family Felidae. Species affiliations with the respective felid lineages are highlighted with coloured boxes (according to Johnson et al. [12]). An asterisk indicates the presence of a stop codon. COI cymt and numt sequences derived from Genbank were included for comparison and are framed with a yellow box.

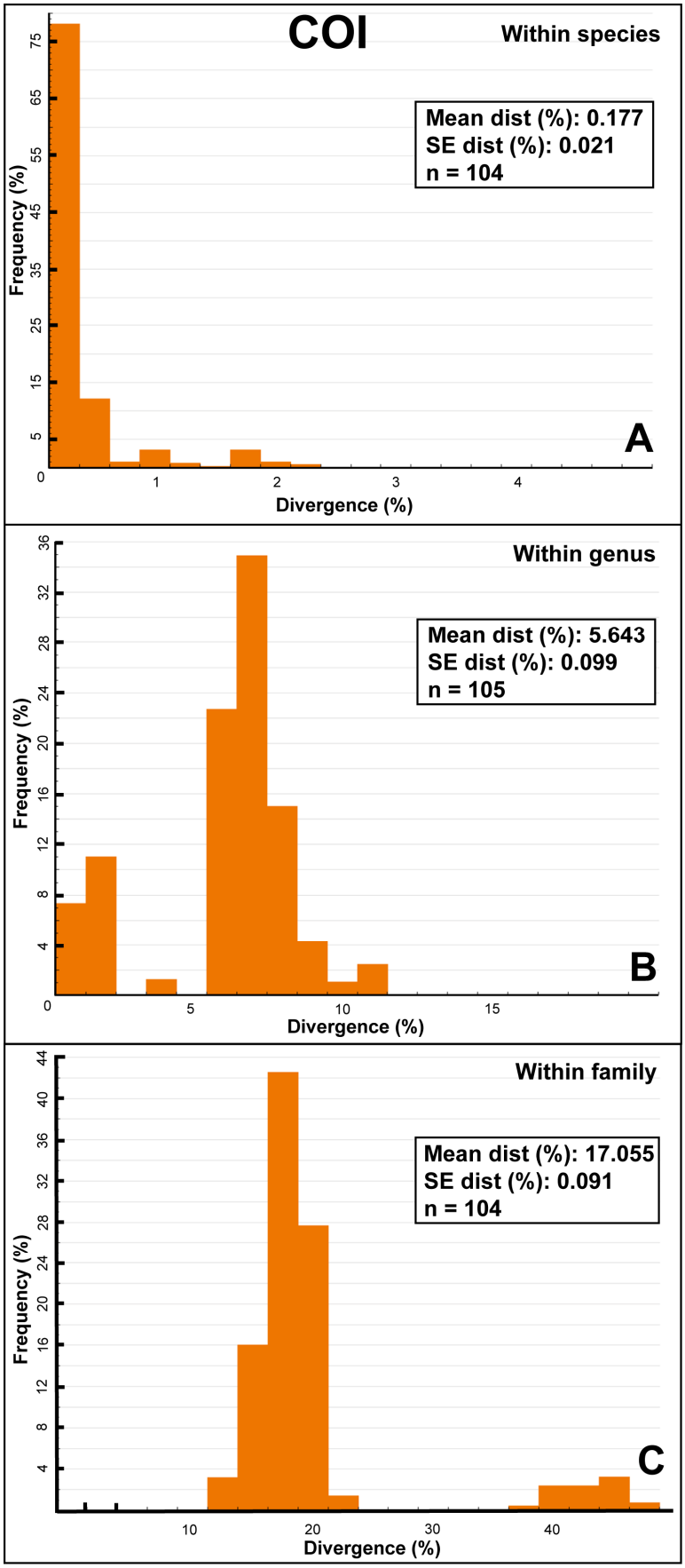

Figure 5. Pairwise comparisons of nucleotide sequence differences in COI among 23 species of Felidae at various levels of taxonomic hierarchy: (A) intraspecific; (B) intragenic; (C) intergenic differences between individuals.

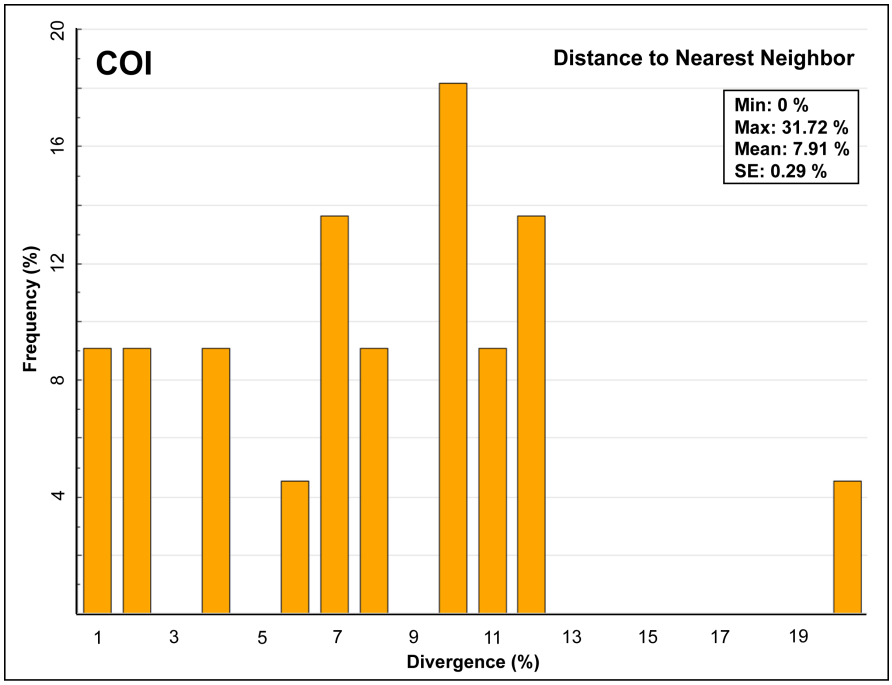

Figure 6. Histogram showing the distribution of the nearest neighbor distances for COI across 23 felid species.

2.3.2. ATP6 barcode marker

198 full-length ATP6 sequences were recovered from 28 taxa (74%) of the 38 extant species of Felidae, distributed among 11 genera and 8 felid lineages (Appendix 1 and 2). Individual species were represented by multiple individuals (average = 6.5, range = 1–18) for a total of 198 sequences of a length of 126 bp. The original felid dataset consisted of 210 specimens from 30 species. However, we failed to obtain sequences from 12 specimens of 2 species. In addition, we excluded all sequences with >1% ambiguous nucleotides from the analyses (n = 20).

2.3.2.1. Putative ATP6 numts

We detected putative numts in 13 (46%) of the 28 species sequenced for ATP6. Putative pseudogenes were recovered from the following cat species: *Acinonyx jubatus, Felis silvestris, Panthera leo, Panthera onca, Panthera pardus, Panthera tigris, Panthera uncia, Puma yaguarundi, Puma concolor, Leopardus pardalis, Leopardus tigrinus, Leopardus wiedii, Leopardus geoffroyi*. The putative numt sequences showed no evidence of frame shifts, stop codons or base pair insertions. However all putative numt sequences derived from 13 different felid species were completely identical and a Blast search revealed 98% sequence similarity with *Panthera pardus* (see Figure 7). This putative ATP6 numt sequence differed from *Panthera pardus* in two bases located in bp-position 54 and 80 of the amplicon and in one amino acid. The coding triplet in bp-location 79-81 of the ATP6 numt codes for the amino acid serine, whereas the corresponding cymt sequences of all other felid species code for the amino acid asparagine (Figure 8).

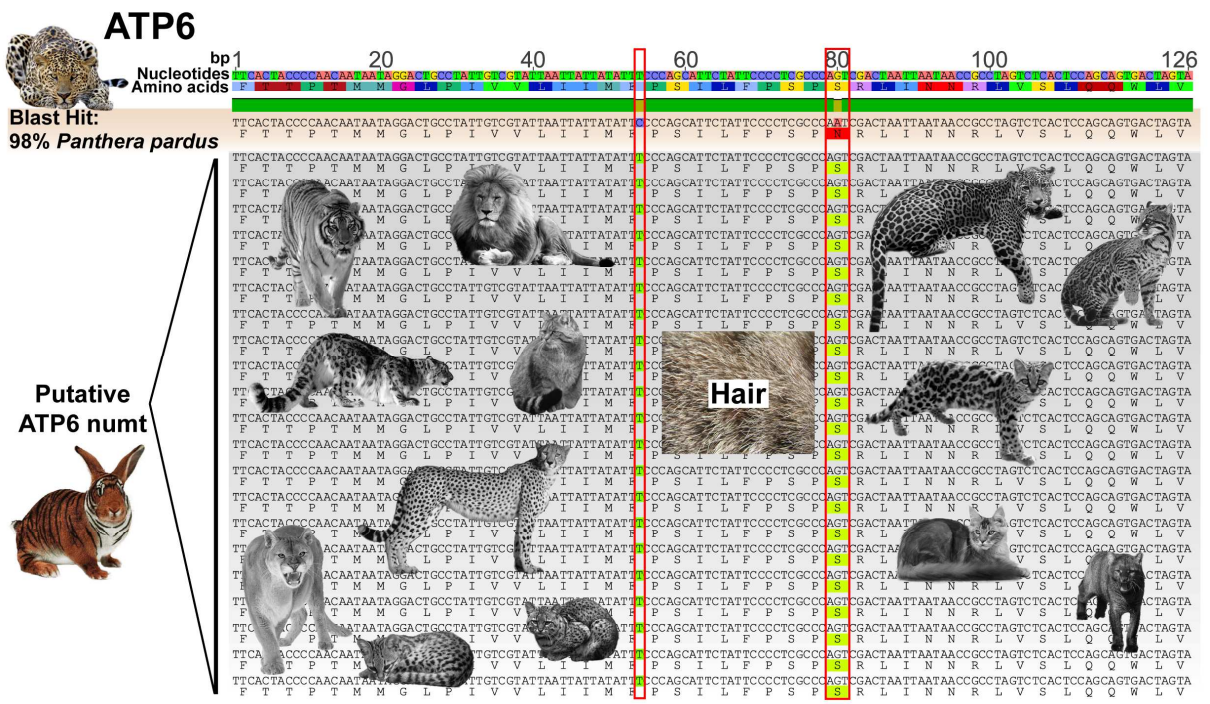

Figure 7. ATP6 numt and cymt sequences of cat hair. Nucleotide and amino acid sequence alignment of the ATP6 gene from *Panthera pardus* (Genbank: NC010641) and the putative ATP6 numt sequences. One putative ATP6 numt haplotype was obtained from hair of 13 different felid species. The putative ATP6 numt shows highest sequence similarity (Blast hit: 98%) with the cymt ATP6 sequence of *Panthera pardus*. The cymt and numt sequences of the protein coding ATP6 gene differ (i) in two bases at positions 54 and 80 and (ii) in the coded amino acid at bp-position 79-81. Sequence differences are highlighted with red boxes.

2.3.2.2. ATP6 tissue-type comparison

The ATP6 sequence comparison of different tissues (hair, blood, muscle) from the same individuals was performed for five felid species (Felis *silvestris, Panthera tigris, Panthera leo, Panthera uncia, Puma yaguarundi*) and resulted in the detection of several nucleotide and amino acid substitutions between different tissue types (Figure 9). ATP6 sequences obtained from blood or muscle yielded the authentic cymt sequence, which was confirmed by correct blast results. Sequences derived from hair resulted in a putative numt sequence perfectly matching the above mentioned putative ATP6 numt haplotype.

2.3.2.3. ATP6-barcode analysis

The NJ tree of sequence divergences (K2P) at the ATP6 region indicated that most genera formed cohesive units (Figure 10). Putative numts are highlighted in grey and cluster separately from the respective cymt sequences. All species possessed a distinctive set of ATP6 sequences, which showed low intraspecific divergences. The mean K2P sequence distance within species was 0.15%, while the mean divergence between congeners was 57-fold higher at 8.55% (see Table 2, Figure 11). Regression analysis indicated that neither mean nor maximum divergence values were significantly correlated to sample size (mean dist.: R^2 = 0.000, P = 0.932; max dist.: R^2 = 0.079, P = 0.182) (Figure 12). The distance to

the nearest neighbour is more than 3.28% and thus higher than the maximum intra-specific distance of 0.16% (see Figure 13). The distance of one individual of *Felis catus* to its nearest neighbour *Felis silvestris* is 0.8% and thus less than the maximum intra-specific distance of 1.22%.

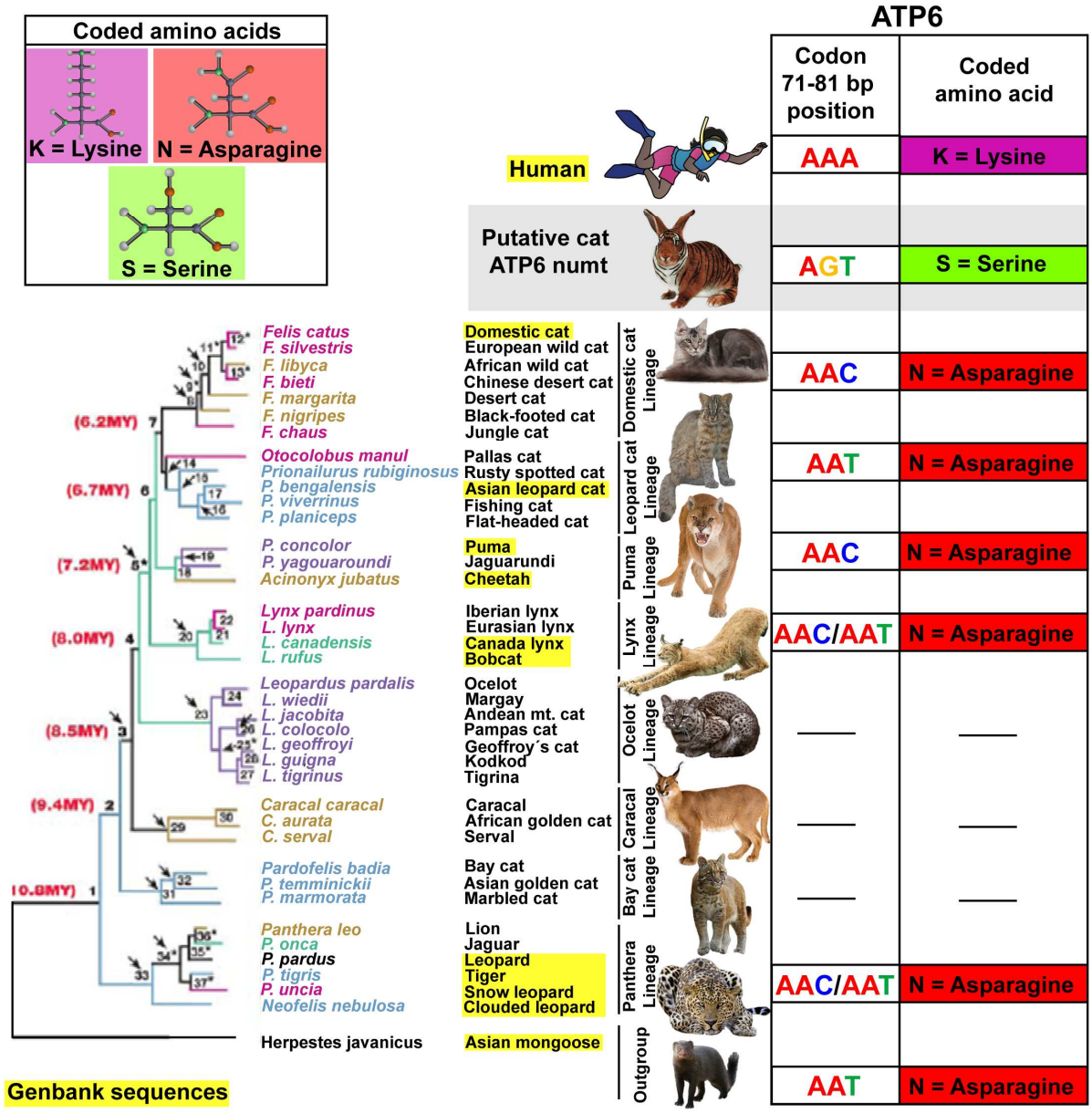

Figure 8. Schematic diagram of the coding triplets and the corresponding coded amino acids at the 79-81 bp-region in the ATP6 gene (126 bp segment) represented for cymt of almost all felid lineages, humans, and the putative ATP6 cat numt. The putative ATP6 cat numt differs in its codon (AGT) and the coded amino acid (S = Serine) from all other felids (codons: AAC, AAT; amino acid: N = Asparagine) and humans (codon: AAA; amino acid: K = Lysine).
*Cymt ATP6 reference sequences were obtained from the following complete mtDNA genome sequences in Genbank (framed with a yellow box): *Acinonyx jubatus*: NC_005212.1, AY463959.1, AF344830.1; *Panthera tigris altaica*: HM185182.1; *Prionailurus bengalensis*: HM185183.1; *Panthera tigris amoyensis*: NC_014770.1, HM589215.1, HM589214.1; *Puma concolor*: AH014071.1; *Lynx canadensis*: AH014070.1; *Lynx rufus*: NC_014456.1, GQ979707.3; *Panthera uncia*: EF551004.1, NC_010638.1; *Felis catus*: NC_001700.1; *Neofelis nebulosa*: NC_008450.1, DQ257669.1; *Panthera tigris*: NC_010642.1, EF551003.1; *Panthera pardus*: NC_010641.1, EF551002.1; *Homo sapiens*: GU392106.1; *Herpestes javanicus*: NC_006835.1.

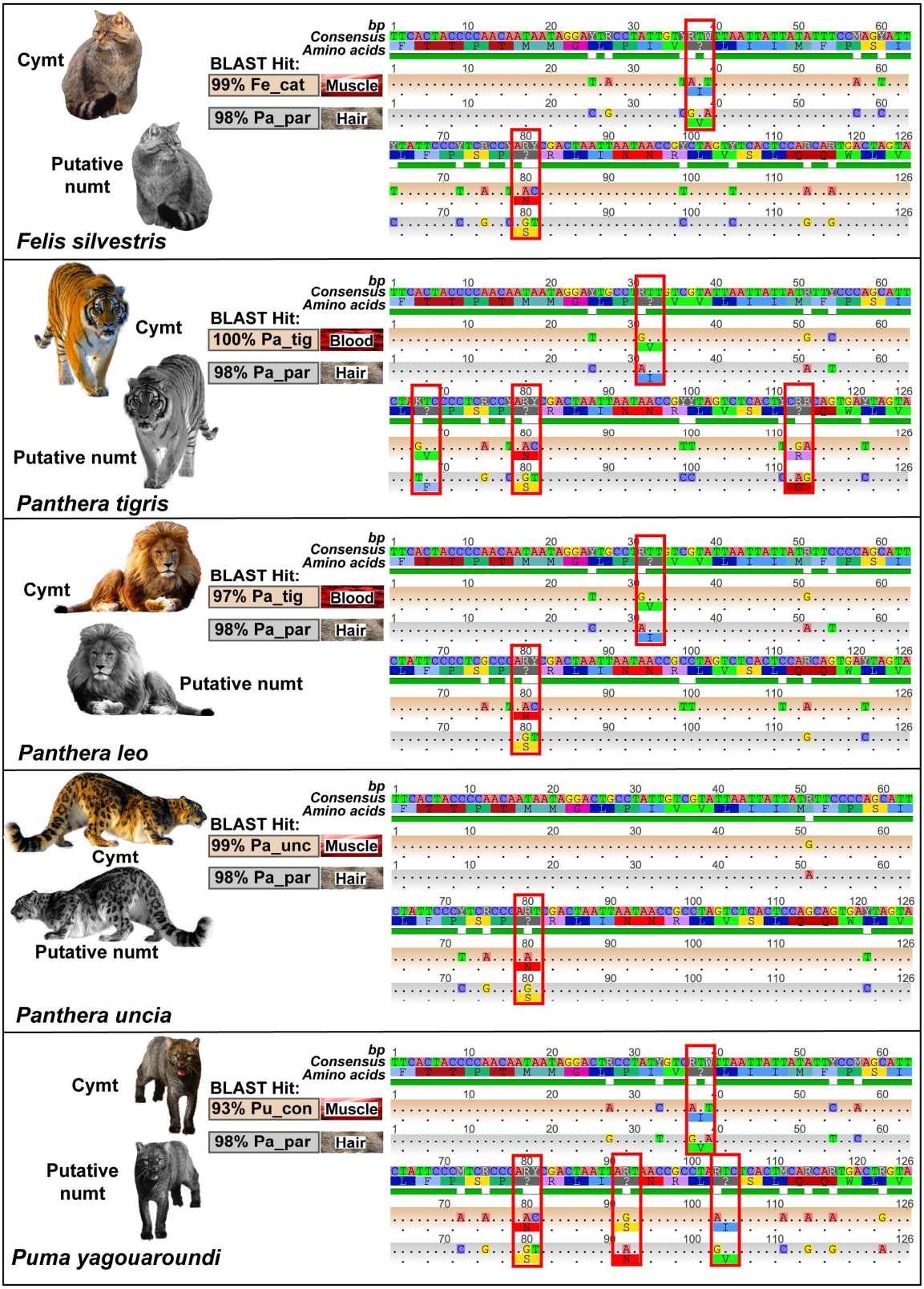

Figure 9. Tissue-specific amplification of ATP6 numts. ATP6 sequences determined from hair, blood or muscle of five different felid species. Sequences obtained from blood or muscle resulted in the authentic cymt sequence verified by Blast sequence search. If no reference sequences were available in Genbank (i.e., *Felis silvestris, Panthera leo, Puma yagouaroundi*), the sequence matching the sister species was classified as the authentic cymt sequence. The putative ATP6 numts derived from hair of all five felids are identical and show 98% sequence similarity with *Panthera pardus* (NC_010641.1). Differences in nucleotides and amino acids between numt sequences obtained from hair, and cymt sequences from blood or muscle were colour-shaded and highlighted with a red box.

2.3.3. Nuclear DNA barcode markers

Initial tests using primers targeting the nuclear LSU D1-D2 region [61] and another region of the 28S [48] showed either no amplification success or no sequence variability between the closely related felid species (data not shown). It is known that compared to mtDNA, nuclear markers show less performance in species delineation of closely related taxa due to slower rates of evolution in the nucleus [64], and less amplification efficiency with vertebrate samples [61].

Table 2. Pairwise ATP6 barcode nucleotide divergences for the Felidae using K2P distances (%).

Level	n	Taxa	Comparisons	Min. Dist (%)	Mean Dist (%)	Max. Dist (%)	SE Dist (%)
Within Species	160	24	157	0	0.145	2	0.016
Within Genus	161	11	165	1	9	18.919	0.112
Within Family	161	1	1889	4.135	14.949	26.691	0.036

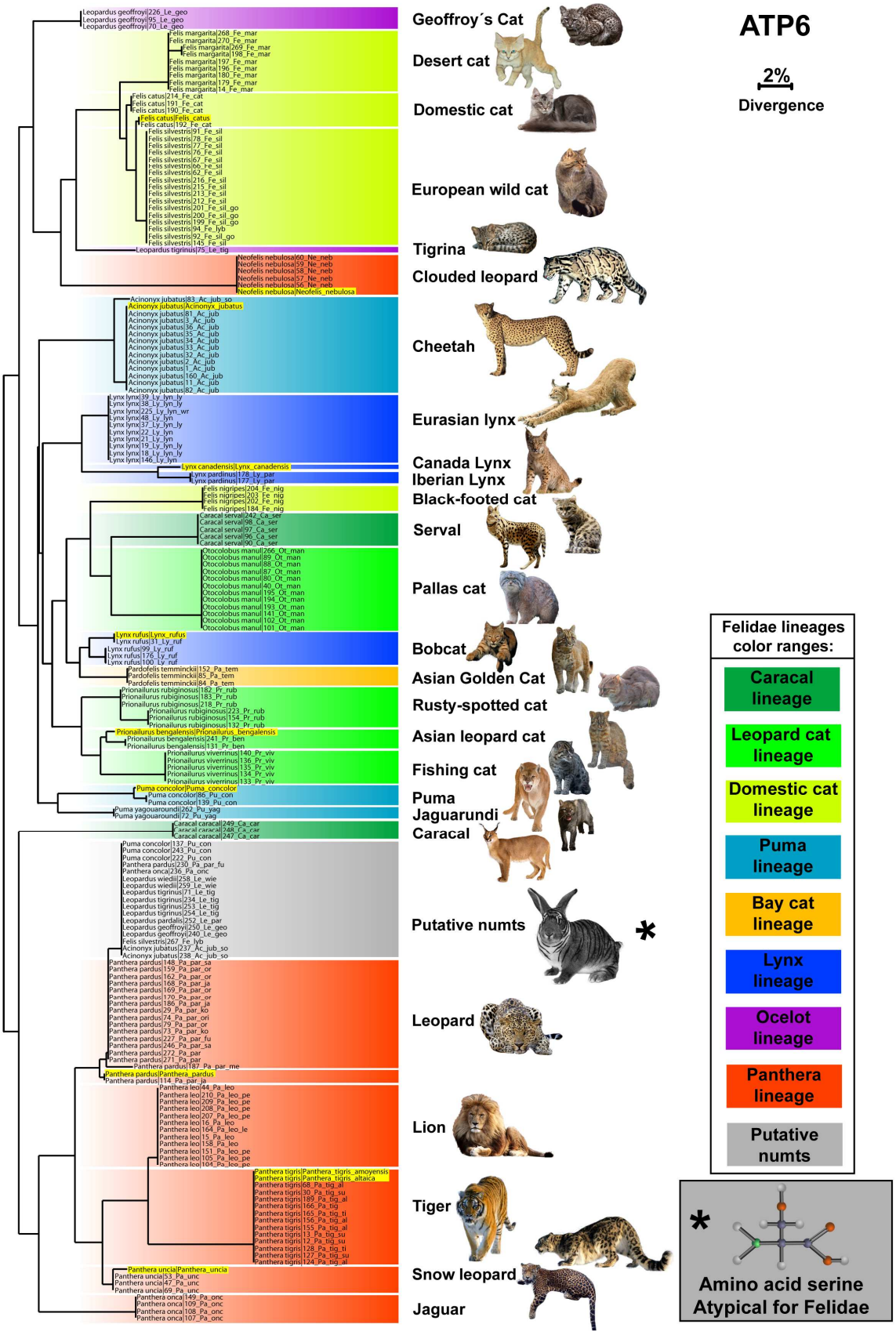

Figure 10. **ATP6 NJ tree of Felidae.** NJ tree of ATP6 sequences from 28 species in the family Felidae. Species affiliations with the respective felid lineages are highlighted with coloured boxes (according to Johsnon et al. [12]). COI cymt sequences derived from Genbank were included for comparison and are framed with a yellow box.

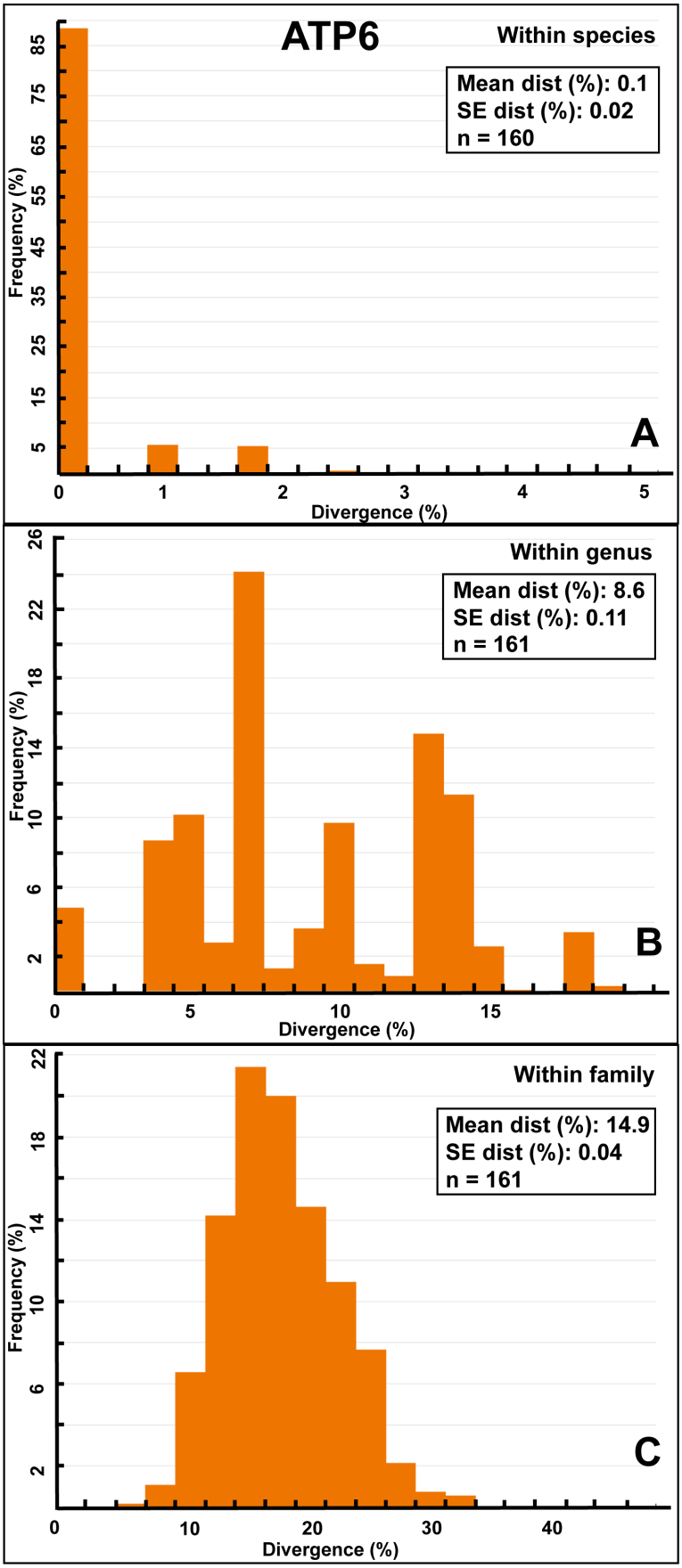

Figure 11: Pairwise comparisons of nucleotide sequence differences in ATP6 among 28 species of Felidae at various levels of taxonomic hierarchy: (A) intraspecific; (B) intragenic; (C) intergenic differences between individuals. *Putative ATP6 numts were excluded for this analysis.

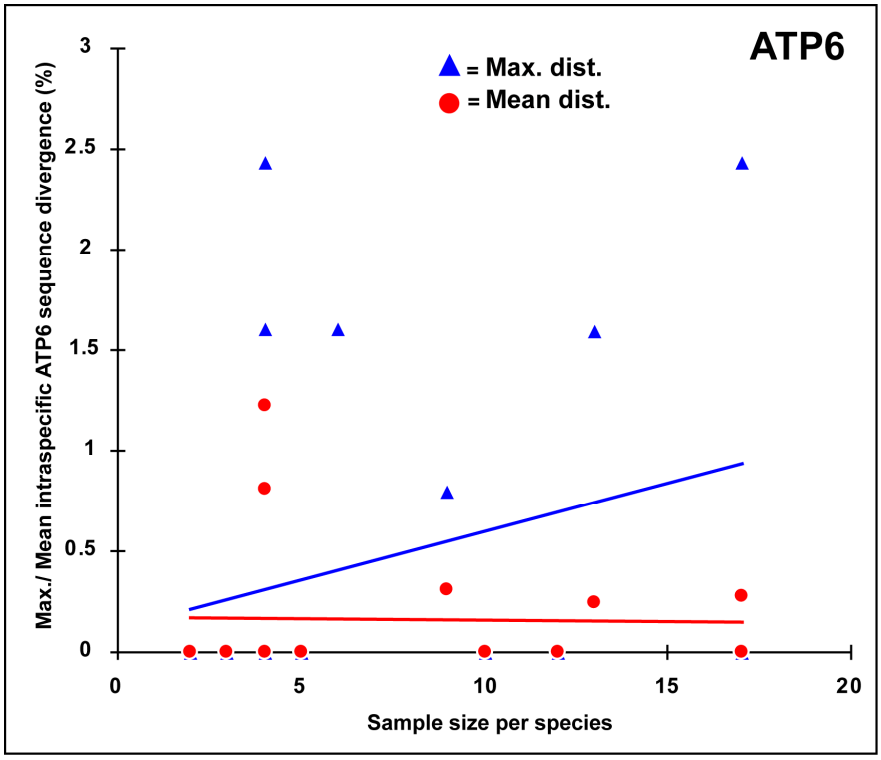

Figure 12. The relationship between maximum and mean intraspecific sequence divergence (K2P) at ATP6 and the number of individuals analysed for each species (mean dist.: R^2 = 0.000, P = 0.932; max dist.: R^2 = 0.079, P = 0.182).

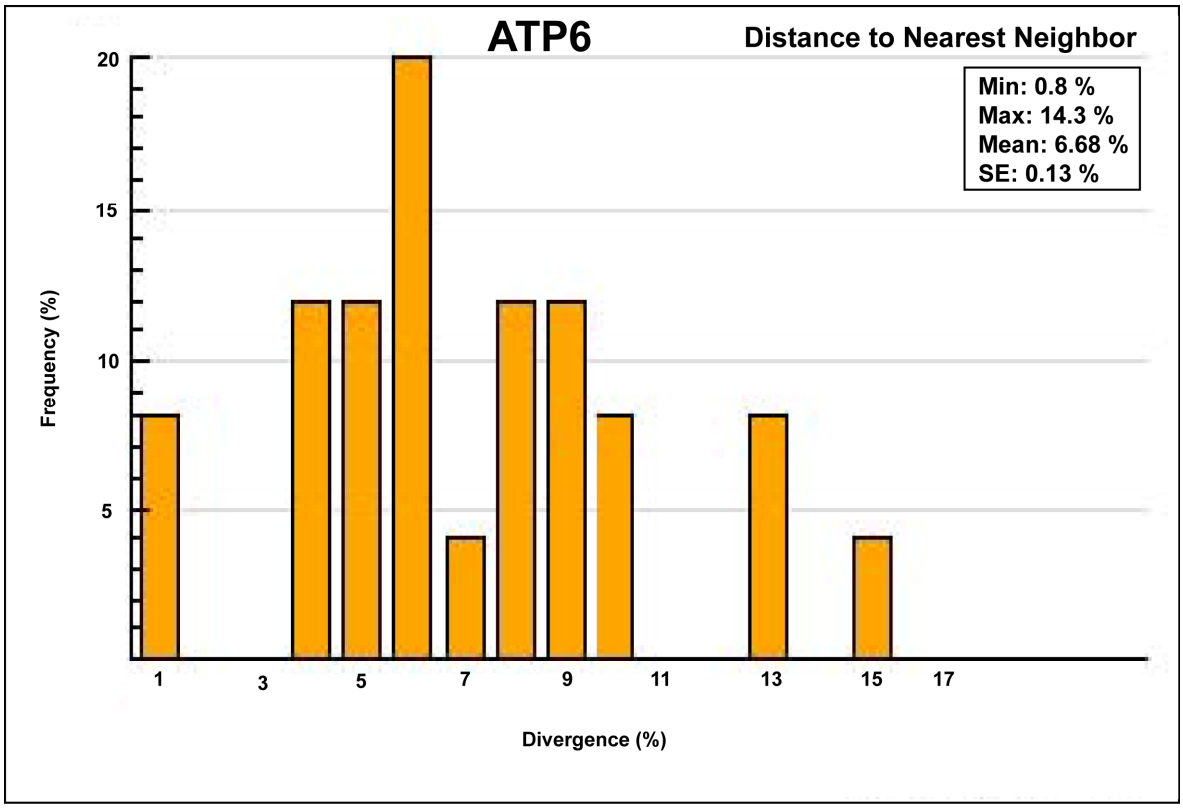

Figure 13. Histogram showing the distribution of the nearest neighbor distances for ATP6 across 23 felid species.

2.4. DISCUSSION

Amplification and sequencing of felid sample material provided 120 COI sequences and 198 ATP6 sequences. They originate from a total of 28 species for ATP6 and 23 species for COI (see Appendix 1). The sequences were generated to assess their validity as barcoding markers and to identify numt contaminations that could potentially constitute substantial challenges for reliable species identification. To date, numts in felids have been identified in two species- the tiger [46] and the domestic cat [28] (see Figure 2).

2.4.1. Characterization of numts

Among the 120 sequences generated for COI, 43 sequences of 6 species exhibited high sequence similarities with previously reported numts (see Figure 4). The amplification of numts was most likely caused by the interaction of two different factors: (i) the existence of very high numt copy numbers in the COI region of cats [51] and (ii) the use of universal Folmer primers preferentially targeting numt sequences. Numts are generally more conserved among taxa, due to slower rates of evolution in the nucleus, and can thus represent ideal binding sites for universal primers [25,32,65].

Among the 198 sequences generated for ATP6, 21 sequences of 13 species indicated putative numts (see Figure 10). Two factors most probably controlled numt amplification predominately from hair samples: (i) hair exhibit rather low mtDNA content and ATP6 primers thus most likely anneal to nuclear sequences of mitochondrial origin (numts), present in higher copy numbers [48] and (ii) the existence of high numt copy numbers in the ATP6 region of cats [51]. High copy numbers of numts homolog to the ATP6 gene region result from multiple independent numt insertions into the cat genome since the origin of Felidae approximately 10.8 MYA ago [12]. These numts are distributed across most cat chromosomes and include gene regions present (e.g. COI) and absent (e.g. ATP6) in the previous reported cat numt [28] and tiger numt [46].

2.4.2. Criteria for numt identification

For the identification of putative numts in the ATP6 and COI dataset, we applied the “anti-numt” quality control strategies suggested by Song et al. [25]. The numt identification was based on the following criteria:

2.4.2.1. COI numts

In most species, COI numt sequences could be differentiated from cymt protein coding gene sequences due to the presence of extra stop codons, insertions–deletions (indels), or frame-shift mutations (see Table 1). The COI sequences generated from lions, however, lacked these typical molecular features. Similarly, Moulton et al. [47] detected a number of COI numts without stop codons or indels, making it difficult to distinguish them from mitochondrial

orthologues. However, we could identify this COI lion numt based on its high sequence similarity (97%) with the previous reported tiger numt. The observation of shared numts in two sister species (lion and tiger) can be explained by the age of the reported tiger numt. The tiger numt diverged from cymt around 3.45 MYA ago, exactly when the *Panthera* lineage began to diverge from the common felid ancestor [46]. This means that all *Panthera* species, and hence also the lion (*Panthera leo*), exhibit a similar numt haplotype belonging to the reported tiger-numt lineage.

2.4.2.2. ATP6 numts

ATP6 numt sequences lack additional stop codons, insertions–deletions (indels), or frame-shift mutations for reliable identification (see Figure 10). ATP6 numts were hence identified by unusual amino acid changes absent from the cymt of all other Felidae. Uncommon amino acid changes were previously used by Magnacca et al. [66] to differentiate numts and cymt sequences. The unusual amino acid Serine in position 79-81bp of the ATP6 numt not only differs from the amino acid Asparagine common in cymt of all other felids but also from the amino acid Lysine typical for humans (see Figure 8). Thereby we could not only corroborate the identity of a putative ATP6 numt but also exclude an inadvertent cross-contamination with human or felid DNA.

Despite the rigorous implementation of the above mentioned criteria for numt identification, we can not fully exclude that numts remained undetected in our dataset. Many studies document the failure of numt identification and inadvertent incorporation of numts in data analysis and this certainly poses a challenge for quality control measures typically suggested for standard DNA barcoding studies (e.g. [25,37]). For example, Anthony et al. [67] and others documented not only the exclusive amplification of either numts or authentic cymt sequences but also the presence of numt recombinants (co-amplifications), where cymt and numts combine during PCR (e.g. [32,53,67,68]).

2.4.3. Tissue-specific numt amplification

Several studies documented that DNA extracted from noninvasive samples may prove particularly likely to yield numts [32,42,48]. To test whether numts are preferentially amplified from specific tissue types, barcode sequences were generated from hair, blood muscle and faeces of a single specimen.

COI sequences were obtained from a single tiger individual using four different tissues types. All sequences obtained matched with 99% identity the previous reported tiger numt [46] (Figure 3). We conclude that at least for the tiger, numt amplification cannot be excluded by tissue-type selection. Similar observations of tissue-independent numt amplification were reported for muskox by Koloktronis et al. [49]. Explanations for this phenomenon include the

high copy number of numts in the COI gene region [51,52], numt age [52,53], and universal primer use [25].

Tissue-specific numt amplification in the ATP6 gene was performed for 5 species using either blood or muscle and hair (see Figure 9). For all species tested, sequences generated from hair samples resulted in the amplification of one putative ATP6 numt haplotype. Sequences obtained from muscle and blood, however, provided the authentic cymt sequences. We conclude that for the ATP6 gene, numts are preferentially amplified from specific tissues like hair. This phenomenon has previously been reported by Greenwood et al. [48] for elephants. A possible explanation for this observation is that hair has a relatively low mtDNA content and hence numts may be preferentially retrieved over cymt by PCR [48]. Similarly, blood from birds has been observed to predominately yield numt sequences, which has been attributed to the fact that bird erythrocytes are nucleated and thus contain predominantly nuclear DNA as target for numt amplification [50]. The molecular genetic data reported here for ATP6 constitute the first report that tissue-specific numt amplification also exists in Felidae. For ATP6 the tissue specific amplification of authentic cymt DNA is considered to be dependent on the favourable ratio of mtDNA versus nuclear DNA copies [55]. Mitochondrial-rich tissues like muscle and mammalian blood, which contains anucleated red blood cells, represent a good source of mtDNA und thus enable organellar cymt DNA amplification [24,48]. However the numt age might also play an important role in tissue-specific numt amplification [52,53]. We conclude that the ATP6 numt sequence haplotype derived from hair of several felid species, must have diverged from cymt around 10 MYA ago, before the eight Felidae lineages began to diverge from the common felid ancestor. The estimated old numt age seems to be correlated with the tissue-specific numt amplification. Similar observations were made for gorillas by Chung et al. [52], who found that “phylogenetically more anciently transferred numts were amplified with a greater incidence from the gorilla faecal DNA sample than from the high-quality gorilla sample”.

Unlike for ATP6, numt amplification in the COI region of the tiger was shown to be independent of the tissue type. This is probably primarily related to the relative copy number of numts homolog to the corresponding protein-coding genes (see Figure 14). The domestic cat genome harbours more copies of independent numt insertions homolog to the COI gene versus the ATP6 gene region [51], (Figure 14). We assume that a similar distribution of numt copies (homolog to the COI gene) exists in the tiger genome based on observations made by Patterson et al. [69] for chimpanzees and humans. They found that the proportion of shared numts (that are orthologous numts present in both sister species genomes at identical loci) can be quite high (80%) for species which diverged less than 6.3 million years ago [70]. Antunes et al. [51] therefore concluded that “the domestic cat numts’s catalogue has potential utility for studies across the 38 species of the Felidae family, which originated less

than 10.8 million years ago [12].” Our observation of numt contaminations existing for both mtDNA gene regions and different felid taxa (other than domestic cat and tiger, for which numts where previously reported) confirm this hypothesis of shared numts.

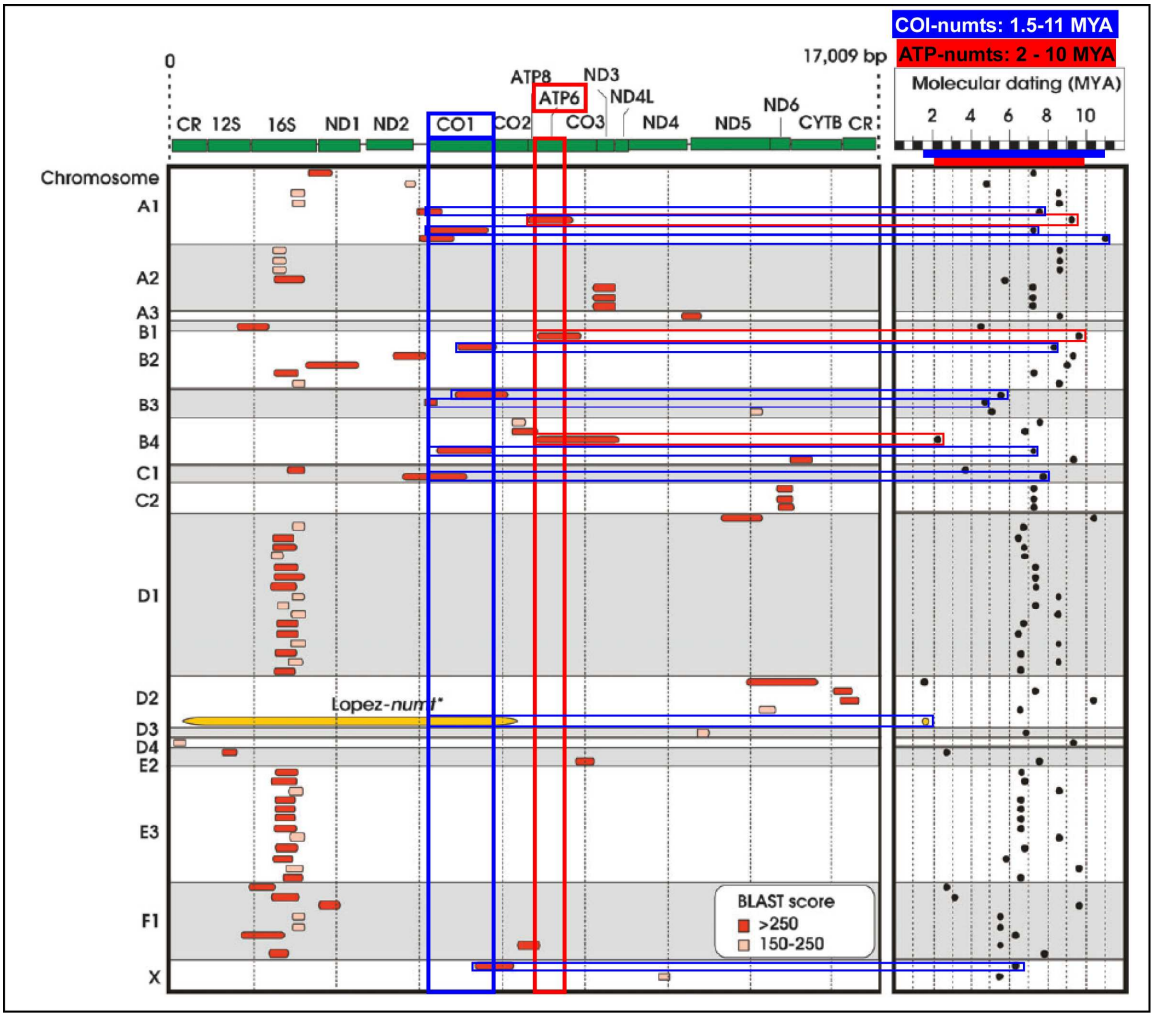

Figure 14. Numt fragments (in red/pink) are mapped onto domestic cat chromosomes. Their molecular dating (MYA—million of years ago) is given on the right side. MtDNA genes are highlighted in green. The relative position of independent numt copies within the ATP6 and COI barcode marker region is marked with a red and blue box, respectively. The Lopez-numt copy is represented in yellow. Modified after Antunes et al. [51].

2.4.4. DNA barcoding analysis with numts

The ultimate goal of the COI and ATP6 barcoding study conducted here was the identification of felid species. The current threat to Felidae imposed by humans (i.e., illegal poaching and trade), require a reliable tool for rapid molecular identification in wildlife forensic investigations. As outlined above numts constitute a potential challenge for species identification in DNA barcoding analyses. Numt contamination was also found among our sequence data sets. Moreover, our results confirm that various factors contribute to the amplification of numts such as taxon [38], gene region [51,52], individuals [48], numt age [53], universal primer use [25] and tissue-type [48-50].

Despite strong numt contamination, our analyses revealed that most individual felid taxa are characterized by unique and species diagnostic barcode sequences. The barcode sequences obtained indicate that this holds true for both ATP6 and COI (see Figure 4 and 10). As such the unique features of individual felid sequences provide a molecular database that can be used for the identification of unknown felid material for forensic applications. The central concept in forensic species identification is to match an unknown sequence of a target item to a reference sequence through DNA similarity searches (Blast search: [71]). All sequences obtained in this study constitute the felid marker reference database and will be deposited in both BOLD and NCBI sequence databases. The intraspecific variability and authenticity of individual felid species was verified by analysing multiple voucher specimens (see Figure 12). Our findings thus indicate that both authentic cymt as well as numt sequences of the COI and ATP6 gene can be used as species-diagnostic barcode markers applicable for felid forensic investigations. The few exceptional cases, where the COI and ATP6 barcode markers show less performance at species level identification, are indicated below:

The COI sequences generated so far allow the rapid and reliable identification of 21 felid species. To date, however two felid taxa are challenging. *Felis catus* and *Felis silvestris* share the same COI numt haplotype (see Figure 4), which enables generic-level assignment but not the identification of individual species. Low levels of species resolution are not a specific problem of numts. The diagnosis of species using authentic mtDNA was previously reported to be particularly difficult when species are young [72], or affected by hybridisation and introgression (e.g. [73]). Indeed, precisely these factors apply to *F. catus* (Domestic cat) and *F. silvestris* (European wild cat). The two sister species diverged less than 1 MYA ago (e.g. [12,74]) and introgressive hybridization between wild species and their domesticated relatives is a widespread phenomenon also common in these taxa (e.g. [75-77]). We conclude, that it is impossible for any mitochondrial-based barcode system, no matter whether cymt or numts, to fully resolve species identity in *F. catus* and *F. silvestris* so that supplemental analyses of one or more nuclear genes will be required (e.g. [78]). A similar situation has been reported for the differentiation of wolf and dog [79].

The ATP6 sequences generated so far allow the rapid and reliable identification of 28 felid species. To date, however amplification of ATP6 numts from hair of several felid species remains problematic. In particular, phylogenetically more anciently transferred numts, like this ATP6 numt, can be preferentially amplified from tissues like hair (e.g. [48,52]) regardless of which felid species was investigated. In wildlife forensic applications, the tissue-specific amplification of this ATP6 numt does not allow any inference about the identity of the felid species under investigation. However, a solution to this problem is either the DNA analysis of other tissues or the additional amplification of another barcode marker like the COI gene.

We conclude that in general the presence of numts can potentially compromise DNA barcoding analyses but in certain cases does not necessarily affect reliable species diagnosis. Our study demonstrates that DNA barcoding of well-documented felid taxa can be reliably performed using species diagnostic cymts and numts of the ATP6 and COI gene. This holds true even, if we cannot fully exclude unidentified numt contamination in our dataset. The availability of an existing numts catalogue for the domestic cat [51] and detailed investigation of further felid numts in this study form the basis for effective cymt-numt barcode-based species identification of Felidae in future forensic investigations.

2.5. CONCLUSIONS

The analysis of two felid DNA barcode markers leads to the following principal conclusions:

a. Felid DNA barcoding using the two mitochondrial markers ATP6 and COI is accompanied by numt contaminations. Except for a few cases, numt amplification does not constitute serious limitations for reliable identification of felids species.

b. The full extent of numts present in felids was not a priori known and varied among the selected mtDNA markers, tissue types, individuals and species.

c. In a few cases numts can potentially compromise the species-diagnostic performance of the felid mtDNA barcoding system in wildlife forensic investigations. The tissue-specific amplification of ATP6 numts in several felid species and a shared COI numt in domestic and wild cats require the analysis of additional tissue materials and nuclear markers.

AUTHOR CONTRIBUTIONS

Conceived and designed the experiments: SJP. Analyzed the data: SJP. Wrote the manuscript: SJP.

ACKNOWLEDGMENTS

I thank Bernard Misof for fruitful discussions and Claudia Etzbauer for technical assistance in the lab. I appreciate the efforts of all collaborators listed in Appendix 1, who provided biological specimens used in this study. All tissues were collected in full compliance with the Convention on International Trade in Endangered Species of Wild Fauna and Flora (CITES). Sequences will be deposited in GenBank. The animal images used for figures are derived from the internet (Appendix 3).

CHAPTER 3

3. Tracking cats: Problems with placing feline carnivores on $\delta^{18}O$, δD isoscapes

Stephanie J. Pietsch[1]*, Keith A. Hobson[2], Leonard I. Wassenaar[2] and Thomas Tütken[3]

(1) Zoologisches Forschungsmuseum Alexander Koenig, Universität Bonn, Bonn, Germany
(2) Environment Canada, Saskatoon, Saskatchewan, Canada
(3) Steinmann-Institut für Geologie, Mineralogie und Paläontologie, Universität Bonn, Bonn, Germany.

* Corresponding author: Stephanie J. Pietsch
E-mail address: feliden.zfmk@googlemail.com

This is the author's version of a work already accepted for publication in Plos One.

ABSTRACT

Background

Several felids are endangered and threatened by the illegal wildlife trade. Establishing geographic origin of tissues of endangered species is thus crucial for wildlife crime investigations and effective conservation strategies. As shown in other species, stable isotope analysis of hydrogen and oxygen in hair (δD_h, $\delta^{18}O_h$) can be used as a tool for provenance determination. However, reliably predicting the spatial distribution of δD_h and $\delta^{18}O_h$ requires confirmation from animal tissues of known origin and a detailed understanding of the isotopic routing of dietary nutrients into felid hair.

Methodology/Findings

We used coupled δD_h and $\delta^{18}O_h$ measurements from the North American bobcat (*Lynx rufus*) and puma (*Puma concolor*) with precipitation-based assignment isoscapes to test the feasibility of isotopic geo-location of Felidae. Hairs of felid and rabbit museum specimens from 75 sites across the United States and Canada were analyzed. Bobcat and puma lacked a significant correlation between H/O isotopes in hair and local waters, and also exhibited an isotopic decoupling of $\delta^{18}O_h$ and δD_h. Conversely, strong δD and $\delta^{18}O$ coupling was found for key prey, eastern cottontail rabbit (*Sylvilagus floridanus*; hair) and white-tailed deer (*Odocoileus virginianus*; collagen, bone phosphate).

Conclusions/Significance

Puma and bobcat hairs do not adhere to expected pattern of H and O isotopic variation predicted by precipitation isoscapes for North America. Thus, using bulk hair, felids cannot be placed on $\delta^{18}O$ and δD isoscapes for use in forensic investigations. The effective application of isotopes to trace the provenance of feline carnivores is likely compromised by major controls of their diet, physiology and metabolism on hair $\delta^{18}O$ and δD related to body water budgets. Controlled feeding experiments, combined with single amino acid isotope analysis of diets and hair, are needed to reveal mechanisms and physiological traits explaining why felid hair does not follow isotopic patterns demonstrated in many other taxa.

3.1. INTRODUCTION

Many carnivore species are currently threatened and are the focus of intense conservation concern [13]. Feline carnivores are often subject to illegal wildlife trade, thus the ability to estimate the geographic provenance of illegal tissue samples would constitute important information in wildlife crime investigations [11]. Probabilistic provenance determination based on O and H isotopes has strong potential to be applied to animal tissues as an investigative tool in wildlife forensic science [80-83]. Validation of isotopic methods has relevance and practical application in various fields like wildlife forensics and conservation biology.

Measurements of the stable isotopes of hydrogen (δD) and oxygen ($\delta^{18}O$) of animal keratinous tissues have been used to track the geographic origin and migratory patterns in a wide variety of animals (e.g. [80,81,84-86]). To date, this approach is based on strong empirical correlations between δD values in animal tissues (δD_t) with the isotopic composition of the amount-weighted mean annual or mean-growing season precipitation (δD_w). The latter correlates inversely with latitude and elevation across the continents, especially in North America [87-89]. Few studies have coupled δD and $\delta^{18}O$ measurements of the organic or inorganic fractions of animal tissues despite the strong covariance between these isotopes in environmental waters (hairs and nails: human [85,90-93]; CO_2, body water, hair and enamel: woodrat [94]; chitin: brine shrimp [95]; chitin: chironomids [96]; plasma, blood and feathers: birds [97,98]; fat, blood, muscle, hair and collagen: pig [99]; carbonate and phosphate tooth enamel, bone collagen, subcutaneous fat and hair: laboratory rat [100]). Strong correlations between δD_w and δD_t have been found for many species [81]. The hydrogen and oxygen isotopic composition of animal tissues (hair, feathers, teeth) is related to the isotopic composition of body water (e.g. [101-104]) and ultimately to that of ingested water. Influences on isotopic composition of body water (δD_{bw}, $\delta^{18}O_{bw}$) of animals include abiotic (climate, drinking water) and biotic (diet and physiology) factors [105-112]. The incorporation of H and O isotopes from the hydrosphere via diet and drinking water into animal tissues is a complex process and our understanding of how these mechanisms affect the nature and variability of the empirically observed relationships is still poor (e.g. [90]). However, to reliably track the geographic origin of an animal requires a detailed understanding of the metabolic routing of dietary nutrients and mechanisms of H and O isotopic incorporation into animal tissues [113].

Hydrogen and oxygen in animal tissues can be derived from two potential sources: dietary nutrients and body water, whereas oxygen is also derived from inhaled air. The body-water pool, in turn, is derived from ingested drinking-, food-, and metabolic-water produced during the catabolism of food macromolecules [105,107,109,112,114-116]. The relative

contributions of all these sources to protein synthesis (i.e. keratin and collagen) are likely to vary among animals [117-119]. Controlled experiments are key to understand and model the incorporation of H and O isotopes into proteinaceous tissues like keratins (hair and feathers), collagen, and chitin, and have so far been developed for only a small number of species like woodrat (*Neotoma cinerea* and *Neotoma stephensi*; [94]), rat (*Rattus norvegicus*; [100]), Japanese quail (*Coturnix japonica*; [101]), house sparrow (*Passer domesticus*; [98]), humans (*Homo sapiens*; [85,90-93,104]), pig (*Sus scrofa domesticus*; [99]), brine shrimp (*Artemia franciscana*; [95]) and chironomids (*Chironomus dilutus*; [96]). These studies revealed that keratin δD and $\delta^{18}O$ reflect both biological (diet, physiology) and environmental signals (water, geographic movement, climate; [90]). Deviations from a strong coupling between δD_t and δD_w, and $\delta^{18}O_t$ and $\delta^{18}O_w$ have been shown (e.g. [90,120]) and may be linked to: 1) climatic factors like relative humidity [114,121]; 2) isotopic disequilibrium of food and water contributions to δD_t [104]; 3) possible trophic-level effects on δD_t [122]; 4) impacts of metabolic rate and drinking water flux on δD_{bw} and $\delta^{18}O_{bw}$ [103,105,107,109] ($\delta^{18}O$ of phosphate ($\delta^{18}O_p$) in urinary stone [123], bone [102] and tooth [124]); and 5) dietary and physiological controls on $\delta^{18}O_h$ and δD_h of hair [90].

Previous studies that successfully applied combined δD_t and $\delta^{18}O_t$ analysis to track the geographic origin and migration of animals focused on herbivores and omnivores (e.g. [80,86,94,98,99,101]). The fact that this method performs particularly well in omnivorous modern humans [85,90-93,125] is not surprising, because humans are well-hydrated and typically consume a constant local water source (e.g. tap water: [126-128]) and consistent homogenous diet across regions (e.g. fast food: [129]). But even for humans, hydrogen isotopic incorporation during keratin synthesis likely varies between different keratinous tissues like nail and hair [130]. Free-ranging carnivores, however, differ significantly in their nutritional, physiological and metabolic characteristics from herbivores and omnivores [131,132]. The house cat, *Felis catus*, is the most thoroughly studied mammalian carnivore [131]. Felids are strict carnivores and thus obtain much of their body water from the consumption of prey [131]. Owing to the lack of empirical H/O isotope studies on strict carnivores (other than raptors) it is unclear whether carnivore hairs track the spatially predictable meteoric water signal (despite their integrative high trophic position). However, Kohn [107] hypothesized, that “carnivore bone phosphate should track the meteoric water signal more closely than do herbivores”. For this reason, the concept of geographic source determination based on H/O isotopes using carnivore hairs as an investigative tool in wildlife forensic science needs to be tested.

Here, we provided the first large-scale δD and $\delta^{18}O$ analysis of hair samples from wild individuals of two North American feline carnivores, bobcat (*Lynx rufus*) and puma (*Puma concolor*). Both species were ideally suited to test the strength of the isotope approach in

assigning geographic origins of Felidae. The availability of skins from museum collections, high-resolution precipitation $\delta^{18}O$ and δD isoscapes for North America and ecological differences between these study animals (e.g. body size, home-range size, habitat use, distribution and prey preferences) allowed us to assess the application and efficacy of H/O isotope fingerprinting for forensic spatial assignment in feline carnivores.

Our study was designed to determine whether puma and bobcat hairs varied predictably in their isotopic composition among isotopically distinct geographic locations and reflected the spatial pattern of isotopic variation in precipitation. Furthermore, we examined if species- or sex-specific effects existed, and whether these could be explained by differences in diet, body size and foraging ecology. Our results demonstrated that the application of water isotopes for provenance determination of feline carnivores was compromised by major controls of their diet, physiology and metabolism on $\delta^{18}O_h$ and δD_h. The controlling factors and possibilities to quantify these will be discussed.

3.2. MATERIALS AND METHODS

3.2.1. Study species and sampling

Eighty-eight hair samples from two North American felid species bobcat (*Lynx rufus*, n = 45) and puma (*Puma concolor*, n = 30), as well as the eastern cottontail rabbit (*Sylvilagus floridanus*, n = 13), the latter representing the preferred prey species of the bobcat, were obtained from the Smithsonian National Museum of Natural History in Washington D.C. and the Utah Museum of Natural History, Utah. Published isotope data of bone-phosphate ($\delta^{18}O_p$) and bone collagen ($\delta^{18}O_{bc}$) from white tailed deer (*Odocoileus virginianus*), constituting the major prey of the puma, were included for comparative analysis [133]. For each specimen, geographic location, sex and elevation was recorded (Table S1). All specimens studied originated from 75 different sites across the United States and Canada (Figure 1). Sample locations ranged in latitude from 25.8 to 48.2ºN and longitude from 124.4 to 65.8ºW, covering strong altitudinal (2 to 3400m) and isotopic gradients ($\delta^{18}O_{riv}$ = –17.5‰ to –0.1‰; δD_{riv} = –132.7‰ to 0.6‰).

3.2.2. Stable isotope analysis

Sample preparation and H/O isotope analysis were conducted at Environment Canada. All keratin samples were physically cleaned of adhering debris and washed twice in a 2:1 mixture of chloroform and methanol to remove lipids from the keratin surface. After cleaning, all samples were air-dried for 24h. Hair samples were then cut into 0.5cm increments (H: 350±20µg; O: 700±50µg) and weighed into pre-combusted silver foil capsules for H and O isotope ratio analysis. For δD, in order to account for exchangeable hydrogen in hair proteins, we used comparative equilibration with in-house keratin working standards,

BWB (–108‰), CFS (–147.7‰), CHS (–187‰), for which the δD value of non-exchangeable H had been previously established [134]. For $\delta^{18}O$, we used the IAEA benzoic acid standards IAEA 601 and 602, with assigned $\delta^{18}O$ values of +23.1‰ and +71.4‰, respectively. For H/O isotopic analyses, samples and reference materials were separately pyrolyzed on a Hekatech HTO elemental analyser at 1350ºC to H_2 and CO for isotopic analysis on an Isoprime™ dual-inlet isotope-ratio mass spectrometer. The reference standards were used to normalize unknown samples to the Vienna Standard Mean Ocean Water-Standard Light Antarctic Precipitation (VSMOW-SLAP) standard scale [134].

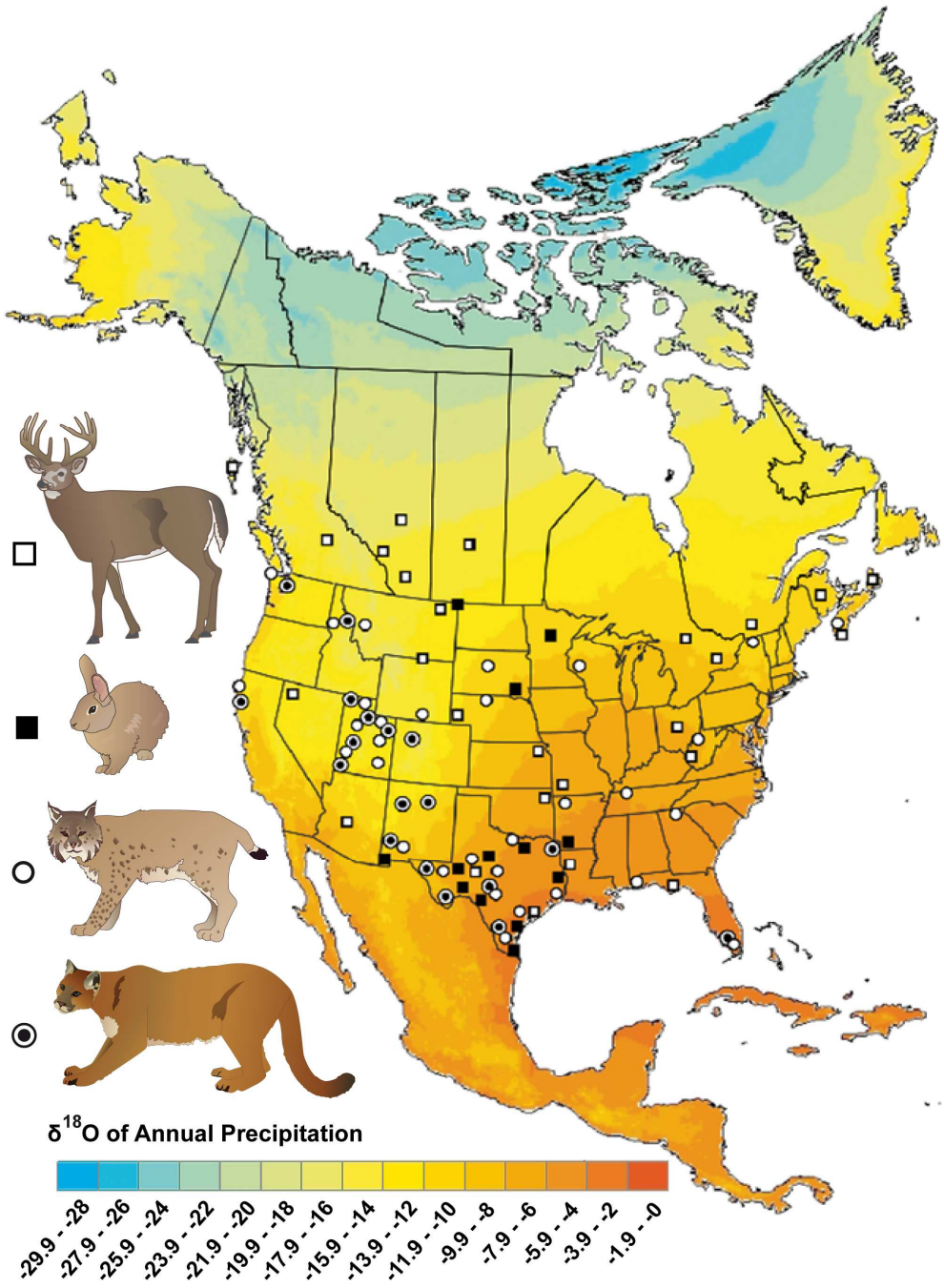

Figure 1. Map of sampling sites. Sample locations for both felines bobcat (n = 45) and puma (n = 30) as well as their preferred prey species eastern cottontail rabbit (n = 13) and white-tailed deer (n = 31,[133]), respectively, plotted on the $\delta^{18}O$ precipitation map of North America [87].

3.2.3. Estimates of drinking water isotope compositions (δD, $\delta^{18}O$)

The H and O isotopic composition of water ingested by both felid species indirectly from their prey were inferred from modelled isoscape values [135] as well as measured river water values across North America [136,137]. It was assumed that the place of death of each puma and bobcat reflected their lifetime habitat. For each locality the average δD and $\delta^{18}O$ values for precipitation were determined using the Online Isotopes in Precipitation Calculator (OIPC) version 2.2 (http://www.waterisotopes.org). The OIPC provided a model estimation of long-term annually or monthly averaged precipitation isotope ratios at specified locations through spatial modelling of a large database of precipitation isotopic data covering the time period 1960–2004 [87,135]. The δD and $\delta^{18}O$ data of the OIPC model were compared to those measured for local river waters [136,137]. In general, there was a good correlation between δD_{riv} and $\delta^{18}O_{riv}$ and δD_w and $\delta^{18}O_w$ for relatively small- to medium-sized drainage catchments (<130,000km^2) [86]. As puma and bobcats have smaller home-range sizes (female bobcat: 21.7km^2, [138,139]; female puma 175.8km^2, [138]) local river water should reflect the average δD and $\delta^{18}O$ values of ingested prey-derived drinking water. Therefore we compared the hair δD_h and $\delta^{18}O_h$ data with the river water data.

Bobcat and puma hair isotope values were plotted against amount-weighted long-term annual, spring (three months mean of March, April, May) and summer (three months mean of June, July and August) precipitation δD_w and $\delta^{18}O_w$ values, because the formation and isotopic incorporation of cat hair is limited to a rather short time period. For instance hair growth in domestic cats is not continuous [140], but rather includes an anagen phase of active growth and a telogen phase of rest [141]. The hair-growth phase takes 6-8 weeks and 70% percent of the hair follicles are in the anagen phase during the summer [142]. Isotopic signals from drinking water and prey consumed during the anagen phase of growth are most likely integrated into the growing hairs. For this reason we related the isotope values of hair δD_h and $\delta^{18}O_h$ not only to annual average δD_w and $\delta^{18}O_w$ values but also to seasonal spring and summer precipitation to test if a better relation with water isotope values of the likely main hair growing season was obtained (Table S2).

3.2.4. Statistical analysis

First, we analysed the H and O isotopic variation of puma and bobcat hairs among locations and their correlation with the large-scale patterns of isotopic variation in precipitation. We tested whether the correlations significantly changed when using the annual and summer modelled precipitation or local river water data (Table S2). We compared hair H and O isotope data of predators and respective prey species and tried to establish a calibration equation between river water and hair for a feline carnivore. Relationships between mean annual $\delta^{18}O_{riv}$, δD_{riv} and $\delta^{18}O_h$, δD_h of puma, bobcat and rabbit

hairs were investigated using linear regressions (Figure 2 and 3). We also examined the relationship between $\delta^{18}O_h$ and δD_h (Figure 4). The effects of species, age, sex, seasonal precipitation and relative humidity on hair isotope values were examined using a General Linear Model (GLM) (Table S2). Statistical tests were conducted using XLSTAT (V 7.5.2).

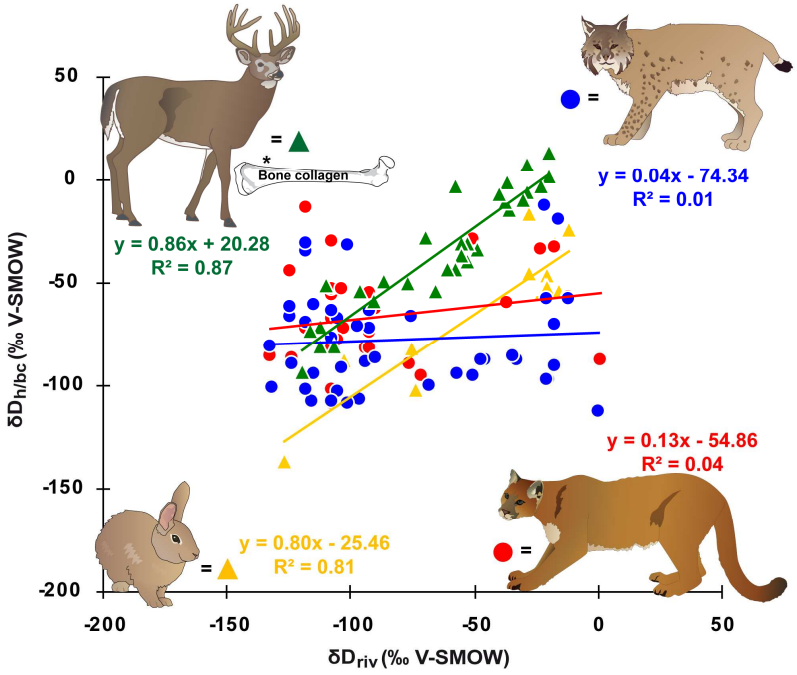

Figure 2. Hydrogen isotope values of keratin relative to river water. Plot of δD of hair (δD_h) from bobcat, puma and eastern cottontail rabbit as well as bone collagen (δD_{bc}) from white-tailed deer [133] vs. mean annual δD of river water (δD_{riv}).

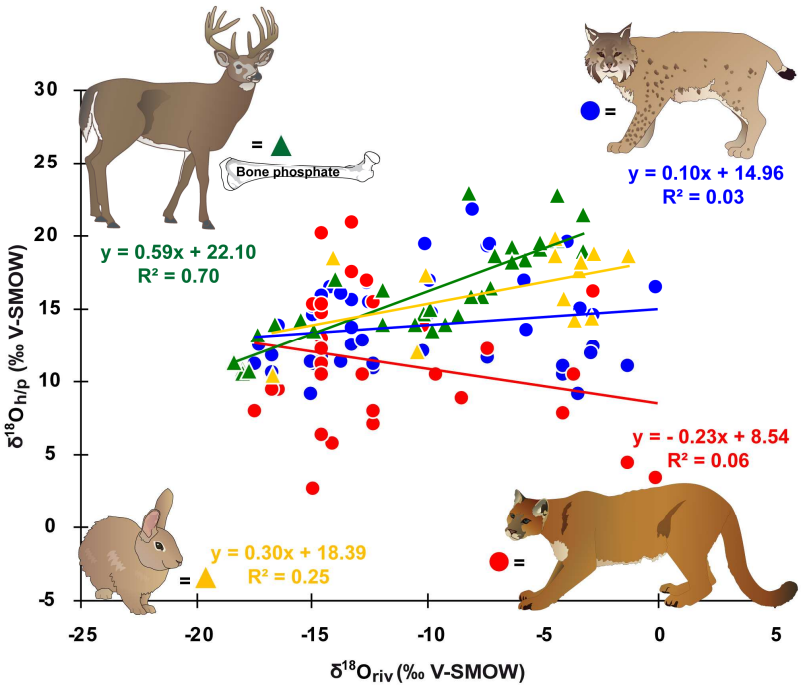

Figure 3. Oxygen isotope values of keratin relative to river water. Plot of $\delta^{18}O$ of hair ($\delta^{18}O_h$) from bobcat, puma and eastern cottontail rabbit and bone phosphate ($\delta^{18}O_p$) from white-tailed deer [133] vs. mean annual $\delta^{18}O$ of river water ($\delta^{18}O_{riv}$).

3.3. RESULTS

All hair δD_h and $\delta^{18}O_h$ values were plotted against mean annual δD_{riv} and $\delta^{18}O_{riv}$ values because using either amount-weighted mean annual, summer (June, July and August) or spring (March, April and May) OIPC modelled precipitation values did not significantly change the results (Table S2). The $\delta^{18}O_h$ - $\delta^{18}O_w$ correlation of bobcats was slightly improved by including relative humidity in the regression (R^2 = 0.21, p = 0.01, n = 44). Relative humidity did show a significant modest effect on $\delta^{18}O_h$ of bobcats (R^2 = 0.21, p = 0.002, n = 44) but no effect on $\delta^{18}O_h$ of puma (R^2 = 0.00, p = 0.818, n = 30). Relative humidity, however, did not affect δD_h of bobcats (R^2 = 0.05, p = 0.146, n = 44) and puma (R^2 = 0.068, p = 0.164, n = 30) (Table S2). The isotope composition of the analyzed hair samples spanned a range of 99.3 ‰ for δD_h and 12.6 ‰ for $\delta^{18}O_h$ in bobcat, and 95.4 ‰ for δD_h, and 18.2 ‰ for $\delta^{18}O_h$ in puma (Figures 2 and 3). No significant relationship was found between δD_h and δD_{riv} for both species (bobcat: R^2 = 0.005, p = 0.65, n = 44; puma: R^2 = 0.040, p = 0.291, n = 30) (Figure 2). Likewise $\delta^{18}O_h$ and $\delta^{18}O_{riv}$ were not significantly correlated (bobcat: R^2 = 0.030, p = 0.261, n = 44; puma: R^2= 0.055, p = 0.211, n = 30) (Figure 3). No effect of sex on the isotopic relationship between hair and water was observed for both species (Table S2). There was a weak correlation between δD_h and $\delta^{18}O_h$ values of the same hair samples in bobcat (R^2 = 0.195, p = 0.003, n = 43) but not in puma (R^2 = 0.0002, p = 0.939, n = 30) (Figure 4).

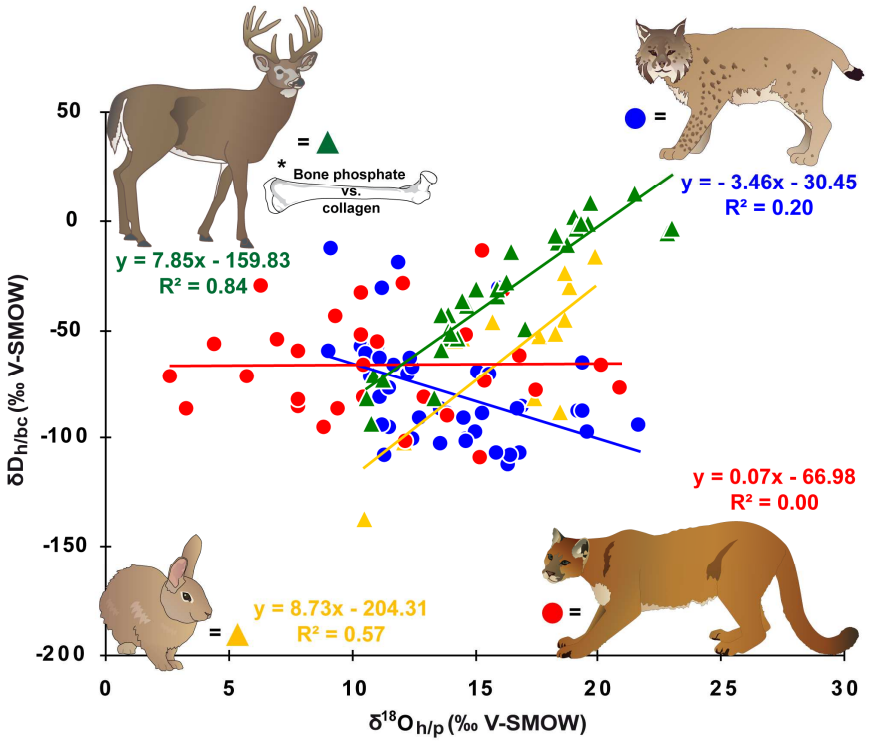

Figure 4. Hydrogen and oxygen isotope ratios of keratin. Hydrogen and oxygen isotope compositions are shown for hair samples (δD_h, $\delta^{18}O_h$) from puma, bobcat and eastern cottontail rabbit as well as collagen (δD_{bc}) and bone phosphate ($\delta^{18}O_p$) data from white-tailed deer [133].

Results for the hair isotope compositions of cottontail rabbits exhibited a strong δD_h–δD_{riv} (δD_h: $R^2 = 0.81$, $p < 0.0001$, $n = 13$) and a moderate $\delta^{18}O_h$ – $\delta^{18}O_{riv}$ ($\delta^{18}O_h$: $R^2 = 0.25$, $p = 0.083$, $n = 13$) positive relationship (Figures 2 and 3). The eastern cottontail rabbits also displayed a significant positive correlation between δD_h and $\delta^{18}O_h$ values of the same hair samples ($R^2 = 0.571$, $p = 0.003$, $n = 13$) (Figure 4).

3.4. DISCUSSION

Both puma and bobcat lacked the expected correlation between water isotopes in local water and hair, and also exhibited a complete decoupling between $\delta^{18}O_h$ and δD_h. This finding contrasted strongly with results from numerous previously published studies on keratin tissues of omnivores and herbivores. Hence, tracing the provenance of feline carnivores such as puma and bobcat based on $\delta^{18}O_h$ and δD_h isoscapes does not appear to be possible, as individuals could not be reliably placed on $\delta^{18}O_w$ and δD_w maps. Potential explanations for this lack of correlation between hair and ambient water isotope compositions are discussed below.

3.4.1. Can relative humidity affect carnivore $\delta^{18}O_h$ and δD_h?

In our study, relative humidity showed a significant modest effect on $\delta^{18}O_h$ of bobcats ($R^2 = 0.21$, $p = 0.002$) but not on puma ($R^2 = 0.00$, $p = 0.818$) (Table S2). Previous studies on mammalian bone phosphate showed that relative humidity controls the $\delta^{18}O_p$ values of herbivore species with low drinking water requirements (e.g. [107]). For example, $\delta^{18}O_p$ values of Australian macropods [114], rabbits and hares [121] have been shown to correlate strongly with changes in relative humidity independent of $\delta^{18}O_w$, whereas the $\delta^{18}O_p$ of North American deer [115] were influenced by both relative humidity and $\delta^{18}O_w$. Low humidity increases the rate of evaporation of surface water and evapotranspiration of leaf- and grass-water and thus leads to oxygen isotopic enrichment effects in plants [143,144]. Drought-tolerant animals who obtain most of their water from plants thus reflect levels of environmental humidity, in particular their $\delta^{18}O_p$ increases with decreasing relative humidity. However, Kohn [107] hypothesized that the importance of relative humidity diminishes with increasing trophic level. Our data support Kohn's hypothesis that predators are less controlled by relative humidity than herbivores. Bobcat $\delta^{18}O_h$ compositions were weakly affected by relative humidity ($R^2 = 0.21$, $p = 0.002$), most likely because they prey upon rabbits, whose $\delta^{18}O_p$ compositions are humidity dependent ($R^2 = 0.86$; [121]). In contrast, puma $\delta^{18}O_h$ compositions were not influenced by relative humidity ($R^2 = 0.00$, $p = 0.818$), probably because they feed on white-tailed deer, whose $\delta^{18}O_p$ is affected by both relative humidity and $\delta^{18}O_w$ [115]. Unlike oxygen isotopes, δD_h values of both feline carnivores were not influenced by relative humidity (bobcat: $R^2 = 0.05$, $p = 0.15$; puma: $R^2 = 0.07$, $p = 0.16$).

Similar observations were made for δD_{bc} (bone collagen) of white-tailed deer by Cormie et al. [145]. We conclude that relative humidity particularly affects $\delta^{18}O_t$ of predators (e.g. bobcats) that feed on drought -tolerant herbivore species like rabbits. However, relative humidity did not explain the lack of a correlation between δD_h - $\delta^{18}O_h$ observed in both felids we studied.

3.4.2. Does an isotopic disequilibrium between food and water affect δD_h?

It was documented previously [90,104], that δD_h is not well correlated with δD_w, if (i) ingested food or water sources (e.g. exotic foods, marine-based diet, high altitude food or snow melt drinking water) are not isotopically related to local meteoric water and/or (ii) migration between isotopically distinct habitats takes place. We tested whether the ingested food sources (i.e. key prey species) of bobcat and puma were in disequilibrium with δD_w, and so caused the lack of a correlation between H/O isotopes in precipitation and those in felid hair. In North America, the preferred prey species of puma is the white-tailed deer (*Odocoileus virginianus*) [146], whose $\delta^{18}O$ of bone phosphate ($\delta^{18}O_p$) [115] and δD bone collagen values (δD_{bc}) [133] strongly correlate with $\delta^{18}O_w$ and δD_w, respectively (Figure 2 and 3). In contrast, bobcats mainly prey on lagomorphs [147], whose $\delta^{18}O_h$ and δD_h values we also found to show a direct relationship with $\delta^{18}O_w$ and δD_w (Figure 2 and 3). Thus the oxygen and hydrogen isotopic composition of prey are not reflected in the hair of their respective predators. Cats are not obligate drinkers [148] and hence isotopic content of drinking water does not explain the lack of a correlation between δD_w and δD_h in felines.

Migration between isotopically distinct biomes during biosynthesis of hair might also affect the correlation of δD_h with δD_w. We would have expected this effect based on potential species- or sex-specific behavioural differences characterizing our study species. Puma and bobcat, for instance, have significantly different home range sizes [11,149], which are also known to vary between seasons and sex. Although carnivores exhibit typical mammalian dispersal behaviour, where males disperse and females are philopatric [150]; we did however not observe an effect of sex on the hair/water isotope correlation for both carnivore species (Table S2). We therefore concluded that the isotopic disequilibrium of food and water does not explain the lack of a relationship between δD_h and δD_w observed in puma and bobcats.

3.4.3. Does a carnivorous diet affect δD_h?

Some studies have suggested a dietary trophic-level effect on H isotope systematics of animal tissues [90,119,122,151,152]. Possibly, high levels of animal protein consumption leads to a decoupling of δD in keratins from δD_w and a deviation from the mean relationship between keratin δD and $\delta^{18}O$ [122,153]. Diet may thus represent a confounding factor in the use of H and O isotopes for geographic tracking [90].

We developed a simple model of hydrogen isotope incorporation in carnivores to illustrate possible trophic-level enrichment and isotopic decoupling of δD_h in carnivores. Various fractionation factors and source pools contributing to non-exchangeable hydrogen in hair were considered (Figure 5). Controlled experiments on domestic cats have shown that, on average, only 1% of their total water input originates from drinking water [148]. So, drinking water likely has minor control on deuterium enrichment in felids, leaving the isotopic input of prey as a major determinant of the isotopic signature of carnivore body water.

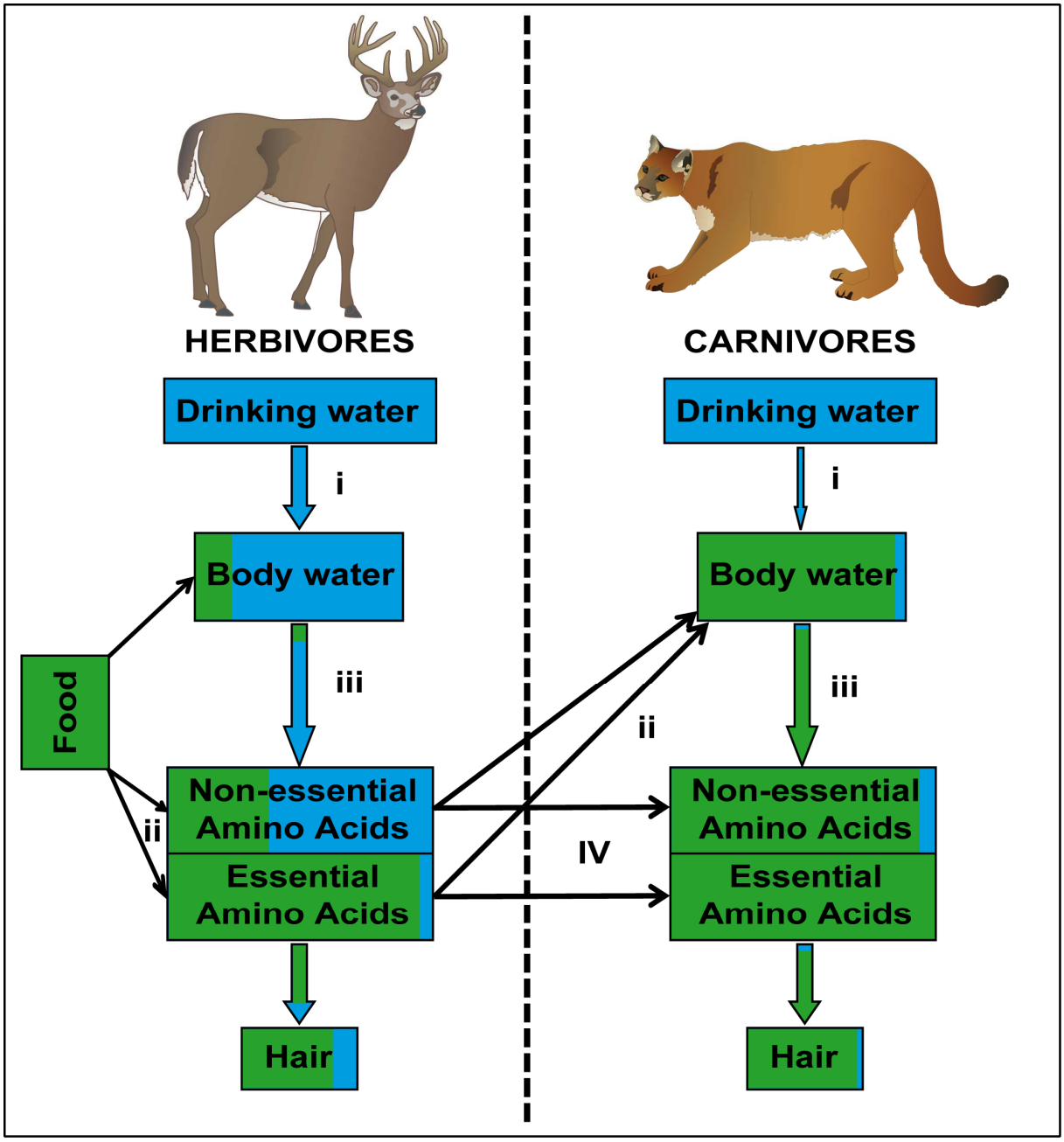

Figure 5. Hydrogen isotope model of herbivores and carnivores. Model of hydrogen isotope physiology and the contribution of food and water to non-exchangeable hydrogen in the hair of herbivores and carnivores. Letters represent processes where isotope fractionation occurs (see text for detailed discussion). Blue colouring represents water inputs and green food inputs.

In this aspect, strict carnivores differ significantly from herbivores and omnivores, whose body water is to a large extent (64 – 80%, see Table 1) obtained from drinking water (Figure 5(i)). Isotope fractionation from drinking water to body water occurs [112,119,154] and may play an important role in δD_h enrichment of carnivore proteins. Feline carnivores consume prey species whose δD_{bw} and $\delta^{18}O_{bw}$ are expected to be higher than δD_w and $\delta^{18}O_w$ due to evaporative enrichment from insensible water loss through skin and breath vapour loss [111,155]. Consequently, carnivores mainly consuming deuterium-enriched prey should have higher δD_{bw} values over those of their prey. A similar process has been documented in humans for the consumption of cow milk and the resulting enrichment in deuterium of consumer tissue [119,156]. Otherwise the consumption of D-depleted prey might decrease the carnivore δD_{bw} values particularly during winter when prey species have built up their body fat reserves. Fat reserves are known to have significantly more negative δD values than proteinaceous tissues [101,153,157,158]. The temporary alternation of D-depleted and -enriched carnivore diets relative to δD_w, based on differential seasonal consumption of lipids and proteins, respectively, might change the δD_{bw} [112] and is finally recorded in δD_h during carnivore hair growth [159].

Table 1. Food and drinking water inputs of hydrogen in the body water of different organisms under laboratory conditions.

Species	Food (%)	Drinking water (%)	Reference
Lab rats	37	64	[160]
Woodrats	29	71	[94]
Doves	15	85	[110]
Humans	20	80	[111]
European roe deer	24	76	[161]

Hydrogen isotope fractionation can also occur during the oxidation of food to form body water (see Figure 5 (ii)). Carnivores have the ability to digest and utilize high levels of dietary fat and protein and so produce relatively higher levels of metabolic water [131,162,163]. Catabolism of macronutrients and production of metabolic water could cause hydrogen isotope fractionation processes leading to deuterium enrichment [112,118]. In addition, isotopic fractionation most likely happens during the incorporation of body water into tissue amino acids (see Figure 5 (iii)). Water from food, drinking water and metabolism are the three source pools which can be fixed into newly synthesized non-essential amino acids [90].

However, the fraction of hydrogen fixed into amino acids may scale with the extent of non-essential amino acid synthesis in the body. This, in turn, is related to the level and amino acid composition of dietary protein intake [164]. Carnivores exhibit low levels of non-essential amino acid synthesis because their natural meat-rich diet contains all required amino acids [165]. Consequently, low levels of hydrogen fixed into amino acids in vivo could maximize the transfer of hydrogen from diet to hair thereby enhancing the contribution of isotopically heavy, prey-derived hydrogen in carnivore hair [90]. Finally, it is also possible that isotope fractionation occurs during the transfer of food amino acids to tissue amino acids (Figure 5 (iv)). δD_h enrichment of carnivore proteins could also occur through selective catabolism of isotopically lighter amino acids [122]. We conclude that there are several possible isotopic fractionation steps during the metabolic incorporation of hydrogen into carnivore hair that could induce enrichment in deuterium and leading to higher δD_h and a loss of correlation with δD_w.

3.4.4. Effects of carnivore physiology and metabolism on δD_h and $\delta^{18}O_h$

If diet rather than drinking water solely controls carnivore δD, we would have expected a variation of the hair/water regression in slope and intercept compared to herbivores and omnivores. Because there was no significant correlation between oxygen and hydrogen isotope compositions of hair and precipitation and δD_h and $\delta^{18}O_h$, we therefore suspected the dietary trophic-level effect was potentially obscured by physiological and metabolic adaptations in carnivores [166]. Animals which display deviations from the normal covariance between δD and $\delta^{18}O$ values in keratin are carnivorous fish, birds and mammals [122] and ancient human populations with a meat-rich diet [90,119,151], which all consume high levels of animal protein and fat. From a purely nutritional perspective, they are all strict carnivores. Through evolution, their adherence to a specialized meat-rich diet induced changes in their metabolic pathways and nutritional requirements [131]. These physiological and metabolic adaptations in strict carnivores could considerably affect the H and O isotope systematics of their keratins.

The H and O isotope compositions of human hair strongly covary, and are closely related to meteoric (drinking) water at the place of residence [85] with the exception of mid 20th century Inuit people [90]. Bowen et al. [90] did not find strong support for ubiquitous effects on the H/O isotope systematics of human hair related to physiological adaptations. However, in pre-globalization times, the typical diet of the Inuit contained high levels of dietary protein and fat from high trophic-level marine animals [167]. Mid 20th century Inuit people thus fed at the highest trophic level of all humans. Since marine food webs have typically longer chain lengths than terrestrial food webs [168], the consumption of marine predators may confer a trophic-level enrichment of Inuit δD_h [90]. Historic Inuit are also classified as obligate

carnivores among omnivorous humans because they require nutrients that are present only in animal tissue of their diet [169] and so differ from other ancient humans who used a marine-dominated but omnivorous diet like the Ainu from Japan and Thai from Thailand [90].

Measurements of δD in feathers have been successfully applied in many bird species to estimate the origins of migrating and wintering individuals [113]. However, in strictly carnivorous raptors like Amur Falcons (*Falco amurensis*; [170]) and Cooper's Hawks (*Accipiter cooperii*; [171]) the linkage between feather δD and δD_w was weaker [86,172]. However, this may be complicated due to the fact that several raptors grow feathers during periods of high work associated with breeding and so may produce more deuterium enriched feathers due to evaporative water loss.

The natural diet of wild felids contains a high proportion of the energy as protein, a variable percentage as fat and a very low percentage as carbohydrate [132]. Metabolic adaptations mainly concern the loss of anabolic pathways required for the synthesis of nutrients universally present in their natural meat-based diet [173]. One of the most striking aspects here is that strict carnivores have lost the ability to produce metabolic compounds that are commonly synthesized by virtually all herbivores and omnivores. For example, cats lack the enzymatic machinery to synthesize some amino and fatty acids, thereby significantly increasing their basal requirement for proteins and essential amino acids. When ingesting prey, wild cats avoid consuming plant materials contained in the intestines [166] and hence the digestion of dietary starches and sugars has adapted to low carbohydrate intake [174].

Currently we lack a testable explanation for our observed and confounding isotopic patterns, but considering the unique felid physiology, we hypothesized that the food metabolism of strict carnivores may exert a vital effect particularly on δD_h. This may also affect the relative contributions of all sources to protein synthesis and hair formation. Recent findings from Pecquerie et al. [118] support our hypothesis. They propose two mechanisms involved in stable isotope fractionation during metabolic reactions: First, the selection of molecules for the anabolic or the catabolic pathway routes depends on their isotopic composition. Second, the concept of atom recombination recognizes that molecules are not completely disassembled into elements during chemical reactions [175]. A non-random allocation of atoms of a particular substrate (e.g. food amino acids) to a particular product (e.g. keratin amino acids) impacts isotopic composition of a given product (e.g. hair). While isotope fractionation takes place in metabolic reactions [118], these were particularly modified during the evolutionary history of carnivores. Knowing that approximately two thirds of the hydrogen in human hair is derived from food [104], we suspect that carnivores might be affected by alternate modes of isotopic routing of macronutrients into hair (Table 2).

Table 2. Food and drinking water inputs of hydrogen in hair and feathers of different organisms.

Species	Food (%)	Drinking water (%)	Reference
Woodrats	75	25	[94]
Japanese quail	74 – 69	26 – 32	[101]
House sparrow	82	18	[98]
Humans	69, 64[a], 73[b]	31, 36[a], 27[b]	[104]

[a] Data after [92]; [b] Data after [85]

The water metabolism in feline carnivores also differs from herbivores and omnivores. Cats drink to a limited extent [132,162] and excrete concentrated urine [176-178]. In addition they produce relatively high levels of metabolic water, which contributes on average 10% to their total water intake [131,162]. Drinking water volume, however, exerts a significant physiological control on the isotopic composition of hydrogen and oxygen in human body water [103] (Table 1). Besides various water conservation adaptations, strict carnivores have higher basal metabolic rates than other mammals [179,180]. A high metabolic rate associated with a low rate of drinking, results in a weak correlation of $\delta^{18}O_p$ with $\delta^{18}O_w$ [102]. We infer that this applies to strict carnivores and assumed that relatively smaller contributions of oxygen in carnivore hair originate from drinking water. In addition, cats lose water primarily through panting [181] vs. from sweat glands of foot pads [182]. Differences in the isotope compositions of liquid water during sweating vs. vapour during panting should affect their body isotopic compositions. Panting animals should thus have higher $\delta^{18}O_{bw}$ and $\delta^{18}O_h$ values than animals that sweat because water vapour lost in panting is more depleted in ^{18}O [107,183]. The same should apply to δD_{bw} and δD_h.

In contrast to the weak correlation between feline carnivore hairs δD_h and $\delta^{18}O_h$ and meteoric water $\delta^{18}O_w$ and δD_w (Figures 2 and 3), a good correlation between claw δD_c and δD_w was observed in a recently published study of migrating pumas in the USA [83]. The reason why the two keratinous tissues do not reflect meteoric water values in the same way remains unclear. However, a similar paradox is known for human fingernails and hair, with nails displaying a more variable H/O isotope composition and a comparatively weaker correlation between δD_c and δD_w ($R^2 = 0.6$) compared to hair ($R^2 = 0.9$) from the same individuals [91,130]. The reverse trend in feline carnivores may result from different formation rates of hairs [140] and nails [184], alternate modes of isotopic routing of macronutrients into hair and nail as well as different amino acid compositions of hair and nail [185].

3.4.5. Amino acid composition of cat hair

The isotopic values of keratins are generally defined by the isotopic composition of their constituent amino acids [185]. For example, cysteine, serine and glutamate, all non-essential, metabolically active amino acids are present at very high proportions in hair [186]. Their isotopic composition reflects both food and drinking water, with a slight bias towards food. Due to the high relative abundance of non-essential amino acids, their isotope composition can often dominate the bulk H and O isotope hair signature and mask the isotope composition from essential amino acids. The latter are present at lower proportions and routed directly from dietary sources [187]. The constancy of amino acid composition and hence isotopic values between tissues, even for related proteins like nail and hair, cannot be implied [185]. Large isotopic differences between amino acids of different components have been observed [188-190], reflecting their formation via different metabolic, synthetic and catabolic processes. However, the amino acid composition of cat hair protein is comparable with that of dog, horse, sheep and human hair [186]. Apparently only the proline content of cat hair protein appears to be lower and glycine appears to be higher than in the other species [186]. Variations in amino acid composition of cat hair might thus be responsible for some of the differences in isotopic patterns we have observed.

3.4.6. Does tanning of museum skins have an effect on the H/O isotopic composition of hairs?

To our knowledge this is the first H/O isotope study on mammal hair which benefits from large museum collections as a valuable source of sample material. However, it has not been assessed whether the tanning process used for preserving hides affects the H/O isotopic composition of taxidermy skins. Tanning chemicals are intended to stop deterioration processes of the skin. At a molecular level tanning chemicals act as solid spacers, which replace the H bonds linking the polypeptide chains of the collagen fiber and thus stabilize the collagen structure of museum skins [191]. Collagen and hair are both proteinaceous tissues and interpeptide H-bonding is abundant and important for maintaining the alpha-helical structure of collagen and hair [192]. Thus, tanning chemicals could potentially alter the non-exchangeable H isotope composition of hairs. However, we hypothesize that tanning chemicals did not affect the H/O isotopic composition of the analyzed felid hairs. First, the rabbit hairs which have most likely undergone the same tanning process as felid hides, showed good isotopic (δD_h and $\delta^{18}O_h$) correlation between hair and meteoric waters (Figure 2 and 3). Second, initial results from a small “before and after tanning experiment” using a common mineral tanning technique (aluminium salts [193]) on hairs from different mammal species indicated that there was no significant effect of the tanning process on the H isotopic values of these hair samples (data not shown).

3.5. CONCLUSIONS

Stable isotope (H, O) data from bobcat and puma hairs from a range of locations across North America revealed that feline carnivores cannot be placed on $\delta^{18}O$ and δD isoscapes for forensic investigation purposes. The effective application of water isoscapes for geographic source determination of feline carnivores is most likely compromised by major controls of their diet, physiology and metabolism on $\delta^{18}O_h$ and δD_h. However, we noted that the integration of H and O isotopes into animal proteins in general remains poorly understood. Isotope fractionation and routing during metabolic and tissue formation processes is complex and presumably varies between herbivores, omnivores and carnivores. Significant research thus remains to be performed to characterize the precise origin and sensitivities of the observed isotope signals. Controlled feeding experiments on strict carnivores like domestic cats are now needed to track isotope routing of macronutrients and their incorporation into different tissue types (e.g. [94,101]). With the objective to enhance the resolution of H and O isotope analysis of proteins, we suggest compound-specific single amino acid isotope analysis may give improved insights into isotope fractionation processes during protein, and by a comparative isotope analysis of essential versus non-essential amino acids. To date most studies have used bulk tissue protein isotopic values of hydrogen and oxygen [85,90,97] but little research has been conducted at the level of single amino acids in hair that was limited to C, N and S isotopes [194-196]. Unfortunately, there are no reported applications of hair $\delta^{18}O$ and δD compound-specific isotope analysis of amino acids. This represents an important area of future research and will contribute to a better understanding of the observed variations in bulk protein H and O isotope ratios.

AUTHOR CONTRIBUTIONS

Conceived and designed the experiments: SJP, TT. Analyzed the data: SJP. Wrote the paper: SJP, KAH, LIW, TT. Conducted stable isotope assays: LIW.

ACKNOWLEDGMENTS

We thank Robert Fischer and Suzanne C. Peurach from the mammal collection at the Smithsonian Natural History Museum in Washington D.C., Eric A. Rickart from the Utah Museum of Natural History, and Bryan T. Hamilton from the Great Basin National Park in Nevada for their assistance with the sample collection. We thank Aurélien Bernard and Jürgen Hummel for their constructive and helpful comments. We also thank David Soto for his assistance with the stable isotope assays. The animal symbols used for figures are courtesy of the Integration and Application Network (www.ian.umces.edu/symbols), University of Maryland Center for Environmental Science.

CHAPTER 4

4. Oxygen isotope composition of North American bobcat and puma bone phosphate: Implications for provenance and climate reconstruction

Stephanie J. Pietsch[1]* and Thomas Tütken[2]

(1) Zoologisches Forschungsmuseum Alexander Koenig, Universität Bonn, Bonn, Germany
(2) Steinmann-Institut für Geologie, Mineralogie und Paläontologie, Universität Bonn, Bonn, Germany.

* Corresponding author: Stephanie J. Pietsch
E-mail address: feliden.zfmk@googlemail.com

This is the author's version of a work prepared for submission to the Journal of Applied Ecology.

ABSTRACT

Background

Feline carnivores are threatened and particularly affected by illegal wildlife trade. Tracing unknown tissues to the origin via stable isotope analysis would hence constitute important information in wildlife crime investigations. The oxygen isotope composition of mammalian skeletal phosphate ($\delta^{18}O_p$) can be used as a proxy for animal provenance and migratory patterns in paleontological, archaeological, ecological and wildlife forensics applications. Terrestrial mammals are generally characterized by a constant oxygen isotope fractionation between meteoric water ($\delta^{18}O_w$) and bone phosphate ($\delta^{18}O_p$) but deviations have been documented for some species. Carnivore $\delta^{18}O_p$ values are considered to be potentially promising proxies for meteoric water ($\delta^{18}O_w$) but far little work has been done on carnivores and none on felids.

Methodology/Findings

We analysed the oxygen isotopic variation of North American puma (*Puma concolor*) and bobcat (*Lynx rufus*) bone phosphate ($\delta^{18}O_p$) and their correlation with the pattern of oxygen isotopic variation in precipitation ($\delta^{18}O_w$) to test the performance of isotopic provenancing in Felidae. Bone samples of felid museum specimens originating from 107 locations across the United States, Canada and Mexico were analyzed. The feline carnivore $\delta^{18}O_p$ - $\delta^{18}O_w$ regressions were determined and compared with those from their respective prey species (deer and rabbit), another carnivore (fox) and other placental mammals. The effects of species, sex and relative humidity on the feline $\delta^{18}O_p$ - $\delta^{18}O_w$ correlation were examined and additional intra-individual tissue comparisons were performed. Bobcats and pumas exhibit only a moderate $\delta^{18}O_p$ - $\delta^{18}O_w$ correlation, which differs statistically from canid carnivores and all other placental mammals. Feline $\delta^{18}O_p$ values, also, revealed a much better relation with $\delta^{18}O_w$, than oxygen isotope ratios of hair ($\delta^{18}O_h$) from the same bobcat individuals.

Conclusions/Significance

The oxygen isotope compositions of bone phosphate and especially hair of feline carnivores do not reliably track meteoric water $\delta^{18}O_w$ values. Hence modern and fossil felid tissues are neither well-suited for provenance determination with high spatial resolution in wildlife forensics nor for precise palaeoclimate-reconstructions. In this regard, feline carnivores differ considerably from most herbivores and omnivores, which better track $\delta^{18}O_w$ values. Oxygen isotopic fingerprinting of bobcat and puma is most likely hampered by factors related to climate, diet, behaviour, physiology and metabolism. Controlled feeding experiments, where body water (i.e. blood) and different tissue types are isotopically monitored, are crucial to elucidate the mechanisms of oxygen isotopic routing and incorporation in feline carnivores.

4.1. INTRODUCTION

Many carnivore species are threatened and focus of intense conservation concern [13]. Feline carnivores are of particular relevance for illegal wildlife trade. The ability to estimate the geographic provenance of tissue samples with unknown origin using stable isotope analysis would hence constitute important information in wildlife crime investigations [11]. Especially the phosphate oxygen isotope composition ($\delta^{18}O_p$) of mammalian biogenic apatite is a proxy for the reconstruction of climate [108,109,114-116,197], topography and elevation [198-200], animal physiology [201,202], animal behaviour [203,204], animal ecology [205,206] which allow the reconstruction of habitat-use, provenance and migratory patterns [207-211] in wildlife forensics and ecology as well as in paleontological and archaeological applications. Carnivore $\delta^{18}O_p$ values are considered to be potentially promising proxies for meteoric water [212] but thus far little work has been done on carnivores (i.e. bear: [213], fox: [214]) and none on felids. However, to infer $\delta^{18}O_w$ of ingested water for palaeoclimate reconstruction using $\delta^{18}O_p$ from fossil carnivores requires the testing of related modern species [108]. In this study we establish for the first time the relations between $\delta^{18}O_p$ and $\delta^{18}O_w$ for two modern felids from North America the bobcat and the puma. These were compared to those relations of their preferred prey species cottontail-rabbit and white-tailed deer, respectively. Controlling factors of carnivore $\delta^{18}O_p$ values and implications for the reconstruction of environmental water, respectively, provenance will be discussed.

4.1.1. Oxygen isotope systematics in mammals

Bioapatite $\delta^{18}O_p$ values of mammal bones and teeth record during their mineralization environmental water $\delta^{18}O_w$ values. This enables to determine the climatic setting in which the animal or human lived and hence its provenance. The retention period of phosphate in bones of large mammals is in the range of several years [108], and hence $\delta^{18}O_p$ is affected by the long-term average factors controlling $\delta^{18}O_{bw}$ in the lifetime habitat of the animal. Mammalian bone mineralisation is catalyzed by the enzyme adenosine triphosphate (ATP) [215-217], which promotes the equilibrium oxygen isotopic fractionation between body water ($\delta^{18}O_{bw}$) and skeletal phosphate ($\delta^{18}O_p$) at a constant body temperature (~37°C for most mammals) [108,109,197]. Thus the oxygen isotopic composition of mammalian biogenic apatite (i.e., carbonate ($\delta^{18}O_c$) and phosphate ($\delta^{18}O_p$)) is related to that of ingested meteoric water ($\delta^{18}O_w$) [108,109,115,116]. The basic principle of the mammal $\delta^{18}O_p$ - $\delta^{18}O_w$ relation is: ingested meteoric water ($\delta^{18}O_w$) controls the $\delta^{18}O_{bw}$, at least for those animals that obtain most of their body water from drinking water [105,212,218]. $\delta^{18}O_p$ of terrestrial mammals is controlled by: (a) oxygen input fluxes: atmospheric O_2, liquid drinking water, oxygen bound in food (plant and animal tissue), and metabolic water [105,106,212,219], and (b) oxygen output fluxes: exhaled water vapour, sweat and urine [109] (see Figure 1). While the $\delta^{18}O$ of atmospheric

oxygen is rather constant ($\delta^{18}O$ = 23.5‰) [220], ingestion of drinking water, food, and food water are the main sources controlling the body water $\delta^{18}O_{bw}$ [108].

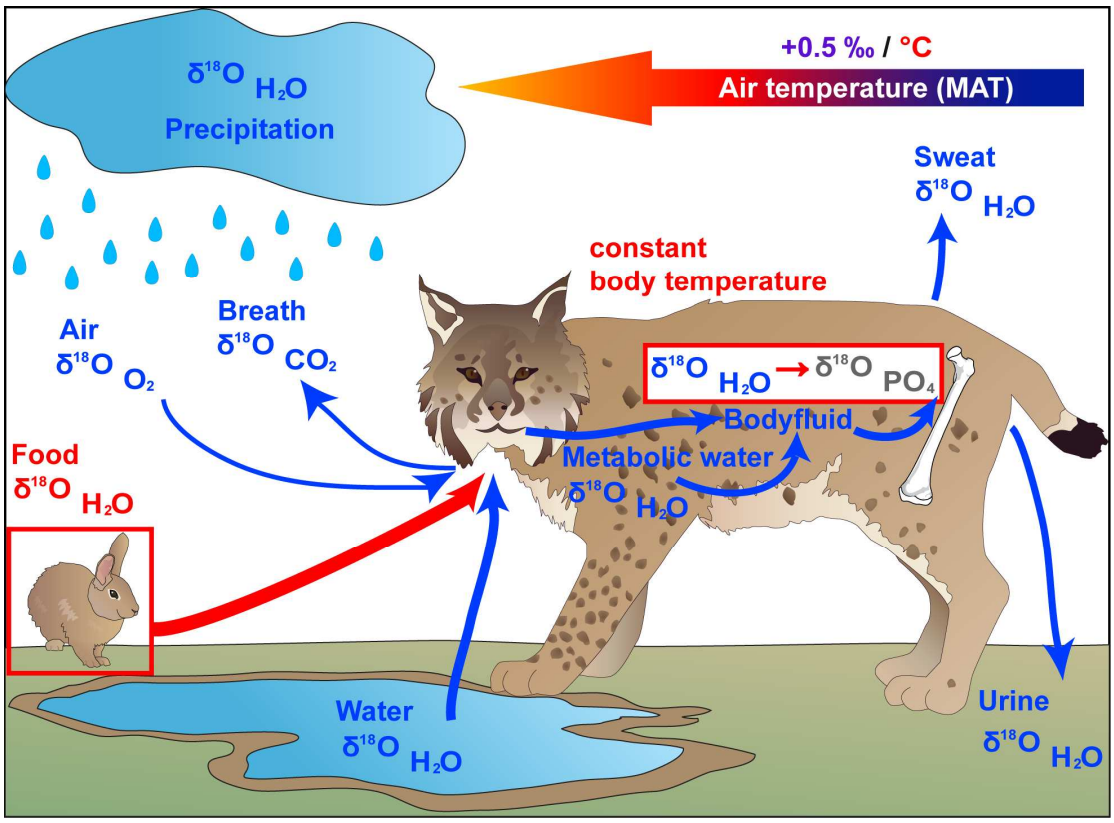

Figure 1. Main oxygen fluxes controlling the oxygen isotope composition of felid body water ($\delta^{18}O_{bw}$). The $^{18}O/^{16}O$ of local environmental water is recorded in the consumer tissues via both diet and drinking water. Homoeothermic vertebrates have a constant body temperature of 37℃ ± 2℃. The temperature dependent fractionation of the oxygen isotope composition during mineralization of apatite in skeletal elements (bone, teeth) from body fluids thus remains constant. The $\delta^{18}O_w$ of the ingested water and hence the climate of the region where the animal lived during tissue formation can be inferred.

$\delta^{18}O_p$ of terrestrial mammals reflects a rather complex mixture of (i) climate, (ii) diet, (iii) animal behaviour and (iv) physiology [108,114,116,219,221-226]. Climatic factors causing variations in the $\delta^{18}O_w$ values of meteoric water are differences in the amount of precipitation, relative humidity, evaporation, distance to the sea, altitude, latitude and temperature [88,227-229]. The effect of diet on $\delta^{18}O_p$ values is particularly well documented for wild herbivores, whose $\delta^{18}O_p$ values are affected by the type of plant consumed, i.e. C_4 versus C_3 plants [219,226,230-233]. Behavioural and physiological factors contributing to a species-specific $\delta^{18}O_p$ - $\delta^{18}O_w$ relation include water turnover [105], water conservation mechanisms [218,219,234], metabolic rate [102], body water loss via sweating or panting [212,219] and suckling [223,235].

During the past three decades $\delta^{18}O_p$ - $\delta^{18}O_w$ relations have been determined empirically for several modern terrestrial mammal species (Table S1).

Table S1. Oxygen isotope equations calibrated on skeletal phosphate of different terrestrial mammal species.

Diet type: Herbivore/ Omnivore/ Carnivore	Sample material (Teeth, Bone, Urinary stones)	Species	Regression equations	R^2	Reference	Drinking water value (Tap or precip water)
O	B	Human	y = 1.53 x -34.30*	0.97	[108]	precip
O	B	Human	y = 1.19 x -27.42*	0.95	[116]	precip
O	T	Human	y = 1.93 x -38.51*	0.92	[123]	precip
O	U	Human	y =1.84 - 41.39*	0.75	[123]	precip
O	T	Human	y = 1.73 x -37.25*	0.87	[203]	tap
O	T + B	Human	y = 1.54 x - 33.72*	0.87	[203]	precip + tap
O	B	Pig	y = 0.86x + 22.71	0.98	[108]	precip
O	T + B	Foxes	y = 1.34x + 25.49	0.98	[214]	precip
O	B	Rats	y = 0.45x + 17.86	0.99	[109]	tap
O	B	Wood & yellow-necked mouse	y = 0.79x + 21.61	0.98	[197]	precip
H	B	White-tailed deer	y = 0.53x + 21.5	0.81	[115]	precip
H	B	Red deer	y = 1.13x + 25.55	0.99	[197]	precip
H	B	Cattle	y = 1.01x + 24.90	0.99	[197]	precip
H	B	Sheep	y = 1.48x + 27.21	0.96	[197]	precip
H	T + B	Asiatic & African elephant	y = 1.06x + 24.30	0.86	[236]	precip
H	T + B	Equidae	y = 0.72x + 22.29	0.9	[121]	precip
H	T + B	Equidae	y = 0.73x + 22.04	0.94	[237]	precip
H	T	Equidae	y = 0.69x + 22.90	0.69	[223]	precip
H	T + B	Equidae	y = 0.71x + 22.60	0.77	[121]	precip
H	B	Goat and moufflon	y = 0.91x + 24.39	0.99	[121]	precip
H	B	Goat, moufflon, roe-bucks	y = 0.88x + 24.10	0.98	[121]	precip
H	T + B	Reindeer	y = 0.39x + 15.96	0.79	[214]	precip
H	T	Bison	y = 0.70x + 21.23	0.83	[209]	precip
H	B	Kangaroo	Correlation of $\delta^{18}O_p$ with rel. humidity		[114]	precip
H	B	Rabbit	y = 0.47x + 22.73	0.23	[121]	precip
O	T	Arvicolinae	y = 0.617x + 21.356	0.86	[238]	precip

*X-Axis= $\delta^{18}O_p$, Y-Axis = $\delta^{18}O_w$ and otherwise vice versa

For all mammals the oxygen isotope fractionation between $\delta^{18}O_w$ and $\delta^{18}O_p$ follows linear regressions, however, the slope and intercept show inter-specific variability. A general trend was identified for $\delta^{18}O_p$ - $\delta^{18}O_w$ relations, i.e. large mammals with low metabolisms being obligate drinkers do track $\delta^{18}O_w$ values of meteoric waters more closely [105,108,116]. However, deviations from a constant oxygen fractionation between $\delta^{18}O_p$ and $\delta^{18}O_w$ have been documented for some species (e.g. Australian macropods [114] and rabbits [121]) and are primarily related to the rate of drinking and metabolism [109]. The previously-published fractionation equations for mammals focused primarily on herbivores and omnivores. So far $\delta^{18}O_p$ - $\delta^{18}O_w$ calibrations have only been attempted for two carnivores, bear [213] and fox [214], which, however, do not represent strict carnivores but rather exhibit an omnivorous lifestyle [239]. While a good $\delta^{18}O_p$ - $\delta^{18}O_w$ regression was obtained for foxes [214], the study for bears was not successful [213]. The latter was related to the fact that investigated zoo animals might have had a different physiology than wild animals.

Free-ranging carnivores, however, differ significantly in their nutritional, physiological and metabolic characteristics from herbivores and omnivores [131,132]. The house cat, *Felis catus*, is one of the best investigated mammalian carnivores [131]. Felids are strict carnivores that obtain much of their body water from the consumption of prey. On average only 1% of their total water input originates from drinking water [131,148]. Food water and drinking water in free-ranging cats are hence primarily ingested from the same source - the prey. In addition to a low rate of drinking, felids are known to have higher body temperatures and basal metabolic rates by general mammalian standards [180]. Thus it is not clear whether carnivore phosphate tracks the spatially predictable meteoric water compositions despite their low drinking intake and high metabolic rate. The few published carbonate oxygen isotope data ($\delta^{18}O_{CO3}$) for carnivores yield ambiguous results regarding the importance of climate versus physiology and diet. For instance, Sponheimer and Lee-Thorp [226] report carnivore $\delta^{18}O_{CO3}$ values similar to their consumed herbivore prey, while others demonstrate very low carnivore $\delta^{18}O_{CO3}$ values due to an ^{18}O-depleted protein- and lipid-rich meat diet [240]. In contrast, Feranec et al. [205] showed enriched carnivore $\delta^{18}O_{CO3}$ values, caused by the consumption of prey whose $\delta^{18}O_{bw}$ was affected by evaporative ^{18}O-enrichment. However, Kohn [212] hypothesized, that “the importance of relative humidity becomes progressively diminished with increasing trophic level”, and consequently “carnivore bone phosphate should track the meteoric water signal more closely than do herbivores”. Therefore the concept of geographic source determination based on oxygen isotopes of carnivore bone phosphate as a potential investigative tool in wildlife forensics and palaeontology needs to be tested on extant species.

Modern felids are a suitable group to test the strength of oxygen isotope fingerprinting for geographic provenancing of living and extinct carnivores. Felids evolved about 35 Ma ago

[241] and are now distributed over all continents except Antarctica, thus covering almost all environmental gradients [11,242]. Although the available fossil record of felids is sparse compared to other carnivoran families such as dogs (Canidae) and bears (Ursidae), the Felidae are the only representatives of strict carnivory within the order Carnivora. North American puma and bobcat are particularly appropriate for isotopic investigations due to the availability of provenanced skeletons from museum collections, high-resolution precipitation $\delta^{18}O$ isoscapes for North America and ecological differences between these two taxa (e.g. body size, home-range size, habitat use, geographic distribution and prey preferences).

Our study was designed to determine, if bone phosphate $\delta^{18}O_p$ values of puma and bobcat vary predictably among isotopically distinct geographic locations and reflected the spatial pattern of $\delta^{18}O_w$ variation in precipitation. We report the first large-scale survey of $\delta^{18}O_p$ data of bone phosphate samples of two feline carnivores, bobcat (*Lynx rufus*) and puma (*Puma concolor*) from across North America. Furthermore, we examined potential effects of species, sex, and relative humidity on the $\delta^{18}O_w$ - $\delta^{18}O_p$ correlation, and whether these could be explained by differences in diet, behaviour, physiology and foraging ecology. The controlling factors and possibilities to quantify these will be discussed.

4.2. MATERIALS AND METHODS

4.2.1. Study species and sampling

A total of 107 bone samples, representing the North American felid species bobcat (*Lynx rufus*; n = 63) and puma (*Puma concolor*; n = 43) were sampled at the Smithsonian National Museum of Natural History in Washington, D.C., the Utah Museum of Natural History in Salt Lake City, Utah and the Laboratory of Genomic Diversity in Frederick, Maryland. Powder samples from defined areas of the lower jaw bone were drilled using a hand-held Proxxon-Minidrill to yield ~60mg of bone powder. For each felid sample, geographic location, sex, and elevation were recorded (Appendix 1). The specimens originate from 107 sites across the United States, Canada and Mexico (Figure 2). Sample locations range in latitude from 25.8 to 64.8ºN and longitude from 162.3 to 74.5ºW and hence cover strong environmental gradients of altitude (1 to 2500m) and meteoric water oxygen isotope composition ($\delta^{18}O_w$ = –21.3‰ to –1.4‰). Published bone-phosphate oxygen isotope data ($\delta^{18}O_p$) from other placental mammals (compiled in [243]), another carnivore, the fox [214] and major prey species like white tailed deer (*Odocoileus virginianus*; [115]) and eastern cottontail rabbit (*Sylvilagus floridanus* [121]) of puma and bobcat, respectively, were included for comparison.

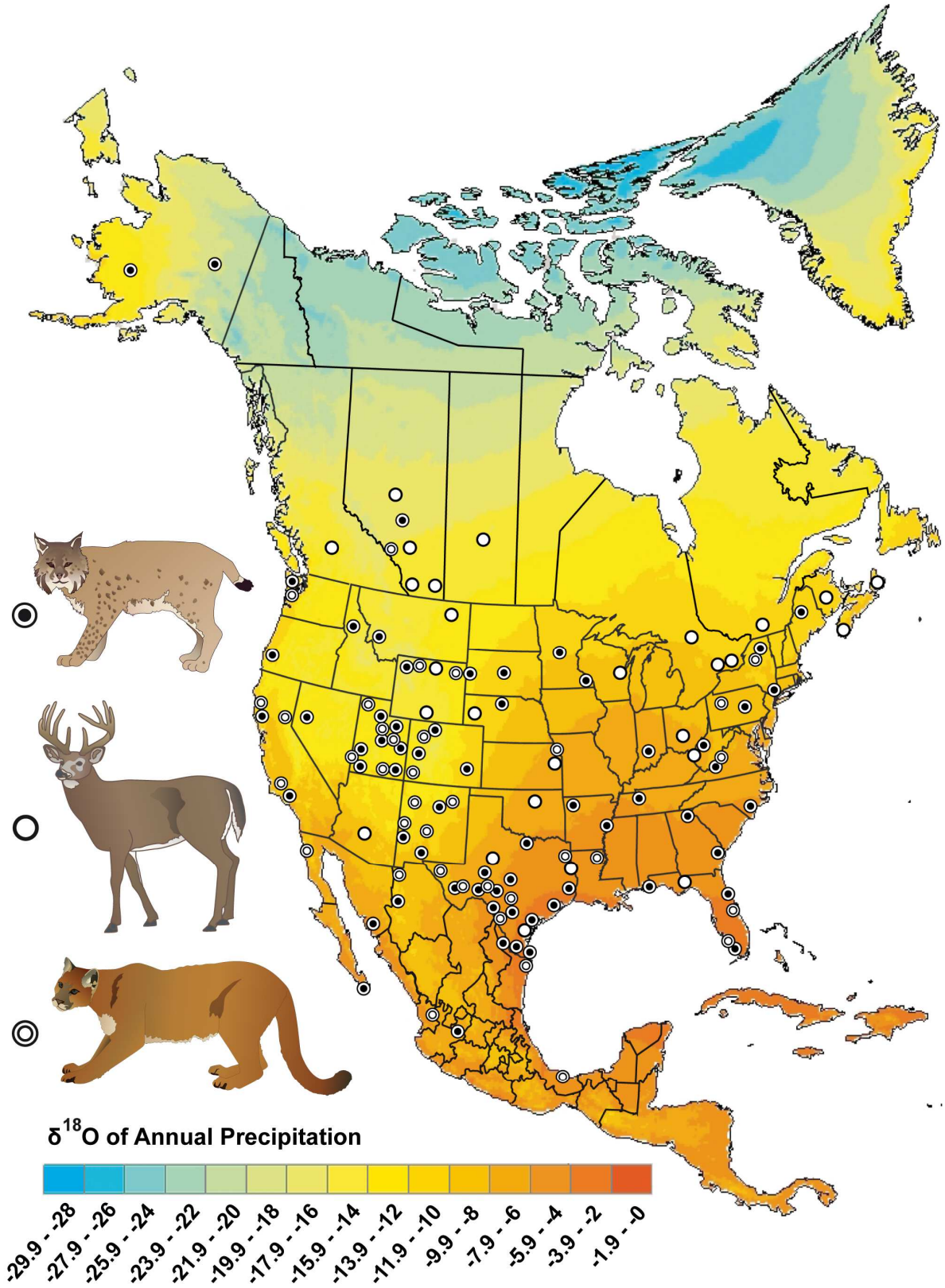

Figure 2. Map of sampling sites. Sample locations for both felines bobcat (n = 63) and puma (n = 43) as well as the preferred prey species of pumas, the white-tailed deer (n = 46, [115]), plotted on the $\delta^{18}O$ precipitation map of North America [87].

4.2.2. Sample preparation and oxygen isotope analysis of bone phosphate ($\delta^{18}O_p$)

Sample preparation was conducted in the chemical laboratory of the Geochemistry department at the Steinmann-Institute, University of Bonn. We followed the protocol for bioapatite preparation of Clementz et al. [244]. 20mg of the powdered samples were chemically pre-treated with 30% H_2O_2 to oxidize organic matter, followed by a treatment with 1M calcium acetate/acetic acid buffer solution at 4℃ to remove carbonate contaminants. Finally, the samples were rinsed five times in double distilled water and dried at 60℃. 5 mg of the pre-treated sample powder was dissolved in 2 M HF overnight and the HF solution was transferred to a new vessel, neutralized with 25% NH_4OH, and the PO_4^{3-} in solution was rapidly precipitated as Ag_3PO_4 by adding 2M $AgNO_3$ according to the method described in Tütken et al. [245].

The phosphate oxygen isotope composition ($\delta^{18}O_p$) of the thoroughly rinsed silver phosphate of each sample was analyzed in triplicate (~500 µg aliquots) using a Finnigan TC-EA at 1450 ℃ connected via a Finnigan Conflow III to a Thermo Finnigan Delta Plus XL CF-IRMS at the University of Tübingen. Oxygen isotope compositions are expressed in per mil (‰) in the δ-notation relative to the Vienna Standard Mean Ocean Water (V-SMOW). The external analytical precision of $\delta^{18}O_P$ values for a synthetic hydroxyl apatite (HAP) from Merck used as internal standard was better than ±0.3‰. The international NBS 120c standard yielded $\delta^{18}O_P$ value of 21.8±0.6‰ (n = 3).

4.2.3. Estimation of $\delta^{18}O_w$ of ingested water

Most wild mammals get their drinking water primarily from running (streams) and standing (lakes) water sources. The primary source of isotopic variability in surface, ground, and soil waters is variation in the $\delta^{18}O_w$ values of precipitation supplying these reservoirs. For each sample location we used the unweigthed mean annual precipitation values ($\delta^{18}O_w$) based on climatic records from nearby IAEA–WMO meteorological stations [137]. We assume that $\delta^{18}O_w$ represents most likely the isotopic composition of the water ingested by the preferred prey species and hence their predators (bobcat and puma) sampled here.

4.2.4. Data analysis

First, we analysed the oxygen isotopic variation of puma and bobcat bone phosphate ($\delta^{18}O_p$) among locations and their correlation with the pattern of oxygen isotopic variation in precipitation ($\delta^{18}O_w$). Linear regression models were used to determine the relation between $\delta^{18}O_w$ and $\delta^{18}O_p$ for bobcat and puma, their respective prey species, rabbit and white-tailed deer, a canid carnivore (fox) and other placental mammals (see Appendix 2 and Figures 3, 4, 5, 6). The effects of species, sex and relative humidity on the $\delta^{18}O_p$ - $\delta^{18}O_w$ correlation were examined using a General Linear Model (GLM) (see Appendix 2, Figures 3 - 7). We tested

whether the $\delta^{18}O_p$ - $\delta^{18}O_w$ fractionation equation of felids statistically differs from other terrestrial mammals. We thus compared the feline carnivore regression line with those from their respective major prey species (deer and rabbit), a canid carnivore (fox) and a group of placental mammals using a single classification Analysis of Covariance (ANCOVA: Tukey test; [246]) (see Appendix 3). Additionally, $\delta^{18}O$ values of bone phosphate ($\delta^{18}O_p$) and hair ($\delta^{18}O_h$) from the same individuals were compared for thirty bobcat specimens. We thus tested, if $\delta^{18}O$ of multiple-both tissue types are correlated within individuals and if $\delta^{18}O_p$ and $\delta^{18}O_h$ of these specimens display similar correlations with $\delta^{18}O_w$ (Figures 8 and 9, Appendix 4). The $\delta^{18}O_h$ data were taken from a previous study [247]. Statistical tests were conducted using XLSTAT (V 7.5.2).

4.3. RESULTS

4.3.1. Variation and range of $\delta^{18}O_p$ and $\delta^{18}O_w$

The oxygen isotope composition of the phosphate fraction ($\delta^{18}O_p$) from feline carnivore bones ranged from 11.5 to 21.7‰ in puma and 9.1 to 21.9‰ in bobcat (Figures 4 and 5). These ranges were smaller than that of the corresponding average $\delta^{18}O_w$ values (–21.3 to –1.4‰ after [137]) estimated for the unweighted mean annual precipitation of the animal's lifetime habitat.

4.3.2. Effect of species on $\delta^{18}O_p$

The $\delta^{18}O_p$ - $\delta^{18}O_w$ relation is known to be species-specific (e.g. [105,212]) and we thus compared $\delta^{18}O_p$ values of puma and bobcat with those of their prey species, canid carnivores and other placental mammals.

4.3.2.1. Among species within feline carnivores

Feline carnivore bone $\delta^{18}O_p$ values exhibited a moderate linear relationship between $\delta^{18}O_p$ and $\delta^{18}O_w$ following the equation:

$$\text{Feline carnivores: } \delta^{18}O_p = 0.40(\pm 0.04)\ \delta^{18}O_w + 20.10(\pm 0.40)\ (R^2 = 0.46).$$

The puma showed a slightly weaker $\delta^{18}O_p$ - $\delta^{18}O_w$ relation than the bobcat (Appendix 2, Figures 4 and 5) indicated by the following equations:

$$\text{Bobcat: } \delta^{18}O_p = 0.41(\pm 0.05)\ \delta^{18}O_w + 20.15(\pm 0.49)\ (R^2 = 0.50),$$

$$\text{Puma: } \delta^{18}O_p = 0.38(\pm 0.07)\ \delta^{18}O_w + 20.00(\pm 0.67)\ (R^2 = 0.39).$$

However, the bobcat and puma $\delta^{18}O_p$ - $\delta^{18}O_w$ regressions are statistically identical (ANCOVA Tukey test: $p = 0.722$) (Appendix 3).

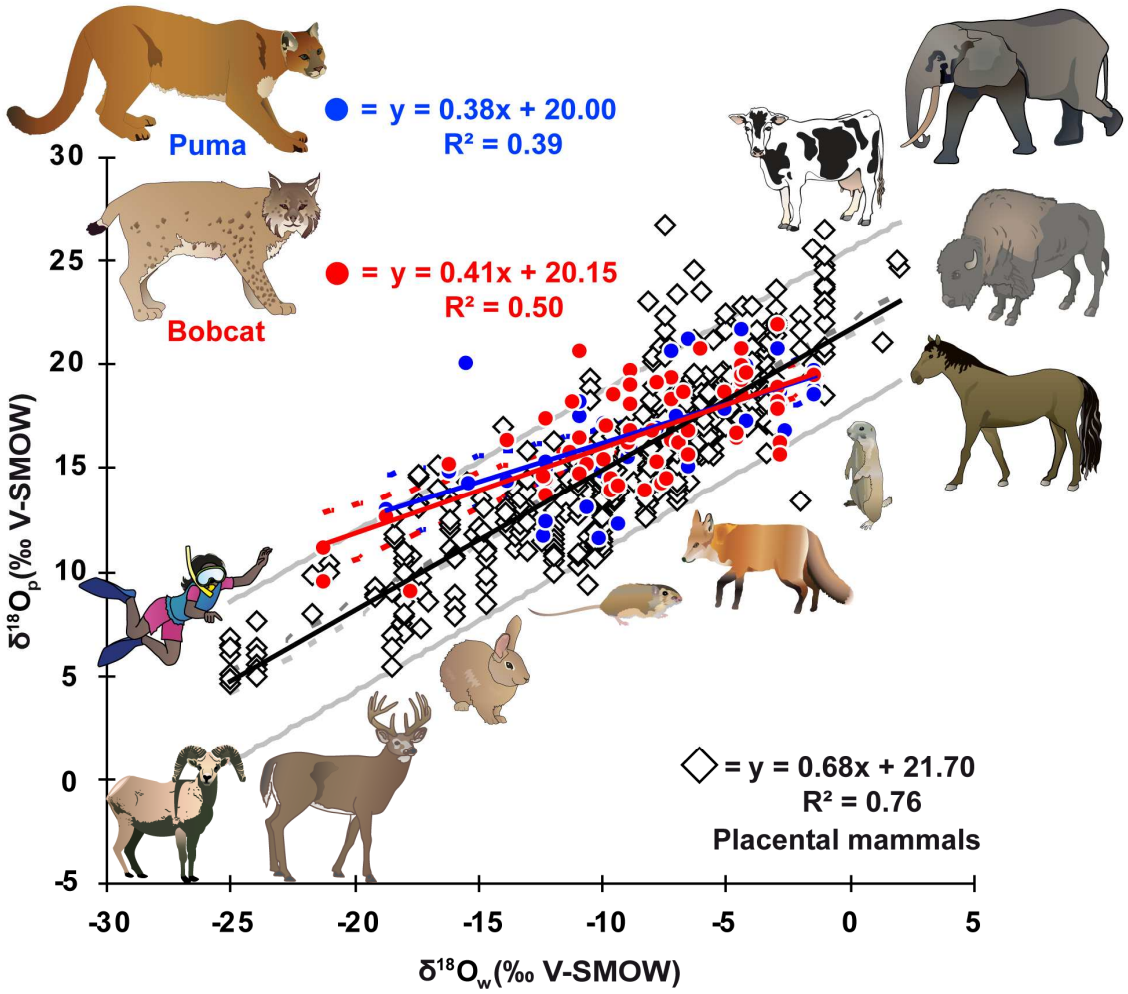

Figure 3. Oxygen isotope values of mammalian bone phosphate relative to meteoric water. Plot of bone phosphate ($\delta^{18}O_p$) from felids in comparison to published data from other placental mammals (Table S1, [243]) versus mean annual $\delta^{18}O$ of precipitation water ($\delta^{18}O_w$).

4.3.2.2. Between feline carnivores, fox and other placental mammals

The $\delta^{18}O_p$ - $\delta^{18}O_w$ relation of feline carnivores differed in their R^2 and slope from other placental mammals and canid carnivores (i.e. foxes).

$$\text{Placental mammals: } \delta^{18}O_p = 0.68(\pm 0.02)\ \delta^{18}O_w + 21.70(\pm 0.17)\ (R^2 = 0.76),$$

$$\text{Fox: } \delta^{18}O_p = 1.38(\pm 0.03)\ \delta^{18}O_w + 25.85(\pm 0.17)\ (R^2 = 0.98).$$

The R^2 of 0.46 and slope of 0.4 for both feline carnivores was lower than those usually measured for other placental mammals and canid carnivores, which are typically higher (placental mammals: $R^2 = 0.76$, slope = 0.68; foxes: $R^2 = 0.98$, slope = 1.38) (Figures 3 and 6). Accordingly the feline carnivore $\delta^{18}O_p$ - $\delta^{18}O_w$ relation was statistically different compared to the global placental mammals (Tukey test: $p = 0.001$) and the fox relationship (Tukey test: $p = 0.050$) (Appendix 3).

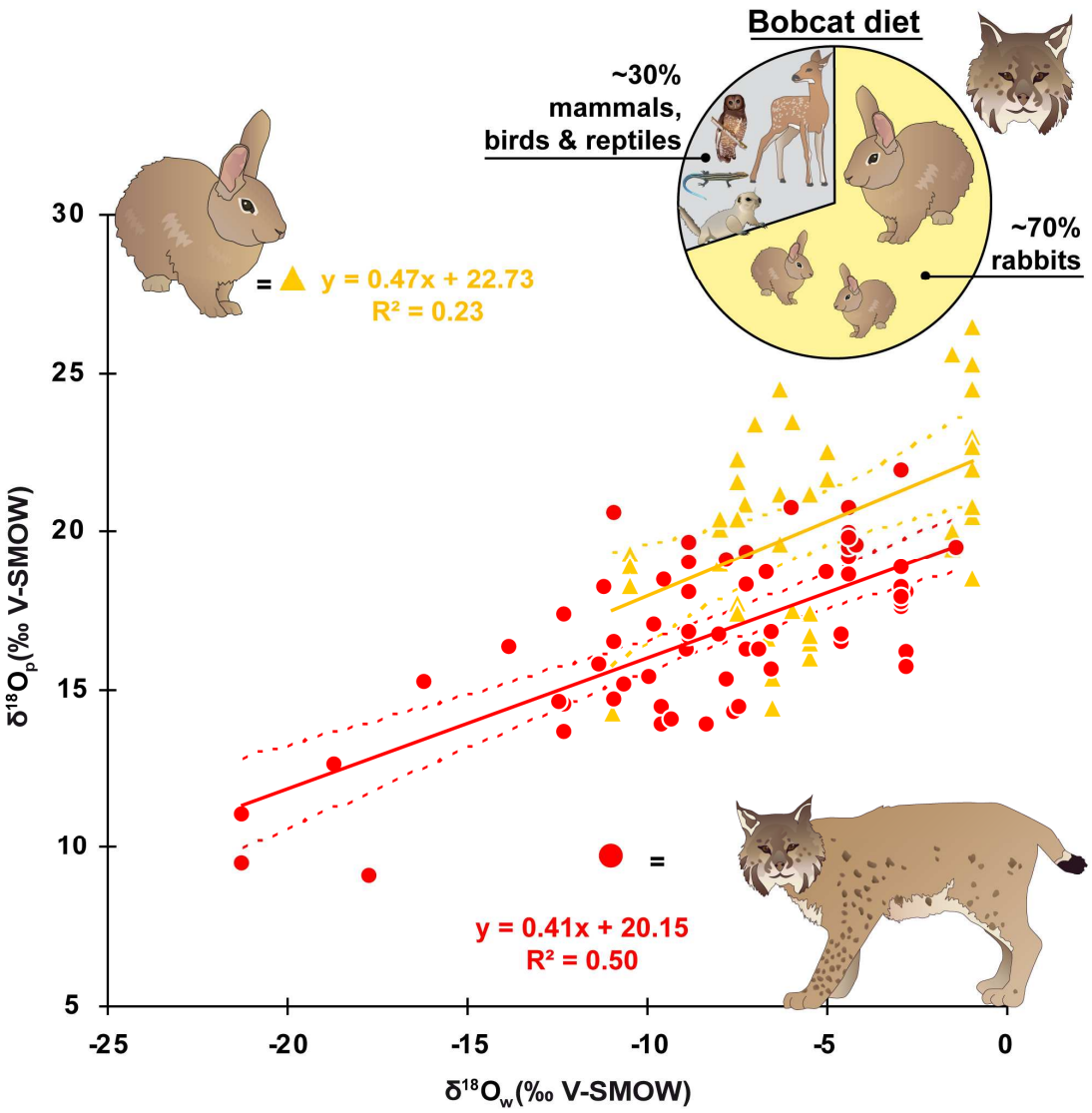

Figure 4. Oxygen isotope values of bobcat and rabbit bone phosphate relative to meteoric water. Plot of bone phosphate ($\delta^{18}O_p$) from bobcat and rabbits [121] vs. mean annual $\delta^{18}O$ of precipitation water ($\delta^{18}O_w$). The pie chart illustrates the typical prey spectrum of bobcats in North America (according to [147]).

4.3.2.3. Between feline carnivores and their respective prey species

The major prey species of bobcat and puma, the eastern cottontail rabbit and white-tailed deer, respectively, showed quite different $\delta^{18}O_p$ - $\delta^{18}O_w$ relationships, with the rabbit having a weak (R^2 = 0.23, p = 0.001, n = 41) and the deer having a strong positive relation (R^2 = 0.71, p < 0.0001, n = 41) (Figures 4 and 5). The key prey species yielded the following equations:

White tailed deer: $\delta^{18}O_p = 0.54(\pm0.05)\ \delta^{18}O_w + 21.70(\pm 0.63)$ ($R^2 = 0.70$),

Rabbits: $\delta^{18}O_p = 0.47(\pm0.14)\ \delta^{18}O_w + 22.73(\pm 0.86)$ ($R^2 = 0.23$).

The $\delta^{18}O_p$ - $\delta^{18}O_w$ relationship of rabbits was not reflected in the $\delta^{18}O_p$ of its respective predator (Tukey test: bobcat/rabbit, p < 0.0001).

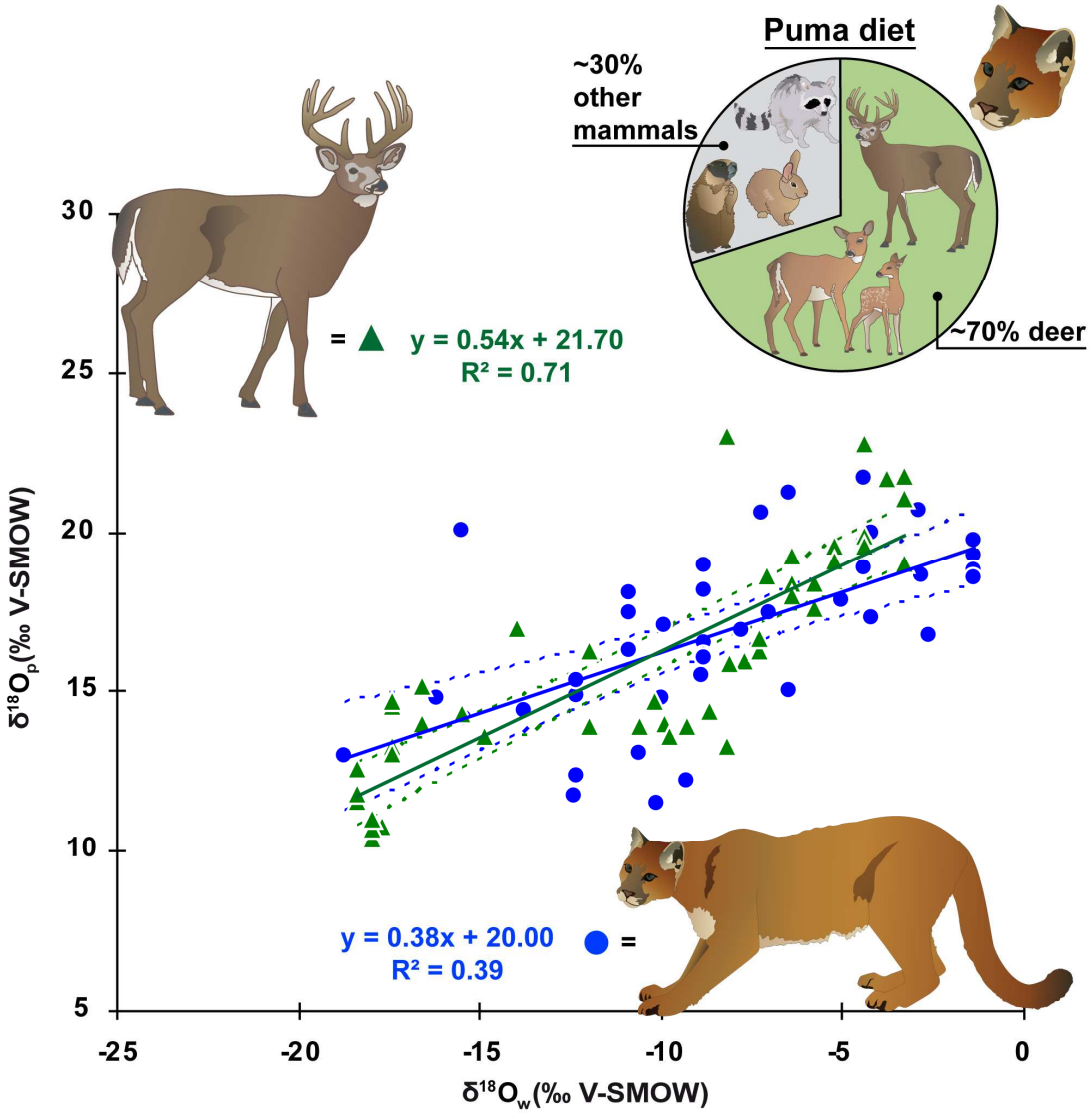

Figure 5. Oxygen isotope values of puma and white-tailed deer bone phosphate relative to meteoric water. Plot of bone phosphate ($\delta^{18}O_p$) from puma and white-tailed deer [115] vs. mean annual $\delta^{18}O$ of precipitation water ($\delta^{18}O_w$). The pie chart illustrates the typical prey spectrum of pumas in North America (according to [248,249]).

A parallel upward shift in the $\delta^{18}O_p$ - $\delta^{18}O_w$ regression line of rabbits versus bobcats could be observed, which indicates on average an ^{18}O enrichment of ~ +2‰ for rabbits relative to its predator (Figure 4). The puma and deer $\delta^{18}O_p$ - $\delta^{18}O_w$ equations however were statistically indistinguishable (Tukey test: p = 0.629) (Appendix 3, Figure 5).

4.3.3. Effect of sex on $\delta^{18}O_p$

Animal behaviour can vary with sex and is documented to be a major factor influencing the $\delta^{18}O_p$ - $\delta^{18}O_w$ relationship of mammals (e.g. [212,250]). However, no effect of sex on the isotopic relationship between $\delta^{18}O_p$ - $\delta^{18}O_w$ was observed for both carnivore species (ANCOVA, Tukey HSD test: male/female bobcat: p = 0.789, n = 45; male/female puma: p = 0.350, n = 24) (Appendix 3).

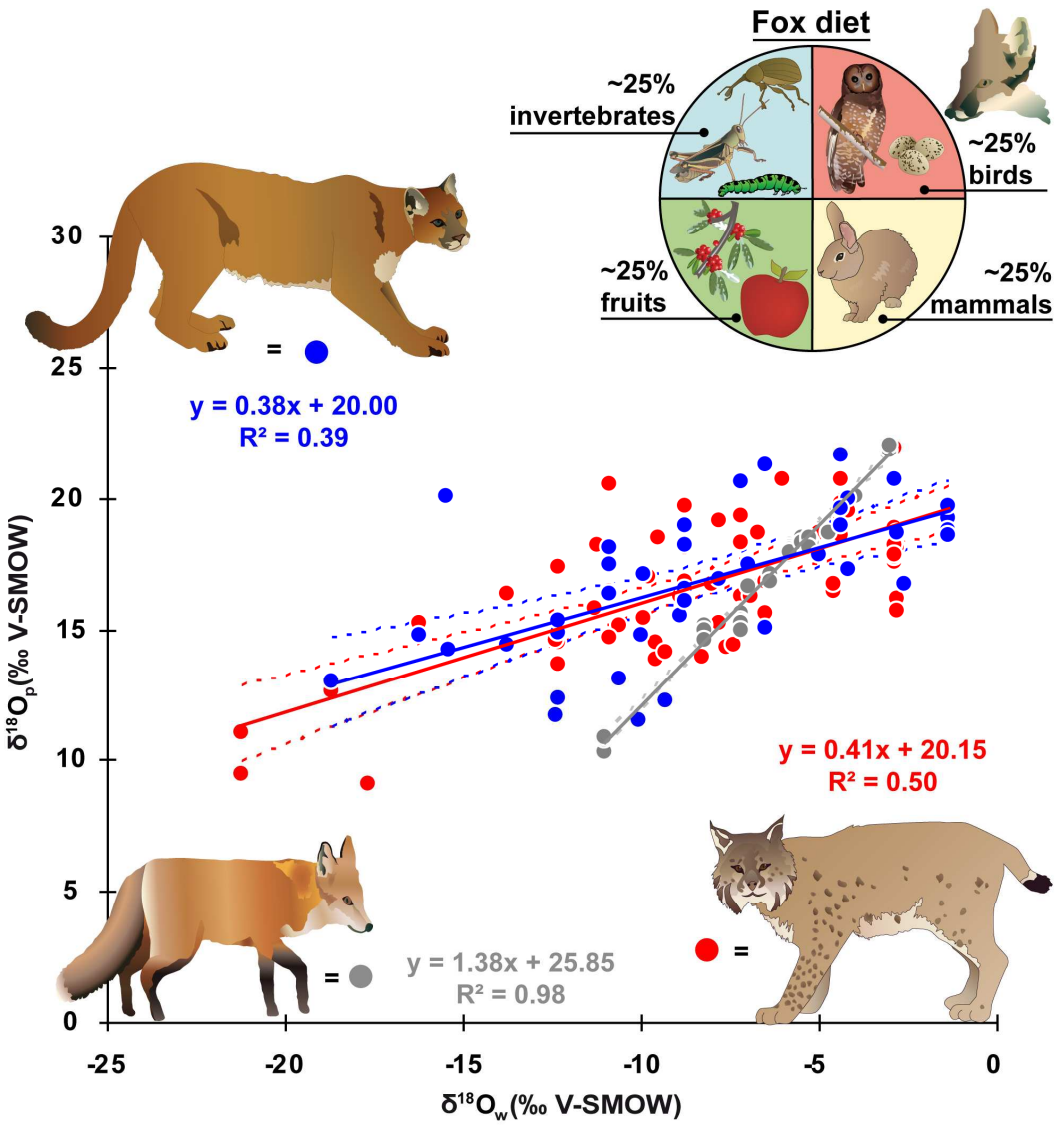

Figure 6. Oxygen isotope values of puma, bobcat and fox bone phosphate relative to meteoric water. Plot of bone phosphate ($\delta^{18}O_p$) from two feline carnivores (bobcat and puma) and a canid carnivore (fox, [214]) vs. mean annual $\delta^{18}O$ of precipitation water ($\delta^{18}O_w$). The pie chart illustrates the typical prey spectrum of omnivorous foxes (*Vulpes vulpes*) in North America (according to [239]).

4.3.4. Effect of relative humidity on $\delta^{18}O_p$

Relative humidity has been documented to control the $\delta^{18}O_p$ values of mammalian herbivore species with low drinking water requirements (e.g. [212]) and could thus also affect their predators. The $\delta^{18}O_p$ - $\delta^{18}O_w$ regression of both predators and prey was in fact improved by including relative humidity (h) in the regression:

Bobcat: $\delta^{18}O_p = 26.75(\pm 1.29) + 0.45(\pm 0.04) * \delta^{18}O_w - 0.10(\pm 0.02) * h$ ($R^2 = 0.664$),

Puma: $\delta^{18}O_p = 25.78(\pm 2.00) + 0.47(\pm 0.07) * \delta^{18}O_w - 0.08(\pm 0.03) * h$ ($R^2 = 0.507$),

Rabbit: $\delta^{18}O_p = 30.65(\pm 1.88) + 0.41(\pm 0.11) * \delta^{18}O_w - 0.13(\pm 0.03) * h$ ($R^2 = 0.502$),

Deer: $\delta^{18}O_p = 34.83(\pm 1.48) + 0.67(\pm 0.03) * \delta^{18}O_w - 0.17(\pm 0.02) * h$ ($R^2 = 0.909$).

Compared to other humidity-dependent herbivore species like Australian macropods [251], relative humidity did show a moderate but significant effect on $\delta^{18}O_p$ of rabbits ($R^2 = 0.34$, $p < 0.0001$, $n = 41$) and a weak effect on $\delta^{18}O_p$ of bobcats ($R^2 = 0.08$, $p = 0.026$, $n = 63$). There was no significant effect of relative humidity observed for puma ($R^2 = 0.002$, $p = 0.786$, $n = 43$) and deer ($R^2 = 0.01$, $p = 0.546$, $n = 44$) (Figure 7, Appendix 2).

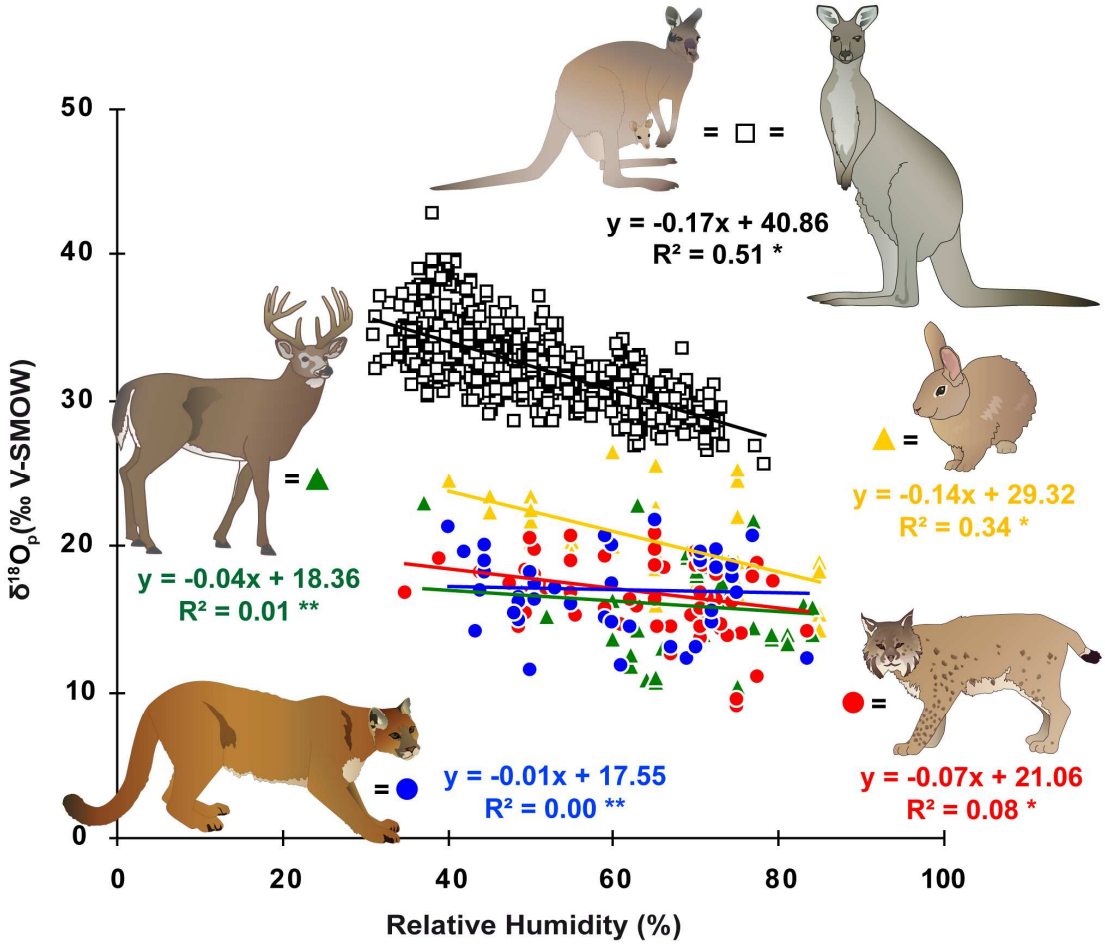

Figure 7. Oxygen isotope values of kangaroo, feline carnivore and herbivore bone phosphate ($\delta^{18}O_p$) versus relative humidity (%). Plot of bone phosphate ($\delta^{18}O_p$) from two feline carnivores (bobcat and puma), Australian macropods [251], white-tailed deer [115] and rabbits [121] vs. mean annual relative humidity (%). * Statistically significant, **statistically not significant.

4.3.5. Intra-individual comparison of tissue $\delta^{18}O$

Different tissue types within individual specimens were demonstrated to exhibit similar $\delta^{18}O_{tissue}$ - $\delta^{18}O_w$ relations [252]. We thus compared $\delta^{18}O$ values of hair keratin and bone phosphate of the same individuals from thirty bobcat specimens. The $\delta^{18}O_p$ values revealed a much better relation with $\delta^{18}O_w$, than $\delta^{18}O_h$ from the same bobcat individuals (Bone phosphate: $R^2 = 0.46$, $p < 0.0001$, $n = 30$; hair: $R^2 = 0.00$, $p = 0.830$, $n = 30$) (Figure 8, Appendix 4). There is no significant correlation between $\delta^{18}O_p$ and $\delta^{18}O_h$ of the same bobcat individuals ($\delta^{18}O_p$ - $\delta^{18}O_h$: $R^2 = 0.057$, $p = 0.203$, $n = 30$) (Figure 9, Appendix 4).

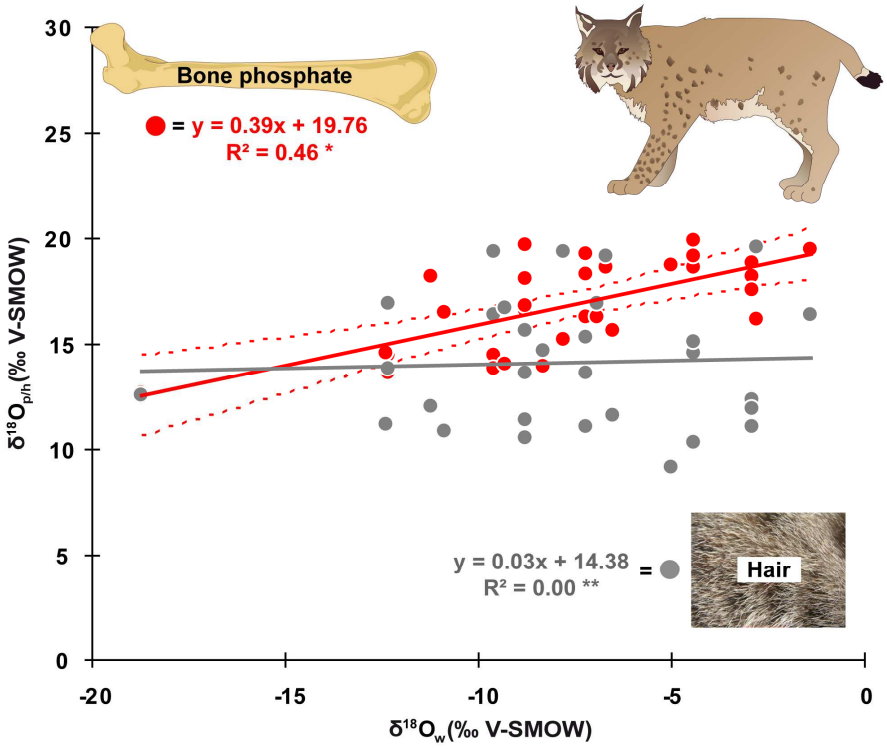

Figure 8. Oxygen isotope values of bobcat bone phosphate and hair relative to meteoric water. Plot of bone phosphate ($\delta^{18}O_p$) and hair ($\delta^{18}O_h$) [247] from single bobcat specimens vs. mean annual $\delta^{18}O$ of precipitation water ($\delta^{18}O_w$). * Statistically significant, ** statistically not significant.

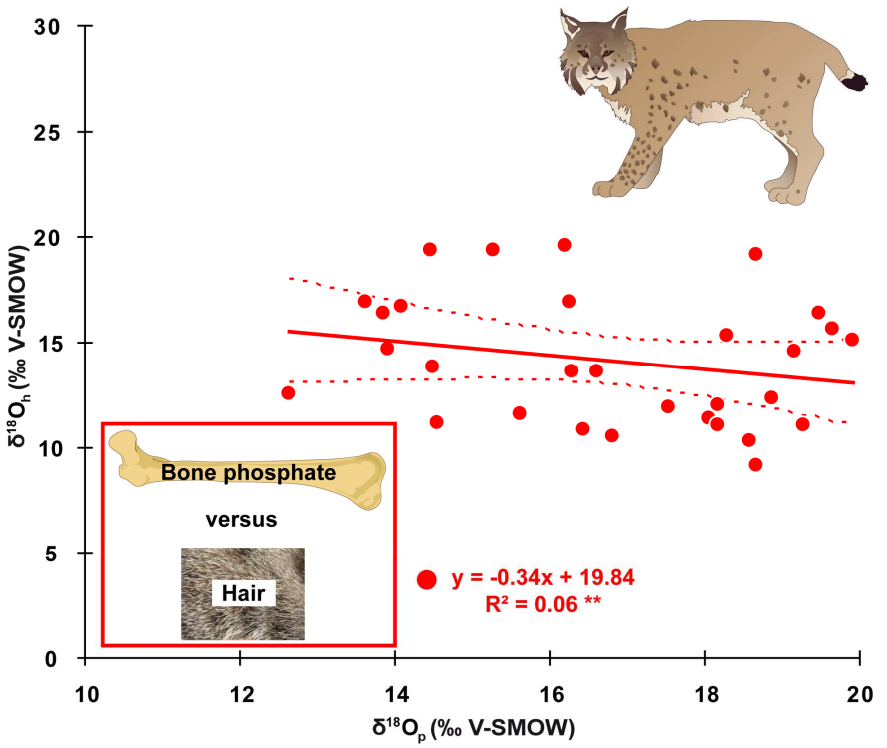

Figure 9. Oxygen isotope values in hair relative to bone phosphate of bobcat. Plot of bone phosphate ($\delta^{18}O_p$) vs. hair ($\delta^{18}O_h$) [247] from single bobcat specimens. ** Statistically not significant.

4.4. DISCUSSION

Our results demonstrate that bobcat and puma exhibit only a moderate linear relationship between $\delta^{18}O_w$ and $\delta^{18}O_p$. Moreover, this relation also differs statistically from their respective prey species, other placental mammals and other carnivores (Figures 3, 4, 5, 6). Compared to most previously published studies on $\delta^{18}O$ of biogenic apatite of omnivores and herbivores, feline carnivores have a weaker and statistically different $\delta^{18}O_p$ - $\delta^{18}O_w$ relationship. Provenance determination of modern feline carnivores, such as puma and bobcat, solely based on $\delta^{18}O_p$ is thus far from precise. Potential explanations causing the deviations from a strong relation between $\delta^{18}O_p$ and $\delta^{18}O_w$ in feline carnivores are discussed below and include climate, diet, animal behaviour as well as physiology and metabolism.

4.4.1. How do climatic factors affect carnivore $\delta^{18}O_p$?

One possibility to explain the significantly weaker feline carnivore $\delta^{18}O_p$ - $\delta^{18}O_w$ correlation compared to other mammals, is that relative humidity affects their $\delta^{18}O_p$. So far it has only been documented that relative humidity controls the $\delta^{18}O_p$ values of mammalian herbivore species with low drinking water requirements (e.g. [212,219]). For example, $\delta^{18}O_p$ values of Australian macropods [114], rabbits and hares [121] have been shown to correlate strongly with changes in relative humidity independent of $\delta^{18}O_w$ (Figure 7), whereas the $\delta^{18}O_p$ of North American deer [115] were reported to be primarily influenced by $\delta^{18}O_w$ and only slightly by relative humidity. Low humidity increases the rate of evaporation of surface water and evapotranspiration of leaf- and grass-water and thus leads to oxygen isotopic enrichment effects in plants [143,253,254]. Drought-tolerant animals who obtain most of their water from plants thus reflect levels of environmental humidity and their $\delta^{18}O_p$ increases with decreasing relative humidity. However, Kohn [212] hypothesized that “the importance of relative humidity becomes progressively diminished with increasing trophic level”. Our data support Kohn’s hypothesis that predators are less controlled by relative humidity than herbivores. However, their $\delta^{18}O_p$ - $\delta^{18}O_w$ correlations were slightly improved by including relative humidity in the regression (Appendix 2). Puma and its respective prey, the white-tailed deer are both unaffected by relative humidity (puma: $R^2 = 0.002$, $p = 0.786$; deer: $R^2 = 0.01$, $p = 0.546$; Figure 7). In contrast, bobcat $\delta^{18}O_p$ compositions are weakly affected by humidity (bobcat: $R^2 = 0.08$, $p = 0.026$; Figure 7), most likely because they prey upon rabbits whose $\delta^{18}O_p$ values in turn are humidity dependent ($R^2 = 0.34$, $p < 0.0001$; Figure 7).

Furthermore, Kohn [212] concludes that carnivore $\delta^{18}O_p$ “should track the meteoric water signal more closely than do herbivores”, due to a reduced humidity effect on their $\delta^{18}O_{bw}$. In this case our results, however, do not confirm the hypothesis. The R^2 of 0.46 for both feline carnivores ($p < 0.0001$, Figure 3) was lower than those usually determined for placental mammals, which are typically higher ($R^2 = 0.73$, $p < 0.0001$, Figure 3). The feline carnivore

$\delta^{18}O_p$ - $\delta^{18}O_w$ relation was also statistically different compared to the global placental mammals (Tukey test: $p < 0.0001$; Appendix 3). The simplest interpretation is that factors other than relative humidity are responsible for a weaker relation between $\delta^{18}O_p$ and $\delta^{18}O_w$ in feline carnivores.

4.4.2. Does diet have a significant impact on carnivore $\delta^{18}O_p$?

The oxygen isotope compositions of food macronutrients (protein, fat and carbohydrate), food water as well as metabolic water from catabolism of nutrients, influence $\delta^{18}O_{bw}$ and hence $\delta^{18}O_p$ values of herbivores and carnivores (e.g. [212,219]). The $\delta^{18}O_p$ values of herbivores are also affected by the type of plant consumed. The $\delta^{18}O$ values of plants using the C_4 photosynthetic pathway can be higher than those of C_3 plants (up to 10‰ $\delta^{18}O_{C4-C3}$ difference, [255]), because they are adapted to arid conditions, which leads to extreme ^{18}O enrichment effects in their leaf water and plant cellulose [256]. Differences in $\delta^{18}O_p$ between grazers (C_4-feeders) and browsers (C_3-feeders) have been assigned to a difference in the leaf water $\delta^{18}O$ of the ingested C_3 and C_4 plants [219,226,231,233]. The key prey species of bobcat and puma, rabbits and white-tailed deer, respectively, differ in their dietary preferences and hence their $\delta^{18}O_p$ - $\delta^{18}O_w$ relations. While white-tailed deer are considered to be browsers [257], whose $\delta^{18}O_p$ compositions are almost unaffected by relative humidity [115] (Appendix 2, Figure 7); cottontail rabbits are referred to as grazers [258], whose $\delta^{18}O_p$ compositions are humidity-dependent [121] (Appendix 2, Figure 7). Based on the various prey preferences of bobcat and puma, we would have expected species-specific differences reflected in their $\delta^{18}O_p$ values. However, both feline carnivores exhibited a statistically indistinguishable linear relationship of $\delta^{18}O_p$ and $\delta^{18}O_w$ (Figure 6, Appendix 3), with the puma showing a slightly weaker $\delta^{18}O_p$ - $\delta^{18}O_w$ relation ($R^2 = 0.39$, $p < 0.0001$; Figure 5) than the bobcat ($R^2 = 0.50$, $p < 0.0001$; Figure 4).

A review of the few stable isotope studies on fossil carnivores revealed the existence of three contrary hypotheses concerning the impact of diet on carnivore $\delta^{18}O_p$ values (Figure 10):
First, carnivores have $\delta^{18}O_p$ values similar to those of their consumed herbivore prey [226]. This explanation seems plausible especially for felids, which are strict carnivores that obtain much of their body water from the consumption of prey [131]. The $\delta^{18}O_p$ data from puma and deer of our study confirm this hypothesis, as their $\delta^{18}O_p$ - $\delta^{18}O_w$ relationship was statistically identical (Tukey test: $p = 0.629$; Appendix 3, Figures 5 and 10A). However this does not apply to bobcats, whose $\delta^{18}O_p$ - $\delta^{18}O_w$ relationship was statistically different from rabbits (Appendix 3, Figures 4 and 10A).

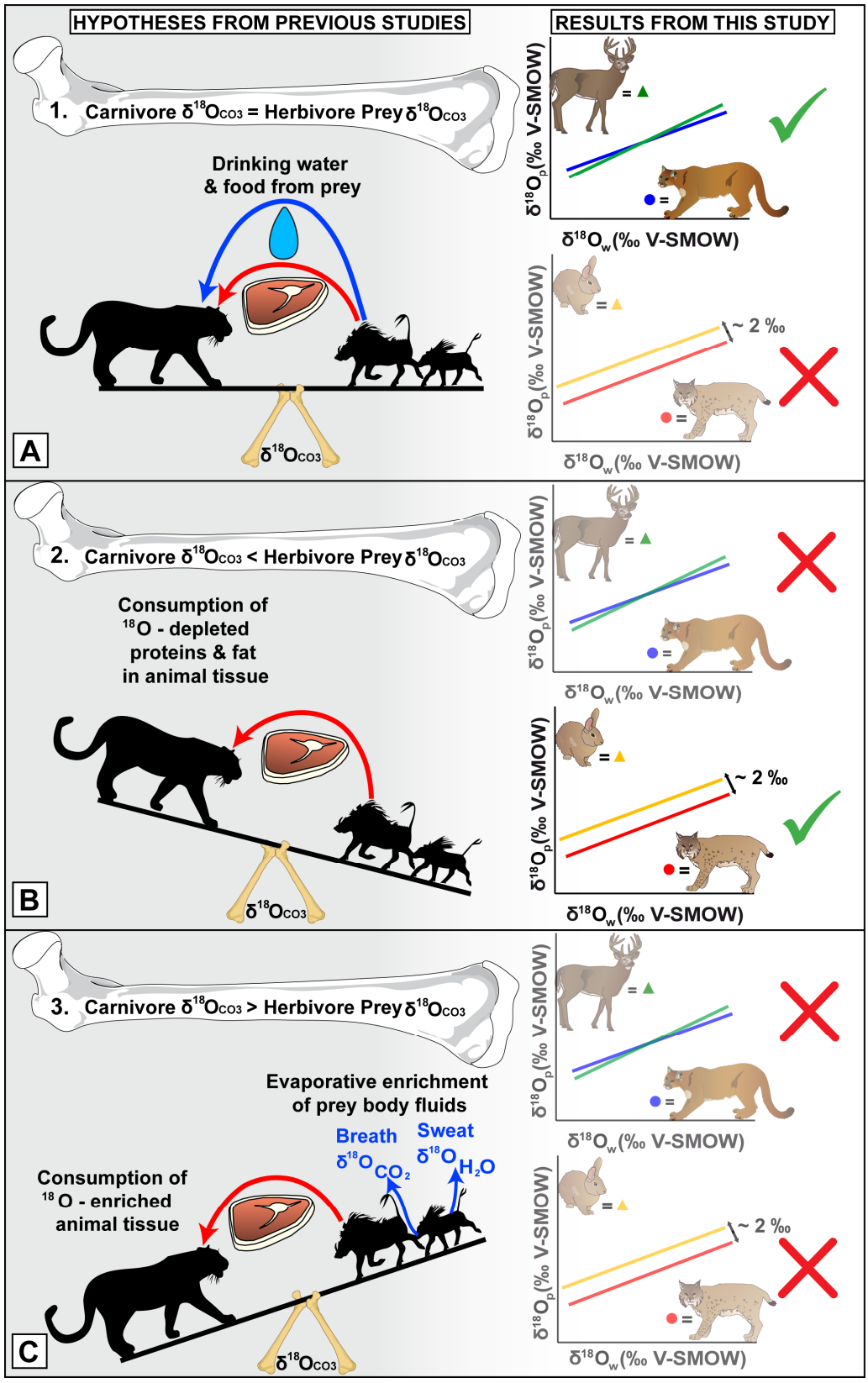

Figure 10. Oxygen isotope model of herbivores and carnivores. A model of oxygen isotopes in skeletal apatite of herbivorous prey versus carnivorous predators. Three contrary hypotheses concerning the impact of diet on carnivore $\delta^{18}O_{CO3}$ values are schematically illustrated and compared with the results obtained for $\delta^{18}O_p$ in our study (on the right). The capital letters illustrate the three published hypotheses: A: Carnivore $\delta^{18}O_{CO3}$ = Herbivore $\delta^{18}O_{CO3}$ [226]; B: Carnivore $\delta^{18}O_{CO3}$ < Herbivore $\delta^{18}O_{CO3}$ [240,259]; C: Carnivore $\delta^{18}O_{CO3}$ > Herbivore $\delta^{18}O_{CO3}$ [205].

Second, carnivores have significantly lower $\delta^{18}O_p$ values in comparison to both browsing and grazing herbivores [240,259]. Carnivores consume animal tissues containing high proportions of protein and fat in contrast to herbivores, whose plant-dominated diet consists mainly of carbohydrates. Proteins are depleted in ^{18}O compared to carbohydrates [143,255,256,260], thus carnivores should have lower $\delta^{18}O_p$ values than herbivores [240]. This can be observed for bobcats having about 2‰ lower $\delta^{18}O_p$ values than rabbits but not for pumas and deer, which both have similar $\delta^{18}O_p$ (Figures 4, 5, 10B).

Third, carnivores are enriched over their herbivorous prey [205]. Isotope fractionation from drinking water to body water occurs [112,119,154] and may play an important role in ^{18}O enrichment of carnivore $\delta^{18}O_p$. Feline carnivores consume prey species, whose $\delta^{18}O_{bw}$ are expected to be higher than the local $\delta^{18}O_w$. This isotopic enrichment of prey body fluids (i.e., milk, urine, blood, plasma, etc.) in ^{18}O can be explained by evaporative enrichment from insensible water loss through skin and breath vapour loss [105,111,197,212]. Consequently, carnivores mainly consuming ^{18}O-enriched prey should have higher $\delta^{18}O_{bw}$ (and hence $\delta^{18}O_p$) values compared to those of their prey. A similar process has been documented in humans for the consumption of milk and the resulting ^{18}O enrichment in consumer tissues [204,235,261]. However, our data do not support the hypothesis of ^{18}O enrichment in carnivores relative to their prey (Figures 4, 5, 10C).

Based on this information it seems likely that animals with different diets (i.e. herbivores, omnivores and carnivores) track $\delta^{18}O_w$ values of meteoric water differently. This becomes particularly clear, if we compare feline with canid carnivores, like foxes. Felids and foxes belong both to the same order Carnivora, but from a nutritional perspective canids (i.e. fox) are considered omnivores (Figure 6). Consequently, foxes exhibit a very good linear relationship of $\delta^{18}O_p$ and $\delta^{18}O_w$ ($R^2 = 0.98$, $p < 0.0001$; Figure 6) and thus differ statistically from feline carnivores (Tukey test: $p = 0.050$; Appendix 3). Dietary effects on $\delta^{18}O_p$ are therefore assumed to be of particular importance in feline carnivores, as they predominantly obtain their food water and drinking water from their prey. Significant seasonal variations in carnivore isotope compositions can be expected, if their dietary patterns change throughout the year [212]. Although North American bobcats and pumas are generally specialized on one major prey (i.e. rabbits: [147] and white-tailed deer: [146], respectively), they are capable to catch and eat many different kinds of animals, if their key prey is limited in certain areas or seasons (puma: [248,249]; bobcat: [147]) (Figures 4 and 5). A carnivore prey spectrum that varies irregularly in space and time during bone mineralisation and isotopic incorporation, might thus contribute to the rather moderate $\delta^{18}O_p$ - $\delta^{18}O_w$ relation of feline carnivores ($R^2 = 0.46$, $p < 0.0001$) compared to the good all mammal correlation ($R^2 = 0.76$, $p < 0.0001$; Figure 3). Currently we lack a testable explanation, why the observed $\delta^{18}O_p$ values of predator and prey differ in bobcat and puma (Figure 10 A, B). Considering the different prey

spectra of these felids, we hypothesized that the puma is more a specialist predator (i.e. large mammals, Figure 5), whereas the bobcat is rather a generalist predator (i.e. birds, reptiles, small mammals, Figure 4). This might explain why puma and white-tailed deer have similar $\delta^{18}O_p$ values in contrast to bobcats and rabbits (Figure 10). Nonetheless, we assume that diet explains only a part of the deviation from an all mammal oxygen isotope $\delta^{18}O_p$ - $\delta^{18}O_w$ relation.

4.4.3. How does behaviour affect carnivore $\delta^{18}O_p$?

Behavioural mechanisms like migration were demonstrated to also influence the oxygen isotope composition of biogenic apatite from fish and mammals [113,262,263] as well as humans [208,211,261,264]. Migration between isotopically distinct biomes during bone or tooth formation can affect the correlation between $\delta^{18}O_p$ and $\delta^{18}O_w$.

Such effects would not be unexpected given the known species- or sex-specific behavioural differences characterizing our study species. Puma and bobcat, and their respective prey species, have significantly different home range sizes, which are also known to vary between seasons and sex [11,149,257,258]. Our data are in accordance with the hypothesis that migratory behaviour might affect feline carnivore $\delta^{18}O_p$. It is a well-known phenomenon that changes in staple prey activity and distribution [265,266] may influence puma migratory behaviour both spatially and temporally [267]. This might explain why migratory puma display a weaker $\delta^{18}O_p$ - $\delta^{18}O_w$ relation ($R^2 = 0.39$, $p < 0.0001$, Figure 5) than non-migratory bobcat ($R^2 = 0.50$, $p < 0.0001$, Figure 4). However, although carnivores exhibit typical mammalian dispersal behaviour, where males disperse and females are philopatric [150], we did not observe an effect of sex on the $\delta^{18}O_p$ - $\delta^{18}O_w$ relation for both carnivore species (Appendix 2). Given that even bobcat display a much weaker $\delta^{18}O_p$ - $\delta^{18}O_w$ relation than most other mammals, although they (and their key prey) are non-migratory, leads us to the assumption, that additional factors like physiology and metabolism might play an important role.

4.4.4. How do physiological and metabolic adaptations influence carnivore $\delta^{18}O_p$?

Physiological factors contributing to a species-specific $\delta^{18}O_w$ - $\delta^{18}O_p$ relation include body water loss via sweating or panting [212,219], water turnover [105], water conservation mechanisms [212,218,219,234] and metabolic rate [102].

Terrestrial mammals usually use a large amount of water for evaporative cooling of their body, which contributes to evaporative water loss and thus affects their $\delta^{18}O_{bw}$ and hence $\delta^{18}O_p$. Differences in the isotope compositions of liquid water during sweating versus water vapor during panting should affect the animal's body water $\delta^{18}O_{bw}$. Cats lose water primarily through panting [181] and only secondarily from sweat glands of foot pads [182]. Panting cats should thus have higher $\delta^{18}O_{bw}$ and $\delta^{18}O_p$ values than animals that sweat because water vapour lost in panting is more depleted in ^{18}O [107,183].

Moreover, drinking water volume exerts a significant positive physiological control on the oxygen isotopic composition of human body water [103] and presumably also on felid $\delta^{18}O_{bw}$. Felids are strict carnivores that obtain much of their body water from the consumption of prey [131]. Food water and drinking water in free-ranging cats are hence primarily recruited from the same source - the prey. Controlled experiments on domestic cats have shown that felids are not obligate drinkers: on average, only 1% of their total water input originates from drinking water [148]. Reduced water turnover in cats thus appears to be a factor affecting the $\delta^{18}O_p$ - $\delta^{18}O_w$ relation.

In addition, Luz et al. [116] noticed that $\delta^{18}O_p$ values of water-conserving desert animals are not very sensitive to variations in $\delta^{18}O_w$. Cats have developed several water conservation mechanisms which facilitate their survival in extreme environments. For instance, felids are not only known to drink to a limited extent [132,162] but also excrete concentrated urine [176-178]. They have hence developed alternative sources to compensate the drinking water input. Cats have the ability to digest and utilize high levels of dietary fat and protein, and oxidation of these energy-containing substances leads to the production of relatively high levels of metabolic water [131,162,163]. Metabolic water contributes on average 10% to their total water intake [131,162]. However, catabolism of macronutrients and production of metabolic water are both metabolic reactions that potentially alter $\delta^{18}O_{bw}$ which then deviates from $\delta^{18}O_w$ values of the ambient meteoric water [112,118].

Moreover, the animal's basal metabolic rate seems to play a prominent role for a constant fractionation of $\delta^{18}O_p$ and $\delta^{18}O_w$. Large mammals, that are obligate drinkers and tend to have lower metabolisms, are more likely to track $\delta^{18}O_w$ values of drinking waters [105,108,116]. On the contrary, a high basal metabolic rate associated with a low rate of drinking, results in a weak correlation of $\delta^{18}O_p$ with $\delta^{18}O_w$ [102]. Felids are known to have high basal metabolic rates (BMR) by general mammalian standards [180,268]. A recent phylogenetic analysis suggests that BMR is correlated with diet among the order of Carnivora; species that eat meat have larger home ranges and higher mass-adjusted BMRs than herbivorous or omnivorous species [269]. This might explain why other closely related species like foxes, which are characterized by an omnivorous lifestyle [131], display a much better $\delta^{18}O_p$ - $\delta^{18}O_w$ regression ($R^2 = 0.98$, $p < 0.0001$, Figure 6) than strict carnivores like bobcat ($R^2 = 0.50$, $p < 0.0001$, Figure 4) and puma ($R^2 = 0.39$, $p < 0.0001$, Figure 5).

4.4.5. Do different tissue-types display similar $\delta^{18}O_{tissue}$ - $\delta^{18}O_w$ relations?

A recent water isotope study on hair of feline carnivores by Pietsch et al. [247] demonstrates that both puma and bobcat completely lacked the expected correlation between water isotopes in local water and hair, and also exhibited a complete decoupling between oxygen and hydrogen isotopes in hair. In this study, we additionally conducted intra-individual tissue

comparisons of $\delta^{18}O$ in bobcats and found that $\delta^{18}O_p$ shows a much better relation with $\delta^{18}O_w$ than $\delta^{18}O_h$ (Appendix 4, Figure 8). Moreover, there was no significant correlation between $\delta^{18}O_p$ and $\delta^{18}O_h$ of the same bobcat individuals (Appendix 4, Figure 9). This contrasts with observations made for macaque monkeys by O'Regan et al. [252], who found that hair and bone apatite $\delta^{18}O$ are highly correlated within individuals.

In consideration of these findings, different factors in feline carnivores happen to interfere with the oxygen isotopic routing and incorporation from meteoric water into body water and different body tissues like bone phosphate and hair. Given that mammal bone phosphate precipitates in oxygen isotopic equilibrium with body water [108,116], we assume that factors related to diet, physiology and metabolism alter $\delta^{18}O_{bw}$ and thus lead to an only moderate $\delta^{18}O_p$ - $\delta^{18}O_w$ relation, deviating from those of other placental mammals and canid carnivores (Figure 3). Despite this fact, feline carnivore bone phosphate $\delta^{18}O_p$ still better tracks meteoric water $\delta^{18}O_w$ values than hair (Figure 8). Factors causing the deviations of O and H isotopes from environmental $\delta^{18}O_w$ in feline carnivore hair are most likely attributed to isotopic routing (from food and water) and isotopic incorporation during biosynthesis of hair keratin.

4.5. CONCLUSIONS

Our study on $\delta^{18}O_p$ of North American bobcat and puma bone phosphate yields a relationship with ambient meteoric water of $\delta^{18}O_p = 0.40(\pm0.04) * \delta^{18}O_w + 20.10(\pm 0.40)$ that is significantly different and less well defined than the $\delta^{18}O_p$ - $\delta^{18}O_w$ relation for placental herbivores and omnivores. This finding leads to the following principal conclusions:

a. Climatic factors like relative humidity can indirectly affect the $\delta^{18}O_p$ values of feline carnivores via its prey. Carnivores like pumas consuming humidity-independent prey species (i.e. white-tailed deer) are generally little or not affected by relative humidity. However, $\delta^{18}O_p$ values of bobcats, specialized on humidity-dependent prey (i.e. rabbits), are partially controlled by relative humidity.
b. Dietary effects on $\delta^{18}O_{bw}$ and hence $\delta^{18}O_p$ of feline carnivores are likely because strict carnivory implies specific adaptations of the digestion, physiology and metabolism. Thus a carnivorous diet may at least partly explain why bobcat and puma have a $\delta^{18}O_p$ - $\delta^{18}O_w$ relation deviating from that of other omnivorous and herbivorous mammals.
c. Felidae exhibit several water conservation mechanisms, like low surface water drinking rate (<1%), water supply from the consumption of prey, excretion of concentrated urine, high-level production of metabolic water through the oxidation of a protein and fat rich diet, and panting. In particular, the low drinking rate combined with a high metabolic rate lead to a $\delta^{18}O_p$ - $\delta^{18}O_w$ deviation in feline carnivores.

d. Behavioural factors like migration between isotopically distinct biomes during bone mineralisation may be responsible for the observed small differences of $\delta^{18}O_p$ - $\delta^{18}O_w$ relations between non-migrating bobcats and migrating pumas. However, no differences could be detected between sexes.
e. Physiological and metabolic adaptations of felids probably have the greatest impact on the observed deviation between $\delta^{18}O_p$ and $\delta^{18}O_w$ in feline carnivores.
f. One major implication of this study is that $\delta^{18}O_p$ of feline carnivores do not trace meteoric water $\delta^{18}O_w$ values better than those of herbivores and omnivores. Thus palaeoclimate reconstructions using oxygen isotope analysis of fossil carnivore skeletal remains and the $\delta^{18}O_p$ - $\delta^{18}O_w$ transfer function of modern feline carnivores are less precise than using herbivores. Furthermore, $\delta^{18}O_p$ fingerprinting has a lower spatial resolution for provenance determination of carnivores than for herbivores.
g. Controlled feeding experiments in combination with isotopic monitoring of body water (i.e. blood, urine) and different tissue types are now needed to elucidate the mechanisms of oxygen isotopic routing and incorporation in feline carnivores.

AUTHOR CONTRIBUTIONS

Conceived and designed the experiments: SJP, TT. Analyzed the data: SJP. Wrote the manuscript: SJP, TT.

ACKNOWLEDGMENTS

We thank Robert Fischer and Suzanne C. Peurach from the mammal collection at the Smithsonian Natural History Museum in Washington D.C., Eric A. Rickart from the Utah Museum of Natural History, and Bryan T. Hamilton from the Great Basin National Park in Nevada for their assistance with the sample collection. We thank Aurélien Bernard for his constructive and helpful comments. We also thank Philipp Herrmann for his assistance with the stable isotope preparation. The animal symbols used for figures are courtesy of the Integration and Application Network (www.ian.umces.edu/symbols), University of Maryland Center for Environmental Science.

5. REFERENCES

1. Broad S, Mulliken T, Roe D (2003) The nature and extent of legal and illegal trade in wildlife. The trade in wildlife: regulation for conservation. London: Earthscan Publications Ltd.
2. Vince K (2002) Organised gangs target wildlife trade. Available: http://www.newscientist.com/article/dn2413.
3. Knapp A, Affre A (2007) A briefing paper on marking techniques used in the control of wildlife in the European Union. Brussels: A TRAFFIC Europe Report for the European Commission. 36 p.
4. Shepherd C, Njiman V (2008) The wild cat trade in Myanmar. Selangor, Malaysia: TRAFFIC Southeast Asia.
5. Oswell A (2010) The Big Cat Trade in Myanmar and Thailand. Selangor, Malaysia: TRAFFIC Southeast Asia.
6. Meyer R, Höfelein C, Lüthy J, Candrian U (1995) Polymerase chain reaction-restriction fragment length polymorphism analysis: a simple method for species identification in food. Journal of AOAC international 78: 1542-1551.
7. Schwenke PL, Rhydderch JG, Ford MJ, Marshall AR, Park LK (2006) Forensic identification of endangered Chinook Salmon (Oncorhynchus tshawytscha) using a multilocus SNP assay. Conservation Genetics 7: 983-989.
8. Walker JA, Hughes DA, Hedges DJ, Anders BA, Laborde ME, et al. (2004) Quantitative PCR for DNA identification based on genome-specific interspersed repetitive elements. Genomics 83: 518-527.
9. Wan QH, Fang SG (2003) Application of species-specific polymerase chain reaction in the forensic identification of tiger species. Forensic science international 131: 75-78.
10. Wasser SK, Mailand C, Booth R, Mutayoba B, Kisamo E, et al. (2007) Using DNA to track the origin of the largest ivory seizure since the 1989 trade ban. Proceedings of the National Academy of Sciences 104: 4228.
11. Nowell K, Jackson P (1996) Wild cats: status survey and conservation action plan. Gland, Switzerland: International Union for Conservation of Nature and Natural Resources. 383 p.
12. Johnson WE, Eizirik E, Pecon-Slattery J, Murphy WJ, Antunes A, et al. (2006) The late Miocene radiation of modern Felidae: a genetic assessment. Science 311: 73-77.
13. Baillie JEM, Hilton-Taylor C, Stuart SN (2004) IUCN Red List of Threatened Species. A Global Species Assessment. Gland, Switzerland and Cambridge, UK: IUCN.
14. Baker CS, Palumbi SR (1994) Which whales are hunted? A molecular genetic approach to monitoring whaling. Science(Washington) 265: 1538-1539.

15. Wetton JH, Tsang CSF, Roney CA, Spriggs AC (2002) An extremely sensitive species-specific ARMS PCR test for the presence of tiger bone DNA. Forensic science international 126: 137-144.
16. Upadhyay SK, Ali S, Sharma K (2007) Tiger Poaching and Trade in Asia: An Overview. Biodiversity & Environment: 157.
17. Dawnay N, Ogden R, McEwing R, Carvalho GR, Thorpe RS (2007) Validation of the barcoding gene COI for use in forensic genetic species identification. Forensic science international 173: 1-6.
18. Folmer O, Black M, Hoeh W, Lutz R, Vrijenhoek R (1994) DNA primers for amplification of mitochondrial cytochrome c oxidase subunit I from diverse metazoan invertebrates. Molecular Marine Biology and Biotechnology 3: 294-299.
19. Hebert PDN, Cywinska A, Ball SL, DeWaard JR (2003) Biological identifications through DNA barcodes. Proceedings of the Royal Society of London Series B: Biological Sciences 270: 313-321.
20. Eaton MJ, Meyers GL, Kolokotronis SO, Leslie MS, Martin AP, et al. (2010) Barcoding bushmeat: molecular identification of Central African and South American harvested vertebrates. Conservation Genetics 11: 1389-1404.
21. Naro Maciel E, Reid B, Fitzsimmons NN, Le M, DeSalle R, et al. (2010) DNA barcodes for globally threatened marine turtles: a registry approach to documenting biodiversity. Molecular Ecology Resources 10: 252-263.
22. Wong EHK, Hanner RH (2008) DNA barcoding detects market substitution in North American seafood. Food Research International 41: 828-837.
23. Wong EHK, Shivji MS, Hanner RH (2009) Identifying sharks with DNA barcodes: assessing the utility of a nucleotide diagnostic approach. Molecular Ecology Resources 9: 243-256.
24. Bensasson D, Zhang DX, Hartl DL, Hewitt GM (2001) Mitochondrial pseudogenes: evolution's misplaced witnesses. Trends in Ecology & Evolution 16: 314-321.
25. Song H, Buhay JE, Whiting MF, Crandall KA (2008) Many species in one: DNA barcoding overestimates the number of species when nuclear mitochondrial pseudogenes are coamplified. Proceedings of the National Academy of Sciences 105: 13486-13491.
26. Antunes A, Ramos MJ (2005) Discovery of a large number of previously unrecognized mitochondrial pseudogenes in fish genomes. Genomics 86: 708-717.
27. Benesh DP, Hasu T, Suomalainen LR, Valtonen ET, Tiirola M (2006) Reliability of mitochondrial DNA in an acanthocephalan: the problem of pseudogenes. International Journal for Parasitology 36: 247-254.

28. Lopez JV, Yuhki N, Masuda R, Modi W, O'Brien SJ (1994) Numt, a recent transfer and tandem amplification of mitochondrial DNA to the nuclear genome of the domestic cat. Journal of Molecular Evolution 39: 174-190.

29. Sorenson MD, Quinn TW (1998) Numts: a challenge for avian systematics and population biology. The Auk 115: 214-221.

30. Williams ST, Knowlton N (2001) Mitochondrial pseudogenes are pervasive and often insidious in the snapping shrimp genus Alpheus. Molecular Biology and Evolution 18: 1484-1493.

31. Zhang DX, Hewitt GM (1996) Nuclear integrations: challenges for mitochondrial DNA markers. Trends in Ecology & Evolution 11: 247-251.

32. Thalmann O, Hebler J, Poinar HN, Pääbo S, Vigilant L (2004) Unreliable mtDNA data due to nuclear insertions: a cautionary tale from analysis of humans and other great apes. Molecular Ecology 13: 321-335.

33. Hebert PDN, Penton EH, Burns JM, Janzen DH, Hallwachs W (2004) Ten species in one: DNA barcoding reveals cryptic species in the neotropical skipper butterfly Astraptes fulgerator. Proceedings of the National Academy of Sciences of the United States of America 101: 14812-14817.

34. Collura RV, Stewart CB (1995) Insertions and duplications of mtDNA in the nuclear genomes of Old World monkeys and hominoids. Nature 378: 485-489.

35. Zischler H, Geisert H, von Haeseler A, Paabo S (1995) A nuclear 'fossil' of the mitochondrial D-loop and the origin of modern humans. Nature 378: 489-492.

36. Thalmann O, Serre D, Hofreiter M, Lukas D, Eriksson J, et al. (2005) Nuclear insertions help and hinder inference of the evolutionary history of gorilla mtDNA. Molecular Ecology 14: 179-188.

37. Hazkani-Covo E, Zeller RM, Martin W (2010) Molecular poltergeists: mitochondrial DNA copies (numts) in sequenced nuclear genomes. PLoS Genetics 6. Available: http://www.plosgenetics.org/article/info%3Adoi%2F10.1371%2Fjournal.pgen.1000834 .

38. Richly E, Leister D (2004) NUMTs in sequenced eukaryotic genomes. Molecular Biology and Evolution 21: 1081-1084.

39. Richly E, Leister D (2004) NUPTs in sequenced eukaryotes and their genomic organization in relation to NUMTs. Molecular Biology and Evolution 21: 1972-1982.

40. Pereira S, Baker A (2004) Low number of mitochondrial pseudogenes in the chicken (Gallus gallus) nuclear genome: implications for molecular inference of population history and phylogenetics. BMC Evolutionary Biology 4. Available: http://www.biomedcentral.com/1471-2148/4/17.

41. Podnar M, Haring E, Pinsker W, Mayer W (2007) Unusual origin of a nuclear pseudogene in the Italian wall lizard: intergenomic and interspecific transfer of a large section of the mitochondrial genome in the genus Podarcis (Lacertidae). Journal of Molecular Evolution 64: 308-320.

42. Jensen Seaman MI, Sarmiento EE, Deinard AS, Kidd KK (2004) Nuclear integrations of mitochondrial DNA in gorillas. American journal of primatology 63: 139-147.

43. Mirol PM, Mascheretti S, Searle JB (2000) Multiple nuclear pseudogenes of mitochondrial cytochrome b in Ctenomys (Caviomorpha, Rodentia) with either great similarity to or high divergence from the true mitochondrial sequence. Heredity 84: 538-547.

44. Martins Jr J, Solomon S, Mikheyev A, Mueller U, Ortiz A, et al. (2007) Nuclear mitochondrial like sequences in ants: evidence from Atta cephalotes (Formicidae: Attini). Insect Molecular Biology 16: 777-784.

45. Pamilo P, Viljakainen L, Vihavainen A (2007) Exceptionally high density of NUMTs in the honeybee genome. Molecular Biology and Evolution 24. Available: http://mbe.oxfordjournals.org/content/24/6/1340.short.

46. Kim JH, Antunes A, Luo SJ, Menninger J, Nash WG, et al. (2006) Evolutionary analysis of a large mtDNA translocation (numt) into the nuclear genome of the Panthera genus species. Gene 366: 292-302.

47. Moulton MJ, Song H, Whiting MF (2010) Assessing the effects of primer specificity on eliminating numt coamplification in DNA barcoding: a case study from Orthoptera (Arthropoda: Insecta). Molecular Ecology Resources 10: 615-627.

48. Greenwood AD, Pääbo S (1999) Nuclear insertion sequences of mitochondrial DNA predominate in hair but not in blood of elephants. Molecular Ecology 8: 133-137.

49. Kolokotronis SO, MacPhee R, Greenwood A (2007) Detection of mitochondrial insertions in the nucleus (NuMts) of Pleistocene and modern muskoxen. BMC Evolutionary Biology 7. Available: http://www.biomedcentral.com/1471-2148/7/67/abstract/.

50. Sorenson MD, Fleischer RC (1996) Multiple independent transpositions of mitochondrial DNA control region sequences to the nucleus. Proceedings of the National Academy of Sciences 93: 15239-15243.

51. Antunes A, Pontius J, Ramos MJ, O'Brien SJ, Johnson WE (2007) Mitochondrial introgressions into the nuclear genome of the domestic cat. Journal of Heredity 98: 414-420.

52. Chung WK, Steiper ME (2008) Mitochondrial COII introgression into the nuclear genome of Gorilla gorilla. International journal of primatology 29: 1341-1353.

53. Triant DA, DeWoody JA (2008) Molecular analyses of mitochondrial pseudogenes within the nuclear genome of arvicoline rodents. Genetica 132: 21-33.

54. Arthofer W, Schüler S, Steiner FM, Schlick Steiner BC (2010) NEWS AND VIEWS: Chloroplast DNA based studies in molecular ecology may be compromised by nuclear encoded plastid sequence. Molecular Ecology 19: 3853–3856.

55. Calvignac S, Konecny L, Malard F, Douady CJ (2011) Preventing the pollution of mitochondrial datasets with nuclear mitochondrial paralogs (numts). Mitochondrion 11: 246-254.

56. Ibarguchi GIG, Friesen VLFVL, Lougheed SCLSC (2006) Defeating numts: Semi-pure mitochondrial DNA from eggs and simple purification methods for field-collected wildlife tissues. Genome 49: 1438-1450.

57. Gilbert MTP, Tomsho LP, Rendulic S, Packard M, Drautz DI, et al. (2007) Whole-genome shotgun sequencing of mitochondria from ancient hair shafts. Science 317: 1927-1930.

58. Trigo T, Freitas T, Kunzler G, Cardoso L, Silva J, et al. (2008) Inter species hybridization among Neotropical cats of the genus *Leopardus*, and evidence for an introgressive hybrid zone between *L. geoffroyi* and *L. tigrinus* in southern Brazil. Molecular Ecology 17: 4317-4333.

59. Meusnier I, Singer G, Landry JF, Hickey D, Hebert P, et al. (2008) A universal DNA mini-barcode for biodiversity analysis. BMC Genomics 9. Available: http://www.biomedcentral.com/1471-2164/9/214.

60. Ivanova NV, Zemlak TS, Hanner RH, Hebert PDN (2007) Universal primer cocktails for fish DNA barcoding. Molecular Ecology Notes 7: 544-548.

61. Sonnenberg R, Nolte AW, Tautz D (2007) An evaluation of LSU rDNA D1-D2 sequences for their use in species identification. Frontiers in Zoology 4. Available: http://www.frontiersinzoology.com/content/4/1/6.

62. Drummond A, Ashton B, Buxton S, Cheung M, Cooper A, et al. Geneious v5. 1. Biomatters Ltd, Auckland, New Zealand.

63. Kimura M (1980) A simple method for estimating evolutionary rates of base substitutions through comparative studies of nucleotide sequences. Journal of Molecular Evolution 16: 111-120.

64. Rubinoff D, Cameron S, Will K (2006) A genomic perspective on the shortcomings of mitochondrial DNA for “barcoding” identification. Journal of Heredity 97: 581-594.

65. Sorenson MD, Ast JC, Dimcheff DE, Yuri T, Mindell DP (1999) Primers for a PCR-based approach to mitochondrial genome sequencing in birds and other vertebrates. Molecular Phylogenetics and Evolution 12: 105-114.

66. Magnacca K, Brown M (2010) Mitochondrial heteroplasmy and DNA barcoding in Hawaiian Hylaeus (Nesoprosopis) bees (Hymenoptera: Colletidae). BMC Evolutionary Biology 10. Available: http://www.biomedcentral.com/1471-2148/10/174.

67. Anthony NM, Clifford SL, Bawe-Johnson M, Abernethy KA, Bruford MW, et al. (2007) Distinguishing gorilla mitochondrial sequences from nuclear integrations and PCR recombinants: Guidelines for their diagnosis in complex sequence databases. Molecular Phylogenetics and Evolution 43: 553-566.

68. Dubey S, Michaux J, Brünner H, Hutterer R, Vogel P (2009) False phylogenies on wood mice due to cryptic cytochrome-b pseudogene. Molecular Phylogenetics and Evolution 50: 633-641.

69. Hazkani-Covo E, Graur D (2007) A comparative analysis of numt evolution in human and chimpanzee. Molecular Biology and Evolution 24: 13-18.

70. Patterson N, Richter DJ, Gnerre S, Lander ES, Reich D (2006) Genetic evidence for complex speciation of humans and chimpanzees. Nature 441: 1103-1108.

71. Altschul SF, Madden TL, Schäffer AA, Zhang J, Zhang Z, et al. (1997) Gapped BLAST and PSI-BLAST: a new generation of protein database search programs. Nucleic Acids Research 25: 3389-3402.

72. Hebert PDN, Stoeckle MY, Zemlak TS, Francis CM (2004) Identification of birds through DNA barcodes. PLoS Biology 2. Available: http://www.plosbiology.org/article/info%3Adoi%2F10.1371%2Fjournal.pbio.0020312.

73. Moritz C, Cicero C (2004) DNA barcoding: promise and pitfalls. PLoS Biology 2. Available: http://www.plosbiology.org/article/info%3Adoi%2F10.1371%2Fjournal.pbio.0020354.

74. Driscoll CA, Menotti-Raymond M, Roca AL, Hupe K, Johnson WE, et al. (2007) The Near Eastern origin of cat domestication. Science 317: 519-523.

75. Hertwig S, Schweizer M, Stepanow S, Jungnickel A, Böhle UR, et al. (2009) Regionally high rates of hybridization and introgression in German wildcat populations (*Felis silvestris*, Carnivora, Felidae). Journal of Zoological Systematics and Evolutionary Research 47: 283-297.

76. Oliveira R, Godinho R, Randi E, Ferrand N, Alves PC (2008) Molecular analysis of hybridisation between wild and domestic cats (*Felis silvestris*) in Portugal: implications for conservation. Conservation Genetics 9: 1-11.

77. Randi E (2008) Detecting hybridization between wild species and their domesticated relatives. Molecular Ecology 17: 285-293.

78. Frézal L, Leblois R (2008) Four years of DNA barcoding: current advances and prospects. Infection, Genetics and Evolution 8: 727-736.

79. Vila C, Walker C, Sundqvist A, Flagstad Ø, Andersone Z, et al. (2003) Combined use of maternal, paternal and bi-parental genetic markers for the identification of wolf–dog hybrids. Heredity 90: 17-24.

80. Bowen GJ, Wassenaar LI, Hobson KA (2005) Global application of stable hydrogen and oxygen isotopes to wildlife forensics. Oecologia 143: 337–348.

81. Hobson KA, Wassenaar LI (2008) Tracking animal migration with stable isotopes; Hobson KA, Wassenaar LI, editors. London, UK: Academic Press. 143 p.

82. West JB, Bowen GJ, Dawson TE, Tu KP (2009) Isoscapes: Understanding Movement, Pattern, and Process on Earth Through Isotope Mapping. New York: Springer Verlag. 487 p.

83. Hénaux V, Powell LA, Hobson KA, Nielsen CK, LaRue MA (2011) Tracking large carnivore dispersal using isotopic clues in claws: an application to cougars across the Great Plains. Methods in Ecology and Evolution 2. Available: http://dx.doi.org/10.1111/j.2041-210X.2011.00107.x.

84. Cryan PM, Bogan MA, Rye RO, Landis GP, Kester CL (2004) Stable hydrogen isotope analysis of bat hair as evidence for seasonal molt and long-distance migration. Journal of Mammalogy 85: 995–1001.

85. Ehleringer JR, Bowen GJ, Chesson LA, West AG, Podlesak DW, et al. (2008) Hydrogen and oxygen isotope ratios in human hair are related to geography. Proceedings of the National Academy of Sciences of the United States of America 105: 2788–2793.

86. Hobson KA (2005) Stable isotopes and the determination of avian migratory connectivity and seasonal interactions. The Auk 122: 1037–1048.

87. Bowen GJ, Revenaugh J (2003) Interpolating the isotopic composition of modern meteoric precipitation. Water Resources Research 39. Available: http://wateriso.eas.purdue.edu/waterisotopes/media/PDFs/2003WR002086.pdf. Accessed 2011 March 8.

88. Dansgaard W (1964) Stable isotopes in precipitation. Tellus 16: 436-468.

89. Rozanski K, Araguás-Araguás L, Gonfiantini R (1993) Isotopic patterns in modern global precipitation. Climate change in continental isotopic records 78: 1–36.

90. Bowen GJ, Ehleringer JR, Chesson LA, Thompson AH, Podlesak DW, et al. (2009) Dietary and Physiological Controls on the Hydrogen and Oxygen Isotope Ratios of Hair from Mid-20th Century Indigenous Populations. American Journal of Physical Anthropology 139: 494–504.

91. Fraser I, Meier-Augenstein W, Kalin R (2006) The role of stable isotopes in human identification: a longitudinal study into the variability of isotopic signals in human hair and nails. Rapid Communications in Mass Spectrometry 20: 1109–1116.

92. O'Brien DM, Wooller MJ (2007) Tracking human travel using stable oxygen and hydrogen isotope analyses of hair and urine. Rapid Communications in Mass Spectrometry 21: 2422–2430.

93. Thompson AH, Chesson LA, Podlesak DW, Bowen GJ, Cerling TE, et al. (2010) Stable Isotope Analysis of Modern Human Hair Collected From Asia (China, India, Mongolia, and Pakistan). American Journal of Physical Anthropology 141: 440–451.

94. Podlesak DW, Torregrossa AM, Ehleringer JR, Dearing MD, Passey BH, et al. (2008) Turnover of oxygen and hydrogen isotopes in the body water, CO_2, hair, and enamel of a small mammal. Geochimica et Cosmochimica Acta 72: 19–35.

95. Nielson KE, Bowen GJ (2010) Hydrogen and oxygen in brine shrimp chitin reflect environmental water and dietary isotopic composition. Geochimica et Cosmochimica Acta 74: 1812–1822.

96. Wang YV, O'Brien DM, Jenson J, Francis D, Wooller MJ (2009) The influence of diet and water on the stable oxygen and hydrogen isotope composition of Chironomidae (Diptera) with paleoecological implications. Oecologia 160: 225–233.

97. Hobson KA, Bowen GJ, Wassenaar LI, Ferrand Y, Lormee H (2004) Using stable hydrogen and oxygen isotope measurements of feathers to infer geographical origins of migrating European birds. Oecologia 141: 477–488.

98. Wolf N, Bowen GJ, del Rio CM (2011) The influence of drinking water on the δD and $\delta^{18}O$ values of house sparrow plasma, blood and feathers. The Journal of Experimental Biology 214: 98–103.

99. Tuross N, Warinner C, Kirsanow K, Kester C (2008) Organic oxygen and hydrogen isotopes in a porcine controlled dietary study. Rapid Communications in Mass Spectrometry 22: 1741–1745.

100. Kirsanow K, Tuross N (2011) Oxygen and hydrogen isotopes in rodent tissues: Impact of diet, water and ontogeny. Palaeogeography, Palaeoclimatology, Palaeoecology: in press.

101. Hobson KA, Atwell L, Wassenaar LI (1999) Influence of drinking water and diet on the stable-hydrogen isotope ratios of animal tissues. Proceedings of the National Academy of Sciences of the United States of America 96: 8003–8006.

102. Luz B, Kolodny Y (1989) Oxygen isotope variation in bone phosphate. Applied Geochemistry 4: 317-323.

103. O'Grady SP, Wende AR, Remien CH, Valenzuela LO, Enright LE, et al. (2010) Aberrant Water Homeostasis Detected by Stable Isotope Analysis. Plos One 5. Available: http://www.plosone.org/article/info%3Adoi%2F10.1371%2Fjournal.pone.0011699. Accessed 2011 Jan 11.

104. Sharp ZD, Atudorei V, Panarello HO, Fernandez J, Douthitt C (2003) Hydrogen isotope systematics of hair: archeological and forensic applications. Journal of Archaeological Science 30: 1709–1716.

105. Bryant JD, Froelich PN (1995) A model of oxygen isotope fractionation in body water of large mammals. Geochimica et Cosmochimica Acta 59: 4523-4537.

106. Bryant JD, Koch PL, Froelich PN, Showers WJ, Genna BJ (1996) Oxygen isotope partitioning between phosphate and carbonate in mammalian apatite. Geochimica et Cosmochimica Acta 60: 5145–5148.

107. Kohn MJ (1996) Predicting animal $\delta^{18}O$: Accounting for diet and physiological adaptation. Geochimica et Cosmochimica Acta 60: 4811–4829.

108. Longinelli A (1984) Oxygen isotopes in mammal bone phosphate: a new tool for paleohydrological and paleoclimatological research? Geochimica et Cosmochimica Acta 48: 385-390.

109. Luz B, Kolodny Y (1985) Oxygen isotope variations in phosphate of biogenic apatites, IV. Mammal teeth and bones. Earth and Planetary Science Letters 75: 29-36.

110. McKechnie AE, Wolf BO, Martínez del Rio C (2004) Deuterium stable isotope ratios as tracers of water resource use: an experimental test with rock doves. Oecologia 140: 191–200.

111. Schoeller DA, Leitch CA, Brown C (1986) Doubly labeled water method: in vivo oxygen and hydrogen isotope fractionation. American Journal of Physiology- Regulatory, Integrative and Comparative Physiology 251: 1137–1143.

112. Tatner P (1988) A model of the natural abundance of oxygen-18 and deuterium in the body water of animals. Journal of Theoretical Biology 133: 267–280.

113. Hobson KA (1999) Tracing origins and migration of wildlife using stable isotopes: a review. Oecologia 120: 314-326.

114. Ayliffe LK, Chivas AR (1990) Oxygen isotope composition of the bone phosphate of Australian kangaroos: potential as a palaeoenvironmental recorder. Geochimica et Cosmochimica Acta 54: 2603-2609.

115. Luz B, Cormie AB, Schwarcz HP (1990) Oxygen isotope variations in phosphate of deer bones. Geochimica et Cosmochimica Acta 54: 1723–1728.

116. Luz B, Kolodny Y, Horowitz M (1984) Fractionation of oxygen isotopes between mammalian bone-phosphate and environmental drinking water. Geochimica et Cosmochimica Acta 48: 1689-1693.

117. Karasov WH, del Rio CM (2007) Physiological ecology: how animals process energy, nutrients, and toxins. Princeton: University Press. 242 p.

118. Pecquerie L, Nisbet RM, Fablet R, Lorrain A, Kooijman SALM (2010) The impact of metabolism on stable isotope dynamics: a theoretical framework. Philosophical Transactions of the Royal Society B: Biological Sciences 365: 3455–3468.

119. Reynard LM, Hedges REM (2008) Stable hydrogen isotopes of bone collagen in palaeodietary and palaeoenvironmental reconstruction. Journal of Archaeological Science 35: 1934–1942.

120. Lott CA, Meehan TD, Heath JA (2003) Estimating the latitudinal origins of migratory birds using hydrogen and sulfur stable isotopes in feathers: influence of marine prey base. Oecologia 134: 505–510.

121. Delgado Huertas A, Iacumin P, Stenni B, Sánchez Chillón B, Longinelli A (1995) Oxygen isotope variations of phosphate in mammalian bone and tooth enamel. Geochimica et Cosmochimica Acta 59: 4299-4305.

122. Birchall J, O'Connell TC, Heaton THE, Hedges REM (2005) Hydrogen isotope ratios in animal body protein reflect trophic level. Journal of Animal Ecology 74: 877–881.

123. Levinson AA, Luz B, Kolodny Y (1987) Variations in oxygen isotopic compositions of human teeth and urinary stones. Applied Geochemistry 2: 367-371.

124. Levin NE, Cerling TE, Passey BH, Harris JM, Ehleringer JR (2006) A stable isotope aridity index for terrestrial environments. Proceedings of the National Academy of Sciences 103: 11201–11205.

125. Daux V, Lécuyer C, Heran MA, Amiot R, Simon L, et al. (2008) Oxygen isotope fractionation between human phosphate and water revisited. Journal of Human Evolution 55: 1138-1147.

126. Bowen GJ, Ehleringer JR, Chesson LA, Stange E, Cerling TE (2007) Stable isotope ratios of tap water in the contiguous United States. Water Resources Research 43. Available: http://wateriso.eas.purdue.edu/waterisotopes/media/PDFs/USATapMap.pdf.

127. Chesson LA, Valenzuela LO, O'Grady SP, Cerling TE, Ehleringer JR (2010) Links between Purchase Location and Stable Isotope Ratios of Bottled Water, Soda, and Beer in the United States. Journal of Agricultural and Food Chemistry 58: 7311–7316.

128. Kennedy CD, Bowen GJ, Ehleringer JR (2011) Temporal variation of oxygen isotope ratios $\delta^{18}O$ in drinking water: Implications for specifying location of origin with human scalp hair. Forensic science international: in press.

129. Chesson LA, Podlesak DW, Thompson AH, Cerling TE, Ehleringer JR (2008) Variation of hydrogen, carbon, nitrogen, and oxygen stable isotope ratios in an American diet: Fast food meals. Journal of Agricultural and Food Chemistry 56: 4084–4091.

130. Fraser I, Meier-Augenstein W (2007) Stable ^{2}H isotope analysis of modern day human hair and nails can aid forensic human identification. Rapid Communications in Mass Spectrometry 21: 3279–3285.

131. MacDonald M, Rogers Q, Morris J (1984) Nutrition of the domestic cat, a mammalian carnivore. Annual Review of Nutrition 4: 521–562.

132. Zoran DL (2002) The carnivore connection to nutrition in cats. Journal of the American Veterinary Medical Association 221: 1559–1567.

133. Cormie AB, Luz B, Schwarcz HP (1994) Relationship between the Hydrogen and Oxygen Isotopes of Deer Bone and Their Use in the Estimation of Relative-Humidity. Geochimica et Cosmochimica Acta 58: 3439–3449.

134. Wassenaar L, Hobson K (2003) Comparative equilibration and online technique for determination of non-exchangeable hydrogen of keratins for use in animal migration studies. Isotopes in Environmental and Health Studies 39: 211–217.

135. Bowen GJ, Wilkinson B (2002) Spatial distribution of $\delta^{18}O$ in meteoric precipitation. Geology 30: 315–318.

136. Coplen TB, Kendall C, VA GSR (2000) Stable hydrogen and oxygen isotope ratios for selected sites of the US Geological Survey's NASQAN and benchmark surface-water networks. Available: http://pubs.usgs.gov/of/2000/ofr00-160/. Accessed 2011 March 8.

137. Dutton A, Wilkinson BH, Welker JM, Bowen GJ, Lohmann KC (2005) Spatial distribution and seasonal variation in $^{18}O/^{16}O$ of modern precipitation and river water across the conterminous USA. Hydrological Processes 19: 4121–4146.

138. Kitchener A (1991) The natural history of the wild cats. Ithaca: Comstock Publishing Associates. 288 p.

139. Sandell M (1989) The mating tactics and spacing patterns of solitary carnivores. Carnivore behavior, ecology, and evolution 1: 164–182.

140. Baker K (1974) Hair growth and replacement in the cat. The British Veterinary Journal 130: 327.

141. Galbraith H (1998) Nutritional and hormonal regulation of hair follicle growth and development. Proceedings of the Nutrition Society 57: 195–205.

142. Ryder ML (1976) Seasonal changes in the coat of the cat. Research in Veterinary Science 21: 280.

143. Epstein S, Thompson P, Yapp CJ (1977) Oxygen and hydrogen isotopic ratios in plant cellulose. Science 198: 1209-1215.

144. Farquhar GD, Lloyd J, Taylor JA, Flanagan LB, Syvertsen JP, et al. (1993) Vegetation effects on the isotope composition of oxygen in atmospheric CO 2. Nature 363: 439-443.

145. Cormie A, Luz B, Schwarcz H (1994) Relationship between the hydrogen and oxygen isotopes of deer bone and their use in the estimation of relative humidity. Geochimica et Cosmochimica Acta 58: 3439-3449.

146. Iriarte JA, Franklin WL, Johnson WE, Redford KH (1990) Biogeographic variation of food habits and body size of the America puma. Oecologia 85: 185–190.

147. Lariviere S, Walton LR (1997) Lynx rufus. Mammalian Species 563: 1–8.

148. Kane E, Rogers Q, Morris J (1981) Feeding behavior of the cat fed laboratory and commercial diets. Nutrition Research 1: 499–507.

149. Lindzey F (1987) Mountain lion. In: Wild furbearer management and conservation in North America Toronto, Canada: Ontario Ministry of Natural Resources. pp. 656–668.

150. Johnson C (1986) Sex-biased philopatry and dispersal in mammals. Oecologia 69: 626-627.

151. Arnay-De-La-Rosa M, Gonzalez-Reimers E, Yanes Y, Velasco-Vazquez J, Romanek CS, et al. (2010) Paleodietary analysis of the prehistoric population of the Canary Islands inferred from stable isotopes (carbon, nitrogen and hydrogen) in bone collagen. Journal of Archaeological Science 37: 1490–1501.

152. Schimmelmann A, Deniro MJ (1986) Stable Isotopic Studies on Chitin. III. The D/H and $^{18}O/^{16}O$ Ratios in Arthropod Chitin. Geochimica et Cosmochimica Acta 50: 1485–1496.

153. DeNiro MJ, Epstein S (1981) Hydrogen Isotope Ratios of Mouse-Tissues Are Influenced by a Variety of Factors Other Than Diet. Science 214: 1374–1375.

154. Gretebeck RJ, Schoeller DA, Socki RA, Davis-Street J, Gibson EK, et al. (1997) Adaptation of the doubly labeled water method for subjects consuming isotopically enriched water. Journal of Applied Physiology 82: 563–570.

155. d'Angela D, Longinelli A (1990) Oxygen isotopes in living mammal's bone phosphate: further results. Chemical Geology: Isotope Geoscience section 86: 75–82.

156. Masud Z, Vallet C, Martin GJ (1999) Stable isotope characterization of milk components and whey ethanol. Journal of Agricultural and Food Chemistry 47: 4693–4699.

157. Estep MF, Hoering TC (1980) Biogeochemistry of the stable hydrogen isotopes. Geochimica et Cosmochimica Acta 44: 1197–1206.

158. Smith B, Epstein S (1970) Biogeochemistry of the stable isotopes of carbon and hydrogen in salt marsh biota. Plant Physiology 46: 738–742.

159. Warinner C, Tuross N (2010) Brief communication: Tissue isotopic enrichment associated with growth depression in a pig: Implications for archaeology and ecology. American Journal of Physical Anthropology 141: 486–493.

160. Takeda H, Lu HM, Miyamoto K, Fuma S, Yanagisawa K, et al. (2001) Comparative biokinetics of tritium in rats during continuous ingestion of tritiated water and tritium-labeled food. International Journal of Radiation Biology 77: 375–381.

161. Wallach ADWAD, Inbar MIM, Scantlebury MSM, Speakman JRSJR, Shanas USU (2007) Water requirements as a bottleneck in the reintroduction of European roe deer to the southern edge of its range. Canadian Journal of Zoology 85: 1182-1192.

162. Hendriks W, Wamberg S, Tarttelin M (1999) A metabolism cage for quantitative urine collection and accurate measurement of water balance in adult cats (*Felis catus*). Journal of Animal Physiology and Animal Nutrition 82: 94–105.

163. Mellanby K (1942) Metabolic water and desiccation. Nature 150: 21.

164. Kromhout D (2005) Fish consumption, n-3 fatty acids, and coronary heart disease. In: Coronary heart disease epidemiology. New York: Oxford University Press. pp. 264–275.

165. Morris JG (1985) Nutritional and metabolic responses to arginine deficiency in carnivores. Journal of Nutrition 115: 524–531.

166. Kirk CA, Debraekeleer J, Armstrong PJ (2000) Normal cats. In: Hand MS, Thatcher CD, Remillard RL, Roudebush P, editors. Small animal clinical nutrition 4th ed. Marceline, MO: Walsworth Publishing Co. pp. 291–351.

167. Buchardt B, Bunch V, Helin P (2007) Fingernails and diet: stable isotope signatures of a marine hunting community from modern Uummannaq, North Greenland. Chemical Geology 244: 316–329.

168. Cohen JE (1994) Marine and Continental Food Webs - 3 Paradoxes. Philosophical Transactions of the Royal Society of London B 343: 57–69.

169. Gibson R, Sinclair A (1981) Are Eskimos obligate carnivores? Lancet 1: 1100.

170. Symes CT, Woodborne S (2010) Migratory connectivity and conservation of the Amur Falcon *Falco amurensis*: a stable isotope perspective. Bird Conservation International 20: 134–148.

171. Meehan TD, Rosenfield RN, Atudore VN, Bielefeldt J, Rosenfield LJ, et al. (2003) Variation in hydrogen stable-isotope ratios between adult and nestling Cooper's Hawks. Condor 105: 567–572.

172. Smith AD, Donohue K, Dufty Jr AM (2008) Intrafeather and intraindividual variation in the stable-hydrogen isotope δD content of raptor feathers. The Condor 110: 500–506.

173. Legrand-Defretin V (1994) Differences between cats and dogs: a nutritional view. Proceedings of the Nutrition Society 53: 15–24.

174. Kienzle E (1993) Carbohydrate metabolism of the cat 1. Activity of amylase in the gastrointestinal tract of the cat. Journal of Animal Physiology and Animal Nutrition 69: 92–101.

175. Martínez del Rio C, Wolf N, Carleton SA, Gannes LZ (2009) Isotopic ecology ten years after a call for more laboratory experiments. Biological Reviews 84: 91–111.

176. Anderson R (1982) Water balance in the dog and cat. Journal of Small Animal Practice 23: 588–598.

177. Chew RM (1965) Water metabolism of mammals. In: Mayer RV, Van Gelder RG, editors. Physiological mammalogy. New York Academic Press. pp. 43–178.

178. Schmidt-Nielsen K, Schmidt-Nielsen B (1952) Water Metabolism of Desert Mammals. Physiological Reviews 32: 135–166.

179. McNab BK (1986) The influence of food habits on the energetics of eutherian mammals. Ecological Monographs 56: 1–19.

180. McNab BK (2000) The standard energetics of mammalian carnivores: Felidae and Hyaenidae. Canadian Journal of Zoology 78: 2227-2239.

181. Doris PA, Baker MA (1981) Effect of Dehydration on Thermoregulation in Cats Exposed to High Ambient-Temperatures. Journal of Applied Physiology 51: 46–54.

182. Adams T (1966) Characteristics of eccrine sweat gland activity in the footpad of the cat. Journal of Applied Physiology 21: 1004–1012.

183. Wong W, Cochran W, Klish W, Smith EO, Lee L, et al. (1988) In vivo isotope-fractionation factors and the measurement of deuterium-and oxygen-18-dilution spaces from plasma, urine, saliva, respiratory water vapor, and carbon dioxide. American Journal of Clinical Nutrition 47: 1–6.

184. Homberger DG, Ham K, Ogunbakin T, Bonin JA, Hopkins BA, et al. (2009) The structure of the cornified claw sheath in the domesticated cat (*Felis catus*): implications for the claw shedding mechanism and the evolution of cornified digital end organs. Journal of Anatomy 214: 620–643.

185. O'Connell T, Hedges R, Healey M, Simpson A (2001) Isotopic comparison of hair, nail and bone: modern analyses. Journal of Archaeological Science 28: 1247–1255.

186. Hendriks W, Tarttelin M, Moughan P (1998) The amino acid composition of cat (*Felis catus*) hair. Animal Science 67: 165–170.

187. Commerford S, Carsten A, Cronkite E (1983) The distribution of tritium among the amino acids of proteins obtained from mice exposed to tritiated water. Radiation Research 94: 151–155.

188. Gaebler O, Vitti TG, Vukmirovich R (1966) Isotope effects in metabolism of ^{14}N and ^{15}N from unlabeled dietary proteins. Biochemistry and Cell Biology 44: 1249–1257.

189. Hare PE, Fogel ML, Stafford TW (1991) The isotopic composition of carbon and nitrogen in individual amino acids isolated from modern and fossil proteins. Journal of Archaeological Science 18: 277–292.

190. Macko SA, Fogel ML, Hare P, Hoering T (1987) Isotopic fractionation of nitrogen and carbon in the synthesis of amino acids by microorganisms. Chemical Geology: Isotope Geoscience section 65: 79–92.

191. Péquignot A, Tumosa C, Endt DW (2006) The effects of tanning and fixing processes on the properties of taxidermy skins. Collection Forum 21. Available: http://www.crcc.cnrs.fr/IMG/pdf/Collection_Forum_2006-2.pdf.

192. Lees S (1986) Water content in type I collagen tissues calculated from the generalized packing model. International Journal of Biological Macromolecules 8: 66–72.

193. Covington AD (1997) Modern tanning chemistry. Chemical Society Reviews 26: 111-126.

194. McCullagh JSO, Tripp JA, Hedges REM (2005) Carbon isotope analysis of bulk keratin and single amino acids from British and North American hair. Rapid Communications in Mass Spectrometry 19: 3227–3231.

195. Petzke KJ, Fuller BT, Metges CC (2010) Advances in natural stable isotope ratio analysis of human hair to determine nutritional and metabolic status. Current Opinion in Clinical Nutrition and Metabolic Care 13: 532–540.

196. Raghavan M, McCullagh JSO, Lynnerup N, Hedges REM (2010) Amino acid $\delta^{13}C$ analysis of hair proteins and bone collagen using liquid chromatography/isotope ratio mass spectrometry: paleodietary implications from intra-individual comparisons. Rapid Communications in Mass Spectrometry 24: 541–548.

197. d'Angela D, Longinelli A (1990) Oxygen isotopes in living mammal's bone phosphate: further results. Chemical Geology 86: 75-82.

198. Bershaw J, Garzione CN, Higgins P, MacFadden BJ, Anaya F, et al. (2010) Spatial-temporal changes in Andean plateau climate and elevation from stable isotopes of mammal teeth. Earth and Planetary Science Letters 289: 530-538.

199. Kohn MJ, Dettman DL (2007) Paleoaltimetry from stable isotope compositions of fossils. Reviews in Mineralogy and Geochemistry 66: 119-154.

200. Morrill C, Koch PL (2002) Elevation or alteration? Evaluation of isotopic constraints on paleoaltitudes surrounding the Eocene Green River Basin. Geology 30: 151-154.

201. Amiot R, Lécuyer C, Buffetaut E, Escarguel G, Fluteau F, et al. (2006) Oxygen isotopes from biogenic apatites suggest widespread endothermy in Cretaceous dinosaurs. Earth and Planetary Science Letters 246: 41-54.

202. Eagle RA, Schauble EA, Tripati AK, Tütken T, Hulbert RC, et al. (2010) Body temperatures of modern and extinct vertebrates from ^{13}C-^{18}O bond abundances in bioapatite. Proceedings of the National Academy of Sciences 107: 10377.

203. Daux V, Lécuyer C, Héran MA, Amiot R, Simon L, et al. (2008) Oxygen isotope fractionation between human phosphate and water revisited. Journal of Human Evolution 55: 1138-1147.

204. Wright LE, Schwarcz HP (1999) Correspondence between stable carbon, oxygen and nitrogen isotopes in human tooth enamel and dentine: infant diets at Kaminaljuyú. Journal of Archaeological Science 26: 1159-1170.

205. Feranec R, García N, DÍez J, Arsuaga J (2010) Understanding the ecology of mammalian carnivorans and herbivores from Valdegoba cave (Burgos, northern

Spain) through stable isotope analysis. Palaeogeography, Palaeoclimatology, Palaeoecology: 263-272.

206. Kohn MJ, McKay MP, Knight JL (2005) Dining in the Pleistocene—Who's on the menu? Geology 33: 649-652.

207. Britton K, Grimes V, Dau J, Richards MP (2009) Reconstructing faunal migrations using intra-tooth sampling and strontium and oxygen isotope analyses: a case study of modern caribou (Rangifer tarandus granti). Journal of Archaeological Science 36: 1163-1172.

208. Dupras TL, Schwarcz HP (2001) Strangers in a strange land: stable isotope evidence for human migration in the Dakhleh Oasis, Egypt. Journal of Archaeological Science 28: 1199-1208.

209. Hoppe KA (2006) Correlation between the oxygen isotope ratio of North American bison teeth and local waters: Implication for paleoclimatic reconstructions. Earth and Planetary Science Letters 244: 408-417.

210. Pellegrini M, Donahue RE, Chenery C, Evans J, Lee Thorp J, et al. (2008) Faunal migration in late glacial central Italy: implications for human resource exploitation. Rapid Communications in Mass Spectrometry 22: 1714-1726.

211. White C, Longstaffe FJ, Law KR (2004) Exploring the effects of environment, physiology and diet on oxygen isotope ratios in ancient Nubian bones and teeth. Journal of Archaeological Science 31: 233-250.

212. Kohn MJ (1996) Predicting animal $\delta^{18}O$: Accounting for diet and physiological adaptation. Geochimica et Cosmochimica Acta 60: 4811-4829.

213. Reinhard E, de Torres T, O'Neil J (1996) $^{18}O/^{16}O$ ratios of cave bear tooth enamel: a record of climate variability during the Pleistocene. Palaeogeography, Palaeoclimatology, Palaeoecology 126: 45-59.

214. Iacumin P, Longinelli A (2002) Relationship between $\delta^{18}O$ values for skeletal apatite from reindeer and foxes and yearly mean $\delta^{18}O$ values of environmental water. Earth and Planetary Science Letters 201: 213-219.

215. Dahms AS, Boyer PD (1973) Occurrence and characteristics of ^{18}O exchange reactions catalyzed by sodium-and potassium-dependent adenosine triphosphatases. Journal of Biological Chemistry 248: 3155-3162.

216. Faller LD, Elgavish GA (1984) Catalysis of oxygen-18 exchange between inorganic phosphate and water by the gastric proton-potassium ATPase. Biochemistry 23: 6584-6590.

217. Leonard F, Scullin RI (1969) New mechanism for calcification of skeletal tissues. Nature 224: 1113-1115.

218. Levin NE, Cerling TE, Passey BH, Harris JM, Ehleringer JR (2006) A stable isotope aridity index for terrestrial environments. Proceedings of the National Academy of Sciences 103: 11201-11205.

219. Kohn MJ, Schoeninger MJ, Valley JW (1996) Herbivore tooth oxygen isotope compositions: effects of diet and physiology. Geochimica et Cosmochimica Acta 60: 3889-3896.

220. Kroopnick P, Craig H (1972) Atmospheric oxygen: Isotopic composition and solubility fractionation. Science 175: 54-55.

221. Bocherens H, Koch PL, Mariotti A, Geraads D, Jaeger JJ (1996) Isotopic biogeochemistry (^{13}C, ^{18}O) of mammalian enamel from African Pleistocene hominid sites. Palaios: 306-318.

222. Bocherens H, Mashkour M, Billiou D, Pellé E, Mariotti A (2001) A new approach for studying prehistoric herd management in arid areas: intra-tooth isotopic analyses of archaeological caprine from Iran: Une nouvelle approche pour l'étude de la gestion préhistorique des troupeaux en zones arides: analyses isotopiques intra-dentaires de caprinés archéologiques d'Iran. Comptes Rendus de l'Académie des Sciences-Series IIA-Earth and Planetary Science 332: 67-74.

223. Bryant JD, Luz B, Froelich PN (1994) Oxygen isotopic composition of fossil horse tooth phosphate as a record of continental paleoclimate. Palaeogeography, Palaeoclimatology, Palaeoecology 107: 303-316.

224. Koch PL (1998) Isotopic reconstruction of past continental environments. Annual Review of Earth and Planetary Sciences 26: 573-613.

225. Kohn MJ, Cerling TE (2002) Stable isotope compositions of biological apatite. Reviews in Mineralogy and Geochemistry 48: 455.

226. Sponheimer M, Lee-Thorp JA (1999) Oxygen isotopes in enamel carbonate and their ecological significance. Journal of Archaeological Science 26: 723-728.

227. Clark ID, Fritz P (1997) Environmental isotopes in hydrogeology. New York: CRC.

228. Fricke HC, O'Neil JR (1999) The correlation between 18O/16O ratios of meteoric water and surface temperature: its use in investigating terrestrial climate change over geologic time. Earth and Planetary Science Letters 170: 181-196.

229. Rozanski K, Araguás-Araguás L, Gonfiantini R (1993) Isotopic patterns in modern global precipitation. Climate Change in Continental Isotope Records 78: 1-36.

230. Grimes ST, Mattey DP, Hooker JJ, Collinson ME (2003) Paleogene paleoclimate reconstruction using oxygen isotopes from land and freshwater organisms: the use of multiple paleoproxies. Geochimica Et Cosmochimica Acta 67: 4033-4047.

231. Helliker BR, Ehleringer JR (2002) Grass blades as tree rings: environmentally induced changes in the oxygen isotope ratio of cellulose along the length of grass blades. New Phytologist 155: 417-424.

232. Lindars ES, Grimes ST, Mattey DP, Collinson ME, Hooker JJ, et al. (2001) Phosphate [delta] 18O determination of modern rodent teeth by direct laser fluorination: an appraisal of methodology and potential application to palaeoclimate reconstruction. Geochimica Et Cosmochimica Acta 65: 2535-2548.

233. Sternberg LO, Deniro MJ, Johnson HB (1984) Isotope ratios of cellulose from plants having different photosynthetic pathways. Plant Physiology 74: 557-561.

234. Kohn MJ, Schoeninger MJ, Valley JW (1998) Variability in oxygen isotope compositions of herbivore teeth: reflections of seasonality or developmental physiology? Chemical Geology 152: 97-112.

235. Wright LE, Schwarcz HP (1998) Stable carbon and oxygen isotopes in human tooth enamel: identifying breastfeeding and weaning in prehistory. American Journal of Physical Anthropology 106: 1-18.

236. Ayliffe L, Lister A, Chivas A (1992) The preservation of glacial-interglacial climatic signatures in the oxygen isotopes of elephant skeletal phosphate. Palaeogeography, Palaeoclimatology, Palaeoecology 99: 179-191.

237. Chillón BS, Alberdi MT, Leone G, Bonadonna FP, Stenni B, et al. (1994) Oxygen isotopic composition of fossil equid tooth and bone phosphate: an archive of difficult interpretation. Palaeogeography, Palaeoclimatology, Palaeoecology 107: 317-328.

238. Navarro N, Lécuyer C, Montuire S, Langlois C, Martineau F (2004) Oxygen isotope compositions of phosphate from arvicoline teeth and Quaternary climatic changes, Gigny, French Jura. Quaternary Research 62: 172-182.

239. Larivière S, Pasitschniak-Arts M (1996) Vulpes vulpes. Mammalian Species: 1-11.

240. Sponheimer M, Lee-Thorp JA (2001) The oxygen isotope composition of mammalian enamel carbonate from Morea Estate, South Africa. Oecologia 126: 153-157.

241. Rothwell T (2003) Phylogenetic Systematics of North American Pseudaelurus (Carnivora: Felidae). American Museum Novitates: 1-64.

242. Sunquist ME, Sunquist F (2002) Wild cats of the world: University of Chicago Press.

243. Amiot R, Lécuyer C, Buffetaut E, Fluteau F, Legendre S, et al. (2004) Latitudinal temperature gradient during the Cretaceous Upper Campanian-Middle Maastrichtian: $\delta^{18}O$ record of continental vertebrates. Earth and Planetary Science Letters 226: 255-272.

244. Clementz MT, Sorbi S, Domning DP (2009) Evidence of Cenozoic environmental and ecological change from stable isotope analysis of sirenian remains from the Tethys-Mediterranean region. Geology 37: 307.

245. Tütken T, Vennemann T, Janz H, Heizmann E (2006) Palaeoenvironment and palaeoclimate of the Middle Miocene lake in the Steinheim basin, SW Germany: A reconstruction from C, O, and Sr isotopes of fossil remains. Palaeogeography, Palaeoclimatology, Palaeoecology 241: 457-491.

246. Sokal RR, Rohlf FJ (1995) Biometry: the principles and practice of statistics in biological research: WH Freeman.

247. Pietsch SJ, Hobson KA, Wassenaar LI, Tütken T (2011) Tracking cats: Problems with placing feline carnivores on $\delta^{18}O$, δD isoscapes. Plos One: In press.

248. Anderson AE (1983) A critical review of literature on puma (*Felis concolor*). Colorado Division of Wildlife. 54 54. 91 p.

249. Currier MJP (1983) Felis concolor. Mammalian Species: 1-7.

250. Fricke HC, O'Neil JR (1996) Inter-and intra-tooth variation in the oxygen isotope composition of mammalian tooth enamel phosphate: implications for palaeoclimatological and palaeobiological research. Palaeogeography, Palaeoclimatology, Palaeoecology 126: 91-99.

251. Murphy BP, Bowman DMJS, Gagan MK (2007) The interactive effect of temperature and humidity on the oxygen isotope composition of kangaroos. Functional Ecology 21: 757-766.

252. O'Regan HJ, Chenery C, Lamb AL, Stevens RE, Rook L, et al. (2008) Modern macaque dietary heterogeneity assessed using stable isotope analysis of hair and bone. Journal of Human Evolution 55: 617-626.

253. Farquhar G, Lloyd J (1993) Carbon and oxygen isotope effects in the exchange of carbon dioxide between terrestrial plants and the atmosphere. In: Ehleringer JE, editor. Stable isotopes and plant carbon-water relations: Academic press. pp. 47-70.

254. Yakir D, DeNiro MJ, Rundel PW (1989) Isotopic inhomogeneity of leaf water: evidence and implications for the use of isotopic signals transduced by plants. Geochimica et Cosmochimica Acta 53: 2769-2773.

255. Sternberg LSL, Mulkey SS, Wright SJ (1989) Oxygen isotope ratio stratification in a tropical moist forest. Oecologia: 51-56.

256. Yakir D (1992) Variations in the natural abundance of oxygen 18 and deuterium in plant carbohydrates. Plant, Cell & Environment 15: 1005-1020.

257. Smith WP (1991) Odocoileus virginianus. Mammalian Species: 1-13.

258. Chapman JA, Hockman JG (1980) Sylvilagus floridanus. Mammalian Species: 1-8.

259. Palmqvist P, Perez-Claros JA, Janis CM, Figueirido B, Torregrosa V, et al. (2008) Biogeochemical and ecomorphological inferences on prey selection and resource partitioning among mammalian carnivores in an early Pleistocene community. Palaios 23: 724-737.

260. Tredget EE, Forsyth N, Uji-Friedland A, Chambers M, Ghahary A, et al. (1993) Gas chromatography--mass spectrometry determination of $^{18}O_2$ in ^{18}O-labelled 4-hydroxyproline for measurement of collagen synthesis and intracellular degradation. Journal of Chromatography B: Biomedical Sciences and Applications 612: 7-19.

261. White CD, Spence MW, Longstaffe FJ, Law KR (2000) Testing the nature of Teotihuacan imperialism at Kaminaljuyu using phosphate oxygen-isotope ratios. Journal of Anthropological Research: 535-558.

262. Killingley J (1980) Migrations of California gray whales tracked by oxygen-18 variations in their epizoic barnacles. Science 207: 759-760.

263. Meyer-Rochow VB, Cook I, Hendy CH (1992) How to obtain clues from the otoliths of an adult fish about the aquatic environment it has been in as a larva. Comparative Biochemistry and Physiology Part A: Physiology 103: 333-335.

264. White CD, Spence MW, Le Q SW (1998) Oxygen isotopes and the identification of geographical origins: the Valley of Oaxaca versus the Valley of Mexico. Journal of Archaeological Science 25: 643-655.

265. Sabine DL, Morrison SF, Whitlaw HA, Ballard WB, Forbes GJ, et al. (2002) Migration behavior of white-tailed deer under varying winter climate regimes in New Brunswick. The Journal of wildlife management: 718-728.

266. Severinghaus C, Cheatum E (1956) Life and times of the white-tailed deer. In: Taylor WP, editor. The Deer of North America Harrisburg, Pa: Stackpole Books. Washington, D.C., USA: The Wildlife Management Institute. pp. 57–186.

267. Pierce BM, Bleich VC, Wehausen JD, Bowyer RT (1999) Migratory patterns of mountain lions: implications for social regulation and conservation. Journal of Mammalogy 80: 986–992.

268. McNab BK (2008) An analysis of the factors that influence the level and scaling of mammalian BMR. Comparative Biochemistry and Physiology-Part A: Molecular & Integrative Physiology 151: 5-28.

269. Munoz-Garcia A, Williams JB (2005) Basal metabolic rate in carnivores is associated with diet after controlling for phylogeny. Physiological and Biochemical Zoology 78: 1039-1056.

6. ACKNOWLEDGMENTS

7. APPENDIX

7.1. CHAPTER 1: GENERAL INTRODUCTION

Appendix S1. IUCN Red List categories and status for all mammal species.

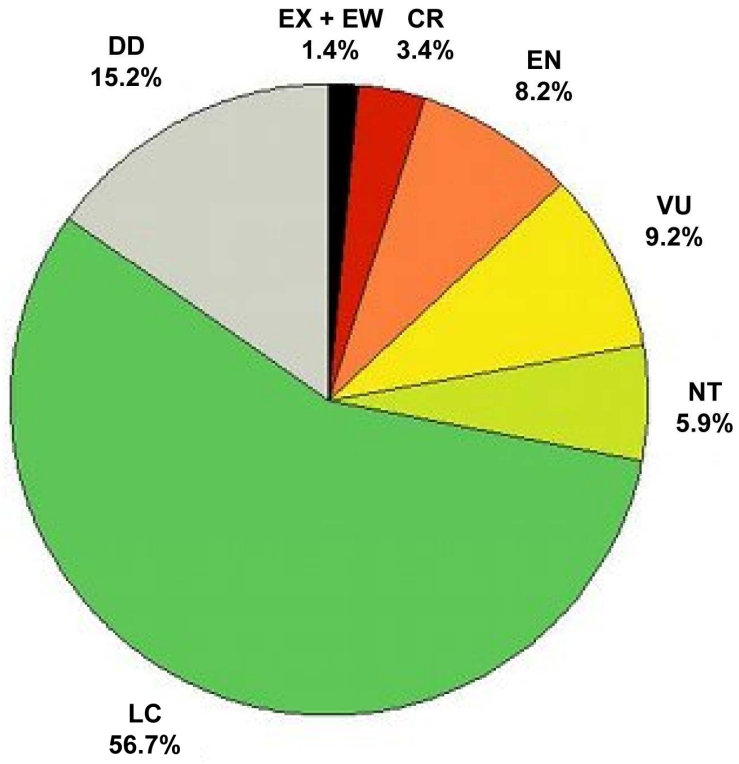

Legend Key	Red List Category	Number of species	Percentage in category
	Extinct (EX)	76	1.4
	Extinct in the Wild (EW)	2	0.04
	Critically Endangered (CR)	188	3.4
	Endangered (EN)	448	8.2
	Vulnerable (VU)	505	9.2
	Near Threatened (NT)	323	5.9
	Least Concern (LC)	3,109	56.7
	Data Deficient (DD)	836	15.2
	TOTAL	5,487	

Appendix S2. IUCN Red List Status (2008) of all mammalian orders.

No.	ORDER	TOTAL	EX	EW	CR	EN	VU	NT	LC	DD	% Threatened or Extinct
1	Afrosoricida	54	0	0	1	7	9	3	30	4	31.5
2	**Carnivora**	**285**	**5**	**0**	**8**	**24**	**39**	**27**	**163**	**19**	**26.7**
3	Cetartiodactyla	329	7	2	14	46	49	26	123	62	35.9
4	Chiroptera	1,150	5	0	25	53	99	77	687	204	15.8
5	Cingulata	21	0	0	0	0	4	5	9	3	19.9
6	Dasyuromorphia	74	1	0	1	6	5	10	47	4	17.6
7	Dermoptera	2	0	0	0	0	0	0	2	0	0
8	Didelphimorphia	95	1	0	1	0	7	2	67	17	9.5
9	Diprotodontia	146	7	0	14	15	16	16	76	2	35.6
10	Eulipotyphla	450	7	0	12	41	31	13	269	77	20.2
11	Hyracoidea	6	0	0	0	0	0	0	5	0	0
12	Lagomorpha	93	1	0	2	10	5	6	61	8	19.4
13	Macroscelidea	16	0	0	0	1	2	1	9	3	18.8
14	Microbiotheria	1	0	0	0	0	0	1	0	0	0
15	Monotremata	5	0	0	3	0	0	0	2	0	60
16	Notoryctemorphia	2	0	0	0	0	0	0	0	2	0
17	Paucituberculata	6	0	0	0	0	2	2	2	0	33.3
18	Peramelemorphia	22	3	0	0	4	2	1	9	3	40.9
19	Perissodactyla	16	0	0	5	5	3	1	2	0	81.3
20	Pholidota	8	0	0	0	2	0	4	2	0	25
21	Pilosa	10	0	0	1	1	0	1	7	0	20
22	Primates	414	2	0	37	86	78	23	132	56	49
23	Proboscidea	2	0	0	0	1	0	1	0	0	50
24	Rodentia	2,255	36	0	64	144	150	103	1,389	369	17.5
25	Scandentia	20	0	0	0	2	0	0	15	3	10
26	Sirenia	5	1	0	0	0	4	0	0	0	100
	TOTAL	5,487	76	2	188	448	505	323	3,109	836	

Appendix S3. IUCN Red List Status (2008) of the 16 carnivoran families.

	FAMILIES OF THE ORDER CARNIVORA	TOTAL	EX	EW	CR	EN	VU	NT	LC	DD	% Threatened or Extinct
1	Ailuridae	1	0	0	0	0	1	0	0	0	100
2	Canidae	36	1	0	3	3	0	4	24	1	19.4
3	Eupleridae	9	1	0	0	1	3	3	1	0	55.6
4	**Felidae**	**36**	**0**	**0**	**1**	**6**	**9**	**9**	**11**	**0**	**44.4**
5	Herpestidae	34	0	0	0	0	3	1	27	3	8.8
6	Hyaenidae	4	0	0	0	0	0	2	2	0	0
7	Mephitidae	12	0	0	0	0	1	0	11	0	8.3
8	Mustelidae	59	1	0	0	7	5	4	36	6	22
9	Nandiniidae	1	0	0	0	0	0	0	1	0	0
10	Odobenidae	1	0	0	0	0	0	0	0	1	0
11	Otariidae	16	1	0	0	4	2	2	7	0	43.8
12	Phocidae	19	1	0	2	1	1	0	12	2	26.3
13	Prionodontidae	2	0	0	0	0	0	0	2	0	0
14	Procyonidae	14	0	0	1	0	0	0	10	3	7.1
15	Ursidae	8	0	0	0	1	5	0	2	0	75
16	Viverridae	33	0	0	1	1	9	2	17	3	33.3

Appendix S4. Conservation status of felid species on the IUCN Red List 2008.

Critically Endangered (Extremely high extinction risk)	
Iberian lynx	*Lynx pardinus*
Endangered (Very high extinction risk)	
Andean cat	*Leopardus jacobita*
Tiger	*Panthera tigris*
Snow leopard	*Panthera uncia*
Borneo bay cat	*Pardofelis badia*
Flat-headed cat	*Prionailurus planiceps*
Fishing cat	*Prionailurus viverrinus*
Vulnerable (High extinction risk)	
Cheetah	*Acinonyx jubatus*
Black-footed cat	*Felis nigripes*
Guingna	*Leopardus guigna*
Oncilla	*Leopardus tigrinus*
Sunda clouded leopard	*Neofelis diardi*
Clouded leopard	*Neofelis nebulosa*
Lion	*Panthera leo*
Marbled cat	*Pardofelis marmorata*
Rusty-spotted cat	*Prionailurus rubiginosus*
Near Threatened (Close to quantifying for higher threat category)	
African golden cat	*Caracal aurata*
Sand cat	*Felis margarita*
Pampas cat	*Leopardus colocolo*
Geoffroy's cat	*Leopardus geoffroyi*
Margay	*Leopardus wiedii*
Pallas's cat	*Otocolobus manul*
Jaguar	*Panthera onca*
Leopard	*Panthera pardus*
Asiatic golden cat	*Pardofelis temminckii*
Least Concern (Relatively widespread and abundant)	
Caracal	*Caracal caracal*
Jungle cat	*Felis chaus*
Wildcat	*Felis silvestris*
Ocelot	*Leopardus pardalis*
Serval	*Leptailurus serval*
Canada lynx	*Lynx canadensis*
Eurasian lynx	*Lynx lynx*
Bobcat	*Lynx rufus*
Leopard cat	*Prionailurus bengalensis*
Puma	*Puma concolor*
Jaguarundi	*Puma yagouaroundi*

7.2. CHAPTER 2: Taming cat numts: DNA barcoding of Felidae using mtDNA and numts

Appendix 1. Sampling list

No.	Sample ID	Common Name	Genus	Species	Sample material (hair, blood, muscle tissue, feces)	Sex	Source/Contact	Barcode sequences generated for:	
								ATP6	COI
1	1/A_Ac_jub	Cheetah	Acinonyx	jubatus	b	f	Dr. Christian Wenker Zoo Basel		
2	2/A_Ac_jub	Cheetah	Acinonyx	jubatus	b	f	Dr. Christian Wenker Zoo Basel		
3	3/A_Ac_jub	Cheetah	Acinonyx	jubatus	b	m	Dr. Christian Wenker Zoo Basel		
4	4/A_Pa_uni	Snowleopard	Panthera	unica	b	f	Dr. Christian Wenker Zoo Basel		
5	5/A_Pa_uni	Snowleopard	Panthera	unica	b	m	Dr. Christian Wenker Zoo Basel		
6	6/A_Pa_unc	Snowleopard	Panthera	uncia	b	f	Dr. Christian Wenker Zoo Basel		
7	7/A_Pa_leo	Lion	Panthera	leo	b	f	Dr. Christian Wenker Zoo Basel		
8	8/A_Pa_leo	Lion	Panthera	leo	b	m	Dr. Christian Wenker Zoo Basel		
9	9/A_Pa_leo	Lion	Panthera	leo	b	m	Dr. Christian Wenker Zoo Basel		
10	10/A_Pa_leo	Lion	Panthera	leo	b	m	Dr. Christian Wenker Zoo Basel		

No.	Sample ID	Common Name	Genus	Species	Sample material (hair, blood, muscle tissue, feces)	Sex	Source/Contact	Barcode sequences generated for:	
								ATP6	COI
11	11/A_Ac_jub	Cheetah	Acinonyx	jubatus	b	f	Herr Andreas Filz Bernburg Tiergarten		
12	12/A_Pa_tig_su	Sumatratiger	Panthera	tigris	b	f	Dr. Ulrike Rademacher (Kuratorin Säugetiere) Wilhelma - der zoologisch botanische Garten		
13	13/A_Pa_tig_su	Sumatratiger	Panthera	tigris	b	m	Dr. Ulrike Rademacher (Kuratorin Säugetiere) Wilhelma - der zoologisch botanische Garten		
14	14/A_Fe_mar	Desertcat	Felis	margarita	t	m	Dr. Susanne Klomburg Zootierärztin Zoo Osnabrück		
15	15/A_Pa_leo	Lion	Panthera	leo	t	m	Dr. Susanne KlomburgZootierärztin Zoo Osnabrück		
16	16/A_Pa_leo	Lion	Panthera	leo	t	f	Dr. Susanne Klomburg Zootierärztin Zoo Osnabrück		
17	17/A_Pa_leo	Lion	Panthera	leo	t	f	Dr. Susanne Klomburg Zootierärztin Zoo Osnabrück		
18	18/A_Ly_lyn_ly	Eurasian lynx	Lynx	lynx	b		Herr Andreas Filz Bernburg Tiergarten		
19	19/A_Ly_lyn_ly	Eurasian lynx	Lynx	lynx	b		Herr Andreas Filz Bernburg Tiergarten		
20	20/A_Fe_sil	European wildcat	Felis	silvestris	h		Dr. Martin Wehrle Natur- und Tierpark Goldau		

No.	Sample ID	Common Name	Genus	Species	Sample material (hair, blood, muscle tissue, feces)	Sex	Source/Contact	Barcode sequences generated for:	
								ATP6	COI
22	22/A_Ly_lyn	Eurasian lynx	Lynx	lynx	h		Mr. Leif Blomqvist (Curator) Helsinki Zoo		
23	25/A_Pa_leo_bl	Lion	Panthera	leo	h	f	Burgers' Zoo Kim van de Put; Arnhem/Netherlands		
24	26/A_Pa_leo_bl	Lion	Panthera	leo	h	f	Burgers' Zoo Kim van de Put; Arnhem/Netherlands		
25	27/A_Pa_leo_bl	Lion	Panthera	leo	h	f	Burgers' Zoo Kim van de Put; Arnhem/Netherlands		
26	28/A_Pa_leo_bl	Lion	Panthera	leo	h	m	Burgers' Zoo Kim van de Put; Arnhem/Netherlands		
27	29/A_Pa_par	Sri Lankan Leopard	Panthera	pardus	h	m	Burgers' Zoo Kim van de Put; Arnhem/Netherlands		
28	30/A_Pa_tig_su	Sumatra Tiger	Panthera	tigris	h	f	Burgers' Zoo Kim van de Put; Arnhem/Netherlands		
29	31/A_Ly_ruf	Bobcat	Lynx	rufus	h	f	Burgers' Zoo Kim van de Put; Arnhem/Netherlands		
30	32/A_Ac_jub	Cheetah	Acinonyx	jubatus	h	f	Burgers' ZooKim van de Put; Arnhem/Netherlands		
31	33/A_Ac_jub	Cheetah	Acinonyx	jubatus	h	f	Burgers' Zoo Kim van de Put; Arnhem/Netherlands		
32	34/A_Ac_jub	Cheetah	Acinonyx	jubatus	h	f	Burgers' Zoo Kim van de Put; Arnhem/Netherlands		

No.	Sample ID	Common Name	Genus	Species	Sample material (hair, blood, muscle tissue, feces)	Sex	Source/Contact	Barcode sequences generated for:	
								ATP6	COI
33	35/A_Ac_jub	Cheetah	Acinonyx	jubatus	h	m	Burgers' Zoo Kim van de Put; Arnhem/Netherlands		
34	36/A_Ac_jub	Cheetah	Acinonyx	jubatus	h	m	Burgers' Zoo Kim van de Put; Arnhem/Netherlands		
35	37/A_Ly_lyn_ly	Eurasian lynx	Lynx	lynx	t	f	Nationalpark Harz Frank Raimer/ Ole Anders		
36	38/A_Ly_lyn_ly	Eurasian lynx	Lynx	lynx	t	m	Nationalpark Harz Frank Raimer/ Ole Anders		
37	39/A_Ly_lyn_ly	Eurasian lynx	Lynx	lynx	h	m	Tierpark Görlitz Dr. A. Gebauer		
38	40/A_Ot_man	Pallas cat	Otocolobus	manul	h		Tierpark Görlitz Dr. A. Gebauer		
39	41/A_Fe_sil	European wildcat	Felis	silvestris	h		Nationalpark Harz Frank Raimer/ Ole Anders		
40	42/A_Fe_sil	European wildcat	Felis	silvestris	h		Nationalpark Harz Frank Raimer/ Ole Anders		
41	43/A_Fe_sil	European wildcat	Felis	silvestris	h		Nationalpark Harz Frank Raimer/ Ole Anders		
42	44/A_Pa_leo	Lion	Panthera	leo	h	m	Zoo Karlsruhe Frau Dr. Klett		
43	45/A_Pa_par_ja	Leopard	Panthera	pardus	h	f	Zoo Karlsruhe Frau Dr. Klett		

No.	Sample ID	Common Name	Genus	Species	Sample material (hair, blood, muscle tissue, feces)	Sex	Source/Contact	Barcode sequences generated for:	
								ATP6	COI
44	46/A_Pa_par_ja	Leopard	Panthera	pardus	b		Zoo Karlsruhe Frau Dr. Klett		
45	47/A_Pa_unc	Snowleopard	Panthera	uncia	h	f	Zoo KarlsruheFrau Dr. Klett		
46	48/A_Ly_lyn	Eurasian lynx	Lynx	lynx	h	f	Zoo Karlsruhe Frau Dr. Klett		
47	49/A_Pa_leo	Lion	Panthera	leo	t	f	Zoo Karlsruhe Frau Dr. Klett		
48	50/A_Pa_leo	Lion	Panthera	leo	h	f	Zoo Karlsruhe Frau Dr. Klett		
49	51/A_Pa_leo	Lion	Panthera	leo	b	f	Zoo Karlsruhe Frau Dr. Klett		
50	52/A_Pa_tig	Tiger	Panthera	tigris	h	f	Zoo Zürich Fr. Gabriele Hürlimann		
51	53/A_Pa_unc	Snowleopard	Panthera	uncia	h	f	Zoo Zürich Fr. Gabriele Hürlimann		
52	54/A_Pa_unc	Snowleopard	Panthera	uncia	h	m	Zoo Zürich Fr. Gabriele Hürlimann		
53	55/A_Pa_unc	Snowleopard	Panthera	uncia	h	m	Zoo Zürich Fr. Gabriele Hürlimann		
54	56/A_Ne_neb	Clouded leopard	Neofelis	nebulosa	h	f	Zoo Zürich Fr. Gabriele Hürlimann		

No.	Sample ID	Common Name	Genus	Species	Sample material (hair, blood, muscle tissue, feces)	Sex	Source/Contact	Barcode sequences generated for:	
								ATP6	COI
55	57/A_Ne_neb	Clouded leopard	Neofelis	nebulosa	h	f	Zoo Zürich Fr. Gabriele Hürlimann		
56	58/A_Ne_neb	Clouded leopard	Neofelis	nebulosa	h	m	Zoo Zürich Fr. Gabriele Hürlimann		
57	59/A_Ne_neb	Clouded leopard	Neofelis	nebulosa	h	m	Zoo Zürich Fr. Gabriele Hürlimann		
58	60/A_Ne_neb	Clouded leopard	Neofelis	nebulosa	h	f	Zoo Zürich Fr. Gabriele Hürlimann		
59	61/A_Fe_sil	European wildcat	Felis	silvestris	h	f	Tierpark Nordhorn Dr. Heike Weber		
60	62/A_Fe_sil	European wildcat	Felis	silvestris	h	m	Tierpark NordhornDr. Heike Weber		
61	63/A_Fe_sil	European wildcat	Felis	silvestris	s		Nationalpark Harz Frank Raimer/ Ole Anders		
62	64/A_Fe_sil	European wildcat	Felis	silvestris	s		Nationalpark Harz Frank Raimer/ Ole Anders		
63	65/A_Fe_cat	Domestic cat	Felis	catus	s		Nationalpark Harz Frank Raimer/ Ole Anders		
64	66/A_Fe_sil	European wildcat	Felis	silvestris	h	m	Alpenzoo Innsbruck Dipl. Biol. Dirk Ullrich		
65	67/A_Fe_sil	European wildcat	Felis	silvestris	h	f	Alpenzoo Innsbruck Dipl. Biol. Dirk Ullrich		

No.	Sample ID	Common Name	Genus	Species	Sample material (hair, blood, muscle tissue, feces)	Sex	Source/Contact	Barcode sequences generated for:	
								ATP6	COI
66	68/A_Pa_tig	Tiger	Panthera	tigris	t		Prof. Dr. Martin Reifinger Institut für pathologische Veterinärmedizin		
67	69/A_Pa_unc	Snowleopard	Panthera	uncia	t	f	Dr. Robert Hoeveler, Veterinäruntersuchungsamt , Krefeld		
68	70/A_Le_geo	Geoffroy`s cat	Leopardus	geoffroyi	t	f	Dr. Robert Hoeveler, Veterinäruntersuchungsamt , Krefeld		
69	71/A_Le_tig	Tigrina	Leopardus	tigrina	t	m	Dr. Robert Hoeveler, Veterinäruntersuchungsamt , Krefeld		
70	72/A_Pu_yag	Jaguarundi	Puma	yaguarundi	t	m	Dr. Robert Hoeveler, Veterinäruntersuchungsamt , Krefeld		
71	73/A_Pa_par_ko	Ceylon Leopard	Panthera	pardus	t	f	Dr. Martin Peters SVUA Arnsberg		
72	74/A_Pa_par_ori	Amurleopard	Panthera	pardus	t	m	Dr. Martin Peters SVUA Arnsberg		
73	75/A_Le_tig	Tigrina	Leopardus	tigrina	t	m	Dr. Martin Peters SVUA Arnsberg		
74	76/A_Fe_sil	European wildcat	Felis	silvestris	t	f	Nationalpark Harz Frank Raimer/ Ole Anders		
75	77/A_Fe_sil	European wildcat	Felis	silvestris	t	f	Nationalpark HarzFrank Raimer/ Ole Anders		
76	78/A_Fe_sil	European wildcat	Felis	silvestris	t	f	Nationalpark Harz Frank Raimer/ Ole Anders		

No.	Sample ID	Common Name	Genus	Species	Sample material (hair, blood, muscle tissue, feces)	Sex	Source/Contact	Barcode sequences generated for:	
								ATP6	COI
77	79/A_Pa_par_ori	Amur leopard	Panthera	pardus	h	f	Mr. Leif Blomqvist (Curator) Helsinki Zoo		
78	80/A_Ot_man	Pallas cat	Otocolobus	manul	h	m	Mr. Leif Blomqvist (Curator) Helsinki Zoo		
79	81/A_Ac_jub	Cheetah	Acinonyx	jubatus	t		IZW Tanja Noventa FG.1		
80	82/A_Ac_jub	Cheetah	Acinonyx	jubatus	t		IZW Tanja Noventa FG.1		
81	83/A_Ac_jub_so	Cheetah	Acinonyx	jubatus	t		IZW Tanja Noventa FG.1		
82	84/A_Pa_tem	Asian golden cat	Pardofelis	temminckii	t		IZW Tanja Noventa FG.1		
83	85/A_Pa_tem	Asian golden cat	Pardofelis	temminckii	t		IZW Tanja Noventa FG.1		
84	86/A_Pu_con	Puma	Puma	concolor	t		IZW Tanja Noventa FG.1		
85	87/A_Ot_man	Palla`s cat	Otocolobus	manul	t		IZW Tanja Noventa FG.1		
86	88/A_Ot_man	Palla`s cat	Otocolobus	manul	t		IZW Tanja Noventa FG.1		
87	89/A_Ot_man	Palla`s cat	Caracal	manul	t		IZW Tanja Noventa FG.1		

No.	Sample ID	Common Name	Genus	Species	Sample material (hair, blood, muscle tissue, feces)	Sex	Source/Contact	Barcode sequences generated for:	
								ATP6	COI
88	90/A_Ca_ser	Serval	Caracal	serval	t		IZW Tanja Noventa FG.1		
89	91/A_Fe_sil	European Wildcat	Felis	silvestris	t		IZW Tanja Noventa FG.1		
90	92/A_Fe_sil_go	Oman wildcat	Felis	silvestris	t		IZW Tanja Noventa FG.1		
91	93/A_Fe_ly	African wildcat	Felis	lybica	t		IZW Tanja Noventa FG.1		
92	94/A_Fe_ly	African wildcat	Felis	lybica	t		IZW Tanja Noventa FG.1		
93	95/A_Le_geo	Geoffroy`s cat	Leopardus	geoffroyi	t		IZW Tanja Noventa FG.1		
94	96/A_Ca_ser	Serval	Caracal	serval	b		IZW Tanja Noventa FG.1		
95	97/A_Ca_ser	Serval	Caracal	serval	b		IZW Tanja Noventa FG.1		
96	98/A_Ca_ser	Serval	Caracal	serval	t		IZW Tanja Noventa FG.1		
97	99/A_Ly_ruf	Bobcat	Lynx	rufus	t		IZW Tanja Noventa FG.1		
98	100/A_Ly_ruf	Bobcat	Lynx	rufus	t		IZW Tanja Noventa FG.1		

No.	Sample ID	Common Name	Genus	Species	Sample material (hair, blood, muscle tissue, feces)	Sex	Source/Contact	Barcode sequences generated for:	
								ATP6	COI
99	101/A_Ot_man	Palla`s cat	Otocolobus	manul	t		IZW Tanja Noventa FG.1		
100	102/A_Ot_man	Palla`s cat	Otocolobus	manul	t		IZW Tanja Noventa FG.1		
101	103/A_Pa_leo	Lion	Panthera	leo	t		IZW Tanja Noventa FG.1		
102	104/A_Pa_leo_pe	Lion	Panthera	leo	t		IZW Tanja Noventa FG.1		
103	105/A_Pa_leo_pe	Lion	Panthera	leo	b		IZW Tanja Noventa FG.1		
104	106/A_Pa_onc	Jaguar	Panthera	onca	b		IZW Tanja Noventa FG.1		
105	107/A_Pa_onc	Jaguar	Panthera	onca	t		IZW Tanja Noventa FG.1		
106	108/A_Pa_onc	Jaguar	Panthera	onca	t		IZW Tanja Noventa FG.1		
107	109/A_Pa_onc	Jaguar	Panthera	onca	t		IZW Tanja Noventa FG.1		
108	110/A_Pa_onc	Jaguar	Panthera	onca	b		IZW Tanja Noventa FG.1		
109	111/A_Pa_onc	Jaguar	Panthera	onca	b		IZW Tanja Noventa FG.1		

No.	Sample ID	Common Name	Genus	Species	Sample material (hair, blood, muscle tissue, feces)	Sex	Source/Contact	Barcode sequences generated for:	
								ATP6	COI
110	112/A_Pa_par	Leopard	Panthera	pardus	t		IZW Tanja Noventa FG.1		
111	113/A_Pa_par_ja	Leopard	Panthera	pardus	b		IZW Tanja Noventa FG.1		
112	114/A_Pa_par_ja	Leopard	Panthera	pardus	b		IZW Tanja Noventa FG.1		
113	115/A_Pa_par_ja	Leopard	Panthera	pardus	b		IZW Tanja Noventa FG.1		
114	116/A_Pa_par_me	Leopard	Panthera	pardus	t		IZW Tanja Noventa FG.1		
115	117/A_Pa_par_or	Leopard	Panthera	pardus	b		IZW Tanja Noventa FG.1		
116	118/A_Pa_par_or	Leopard	Panthera	pardus	b		IZW Tanja Noventa FG.1		
117	119/A_Pa_par_or	Leopard	Panthera	pardus	b		IZW Tanja Noventa FG.1		
118	120/A_Pa_par_or	Leopard	Panthera	pardus	b		IZW Tanja Noventa FG.1		
119	121/A_Pa_par_or	Leopard	Panthera	pardus	t		IZW Tanja Noventa FG.1		
120	122/A_Pa_par_or	Leopard	Panthera	pardus	t		IZW Tanja Noventa FG.1		

No.	Sample ID	Common Name	Genus	Species	Sample material (hair, blood, muscle tissue, feces)	Sex	Source/Contact	Barcode sequences generated for:	
								ATP6	COI
121	123/A_Pa_tig_al	Tiger	Panthera	tigris	t		IZW Tanja Noventa FG.1		
122	124/A_Pa_tig_al	Tiger	Panthera	tigris	t		IZW Tanja Noventa FG.1		
123	125/A_Pa_tig_co	Tiger	Panthera	tigris	t		IZW Tanja Noventa FG.1		
124	126/A_Pa_tig_su	Tiger	Panthera	tigris	t		IZW Tanja Noventa FG.1		
125	127/A_Pa_tig_su	Tiger	Panthera	tigris	t		IZW Tanja Noventa FG.1		
126	128/A_Pa_tig_ti	Tiger	Panthera	tigris	t		IZW Tanja Noventa FG.1		
127	129/A_Pa_tig_ti	Tiger	Panthera	tigris	t		IZW Tanja Noventa FG.1		
128	130/A_Pr_ben	Asian leopard cat	Prionailurus	bengalensis	t		IZW Tanja Noventa FG.1		
129	131/A_Pr_ben	Asian leopard cat	Prionailurus	bengalensis	t		IZW Tanja Noventa FG.1		
130	132/A_Pr_rub	Rusty-spotted cat	Prionailurus	rubiginosus	t		IZW Tanja Noventa FG.1		
131	133/A_Pr_viv	Fishing cat	Prionailurus	viverrinus	t		IZW Tanja Noventa FG.1		

No.	Sample ID	Common Name	Genus	Species	Sample material (hair, blood, muscle tissue, feces)	Sex	Source/Contact	Barcode sequences generated for:	
								ATP6	COI
132	134/A_Pr_viv	Fishing cat	Prionailurus	viverrinus	t		IZW Tanja Noventa FG.1		
133	135/A_Pr_viv	Fishing cat	Prionailurus	viverrinus	t		IZW Tanja Noventa FG.1		
134	136/A_Pr_viv	Fishing cat	Prionailurus	viverrinus	t		IZW Tanja Noventa FG.1		
135	137/A_Pu_con	Puma	Puma	concolor	b		IZW Tanja Noventa FG.1		
136	138/A_Pu_con	Puma	Puma	concolor	b		IZW Tanja Noventa FG.1		
137	139/A_Pu_con	Puma	Puma	concolor	b		IZW Tanja Noventa FG.1		
138	140/A_Pr_viv	Fishing cat	Prionailurus	viverrinus	t	m	IZW Jennifer Ringleb FG 4		
139	141/A_Ot_man	Palla`s cat	Otocolobus	manul	t	m	IZW Jennifer Ringleb FG 4		
140	142/A_Le_par	Ocelot	Leopardus	pardalis	t	m	IZW Jennifer Ringleb FG 4		
141	143/A_Le_par	Ocelot	Leopardus	pardalis	t	m	IZW Jennifer Ringleb FG 4		
142	144/A_Pu_con	Puma	Puma	concolor	t	m	IZW Jennifer Ringleb FG 4		

No.	Sample ID	Common Name	Genus	Species	Sample material (hair, blood, muscle tissue, feces)	Sex	Source/Contact	Barcode sequences generated for:	
								ATP6	COI
143	145/A_Fe_sil	European Wildcat	Felis	silvestris	t	m	IZW Jennifer Ringleb FG 4		
144	146/A_Ly_lyn	Eurasian lynx	Lynx	lynx	t	m	IZW Jennifer Ringleb FG 4		
145	147/A_Pa_tig_al	Tiger	Panthera	tigris	t	m	IZW Jennifer Ringleb FG 4		
146	148/A_Pa_par_sa	Leopard	Panthera	pardus	t	m	IZW Jennifer Ringleb FG 4		
147	149/A_Pa_onc	Jaguar	Panthera	onca	t	m	IZW Jennifer Ringleb FG 4		
148	150/A_Pa_tig_al	Tiger	Panthera	tigris	t	m	IZW Jennifer Ringleb FG 4		
149	151/A_Pa_leo_pe	Lion	Panthera	leo	t	m	IZW Jennifer Ringleb FG 4		
150	152/A_Pa_tem	Asian golden cat	Pardofelis	temminckii	t	m	IZW Jennifer Ringleb FG 4		
151	153/A_Pa_tig_al	Tiger	Panthera	tigris	t	m	IZW Jennifer Ringleb FG 4		
152	154/A_Pr_rub	Rusty-spotted cat	Prionailurus	rubiginosus	t	m	IZW Jennifer Ringleb FG 4		
153	155/A_Pa_tig_al	Tiger	Panthera	tigris	t	m	IZW Jennifer Ringleb FG 4		

No.	Sample ID	Common Name	Genus	Species	Sample material (hair, blood, muscle tissue, feces)	Sex	Source/Contact	Barcode sequences generated for:	
								ATP6	COI
154	156/A_Pa_tig_al	Tiger	Panthera	tigris	t	m	IZW Jennifer Ringleb FG 4		
155	157/A_Pa_unc	Snowleopard	Panthera	uncia	t	m	IZW Jennifer Ringleb FG 4		
156	158/a_Pa_leo	Lion	Panthera	leo	t	m	IZW Jennifer Ringleb FG 4		
157	159/A_Pa_par_or	Leopard	Panthera	pardus	t	m	IZW Jennifer Ringleb FG 4		
158	160/A_Ac_jub	Cheetah	Acinonyx	jubatus	t	m	IZW Jennifer Ringleb FG 4		
159	161/A_Pa_tig_su	Tiger	Panthera	tigris	t	m	IZW Jennifer Ringleb FG 4		
160	162/A_Pa_par_or	Leopard	Panthera	pardus	t	m	IZW Jennifer Ringleb FG 4		
161	163/A_Pa_par_me	Leopard	Panthera	pardus	t	m	IZW Jennifer Ringleb FG 4		
162	164/A_Pa_leo_le	Lion	Panthera	leo	t	m	IZW Jennifer Ringleb FG 4		
163	165/A_Pa_tig_ti	Tiger	Panthera	tigris	t	m	IZW Jennifer Ringleb FG 4		
164	166/A_Pa_tig	Tiger	Panthera	tigris	t	m	IZW Jennifer Ringleb FG 4		

No.	Sample ID	Common Name	Genus	Species	Sample material (hair, blood, muscle tissue, feces)	Sex	Source/Contact	Barcode sequences generated for:	
								ATP6	COI
165	167/A_Pa_leo	Lion	Panthera	leo	t	m	IZW Jennifer Ringleb FG 4		
166	168/A_Pa_par_ja	Leopard	Panthera	pardus	t	m	IZW Jennifer Ringleb FG 4		
167	169/A_Pa_par_or	Leopard	Panthera	pardus	f	f	IZW Jennifer Ringleb FG 4		
168	170/A_Pa_par_or	Leopard	Panthera	pardus	f	m	IZW Jennifer Ringleb FG 4		
169	171/A_Pa_par_or	Leopard	Panthera	pardus	f	f	IZW Jennifer Ringleb FG 4		
170	172/A_Pa_tig_su	Tiger	Panthera	tigris	f	f	IZW Jennifer Ringleb FG 4		
171	173/A_Pa_tig_su	Tiger	Panthera	tigris	f	f	IZW Jennifer Ringleb FG 4		
172	174/A_Pa_tig_al	Tiger	Panthera	tigris	f	f	IZW Jennifer Ringleb FG 4		
173	175/A_Pa_tig_al	Tiger	Panthera	tigris	f	m	IZW Jennifer Ringleb FG 4		
174	176/A_Ly_ruf	Bobcat	Lynx	rufus	f	f	IZW Jennifer Ringleb FG 4		
175	177/A_Ly_par	Iberian lynx	Lynx	pardinus	f	m	IZW Jennifer Ringleb FG 4		

No.	Sample ID	Common Name	Genus	Species	Sample material (hair, blood, muscle tissue, feces)	Sex	Source/Contact	Barcode sequences generated for:	
								ATP6	COI
176	178/A_Ly_par	Iberian lynx	Lynx	pardinus	f	m	IZW Jennifer Ringleb FG 4		
177	179/A_Fe_mar	Desert cat	Felis	margarita	f	f	IZW Jennifer Ringleb FG 4		
178	180/A_Fe_mar	Desert cat	Felis	margarita	f	f	IZW Jennifer Ringleb FG 4		
179	181/A_Le_tig	Tigrina	Leopardus	tigrinus	f	?	IZW Jennifer Ringleb FG 4		
180	182/A_Pr_rub	Rusty-spotted cat	Prionailurus	rubiginosus	f	f	IZW Jennifer Ringleb FG 4		
181	183/A_Pr_rub	Rusty-spotted cat	Prionailurus	rubiginosus	f	f	IZW Jennifer Ringleb FG 4		
182	184/A_Fe_nig	Black-footed cat	Felis	nigripes	f		IZW Jennifer Ringleb FG 4		
183	185/A_Fe_nig	Black-footed cat	Felis	nigripes	f		IZW Jennifer Ringleb FG 4		
184	186/A_Pa_par_ja	Leopard	Panthera	pardus	f		IZW Jennifer Ringleb FG 4		
185	187/A_Pa_par_me	Leopard	Panthera	pardus	f		IZW Jennifer Ringleb FG 4		
186	188/A_Pa_par_me	Leopard	Panthera	pardus	f		IZW Jennifer Ringleb FG 4		

No.	Sample ID	Common Name	Genus	Species	Sample material (hair, blood, muscle tissue, feces)	Sex	Source/Contact	Barcode sequences generated for:	
								ATP6	COI
187	189/A_Pa_tig_al	Tiger	Panthera	tigris	t		IZW Jennifer Ringleb FG 4		
188	190/A_Fe_cat	Domestic cat	Felis	catus	t		IZW Jennifer Ringleb FG 4		
189	191/A_Fe_cat	Domestic cat	Felis	catus	t		IZW Jennifer Ringleb FG 4		
190	192/A_Fe_cat	Domestic cat	Felis	catus	t		IZW Jennifer Ringleb FG 4		
191	193/A_Ot_man	Palla`s cat	Otocolobus	manul	t	m	Kathrin Witzensberger Trier Tierpark Berlin		
192	194/A_Ot_man	Palla`s cat	Otocolobus	manul	h	f	Kathrin Witzensberger Trier Zoo Moscow		
193	195/A_Ot_man	Palla`s cat	Otocolobus	manul	h	m	Kathrin Witzensberger Trier Zoo Moscow		
194	196/A_Fe_mar	Desertcat	Felis	margarita	t	f	Kathrin Witzensberger Trier Zoo Osnabrück		
195	197/A_Fe_mar	Desertcat	Felis	margarita	t	m	Kathrin Witzensberger Trier Zoo Wuppertal		
196	198/A_Fe_mar	Desertcat	Felis	margarita	t	f	Kathrin Witzensberger Trier Zoo Wuppertal		
197	199/A_Fe_sil_go	Oman wildcat	Felis	silvestris	h	m	Kathrin Witzensberger Trier		

No.	Sample ID	Common Name	Genus	Species	Sample material (hair, blood, muscle tissue, feces)	Sex	Source/Contact	Barcode sequences generated for:	
								ATP6	COI
198	200/A_Fe_sil_go	Oman wildcat	Felis	silvestris	h	f	Kathrin Witzensberger Trier		
199	201/A_Fe_sil_go	Oman wildcat	Felis	silvestris	h	m	Kathrin Witzensberger Trier Parc des felins, France		
200	202/A_Fe_nig	Black-footed cat	Felis	nigripes	t	f	Kathrin Witzensberger Trier Zoo Wuppertal		
201	203/A_Fe_nig	Black-footed cat	Felis	nigripes	t	m	Kathrin Witzensberger Trier Zoo Wuppertal		
202	204/A_Fe_nig	Black-footed cat	Felis	nigripes	t	m	Kathrin Witzensberger Trier Zoo Wuppertal		
203	205/A_Pa_leo	Lion	Panthera	leo	b	m	Zoo Köln		
204	206/A_Pa_tig_al	Tiger	Panthera	tigris	h	m	Tierpark Hagenbeck		
205	207/A_Pa_leo_pe	Lion	Panthera	leo	h	m	Mr. Leif Blomqvist (Curator) Helsinki Zoo		
206	208/A_Pa_leo_pe	Lion	Panthera	leo	h	m	Mr. Leif Blomqvist (Curator) Helsinki Zoo		
207	209/A_Pa_leo_pe	Lion	Panthera	leo	h	f	Mr. Leif Blomqvist (Curator) Helsinki Zoo		
208	210/A_Pa_leo_pe	Lion	Panthera	leo	h	f	Mr. Leif Blomqvist (Curator) Helsinki Zoo		

No.	Sample ID	Common Name	Genus	Species	Sample material (hair, blood, muscle tissue, feces)	Sex	Source/Contact	Barcode sequences generated for:	
								ATP6	COI
209	211/A_Pa_par_ori	Amurleopard	Panthera	pardus	h	m	Mr. Leif Blomqvist (Curator) Helsinki Zoo		
210	212/A_Fe_sil	European wildcat	Felis	silvestris	t	f	Veterinärpathologie Zürich Prof. Dr. Pospischil		
211	213/A_Fe_sil	European wildcat	Felis	silvestris	t		Nationalpark Harz Frank Raimer/ Ole Anders		
212	214/A_Fe_cat	Domestic cat	Felis	catus	t		Nationalpark Harz Frank Raimer/ Ole Anders		
213	215/A_Fe_sil	European wildcat	Felis	silvestris	t		Nationalpark Harz Frank Raimer/ Ole Anders		
214	216/A_Fe_sil	European wildcat	Felis	silvestris	t		Nationalpark Harz Frank Raimer/ Ole Anders		
215	217/A_Ly_lyn_ly	Eurasian lynx	Lynx	lynx	t	f	Nationalpark Harz Frank Raimer/ Ole Anders		
216	218_Pr_rub-phi	Rusty-spotted cat	Prionailurus	rubiginosus	h		Zoologischer Garten Frankfurt Frau Dr. Geiger		
217	219_Le_par	Ocelot	Leopardus	pardalis	h	f	Zoo Stralsund Dr. Langner		
218	220_Le_par	Ocelot	Leopardus	pardalis	h	m	Zoo Stralsund Dr. Langner		
219	221_Pr_ben	Asian leopard cat	Prionailurus	bengalensis	h	m/f	Zoo Augsburg Dr. Jantschke		

No.	Sample ID	Common Name	Genus	Species	Sample material (hair, blood, muscle tissue, feces)	Sex	Source/Contact	Barcode sequences generated for:	
								ATP6	COI
220	222_Pu_con	Puma	Puma	concolor	h	f	Zoo Bremerhaven Dr. Schöne		
221	223_Pr_rub	Rusty-spotted cat	Prionailurus	rubiginosus	h	f	Zoo Frankfurt Dr. Schauerte		
222	224_Pa_unc	Snowleopard	Panthera	unica	h		Zoo Wuppertal Dr. A Stadler		
223	225_Ly_ly_wr	Sibirian lynx	Lynx	lynx	h		Zoo Wuppertal Dr. A Stadler		
224	226_Le_geo	Geoffroy`s cat	Leopardus	geoffroyi	h		Zoo Wuppertal Dr. A Stadler		
225	227_Pa_par_fu	Indian Leopard	Panthera	pardus	h		Zoo Wuppertal Dr. A Stadler		
226	228_Fe_ly_go	Oman wildcat	Felis	lybica	h		Zoo Wuppertal Dr. A Stadler		
227	229_Pa_leo	Lion	Panthera	leo	h		Zoo Wuppertal Dr. A Stadler		
228	230_Pa_par_fu	Leopard	Panthera	pardus	h		Zoo Wuppertal Dr. A Stadler		
229	231_Pa_tem	Asian golden cat	Pardofelis	temminckii	h		Zoo Wuppertal Dr. A Stadler		
230	232_Ne_neb	Clouded leopard	Neofelis	nebulosa	h		Zoo Wuppertal Dr. A Stadler		

No.	Sample ID	Common Name	Genus	Species	Sample material (hair, blood, muscle tissue, feces)	Sex	Source/Contact	Barcode sequences generated for:	
								ATP6	COI
231	233_Ac_jub	Cheetah	Acinonyx	jubatus	h		Zoo Wuppertal Dr. A Stadler		
232	234_Le_tig	Tigrina	Leopardus	tigrina	h		Zoo Wuppertal Dr. A Stadler		
233	235_Pa_tig_al	Tiger	Panthera	tigris	h		Zoo Wuppertal Dr. A Stadler		
234	236/A_Pa_onc	Jaguar	Panthera	onca	h	m	Zoo Landau Dr. C. Schubert		
235	237/A_Ac_jub_so	Cheetah	Acinonyx	jubatus	h	m	Zoo Landau Dr. C. Schubert		
236	238/A_Ac_jub_so	Cheetah	Acinonyx	jubatus	h	f	Zoo Landau Dr. C. Schubert		
237	239/A_Ac_jub_so	Cheetah	Acinonyx	jubatus	h	m	Zoo Landau Dr. C. Schubert		
238	240/A_Le_geo	Geoffroy`s cat	Leopardus	geoffroyi	h		Bad Kösen Tierpark Herr Scherling		
239	241/A_Pr_ben	Asian leopard cat	Prionailurus	bengalensis	h, b, t	m	Zoo Heidelberg Dr. Scharpegge		
240	242/A_Ca_ser	Serval	Caracal	serval	h	m	Zoo Hoyerswerda Fr. Dr. Häfner		
241	243_Pu_con	Puma	Puma	concolor	h	?	Parkenzoo Sweden, Jennie Westander		

No.	Sample ID	Common Name	Genus	Species	Sample material (hair, blood, muscle tissue, feces)	Sex	Source/Contact	Barcode sequences generated for:	
								ATP6	COI
242	244_Ot_man	Pallas cat	Otocolobus	manul	h	?	Parkenzoo Sweden, Jennie Westander		
243	245_Fe_mar	Desert cat	Felis	margarita	h	?	Parkenzoo Sweden, Jennie Westander		
244	246_Pa_par_sa	Leopard	Panthera	pardus	h	?	Allwetterzoo Münster Dr. Wewers		
245	247_Ca_car	Caracal	Caracal	caracal	h	m	Grégory Breton, Curator at LE PARC DES FELINS, France		
246	248_Ca_car	Caracal	Caracal	caracal	h	f	Grégory Breton, Curator at LE PARC DES FELINS, France		
247	249_Ca_car	Caracal	Caracal	caracal	h	f	Grégory Breton, Curator at LE PARC DES FELINS, France		
248	250_Le_geo	Geoffroy`s cat	Leopardus	geoffroyi	h	m	Grégory Breton, Curator at LE PARC DES FELINS, France		
249	251_Le_geo	Geoffroy`s cat	Leopardus	geoffroyi	h	m	Grégory Breton, Curator at LE PARC DES FELINS, France		
250	252_Le_par	Ocelot	Leopardus	pardalis	h	m	Grégory Breton, Curator at LE PARC DES FELINS, France		
251	253_Le_tig	Tigrina	Leopardus	tigrinus	h	m	Grégory Breton, Curator at LE PARC DES FELINS, France		
252	254_Le_tig	Tigrina	Leopardus	tigrinus	h	m	Grégory Breton, Curator at LE PARC DES FELINS, France		

No.	Sample ID	Common Name	Genus	Species	Sample material (hair, blood, muscle tissue, feces)	Sex	Source/Contact	Barcode sequences generated for:	
								ATP6	COI
253	255_Le_tig	Tigrina	Leopardus	tigrinus	h	f	Grégory Breton, Curator at LE PARC DES FELINS, France		
254	256_Le_tig	Tigrina	Leopardus	tigrinus	h	f	Grégory Breton, Curator at LE PARC DES FELINS, France		
255	257_Le_wie	Margay	Leopardus	wiedii	h	m	Grégory Breton, Curator at LE PARC DES FELINS, France		
256	258_Le_wie	Margay	Leopardus	wiedii	h	m	Grégory Breton, Curator at LE PARC DES FELINS, France		
257	259_Le_wie	Margay	Leopardus	wiedii	h	f	Grégory Breton, Curator at LE PARC DES FELINS, France		
258	260_Le_wie	Margay	Leopardus	wiedii	h	f	Grégory Breton, Curator at LE PARC DES FELINS, France		
259	261_Ly_lyn	Eurasian lynx	Lynx	lynx	h	m	Grégory Breton, Curator at LE PARC DES FELINS, France		
260	262_Pu_yag	Jaguarundi	Puma	yaguarundi	h	m	Grégory Breton, Curator at LE PARC DES FELINS, France		
261	263_Pu_yag	Jaguarundi	Puma	yaguarundi	h	m	Grégory Breton, Curator at LE PARC DES FELINS, France		
262	264_Pu_yag	Jaguarundi	Puma	yaguarundi	h	f	Grégory Breton, Curator at LE PARC DES FELINS, France		
263	265_Pu_yag	Jaguarundi	Puma	yaguarundi	h	f	Grégory Breton, Curator at LE PARC DES FELINS, France		

No.	Sample ID	Common Name	Genus	Species	Sample material (hair, blood, muscle tissue, feces)	Sex	Source/Contact	Barcode sequences generated for:	
								ATP6	COI
264	266_Ot_man	Palla´s cat	Otocolobus	manul	h	f	Grégory Breton, Curator at LE PARC DES FELINS, France		
265	267_Fe_lyb	African wildcat	Felis	lybica	h	f	Grégory Breton, Curator at LE PARC DES FELINS, France		
266	268_Fe_mar	Desert cat	Felis	margarita	h	m	Grégory Breton, Curator at LE PARC DES FELINS, France		
267	269_Fe_mar	Desert cat	Felis	margarita	h	m	Grégory Breton, Curator at LE PARC DES FELINS, France		
268	270_Fe_mar	Desert cat	Felis	margarita	h	m	Grégory Breton, Curator at LE PARC DES FELINS, France		
269	271_Pa_par	Leopard	Panthera	pardus	h	?	Rebecca Ray, Zambia Luambe NP		
270	272_Pa_par	Leopard	Panthera	pardus	h	?	Rebecca Ray, Zambia Luambe NP		
271	273_Pa_par	Leopard	Panthera	pardus	h	?	Rebecca Ray, Zambia Luambe NP		
272	274_Pa_par	Leopard	Panthera	pardus	t	?	Rebecca Ray, Zambia Luambe NP		
273	275_Pa_par	Leopard	Panthera	pardus	t	?	Rebecca Ray, Zambia Luambe NP		
274	276_Pa_par	Leopard	Panthera	pardus	t	?	Rebecca Ray, Zambia Luambe NP		

No.	Sample ID	Common Name	Genus	Species	Sample material (hair, blood, muscle tissue, feces)	Sex	Source/Contact	Barcode sequences generated for:	
								ATP6	COI
275	277_Pu_con	Puma	Puma	concolor	h	w	Zoo Bremerhaven Dr. Schöne		
276	278_Pu_con	Puma	Puma	concolor	h	w	Zoo Bremerhaven Dr. Schöne		
277	279_Pu_con	Puma	Puma	concolor	h	m	Zoo Bremerhaven Dr. Schöne		

Table S1. Characterization of the size, similarity, and nucleotide substitution patterns from pairwise comparison of COI cymt and putative numt sequences.

Genus	Species	Common name	Number of analysed COI sequences	Size (bp)		Changes bewteen cymt and numt (bp)		Number of numt haplotypes	Base pair insertions (bp)	Number of stop codons	Blast Hit	Numt Genbank Accession number	Reference
				cymt	numt	Subst.	Gaps						
Panthera	*tigris*	Tiger	18	658	663	65	5	1	5	2	99% (Tiger-numt)	DQ151551	[35]
Panthera	*leo*	Lion	4	658	658	n.a.	0	1	0	0	97% (Tiger-numt)	DQ151552	[35]
Felis	*catus*	Dometic cat	4	658	658	47	0	3	0	1	99% (Cat-numt)	U20754	[17]
Felis	*silvestris*	European wild cat	10	658	658	n.a.	0	3	0	1	100 & 99 % (Cat- numt)	U20755	[17]
Felis	*libyca*	African wild cat	2	658	658	n.a.	0	2	0	1	100% (Cat-numt)	U20756	[17]
Otocolobus	*manul*	Pallas cat	4	658	658	n.a.	0	1	0	8	n.a.	n.a.	n.a.

Appendix 2. ATP6 and COI sequence alignments

1 10 20 30 40 50 60 70 80 90 100 110 120 126
Consensus
1. BCATS221-11|237_Ac_jub_so|Acinonyx
2. BCATS222-11|238_Ac_jub_so|Acinonyx
3. BCATS004-10|2_Ac_jub|Acinonyx
4. BCATS005-10|32_Ac_jub|Acinonyx
5. BCATS006-10|33_Ac_jub|Acinonyx
6. BCATS007-10|34_Ac_jub|Acinonyx
7. BCATS008-10|35_Ac_jub|Acinonyx
8. BCATS009-10|36_Ac_jub|Acinonyx
9. BCATS010-10|3_Ac_jub|Acinonyx
10. BCATS001-10|11_Ac_jub|Acinonyx
11. BCATS011-10|81_Ac_jub|Acinonyx
12. BCATS012-10|82_Ac_jub|Acinonyx
13. BCATS013-10|83_Ac_jub_so|Acinonyx
14. BCATS002-10|160_Ac_jub|Acinonyx
15. BCATS003-10|1_Ac_jub|Acinonyx
16. BCATS218-11|247_Ca_car|Caracal
17. BCATS219-11|248_Ca_car|Caracal
18. BCATS220-11|249_Ca_car|Caracal
19. BCATS217-11|242_Ca_ser|Caracal
20. BCATS014-10|90_Ca_ser|Caracal
21. BCATS015-10|96_Ca_ser|Caracal
22. BCATS016-10|97_Ca_ser|Caracal
23. BCATS017-10|98_Ca_ser|Caracal
24. BCATS021-10|214_Fe_cat|Felis
25. BCATS018-10|190_Fe_cat|Felis
26. BCATS019-10|191_Fe_cat|Felis
27. BCATS020-10|192_Fe_cat|Felis
28. BCATS211-11|268_Fe_mar|Felis
29. BCATS213-11|269_Fe_mar|Felis
30. BCATS212-11|270_Fe_mar|Felis
31. BCATS024-10|14_Fe_mar|Felis
32. BCATS025-10|179_Fe_mar|Felis
33. BCATS026-10|180_Fe_mar|Felis
34. BCATS027-10|196_Fe_mar|Felis
35. BCATS028-10|197_Fe_mar|Felis
36. BCATS029-10|198_Fe_mar|Felis
37. BCATS031-10|202_Fe_nig|Felis
38. BCATS032-10|203_Fe_nig|Felis
39. BCATS033-10|204_Fe_nig|Felis
40. BCATS030-10|184_Fe_nig|Felis
41. BCATS037-10|201_Fe_sil_go|Felis
42. BCATS038-10|212_Fe_sil|Felis
43. BCATS039-10|213_Fe_sil|Felis
44. BCATS040-10|215_Fe_sil|Felis
45. BCATS041-10|216_Fe_sil|Felis
46. BCATS216-11|267_Fe_lyb|Felis
47. BCATS044-10|62_Fe_sil|Felis
48. BCATS045-10|66_Fe_sil|Felis
49. BCATS046-10|67_Fe_sil|Felis
50. BCATS047-10|76_Fe_sil|Felis
51. BCATS048-10|77_Fe_sil|Felis
52. BCATS049-10|78_Fe_sil|Felis
53. BCATS050-10|91_Fe_sil|Felis
54. BCATS051-10|92_Fe_sil_go|Felis
55. BCATS214-11|94_Fe_lyb|Felis
56. BCATS034-10|145_Fe_sil|Felis
57. BCATS035-10|199_Fe_sil_go|Felis
58. BCATS036-10|200_Fe_sil_go|Felis
59. BCATS210-11|226_Le_geo|Leopardus
60. BCATS209-11|240_Le_geo|Leopardus
61. BCATS208-11|250_Le_geo|Leopardus
62. BCATS052-10|70_Le_geo|Leopardus
63. BCATS053-10|95_Le_geo|Leopardus
64. BCATS055-10|252_Le_par|Leopardus
65. BCATS205-11|234_Le_tig|Leopardus
66. BCATS206-11|253_Le_tig|Leopardus
67. BCATS207-11|254_Le_tig|Leopardus
68. BCATS056-10|71_Le_tig|Leopardus
69. BCATS057-10|75_Le_tig|Leopardus
70. BCATS203-11|258_Le_wie|Leopardus
71. BCATS204-11|259_Le_wie|Leopardus
72. BCATS061-10|21_Ly_lyn|Lynx
73. BCATS202-11|225_Ly_lyn_wr|Lynx
74. BCATS062-10|22_Ly_lyn|Lynx
75. BCATS063-10|37_Ly_lyn_ly|Lynx

1 10 20 30 40 50 60 70 80 90 100 110 120 126
Consensus
76. BCATS064-10|38_Ly_lyn_ly|Lynx
77. BCATS065-10|39_Ly_lyn_ly|Lynx
78. BCATS066-10|48_Ly_lyn|Lynx
79. BCATS058-10|146_Ly_lyn|Lynx
80. BCATS059-10|18_Ly_lyn_ly|Lynx
81. BCATS060-10|19_Ly_lyn_ly|Lynx
82. BCATS067-10|177_Ly_par|Lynx
83. BCATS068-10|178_Ly_par|Lynx
84. BCATS069-10|100_Ly_ruf|Lynx
85. BCATS072-10|31_Ly_ruf|Lynx
86. BCATS071-10|99_Ly_ruf|Lynx
87. BCATS070-10|176_Ly_ruf|Lynx
88. BCATS073-10|56_Ne_neb|Neofelis
89. BCATS074-10|57_Ne_neb|Neofelis
90. BCATS075-10|58_Ne_neb|Neofelis
91. BCATS076-10|59_Ne_neb|Neofelis
92. BCATS077-10|60_Ne_neb|Neofelis
93. BCATS078-10|101_Ot_man|Otocolobus
94. BCATS201-11|266_Ot_man|Otocolobus
95. BCATS084-10|40_Ot_man|Otocolobus
96. BCATS079-10|102_Ot_man|Otocolobus
97. BCATS085-10|80_Ot_man|Otocolobus
98. BCATS086-10|87_Ot_man|Otocolobus
99. BCATS087-10|88_Ot_man|Otocolobus
100. BCATS088-10|89_Ot_man|Otocolobus
101. BCATS080-10|141_Ot_man|Otocolobus
102. BCATS081-10|193_Ot_man|Otocolobus
103. BCATS082-10|194_Ot_man|Otocolobus
104. BCATS083-10|195_Ot_man|Otocolobus
105. BCATS099-10|207_Pa_leo_pe|Panthe...
106. BCATS100-10|208_Pa_leo_pe|Panthe...
107. BCATS101-10|209_Pa_leo_pe|Panthe...
108. BCATS102-10|210_Pa_leo_pe|Panthe...
109. BCATS105-10|44_Pa_leo|Panthera
110. BCATS090-10|104_Pa_leo_pe|Panthe...
111. BCATS091-10|105_Pa_leo_pe|Panthe...
112. BCATS092-10|151_Pa_leo_pe|Panthe...
113. BCATS093-10|158_Pa_leo|Panthera
114. BCATS094-10|15_Pa_leo|Panthera
115. BCATS095-10|164_Pa_leo_le|Panthera
116. BCATS097-10|16_Pa_leo|Panthera
117. BCATS224-11|236_Pa_onc|Panthera
118. BCATS115-10|149_Pa_onc|Panthera
119. BCATS111-10|107_Pa_onc|Panthera
120. BCATS112-10|108_Pa_onc|Panthera
121. BCATS113-10|109_Pa_onc|Panthera
122. BCATS117-10|114_Pa_par_ja|Panthera
123. BCATS197-11|227_Pa_par_fu|Panthera
124. BCATS196-11|230_Pa_par_fu|Panthera
125. BCATS198-11|246_Pa_par_sa|Panthe...
126. BCATS200-11|271_Pa_par|Panthera
127. BCATS199-11|272_Pa_par|Panthera
128. BCATS133-10|29_Pa_par_ko|Panthera
129. BCATS187-10|73_Pa_par_ko|Panthera
130. BCATS134-10|74_Pa_par_or|Panthera
131. BCATS135-10|79_Pa_par_or|Panthera
132. BCATS125-10|148_Pa_par_sa|Panthe...
133. BCATS126-10|159_Pa_par_or|Panthera
134. BCATS127-10|162_Pa_par_or|Panthera
135. BCATS128-10|168_Pa_par_ja|Panthera
136. BCATS129-10|169_Pa_par_or|Panthera
137. BCATS130-10|170_Pa_par_or|Panthera
138. BCATS131-10|186_Pa_par_ja|Panthera
139. BCATS132-10|187_Pa_par_me|Panth...
140. BCATS157-10|30_Pa_tig_su|Panthera
141. BCATS158-10|68_Pa_tig_al|Panthera
142. BCATS140-10|124_Pa_tig_al|Panthera
143. BCATS143-10|127_Pa_tig_su|Panthera
144. BCATS144-10|128_Pa_tig_ti|Panthera
145. BCATS146-10|12_Pa_tig_su|Panthera
146. BCATS147-10|13_Pa_tig_su|Panthera
147. BCATS151-10|155_Pa_tig_al|Panthera
148. BCATS152-10|156_Pa_tig_al|Panthera
149. BCATS154-10|165_Pa_tig_ti|Panthera
150. BCATS155-10|166_Pa_tig|Panthera

1 10 20 30 40 50 60 70 80 90 100 110 120 126
Consensus
103. BCATS082-10|194_Ot_man|Otocolobus
104. BCATS083-10|195_Ot_man|Otocolobus
105. BCATS099-10|207_Pa_leo_pe|Panthe...
106. BCATS100-10|208_Pa_leo_pe|Panthe...
107. BCATS101-10|209_Pa_leo_pe|Panthe...
108. BCATS102-10|210_Pa_leo_pe|Panthe...
109. BCATS105-10|44_Pa_leo|Panthera
110. BCATS090-10|104_Pa_leo_pe|Panthe...
111. BCATS091-10|105_Pa_leo_pe|Panthe...
112. BCATS092-10|151_Pa_leo_pe|Panthe...
113. BCATS093-10|158_Pa_leo|Panthera
114. BCATS094-10|15_Pa_leo|Panthera
115. BCATS095-10|164_Pa_leo_le|Panthera
116. BCATS097-10|16_Pa_leo|Panthera
117. BCATS224-11|236_Pa_onc|Panthera
118. BCATS115-10|149_Pa_onc|Panthera
119. BCATS111-10|107_Pa_onc|Panthera
120. BCATS112-10|108_Pa_onc|Panthera
121. BCATS113-10|109_Pa_onc|Panthera
122. BCATS117-10|114_Pa_par_ja|Panthera
123. BCATS197-11|227_Pa_par_fu|Panthera
124. BCATS196-11|230_Pa_par_fu|Panthera
125. BCATS198-11|246_Pa_par_sa|Panthe...
126. BCATS200-11|271_Pa_par|Panthera
127. BCATS199-11|272_Pa_par|Panthera
128. BCATS133-10|29_Pa_par_ko|Panthera
129. BCATS187-10|73_Pa_par_ko|Panthera
130. BCATS134-10|74_Pa_par_ori|Panthera
131. BCATS135-10|79_Pa_par_or|Panthera
132. BCATS125-10|148_Pa_par_sa|Panthe...
133. BCATS126-10|159_Pa_par_or|Panthera
134. BCATS127-10|162_Pa_par_or|Panthera
135. BCATS128-10|168_Pa_par_ja|Panthera
136. BCATS129-10|169_Pa_par_or|Panthera
137. BCATS130-10|170_Pa_par_or|Panthera
138. BCATS131-10|186_Pa_par_ja|Panthera
139. BCATS132-10|187_Pa_par_me|Panth...
140. BCATS157-10|30_Pa_tig_su|Panthera
141. BCATS158-10|68_Pa_tig_al|Panthera
142. BCATS140-10|124_Pa_tig_al|Panthera
143. BCATS143-10|127_Pa_tig_su|Panthera
144. BCATS144-10|128_Pa_tig_ti|Panthera
145. BCATS146-10|12_Pa_tig_su|Panthera
146. BCATS147-10|13_Pa_tig_su|Panthera
147. BCATS151-10|155_Pa_tig_al|Panthera
148. BCATS152-10|156_Pa_tig_al|Panthera
149. BCATS154-10|165_Pa_tig_ti|Panthera
150. BCATS155-10|166_Pa_tig|Panthera
151. BCATS156-10|189_Pa_tig_al|Panthera
152. BCATS160-10|47_Pa_unc|Panthera
153. BCATS162-10|53_Pa_unc|Panthera
154. BCATS166-10|69_Pa_unc|Panthera
155. BCATS136-10|84_Pa_tem|Pardofelis
156. BCATS137-10|85_Pa_tem|Pardofelis
157. BCATS138-10|152_Pa_tem|Pardofelis
158. BCATS195-11|241_Pr_ben|Prionailurus
159. BCATS168-10|131_Pr_ben|Prionailurus
160. BCATS194-11|218_Pr_rub|Prionailurus
161. BCATS193-11|223_Pr_rub|Prionailurus
162. BCATS169-10|132_Pr_rub|Prionailurus
163. BCATS170-10|154_Pr_rub|Prionailurus
164. BCATS171-10|182_Pr_rub|Prionailurus
165. BCATS172-10|183_Pr_rub|Prionailurus
166. BCATS173-10|133_Pr_viv|Prionailurus
167. BCATS174-10|134_Pr_viv|Prionailurus
168. BCATS175-10|135_Pr_viv|Prionailurus
169. BCATS176-10|136_Pr_viv|Prionailurus
170. BCATS177-10|140_Pr_viv|Prionailurus
171. BCATS192-11|222_Pu_con|Puma
172. BCATS191-11|243_Pu_con|Puma
173. BCATS181-10|86_Pu_con|Puma
174. BCATS178-10|137_Pu_con|Puma
175. BCATS180-10|139_Pu_con|Puma
176. BCATS190-11|262_Pu_yag|Puma
177. BCATS182-10|72_Pu_yag|Puma

Consensus
1. BCATS004-10|2_Ac_jub|Acinonyx
2. BCATS003-10|1_Ac_jub|Acinonyx
3. BCATS002-10|160_Ac_jub|Acinonyx
4. BCATS001-10|11_Ac_jub|Acinonyx
5. BCATS013-10|83_Ac_jub_so|Acinonyx
6. BCATS012-10|82_Ac_jub|Acinonyx
7. BCATS011-10|81_Ac_jub|Acinonyx
8. BCATS010-10|3_Ac_jub|Acinonyx
9. BCATS017-10|98_Ca_ser|Caracal
10. BCATS016-10|97_Ca_ser|Caracal
11. BCATS015-10|96_Ca_ser|Caracal
12. BCATS014-10|90_Ca_ser|Caracal
13. BCATS021-10|214_Fe_cat|Felis
14. BCATS020-10|192_Fe_cat|Felis
15. BCATS019-10|191_Fe_cat|Felis
16. BCATS018-10|190_Fe_cat|Felis
17. BCATS029-10|198_Fe_mar|Felis
18. BCATS024-10|14_Fe_mar|Felis
19. BCATS033-10|204_Fe_nig|Felis
20. BCATS032-10|203_Fe_nig|Felis
21. BCATS031-10|202_Fe_nig|Felis
22. BCATS051-10|92_Fe_sil_go|Felis
23. BCATS050-10|91_Fe_sil|Felis
24. BCATS049-10|78_Fe_sil|Felis
25. BCATS048-10|77_Fe_sil|Felis
26. BCATS047-10|76_Fe_sil|Felis
27. BCATS041-10|216_Fe_sil|Felis
28. BCATS040-10|215_Fe_sil|Felis
29. BCATS039-10|213_Fe_sil|Felis
30. BCATS038-10|212_Fe_sil|Felis
31. BCATS034-10|145_Fe_sil|Felis
32. BCATS022-10|93_Fe_lyb|Felis
33. BCATS053-10|95_Le_geo|Leopardus
34. BCATS052-10|70_Le_geo|Leopardus
35. BCATS057-10|75_Le_tig|Leopardus
36. BCATS056-10|71_Le_tig|Leopardus
37. BCATS185-10|217_Ly_lyn_ly|Lynx
38. BCATS065-10|39_Ly_lyn_ly|Lynx
39. BCATS064-10|38_Ly_lyn_ly|Lynx
40. BCATS063-10|37_Ly_lyn_ly|Lynx
41. BCATS060-10|19_Ly_lyn_ly|Lynx
42. BCATS059-10|18_Ly_lyn_ly|Lynx
43. BCATS058-10|146_Ly_lyn|Lynx
44. BCATS071-10|99_Ly_ruf|Lynx
45. BCATS069-10|100_Ly_ruf|Lynx
46. BCATS088-10|89_Ot_man|Otocolobus
47. BCATS086-10|87_Ot_man|Otocolobus
48. BCATS081-10|193_Ot_man|Otocolobus
49. BCATS079-10|102_Ot_man|Otocolobus
50. BCATS186-10|28_Pa_leo_bl|Panthera
51. BCATS106-10|49_Pa_leo|Panthera
52. BCATS104-10|27_Pa_leo_bl|Panthera
53. BCATS103-10|26_Pa_leo_bl|Panthera
54. BCATS115-10|149_Pa_onc|Panthera
55. BCATS113-10|109_Pa_onc|Panthera
56. BCATS189-10|211_Pa_par_ori|Panthera
57. BCATS188-10|163_Pa_par_me|Panthera
58. BCATS187-10|73_Pa_par_ko|Panthera
59. BCATS183-10|122_Pa_par_or|Panthera
60. BCATS135-10|79_Pa_par_or|Panthera
61. BCATS134-10|74_Pa_par_ori|Panthera
62. BCATS128-10|168_Pa_par_ja|Panthera
63. BCATS127-10|162_Pa_par_or|Panthera
64. BCATS126-10|159_Pa_par_or|Panthera
65. BCATS125-10|148_Pa_par_sa|Panthera
66. BCATS124-10|121_Pa_par_or|Panthera
67. BCATS119-10|116_Pa_par_me|Panthera
68. BCATS158-10|68_Pa_tig_al|Panthera
69. BCATS156-10|189_Pa_tig_al|Panthera
70. BCATS155-10|166_Pa_tig|Panthera
71. BCATS154-10|165_Pa_tig_ti|Panthera
72. BCATS153-10|161_Pa_tig_su|Panthera
73. BCATS152-10|156_Pa_tig_al|Panthera

140 150 160 170 180 190 200 210 220 230 240
Consensus
1. BCATS004-10|2_Ac_jub|Acinonyx
2. BCATS003-10|1_Ac_jub|Acinonyx
3. BCATS002-10|160_Ac_jub|Acinonyx
4. BCATS001-10|11_Ac_jub|Acinonyx
5. BCATS013-10|83_Ac_jub_so|Acinonyx
6. BCATS012-10|82_Ac_jub|Acinonyx
7. BCATS011-10|81_Ac_jub|Acinonyx
8. BCATS010-10|3_Ac_jub|Acinonyx
9. BCATS017-10|98_Ca_ser|Caracal
10. BCATS016-10|97_Ca_ser|Caracal
11. BCATS015-10|96_Ca_ser|Caracal
12. BCATS014-10|90_Ca_ser|Caracal
13. BCATS021-10|214_Fe_cat|Felis
14. BCATS020-10|192_Fe_cat|Felis
15. BCATS019-10|191_Fe_cat|Felis
16. BCATS018-10|190_Fe_cat|Felis
17. BCATS029-10|198_Fe_mar|Felis
18. BCATS024-10|14_Fe_mar|Felis
19. BCATS033-10|204_Fe_nig|Felis
20. BCATS032-10|203_Fe_nig|Felis
21. BCATS031-10|202_Fe_nig|Felis
22. BCATS051-10|92_Fe_sil_go|Felis
23. BCATS050-10|91_Fe_sil|Felis
24. BCATS049-10|78_Fe_sil|Felis
25. BCATS048-10|77_Fe_sil|Felis
26. BCATS047-10|76_Fe_sil|Felis
27. BCATS041-10|216_Fe_sil|Felis
28. BCATS040-10|215_Fe_sil|Felis
29. BCATS039-10|213_Fe_sil|Felis
30. BCATS038-10|212_Fe_sil|Felis
31. BCATS034-10|145_Fe_sil|Felis
32. BCATS022-10|93_Fe_lyb|Felis
33. BCATS053-10|95_Le_geo|Leopardus
34. BCATS052-10|70_Le_geo|Leopardus
35. BCATS057-10|75_Le_tig|Leopardus
36. BCATS056-10|71_Le_tig|Leopardus
37. BCATS185-10|217_Ly_lyn_ly|Lynx
38. BCATS065-10|39_Ly_lyn_ly|Lynx
39. BCATS064-10|38_Ly_lyn_ly|Lynx
40. BCATS063-10|37_Ly_lyn_ly|Lynx
41. BCATS060-10|19_Ly_lyn_ly|Lynx
42. BCATS059-10|18_Ly_lyn_ly|Lynx
43. BCATS058-10|146_Ly_lyn|Lynx
44. BCATS071-10|99_Ly_ruf|Lynx
45. BCATS069-10|100_Ly_ruf|Lynx
46. BCATS088-10|89_Ot_man|Otocolobus
47. BCATS086-10|87_Ot_man|Otocolobus
48. BCATS081-10|193_Ot_man|Otocolobus
49. BCATS079-10|102_Ot_man|Otocolobus
50. BCATS186-10|28_Pa_leo_bl|Panthera
51. BCATS106-10|49_Pa_leo|Panthera
52. BCATS104-10|27_Pa_leo_bl|Panthera
53. BCATS103-10|26_Pa_leo_bl|Panthera
54. BCATS115-10|149_Pa_onc|Panthera
55. BCATS113-10|109_Pa_onc|Panthera
56. BCATS189-10|211_Pa_par_ori|Panthera
57. BCATS188-10|163_Pa_par_me|Panthera
58. BCATS187-10|73_Pa_par_ko|Panthera
59. BCATS183-10|122_Pa_par_or|Panthera
60. BCATS135-10|79_Pa_par_or|Panthera
61. BCATS134-10|74_Pa_par_ori|Panthera
62. BCATS128-10|168_Pa_par_ja|Panthera
63. BCATS127-10|162_Pa_par_or|Panthera
64. BCATS126-10|159_Pa_par_or|Panthera
65. BCATS125-10|148_Pa_par_sa|Panthera
66. BCATS124-10|121_Pa_par_or|Panthera
67. BCATS119-10|116_Pa_par_me|Panthera
68. BCATS158-10|68_Pa_tig_al|Panthera
69. BCATS156-10|189_Pa_tig_al|Panthera
70. BCATS155-10|166_Pa_tig|Panthera
71. BCATS154-10|165_Pa_tig_ti|Panthera
72. BCATS153-10|161_Pa_tig_su|Panthera
73. BCATS152-10|156_Pa_tig_al|Panthera

240
250
260
270
280
290
300
310
320
330
Consensus
1. BCATS004-10|2_Ac_jub|Acinonyx
2. BCATS003-10|1_Ac_jub|Acinonyx
3. BCATS002-10|160_Ac_jub|Acinonyx
4. BCATS001-10|11_Ac_jub|Acinonyx
5. BCATS013-10|83_Ac_jub_so|Acinonyx
6. BCATS012-10|82_Ac_jub|Acinonyx
7. BCATS011-10|81_Ac_jub|Acinonyx
8. BCATS010-10|3_Ac_jub|Acinonyx
9. BCATS017-10|98_Ca_ser|Caracal
10. BCATS016-10|97_Ca_ser|Caracal
11. BCATS015-10|96_Ca_ser|Caracal
12. BCATS014-10|90_Ca_ser|Caracal
13. BCATS021-10|214_Fe_cat|Felis
14. BCATS020-10|192_Fe_cat|Felis
15. BCATS019-10|191_Fe_cat|Felis
16. BCATS018-10|190_Fe_cat|Felis
17. BCATS029-10|198_Fe_mar|Felis
18. BCATS024-10|14_Fe_mar|Felis
19. BCATS033-10|204_Fe_nig|Felis
20. BCATS032-10|203_Fe_nig|Felis
21. BCATS031-10|202_Fe_nig|Felis
22. BCATS051-10|92_Fe_sil_go|Felis
23. BCATS050-10|91_Fe_sil|Felis
24. BCATS049-10|78_Fe_sil|Felis
25. BCATS048-10|77_Fe_sil|Felis
26. BCATS047-10|76_Fe_sil|Felis
27. BCATS041-10|216_Fe_sil|Felis
28. BCATS040-10|215_Fe_sil|Felis
29. BCATS039-10|213_Fe_sil|Felis
30. BCATS038-10|212_Fe_sil|Felis
31. BCATS034-10|145_Fe_sil|Felis
32. BCATS022-10|93_Fe_lyb|Felis
33. BCATS053-10|95_Le_geo|Leopardus
34. BCATS052-10|70_Le_geo|Leopardus
35. BCATS057-10|75_Le_tig|Leopardus
36. BCATS056-10|71_Le_tig|Leopardus
37. BCATS185-10|217_Ly_lyn_ly|Lynx
38. BCATS065-10|39_Ly_lyn_ly|Lynx
39. BCATS064-10|38_Ly_lyn_ly|Lynx
40. BCATS063-10|37_Ly_lyn_ly|Lynx
41. BCATS060-10|19_Ly_lyn_ly|Lynx
42. BCATS059-10|18_Ly_lyn_ly|Lynx
43. BCATS058-10|146_Ly_lyn|Lynx
44. BCATS071-10|99_Ly_ruf|Lynx
45. BCATS069-10|100_Ly_ruf|Lynx
46. BCATS088-10|89_Ot_man|Otocolobus
47. BCATS086-10|87_Ot_man|Otocolobus
48. BCATS081-10|193_Ot_man|Otocolobus
49. BCATS079-10|102_Ot_man|Otocolobus
50. BCATS186-10|28_Pa_leo_bl|Panthera
51. BCATS106-10|49_Pa_leo|Panthera
52. BCATS104-10|27_Pa_leo_bl|Panthera
53. BCATS103-10|26_Pa_leo_bl|Panthera
54. BCATS115-10|149_Pa_onc|Panthera
55. BCATS113-10|109_Pa_onc|Panthera
56. BCATS189-10|211_Pa_par_ori|Panthera
57. BCATS188-10|163_Pa_par_me|Panthera
58. BCATS187-10|73_Pa_par_ko|Panthera
59. BCATS183-10|122_Pa_par_or|Panthera
60. BCATS135-10|79_Pa_par_or|Panthera
61. BCATS134-10|74_Pa_par_ori|Panthera
62. BCATS128-10|168_Pa_par_ja|Panthera
63. BCATS127-10|162_Pa_par_or|Panthera
64. BCATS126-10|159_Pa_par_or|Panthera
65. BCATS125-10|148_Pa_par_sa|Panthera
66. BCATS124-10|121_Pa_par_or|Panthera
67. BCATS119-10|116_Pa_par_me|Panthera
68. BCATS158-10|68_Pa_tig_al|Panthera
69. BCATS156-10|189_Pa_tig_al|Panthera
70. BCATS155-10|166_Pa_tig|Panthera
71. BCATS154-10|165_Pa_tig_ti|Panthera
72. BCATS153-10|161_Pa_tig_su|Panthera
73. BCATS152-10|156_Pa_tig_al|Panthera

340
350
360
370
380
390
400
410
420
430
Consensus
1. BCATS004-10|2_Ac_jub|Acinonyx
2. BCATS003-10|1_Ac_jub|Acinonyx
3. BCATS002-10|160_Ac_jub|Acinonyx
4. BCATS001-10|11_Ac_jub|Acinonyx
5. BCATS013-10|83_Ac_jub_so|Acinonyx
6. BCATS012-10|82_Ac_jub|Acinonyx
7. BCATS011-10|81_Ac_jub|Acinonyx
8. BCATS010-10|3_Ac_jub|Acinonyx
9. BCATS017-10|98_Ca_ser|Caracal
10. BCATS016-10|97_Ca_ser|Caracal
11. BCATS015-10|96_Ca_ser|Caracal
12. BCATS014-10|90_Ca_ser|Caracal
13. BCATS021-10|214_Fe_cat|Felis
14. BCATS020-10|192_Fe_cat|Felis
15. BCATS019-10|191_Fe_cat|Felis
16. BCATS018-10|190_Fe_cat|Felis
17. BCATS029-10|198_Fe_mar|Felis
18. BCATS024-10|14_Fe_mar|Felis
19. BCATS033-10|204_Fe_nig|Felis
20. BCATS032-10|203_Fe_nig|Felis
21. BCATS031-10|202_Fe_nig|Felis
22. BCATS051-10|92_Fe_sil_go|Felis
23. BCATS050-10|91_Fe_sil|Felis
24. BCATS049-10|78_Fe_sil|Felis
25. BCATS048-10|77_Fe_sil|Felis
26. BCATS047-10|76_Fe_sil|Felis
27. BCATS041-10|216_Fe_sil|Felis
28. BCATS040-10|215_Fe_sil|Felis
29. BCATS039-10|213_Fe_sil|Felis
30. BCATS038-10|212_Fe_sil|Felis
31. BCATS034-10|145_Fe_sil|Felis
32. BCATS022-10|93_Fe_lyb|Felis
33. BCATS053-10|95_Le_geo|Leopardus
34. BCATS052-10|70_Le_geo|Leopardus
35. BCATS057-10|75_Le_tig|Leopardus
36. BCATS056-10|71_Le_tig|Leopardus
37. BCATS185-10|217_Ly_lyn_ly|Lynx
38. BCATS065-10|39_Ly_lyn_ly|Lynx
39. BCATS064-10|38_Ly_lyn_ly|Lynx
40. BCATS063-10|37_Ly_lyn_ly|Lynx
41. BCATS060-10|19_Ly_lyn_ly|Lynx
42. BCATS059-10|18_Ly_lyn_ly|Lynx
43. BCATS058-10|146_Ly_lyn|Lynx
44. BCATS071-10|99_Ly_ruf|Lynx
45. BCATS069-10|100_Ly_ruf|Lynx
46. BCATS088-10|89_Ot_man|Otocolobus
47. BCATS086-10|87_Ot_man|Otocolobus
48. BCATS081-10|193_Ot_man|Otocolobus
49. BCATS079-10|102_Ot_man|Otocolobus
50. BCATS186-10|28_Pa_leo_bl|Panthera
51. BCATS106-10|49_Pa_leo|Panthera
52. BCATS104-10|27_Pa_leo_bl|Panthera
53. BCATS103-10|26_Pa_leo_bl|Panthera
54. BCATS115-10|149_Pa_onc|Panthera
55. BCATS113-10|109_Pa_onc|Panthera
56. BCATS189-10|211_Pa_par_ori|Panthera
57. BCATS188-10|163_Pa_par_me|Panthera
58. BCATS187-10|73_Pa_par_ko|Panthera
59. BCATS183-10|122_Pa_par_or|Panthera
60. BCATS135-10|79_Pa_par_or|Panthera
61. BCATS134-10|74_Pa_par_ori|Panthera
62. BCATS128-10|168_Pa_par_ja|Panthera
63. BCATS127-10|162_Pa_par_or|Panthera
64. BCATS126-10|159_Pa_par_or|Panthera
65. BCATS125-10|148_Pa_par_sa|Panthera
66. BCATS124-10|121_Pa_par_or|Panthera
67. BCATS119-10|116_Pa_par_me|Panthera
68. BCATS158-10|68_Pa_tig_al|Panthera
69. BCATS156-10|189_Pa_tig_al|Panthera
70. BCATS155-10|166_Pa_tig|Panthera
71. BCATS154-10|165_Pa_tig_ti|Panthera
72. BCATS153-10|161_Pa_tig_su|Panthera
73. BCATS152-10|156_Pa_tig_al|Panthera

440
450
460
470
480
490
500
510
520
530
Consensus
1. BCATS004-10|2_Ac_jub|Acinonyx
2. BCATS003-10|1_Ac_jub|Acinonyx
3. BCATS002-10|160_Ac_jub|Acinonyx
4. BCATS001-10|11_Ac_jub|Acinonyx
5. BCATS013-10|83_Ac_jub_so|Acinonyx
6. BCATS012-10|82_Ac_jub|Acinonyx
7. BCATS011-10|81_Ac_jub|Acinonyx
8. BCATS010-10|3_Ac_jub|Acinonyx
9. BCATS017-10|98_Ca_ser|Caracal
10. BCATS016-10|97_Ca_ser|Caracal
11. BCATS015-10|96_Ca_ser|Caracal
12. BCATS014-10|90_Ca_ser|Caracal
13. BCATS021-10|214_Fe_cat|Felis
14. BCATS020-10|192_Fe_cat|Felis
15. BCATS019-10|191_Fe_cat|Felis
16. BCATS018-10|190_Fe_cat|Felis
17. BCATS029-10|198_Fe_mar|Felis
18. BCATS024-10|14_Fe_mar|Felis
19. BCATS033-10|204_Fe_nig|Felis
20. BCATS032-10|203_Fe_nig|Felis
21. BCATS031-10|202_Fe_nig|Felis
22. BCATS051-10|92_Fe_sil_go|Felis
23. BCATS050-10|91_Fe_sil|Felis
24. BCATS049-10|78_Fe_sil|Felis
25. BCATS048-10|77_Fe_sil|Felis
26. BCATS047-10|76_Fe_sil|Felis
27. BCATS041-10|216_Fe_sil|Felis
28. BCATS040-10|215_Fe_sil|Felis
29. BCATS039-10|213_Fe_sil|Felis
30. BCATS038-10|212_Fe_sil|Felis
31. BCATS034-10|145_Fe_sil|Felis
32. BCATS022-10|93_Fe_lyb|Felis
33. BCATS053-10|95_Le_geo|Leopardus
34. BCATS052-10|70_Le_geo|Leopardus
35. BCATS057-10|75_Le_tig|Leopardus
36. BCATS056-10|71_Le_tig|Leopardus
37. BCATS185-10|217_Ly_lyn_ly|Lynx
38. BCATS065-10|39_Ly_lyn_ly|Lynx
39. BCATS064-10|38_Ly_lyn_ly|Lynx
40. BCATS063-10|37_Ly_lyn_ly|Lynx
41. BCATS060-10|19_Ly_lyn_ly|Lynx
42. BCATS059-10|18_Ly_lyn_ly|Lynx
43. BCATS058-10|146_Ly_lyn|Lynx
44. BCATS071-10|99_Ly_ruf|Lynx
45. BCATS069-10|100_Ly_ruf|Lynx
46. BCATS088-10|89_Ot_man|Otocolobus
47. BCATS086-10|87_Ot_man|Otocolobus
48. BCATS081-10|193_Ot_man|Otocolobus
49. BCATS079-10|102_Ot_man|Otocolobus
50. BCATS186-10|28_Pa_leo_bl|Panthera
51. BCATS106-10|49_Pa_leo|Panthera
52. BCATS104-10|27_Pa_leo_bl|Panthera
53. BCATS103-10|26_Pa_leo_bl|Panthera
54. BCATS115-10|149_Pa_onc|Panthera
55. BCATS113-10|109_Pa_onc|Panthera
56. BCATS189-10|211_Pa_par_ori|Panthera
57. BCATS188-10|163_Pa_par_me|Panthera
58. BCATS187-10|73_Pa_par_ko|Panthera
59. BCATS183-10|122_Pa_par_or|Panthera
60. BCATS135-10|79_Pa_par_or|Panthera
61. BCATS134-10|74_Pa_par_ori|Panthera
62. BCATS128-10|168_Pa_par_ja|Panthera
63. BCATS127-10|162_Pa_par_or|Panthera
64. BCATS126-10|159_Pa_par_or|Panthera
65. BCATS125-10|148_Pa_par_sa|Panthera
66. BCATS124-10|121_Pa_par_or|Panthera
67. BCATS119-10|116_Pa_par_me|Panthera
68. BCATS158-10|68_Pa_tig_al|Panthera
69. BCATS156-10|189_Pa_tig_al|Panthera
70. BCATS155-10|166_Pa_tig|Panthera
71. BCATS154-10|165_Pa_tig_ti|Panthera
72. BCATS153-10|161_Pa_tig_su|Panthera
73. BCATS152-10|156_Pa_tig_al|Panthera

540
550
560
570
580
590
600
610
620
630
64
Consensus
1. BCATS004-10|2_Ac_jub|Acinonyx
2. BCATS003-10|1_Ac_jub|Acinonyx
3. BCATS002-10|160_Ac_jub|Acinonyx
4. BCATS001-10|11_Ac_jub|Acinonyx
5. BCATS013-10|83_Ac_jub_so|Acinonyx
6. BCATS012-10|82_Ac_jub|Acinonyx
7. BCATS011-10|81_Ac_jub|Acinonyx
8. BCATS010-10|3_Ac_jub|Acinonyx
9. BCATS017-10|98_Ca_ser|Caracal
10. BCATS016-10|97_Ca_ser|Caracal
11. BCATS015-10|96_Ca_ser|Caracal
12. BCATS014-10|90_Ca_ser|Caracal
13. BCATS021-10|214_Fe_cat|Felis
14. BCATS020-10|192_Fe_cat|Felis
15. BCATS019-10|191_Fe_cat|Felis
16. BCATS018-10|190_Fe_cat|Felis
17. BCATS029-10|198_Fe_mar|Felis
18. BCATS024-10|14_Fe_mar|Felis
19. BCATS033-10|204_Fe_nig|Felis
20. BCATS032-10|203_Fe_nig|Felis
21. BCATS031-10|202_Fe_nig|Felis
22. BCATS051-10|92_Fe_sil_go|Felis
23. BCATS050-10|91_Fe_sil|Felis
24. BCATS049-10|78_Fe_sil|Felis
25. BCATS048-10|77_Fe_sil|Felis
26. BCATS047-10|76_Fe_sil|Felis
27. BCATS041-10|216_Fe_sil|Felis
28. BCATS040-10|215_Fe_sil|Felis
29. BCATS039-10|213_Fe_sil|Felis
30. BCATS038-10|212_Fe_sil|Felis
31. BCATS034-10|145_Fe_sil|Felis
32. BCATS022-10|93_Fe_lyb|Felis
33. BCATS053-10|95_Le_geo|Leopardus
34. BCATS052-10|70_Le_geo|Leopardus
35. BCATS057-10|75_Le_tig|Leopardus
36. BCATS056-10|71_Le_tig|Leopardus
37. BCATS185-10|217_Ly_lyn_ly|Lynx
38. BCATS065-10|39_Ly_lyn_ly|Lynx
39. BCATS064-10|38_Ly_lyn_ly|Lynx
40. BCATS063-10|37_Ly_lyn_ly|Lynx
41. BCATS060-10|19_Ly_lyn_ly|Lynx
42. BCATS059-10|18_Ly_lyn_ly|Lynx
43. BCATS058-10|146_Ly_lyn|Lynx
44. BCATS071-10|99_Ly_ruf|Lynx
45. BCATS069-10|100_Ly_ruf|Lynx
46. BCATS088-10|89_Ot_man|Otocolobus
47. BCATS086-10|87_Ot_man|Otocolobus
48. BCATS081-10|193_Ot_man|Otocolobus
49. BCATS079-10|102_Ot_man|Otocolobus
50. BCATS186-10|28_Pa_leo_bl|Panthera
51. BCATS106-10|49_Pa_leo|Panthera
52. BCATS104-10|27_Pa_leo_bl|Panthera
53. BCATS103-10|26_Pa_leo_bl|Panthera
54. BCATS115-10|149_Pa_onc|Panthera
55. BCATS113-10|109_Pa_onc|Panthera
56. BCATS189-10|211_Pa_par_ori|Panthera
57. BCATS188-10|163_Pa_par_me|Panthera
58. BCATS187-10|73_Pa_par_ko|Panthera
59. BCATS183-10|122_Pa_par_or|Panthera
60. BCATS135-10|79_Pa_par_or|Panthera
61. BCATS134-10|74_Pa_par_ori|Panthera
62. BCATS128-10|168_Pa_par_ja|Panthera
63. BCATS127-10|162_Pa_par_or|Panthera
64. BCATS126-10|159_Pa_par_or|Panthera
65. BCATS125-10|148_Pa_par_sa|Panthera
66. BCATS124-10|121_Pa_par_or|Panthera
67. BCATS119-10|116_Pa_par_me|Panthera
68. BCATS158-10|68_Pa_tig_al|Panthera
69. BCATS156-10|189_Pa_tig_al|Panthera
70. BCATS155-10|166_Pa_tig|Panthera
71. BCATS154-10|165_Pa_tig_ti|Panthera
72. BCATS153-10|161_Pa_tig_su|Panthera
73. BCATS152-10|156_Pa_tig_al|Panthera

640 650 660 670 680 690 700 710 720 730 74
Consensus
1. BCATS004-10|2_Ac_jub|Acinonyx
2. BCATS003-10|1_Ac_jub|Acinonyx
3. BCATS002-10|160_Ac_jub|Acinonyx
4. BCATS001-10|11_Ac_jub|Acinonyx
5. BCATS013-10|83_Ac_jub_so|Acinonyx
6. BCATS012-10|82_Ac_jub|Acinonyx
7. BCATS011-10|81_Ac_jub|Acinonyx
8. BCATS010-10|3_Ac_jub|Acinonyx
9. BCATS017-10|98_Ca_ser|Caracal
10. BCATS016-10|97_Ca_ser|Caracal
11. BCATS015-10|96_Ca_ser|Caracal
12. BCATS014-10|90_Ca_ser|Caracal
13. BCATS021-10|214_Fe_cat|Felis
14. BCATS020-10|192_Fe_cat|Felis
15. BCATS019-10|191_Fe_cat|Felis
16. BCATS018-10|190_Fe_cat|Felis
17. BCATS029-10|198_Fe_mar|Felis
18. BCATS024-10|14_Fe_mar|Felis
19. BCATS033-10|204_Fe_nig|Felis
20. BCATS032-10|203_Fe_nig|Felis
21. BCATS031-10|202_Fe_nig|Felis
22. BCATS051-10|92_Fe_sil_go|Felis
23. BCATS050-10|91_Fe_sil|Felis
24. BCATS049-10|78_Fe_sil|Felis
25. BCATS048-10|77_Fe_sil|Felis
26. BCATS047-10|76_Fe_sil|Felis
27. BCATS041-10|216_Fe_sil|Felis
28. BCATS040-10|215_Fe_sil|Felis
29. BCATS039-10|213_Fe_sil|Felis
30. BCATS038-10|212_Fe_sil|Felis
31. BCATS034-10|145_Fe_sil|Felis
32. BCATS022-10|93_Fe_lyb|Felis
33. BCATS053-10|95_Le_geo|Leopardus
34. BCATS052-10|70_Le_geo|Leopardus
35. BCATS057-10|75_Le_tig|Leopardus
36. BCATS056-10|71_Le_tig|Leopardus
37. BCATS185-10|217_Ly_lyn_ly|Lynx
38. BCATS065-10|39_Ly_lyn_ly|Lynx
39. BCATS064-10|38_Ly_lyn_ly|Lynx
40. BCATS063-10|37_Ly_lyn_ly|Lynx
41. BCATS060-10|19_Ly_lyn_ly|Lynx
42. BCATS059-10|18_Ly_lyn_ly|Lynx
43. BCATS058-10|146_Ly_lyn|Lynx
44. BCATS071-10|99_Ly_ruf|Lynx
45. BCATS069-10|100_Ly_ruf|Lynx
46. BCATS088-10|89_Ot_man|Otocolobus
47. BCATS086-10|87_Ot_man|Otocolobus
48. BCATS081-10|193_Ot_man|Otocolobus
49. BCATS079-10|102_Ot_man|Otocolobus
50. BCATS186-10|28_Pa_leo_bl|Panthera
51. BCATS106-10|49_Pa_leo|Panthera
52. BCATS104-10|27_Pa_leo_bl|Panthera
53. BCATS103-10|26_Pa_leo_bl|Panthera
54. BCATS115-10|149_Pa_onc|Panthera
55. BCATS113-10|109_Pa_onc|Panthera
56. BCATS189-10|211_Pa_par_ori|Panthera
57. BCATS188-10|163_Pa_par_me|Panthera
58. BCATS187-10|73_Pa_par_ko|Panthera
59. BCATS183-10|122_Pa_par_or|Panthera
60. BCATS135-10|79_Pa_par_or|Panthera
61. BCATS134-10|74_Pa_par_ori|Panthera
62. BCATS128-10|168_Pa_par_ja|Panthera
63. BCATS127-10|162_Pa_par_or|Panthera
64. BCATS126-10|159_Pa_par_or|Panthera
65. BCATS125-10|148_Pa_par_sa|Panthera
66. BCATS124-10|121_Pa_par_or|Panthera
67. BCATS119-10|116_Pa_par_me|Panthera
68. BCATS158-10|68_Pa_tig_al|Panthera
69. BCATS156-10|189_Pa_tig_al|Panthera
70. BCATS155-10|166_Pa_tig|Panthera
71. BCATS154-10|165_Pa_tig_ti|Panthera
72. BCATS153-10|161_Pa_tig_su|Panthera
73. BCATS152-10|156_Pa_tig_al|Panthera

	40 750 760 770 780 790 800 810 820 830 840
Consensus	-----------------------------------AGCTCCTGTCACTACCAGTTCTAGCAG
1. BCATS004-10|2_Ac_jub|Acinonyx	
2. BCATS003-10|1_Ac_jub|Acinonyx	
3. BCATS002-10|160_Ac_jub|Acinonyx	
4. BCATS001-10|11_Ac_jub|Acinonyx	
5. BCATS013-10|83_Ac_jub_so|Acinonyx	
6. BCATS012-10|82_Ac_jub|Acinonyx	
7. BCATS011-10|81_Ac_jub|Acinonyx	
8. BCATS010-10|3_Ac_jub|Acinonyx	
9. BCATS017-10|98_Ca_ser|Caracal	
10. BCATS016-10|97_Ca_ser|Caracal	
11. BCATS015-10|96_Ca_ser|Caracal	
12. BCATS014-10|90_Ca_ser|Caracal	
13. BCATS021-10|214_Fe_cat|Felis	
14. BCATS020-10|192_Fe_cat|Felis	
15. BCATS019-10|191_Fe_cat|Felis	
16. BCATS018-10|190_Fe_cat|Felis	
17. BCATS029-10|198_Fe_mar|Felis	
18. BCATS024-10|14_Fe_mar|Felis	
19. BCATS033-10|204_Fe_nig|Felis	
20. BCATS032-10|203_Fe_nig|Felis	
21. BCATS031-10|202_Fe_nig|Felis	
22. BCATS051-10|92_Fe_sil_go|Felis	
23. BCATS050-10|91_Fe_sil|Felis	
24. BCATS049-10|78_Fe_sil|Felis	
25. BCATS048-10|77_Fe_sil|Felis	
26. BCATS047-10|76_Fe_sil|Felis	
27. BCATS041-10|216_Fe_sil|Felis	
28. BCATS040-10|215_Fe_sil|Felis	
29. BCATS039-10|213_Fe_sil|Felis	
30. BCATS038-10|212_Fe_sil|Felis	
31. BCATS034-10|145_Fe_sil|Felis	
32. BCATS022-10|93_Fe_lyb|Felis	
33. BCATS053-10|95_Le_geo|Leopardus	
34. BCATS052-10|70_Le_geo|Leopardus	
35. BCATS057-10|75_Le_tig|Leopardus	
36. BCATS056-10|71_Le_tig|Leopardus	
37. BCATS185-10|217_Ly_lyn_ly|Lynx	
38. BCATS065-10|39_Ly_lyn_ly|Lynx	
39. BCATS064-10|38_Ly_lyn_ly|Lynx	
40. BCATS063-10|37_Ly_lyn_ly|Lynx	
41. BCATS060-10|19_Ly_lyn_ly|Lynx	
42. BCATS059-10|18_Ly_lyn_ly|Lynx	
43. BCATS058-10|146_Ly_lyn|Lynx	
44. BCATS071-10|99_Ly_ruf|Lynx	
45. BCATS069-10|100_Ly_ruf|Lynx	
46. BCATS088-10|89_Ot_man|Otocolobus	-----------------------------------AGCTCCTGTCACTACCAGTTCTAGCAG
47. BCATS086-10|87_Ot_man|Otocolobus	-----------------------------------AGCTCCTGTCACTACCAGTTCTAGCAG
48. BCATS081-10|193_Ot_man|Otocolobus	-----------------------------------AGCTCCTGTCACTACCAGTTCTAGCAG
49. BCATS079-10|102_Ot_man|Otocolobus	-----------------------------------AGCTCCTGTCACTACCAGTTCTAGCAG
50. BCATS186-10|28_Pa_leo_bl|Panthera	
51. BCATS106-10|49_Pa_leo|Panthera	
52. BCATS104-10|27_Pa_leo_bl|Panthera	
53. BCATS103-10|26_Pa_leo_bl|Panthera	
54. BCATS115-10|149_Pa_onc|Panthera	
55. BCATS113-10|109_Pa_onc|Panthera	
56. BCATS189-10|211_Pa_par_ori|Panthera	
57. BCATS188-10|163_Pa_par_me|Panthera	
58. BCATS187-10|73_Pa_par_ko|Panthera	
59. BCATS183-10|122_Pa_par_or|Panthera	
60. BCATS135-10|79_Pa_par_or|Panthera	
61. BCATS134-10|74_Pa_par_ori|Panthera	
62. BCATS128-10|168_Pa_par_ja|Panthera	
63. BCATS127-10|162_Pa_par_or|Panthera	
64. BCATS126-10|159_Pa_par_or|Panthera	
65. BCATS125-10|148_Pa_par_sa|Panthera	
66. BCATS124-10|121_Pa_par_or|Panthera	
67. BCATS119-10|116_Pa_par_me|Panthera	
68. BCATS158-10|68_Pa_tig_al|Panthera	
69. BCATS156-10|189_Pa_tig_al|Panthera	
70. BCATS155-10|166_Pa_tig|Panthera	
71. BCATS154-10|165_Pa_tig_ti|Panthera	
72. BCATS153-10|161_Pa_tig_su|Panthera	
73. BCATS152-10|156_Pa_tig_al|Panthera	
74. BCATS151-10|155_Pa_tig_al|Panthera	

Consensus
32. BCATS022-10|93_Fe_lyb|Felis
33. BCATS053-10|95_Le_geo|Leopardus
34. BCATS052-10|70_Le_geo|Leopardus
35. BCATS057-10|75_Le_tig|Leopardus
36. BCATS056-10|71_Le_tig|Leopardus
37. BCATS185-10|217_Ly_lyn_ly|Lynx
38. BCATS065-10|39_Ly_lyn_ly|Lynx
39. BCATS064-10|38_Ly_lyn_ly|Lynx
40. BCATS063-10|37_Ly_lyn_ly|Lynx
41. BCATS060-10|19_Ly_lyn_ly|Lynx
42. BCATS059-10|18_Ly_lyn_ly|Lynx
43. BCATS058-10|146_Ly_lyn|Lynx
44. BCATS071-10|99_Ly_ruf|Lynx
45. BCATS069-10|100_Ly_ruf|Lynx
46. BCATS088-10|89_Ot_man|Otocolobus
47. BCATS086-10|87_Ot_man|Otocolobus
48. BCATS081-10|193_Ot_man|Otocolobus
49. BCATS079-10|102_Ot_man|Otocolobus
50. BCATS186-10|28_Pa_leo_bl|Panthera
51. BCATS106-10|49_Pa_leo|Panthera
52. BCATS104-10|27_Pa_leo_bl|Panthera
53. BCATS103-10|26_Pa_leo_bl|Panthera
54. BCATS115-10|149_Pa_onc|Panthera
55. BCATS113-10|109_Pa_onc|Panthera
56. BCATS189-10|211_Pa_par_ori|Panthera
57. BCATS188-10|163_Pa_par_me|Panthera
58. BCATS187-10|73_Pa_par_ko|Panthera
59. BCATS183-10|122_Pa_par_or|Panthera
60. BCATS135-10|79_Pa_par_or|Panthera
61. BCATS134-10|74_Pa_par_ori|Panthera
62. BCATS128-10|168_Pa_par_ja|Panthera
63. BCATS127-10|162_Pa_par_or|Panthera
64. BCATS126-10|159_Pa_par_or|Panthera
65. BCATS125-10|148_Pa_par_sa|Panthera
66. BCATS124-10|121_Pa_par_or|Panthera
67. BCATS119-10|116_Pa_par_me|Panthera
68. BCATS158-10|68_Pa_tig_al|Panthera
69. BCATS156-10|189_Pa_tig_al|Panthera
70. BCATS155-10|166_Pa_tig|Panthera
71. BCATS154-10|165_Pa_tig_ti|Panthera
72. BCATS153-10|161_Pa_tig_su|Panthera
73. BCATS152-10|156_Pa_tig_al|Panthera
74. BCATS151-10|155_Pa_tig_al|Panthera
75. BCATS150-10|153_Pa_tig_al|Panthera
76. BCATS149-10|150_Pa_tig_al|Panthera
77. BCATS148-10|147_Pa_tig_al|Panthera
78. BCATS147-10|13_Pa_tig_su|Panthera
79. BCATS146-10|12_Pa_tig_su|Panthera
80. BCATS145-10|129_Pa_tig_ti|Panthera
81. BCATS144-10|128_Pa_tig_ti|Panthera
82. BCATS143-10|127_Pa_tig_su|Panthera
83. BCATS142-10|126_Pa_tig_su|Panthera
84. BCATS140-10|124_Pa_tig_al|Panthera
85. BCATS139-10|123_Pa_tig_al|Panthera
86. BCATS159-10|157_Pa_unc|Panthera
87. BCATS166-10|69_Pa_unc|Panthera
88. BCATS138-10|152_Pa_tem|Pardofelis
89. BCATS137-10|85_Pa_tem|Pardofelis
90. BCATS136-10|84_Pa_tem|Pardofelis
91. BCATS168-10|131_Pr_ben|Prionailurus
92. BCATS167-10|130_Pr_ben|Prionailurus
93. BCATS170-10|154_Pr_rub|Prionailurus
94. BCATS169-10|132_Pr_rub|Prionailurus
95. BCATS176-10|136_Pr_viv|Prionailurus
96. BCATS175-10|135_Pr_viv|Prionailurus
97. BCATS174-10|134_Pr_viv|Prionailurus
98. BCATS173-10|133_Pr_viv|Prionailurus
99. BCATS184-10|144_Pu_con|Puma
100. BCATS181-10|86_Pu_con|Puma
101. BCATS180-10|139_Pu_con|Puma
102. BCATS179-10|138_Pu_con|Puma
103. BCATS178-10|137_Pu_con|Puma
104. BCATS182-10|72_Pu_yag|Puma

Consensus
32. BCATS022-10|93_Fe_lyb|Felis
33. BCATS053-10|95_Le_geo|Leopardus
34. BCATS052-10|70_Le_geo|Leopardus
35. BCATS057-10|75_Le_tig|Leopardus
36. BCATS056-10|71_Le_tig|Leopardus
37. BCATS185-10|217_Ly_lyn_ly|Lynx
38. BCATS065-10|39_Ly_lyn_ly|Lynx
39. BCATS064-10|38_Ly_lyn_ly|Lynx
40. BCATS063-10|37_Ly_lyn_ly|Lynx
41. BCATS060-10|19_Ly_lyn_ly|Lynx
42. BCATS059-10|18_Ly_lyn_ly|Lynx
43. BCATS058-10|146_Ly_lyn|Lynx
44. BCATS071-10|99_Ly_ruf|Lynx
45. BCATS069-10|100_Ly_ruf|Lynx
46. BCATS088-10|89_Ot_man|Otocolobus
47. BCATS086-10|87_Ot_man|Otocolobus
48. BCATS081-10|193_Ot_man|Otocolobus
49. BCATS079-10|102_Ot_man|Otocolobus
50. BCATS186-10|28_Pa_leo_bl|Panthera
51. BCATS106-10|49_Pa_leo|Panthera
52. BCATS104-10|27_Pa_leo_bl|Panthera
53. BCATS103-10|26_Pa_leo_bl|Panthera
54. BCATS115-10|149_Pa_onc|Panthera
55. BCATS113-10|109_Pa_onc|Panthera
56. BCATS189-10|211_Pa_par_ori|Panthera
57. BCATS188-10|163_Pa_par_me|Panthera
58. BCATS187-10|73_Pa_par_ko|Panthera
59. BCATS183-10|122_Pa_par_or|Panthera
60. BCATS135-10|79_Pa_par_or|Panthera
61. BCATS134-10|74_Pa_par_ori|Panthera
62. BCATS128-10|168_Pa_par_ja|Panthera
63. BCATS127-10|162_Pa_par_or|Panthera
64. BCATS126-10|159_Pa_par_or|Panthera
65. BCATS125-10|148_Pa_par_sa|Panthera
66. BCATS124-10|121_Pa_par_or|Panthera
67. BCATS119-10|116_Pa_par_me|Panthera
68. BCATS158-10|68_Pa_tig_al|Panthera
69. BCATS156-10|189_Pa_tig_al|Panthera
70. BCATS155-10|166_Pa_tig|Panthera
71. BCATS154-10|165_Pa_tig_ti|Panthera
72. BCATS153-10|161_Pa_tig_su|Panthera
73. BCATS152-10|156_Pa_tig_al|Panthera
74. BCATS151-10|155_Pa_tig_al|Panthera
75. BCATS150-10|153_Pa_tig_al|Panthera
76. BCATS149-10|150_Pa_tig_al|Panthera
77. BCATS148-10|147_Pa_tig_al|Panthera
78. BCATS147-10|13_Pa_tig_su|Panthera
79. BCATS146-10|12_Pa_tig_su|Panthera
80. BCATS145-10|129_Pa_tig_ti|Panthera
81. BCATS144-10|128_Pa_tig_ti|Panthera
82. BCATS143-10|127_Pa_tig_su|Panthera
83. BCATS142-10|126_Pa_tig_su|Panthera
84. BCATS140-10|124_Pa_tig_al|Panthera
85. BCATS139-10|123_Pa_tig_al|Panthera
86. BCATS159-10|157_Pa_unc|Panthera
87. BCATS166-10|69_Pa_unc|Panthera
88. BCATS138-10|152_Pa_tem|Pardofelis
89. BCATS137-10|85_Pa_tem|Pardofelis
90. BCATS136-10|84_Pa_tem|Pardofelis
91. BCATS168-10|131_Pr_ben|Prionailurus
92. BCATS167-10|130_Pr_ben|Prionailurus
93. BCATS170-10|154_Pr_rub|Prionailurus
94. BCATS169-10|132_Pr_rub|Prionailurus
95. BCATS176-10|136_Pr_viv|Prionailurus
96. BCATS175-10|135_Pr_viv|Prionailurus
97. BCATS174-10|134_Pr_viv|Prionailurus
98. BCATS173-10|133_Pr_viv|Prionailurus
99. BCATS184-10|144_Pu_con|Puma
100. BCATS181-10|86_Pu_con|Puma
101. BCATS180-10|139_Pu_con|Puma
102. BCATS179-10|138_Pu_con|Puma
103. BCATS178-10|137_Pu_con|Puma
104. BCATS182-10|72_Pu_yag|Puma

240
250
260
270
280
290
300
310
320
330
Consensus
32. BCATS022-10|93_Fe_lyb|Felis
33. BCATS053-10|95_Le_geo|Leopardus
34. BCATS052-10|70_Le_geo|Leopardus
35. BCATS057-10|75_Le_tig|Leopardus
36. BCATS056-10|71_Le_tig|Leopardus
37. BCATS185-10|217_Ly_lyn_ly|Lynx
38. BCATS065-10|39_Ly_lyn_ly|Lynx
39. BCATS064-10|38_Ly_lyn_ly|Lynx
40. BCATS063-10|37_Ly_lyn_ly|Lynx
41. BCATS060-10|19_Ly_lyn_ly|Lynx
42. BCATS059-10|18_Ly_lyn_ly|Lynx
43. BCATS058-10|146_Ly_lyn|Lynx
44. BCATS071-10|99_Ly_ruf|Lynx
45. BCATS069-10|100_Ly_ruf|Lynx
46. BCATS088-10|89_Ot_man|Otocolobus
47. BCATS086-10|87_Ot_man|Otocolobus
48. BCATS081-10|193_Ot_man|Otocolobus
49. BCATS079-10|102_Ot_man|Otocolobus
50. BCATS186-10|28_Pa_leo_bl|Panthera
51. BCATS106-10|49_Pa_leo|Panthera
52. BCATS104-10|27_Pa_leo_bl|Panthera
53. BCATS103-10|26_Pa_leo_bl|Panthera
54. BCATS115-10|149_Pa_onc|Panthera
55. BCATS113-10|109_Pa_onc|Panthera
56. BCATS189-10|211_Pa_par_ori|Panthera
57. BCATS188-10|163_Pa_par_me|Panthera
58. BCATS187-10|73_Pa_par_ko|Panthera
59. BCATS183-10|122_Pa_par_or|Panthera
60. BCATS135-10|79_Pa_par_or|Panthera
61. BCATS134-10|74_Pa_par_ori|Panthera
62. BCATS128-10|168_Pa_par_ja|Panthera
63. BCATS127-10|162_Pa_par_or|Panthera
64. BCATS126-10|159_Pa_par_or|Panthera
65. BCATS125-10|148_Pa_par_sa|Panthera
66. BCATS124-10|121_Pa_par_or|Panthera
67. BCATS119-10|116_Pa_par_me|Panthera
68. BCATS158-10|68_Pa_tig_al|Panthera
69. BCATS156-10|189_Pa_tig_al|Panthera
70. BCATS155-10|166_Pa_tig|Panthera
71. BCATS154-10|165_Pa_tig_ti|Panthera
72. BCATS153-10|161_Pa_tig_su|Panthera
73. BCATS152-10|156_Pa_tig_al|Panthera
74. BCATS151-10|155_Pa_tig_al|Panthera
75. BCATS150-10|153_Pa_tig_al|Panthera
76. BCATS149-10|150_Pa_tig_al|Panthera
77. BCATS148-10|147_Pa_tig_al|Panthera
78. BCATS147-10|13_Pa_tig_su|Panthera
79. BCATS146-10|12_Pa_tig_su|Panthera
80. BCATS145-10|129_Pa_tig_ti|Panthera
81. BCATS144-10|128_Pa_tig_ti|Panthera
82. BCATS143-10|127_Pa_tig_su|Panthera
83. BCATS142-10|126_Pa_tig_su|Panthera
84. BCATS140-10|124_Pa_tig_al|Panthera
85. BCATS139-10|123_Pa_tig_al|Panthera
86. BCATS159-10|157_Pa_unc|Panthera
87. BCATS166-10|69_Pa_unc|Panthera
88. BCATS138-10|152_Pa_tem|Pardofelis
89. BCATS137-10|85_Pa_tem|Pardofelis
90. BCATS136-10|84_Pa_tem|Pardofelis
91. BCATS168-10|131_Pr_ben|Prionailurus
92. BCATS167-10|130_Pr_ben|Prionailurus
93. BCATS170-10|154_Pr_rub|Prionailurus
94. BCATS169-10|132_Pr_rub|Prionailurus
95. BCATS176-10|136_Pr_viv|Prionailurus
96. BCATS175-10|135_Pr_viv|Prionailurus
97. BCATS174-10|134_Pr_viv|Prionailurus
98. BCATS173-10|133_Pr_viv|Prionailurus
99. BCATS184-10|144_Pu_con|Puma
100. BCATS181-10|86_Pu_con|Puma
101. BCATS180-10|139_Pu_con|Puma
102. BCATS179-10|138_Pu_con|Puma
103. BCATS178-10|137_Pu_con|Puma
104. BCATS182-10|72_Pu_yag|Puma

340
350
360
370
380
390
400
410
420
430
Consensus
32. BCATS022-10|93_Fe_lyb|Felis
33. BCATS053-10|95_Le_geo|Leopardus
34. BCATS052-10|70_Le_geo|Leopardus
35. BCATS057-10|75_Le_tig|Leopardus
36. BCATS056-10|71_Le_tig|Leopardus
37. BCATS185-10|217_Ly_lyn_ly|Lynx
38. BCATS065-10|39_Ly_lyn_ly|Lynx
39. BCATS064-10|38_Ly_lyn_ly|Lynx
40. BCATS063-10|37_Ly_lyn_ly|Lynx
41. BCATS060-10|19_Ly_lyn_ly|Lynx
42. BCATS059-10|18_Ly_lyn_ly|Lynx
43. BCATS058-10|146_Ly_lyn|Lynx
44. BCATS071-10|99_Ly_ruf|Lynx
45. BCATS069-10|100_Ly_ruf|Lynx
46. BCATS088-10|89_Ot_man|Otocolobus
47. BCATS086-10|87_Ot_man|Otocolobus
48. BCATS081-10|193_Ot_man|Otocolobus
49. BCATS079-10|102_Ot_man|Otocolobus
50. BCATS186-10|28_Pa_leo_bl|Panthera
51. BCATS106-10|49_Pa_leo|Panthera
52. BCATS104-10|27_Pa_leo_bl|Panthera
53. BCATS103-10|26_Pa_leo_bl|Panthera
54. BCATS115-10|149_Pa_onc|Panthera
55. BCATS113-10|109_Pa_onc|Panthera
56. BCATS189-10|211_Pa_par_ori|Panthera
57. BCATS188-10|163_Pa_par_me|Panthera
58. BCATS187-10|73_Pa_par_ko|Panthera
59. BCATS183-10|122_Pa_par_or|Panthera
60. BCATS135-10|79_Pa_par_or|Panthera
61. BCATS134-10|74_Pa_par_ori|Panthera
62. BCATS128-10|168_Pa_par_ja|Panthera
63. BCATS127-10|162_Pa_par_or|Panthera
64. BCATS126-10|159_Pa_par_or|Panthera
65. BCATS125-10|148_Pa_par_sa|Panthera
66. BCATS124-10|121_Pa_par_or|Panthera
67. BCATS119-10|116_Pa_par_me|Panthera
68. BCATS158-10|68_Pa_tig_al|Panthera
69. BCATS156-10|189_Pa_tig_al|Panthera
70. BCATS155-10|166_Pa_tig|Panthera
71. BCATS154-10|165_Pa_tig_ti|Panthera
72. BCATS153-10|161_Pa_tig_su|Panthera
73. BCATS152-10|156_Pa_tig_al|Panthera
74. BCATS151-10|155_Pa_tig_al|Panthera
75. BCATS150-10|153_Pa_tig_al|Panthera
76. BCATS149-10|150_Pa_tig_al|Panthera
77. BCATS148-10|147_Pa_tig_al|Panthera
78. BCATS147-10|13_Pa_tig_su|Panthera
79. BCATS146-10|12_Pa_tig_su|Panthera
80. BCATS145-10|129_Pa_tig_ti|Panthera
81. BCATS144-10|128_Pa_tig_ti|Panthera
82. BCATS143-10|127_Pa_tig_su|Panthera
83. BCATS142-10|126_Pa_tig_su|Panthera
84. BCATS140-10|124_Pa_tig_al|Panthera
85. BCATS139-10|123_Pa_tig_al|Panthera
86. BCATS159-10|157_Pa_unc|Panthera
87. BCATS166-10|69_Pa_unc|Panthera
88. BCATS138-10|152_Pa_tem|Pardofelis
89. BCATS137-10|85_Pa_tem|Pardofelis
90. BCATS136-10|84_Pa_tem|Pardofelis
91. BCATS168-10|131_Pr_ben|Prionailurus
92. BCATS167-10|130_Pr_ben|Prionailurus
93. BCATS170-10|154_Pr_rub|Prionailurus
94. BCATS169-10|132_Pr_rub|Prionailurus
95. BCATS176-10|136_Pr_viv|Prionailurus
96. BCATS175-10|135_Pr_viv|Prionailurus
97. BCATS174-10|134_Pr_viv|Prionailurus
98. BCATS173-10|133_Pr_viv|Prionailurus
99. BCATS184-10|144_Pu_con|Puma
100. BCATS181-10|86_Pu_con|Puma
101. BCATS180-10|139_Pu_con|Puma
102. BCATS179-10|138_Pu_con|Puma
103. BCATS178-10|137_Pu_con|Puma
104. BCATS182-10|72_Pu_yag|Puma

Consensus
32. BCATS022-10|93_Fe_lyb|Felis
33. BCATS053-10|95_Le_geo|Leopardus
34. BCATS052-10|70_Le_geo|Leopardus
35. BCATS057-10|75_Le_tig|Leopardus
36. BCATS056-10|71_Le_tig|Leopardus
37. BCATS185-10|217_Ly_lyn_ly|Lynx
38. BCATS065-10|39_Ly_lyn_ly|Lynx
39. BCATS064-10|38_Ly_lyn_ly|Lynx
40. BCATS063-10|37_Ly_lyn_ly|Lynx
41. BCATS060-10|19_Ly_lyn_ly|Lynx
42. BCATS059-10|18_Ly_lyn_ly|Lynx
43. BCATS058-10|146_Ly_lyn|Lynx
44. BCATS071-10|99_Ly_ruf|Lynx
45. BCATS069-10|100_Ly_ruf|Lynx
46. BCATS088-10|89_Ot_man|Otocolobus
47. BCATS086-10|87_Ot_man|Otocolobus
48. BCATS081-10|193_Ot_man|Otocolobus
49. BCATS079-10|102_Ot_man|Otocolobus
50. BCATS186-10|28_Pa_leo_bl|Panthera
51. BCATS106-10|49_Pa_leo|Panthera
52. BCATS104-10|27_Pa_leo_bl|Panthera
53. BCATS103-10|26_Pa_leo_bl|Panthera
54. BCATS115-10|149_Pa_onc|Panthera
55. BCATS113-10|109_Pa_onc|Panthera
56. BCATS189-10|211_Pa_par_ori|Panthera
57. BCATS188-10|163_Pa_par_me|Panthera
58. BCATS187-10|73_Pa_par_ko|Panthera
59. BCATS183-10|122_Pa_par_or|Panthera
60. BCATS135-10|79_Pa_par_or|Panthera
61. BCATS134-10|74_Pa_par_ori|Panthera
62. BCATS128-10|168_Pa_par_ja|Panthera
63. BCATS127-10|162_Pa_par_or|Panthera
64. BCATS126-10|159_Pa_par_or|Panthera
65. BCATS125-10|148_Pa_par_sa|Panthera
66. BCATS124-10|121_Pa_par_or|Panthera
67. BCATS119-10|116_Pa_par_me|Panthera
68. BCATS158-10|68_Pa_tig_al|Panthera
69. BCATS156-10|189_Pa_tig_al|Panthera
70. BCATS155-10|166_Pa_tig|Panthera
71. BCATS154-10|165_Pa_tig_ti|Panthera
72. BCATS153-10|161_Pa_tig_su|Panthera
73. BCATS152-10|156_Pa_tig_al|Panthera
74. BCATS151-10|155_Pa_tig_al|Panthera
75. BCATS150-10|153_Pa_tig_al|Panthera
76. BCATS149-10|150_Pa_tig_al|Panthera
77. BCATS148-10|147_Pa_tig_al|Panthera
78. BCATS147-10|13_Pa_tig_su|Panthera
79. BCATS146-10|12_Pa_tig_su|Panthera
80. BCATS145-10|129_Pa_tig_ti|Panthera
81. BCATS144-10|128_Pa_tig_ti|Panthera
82. BCATS143-10|127_Pa_tig_su|Panthera
83. BCATS142-10|126_Pa_tig_su|Panthera
84. BCATS140-10|124_Pa_tig_al|Panthera
85. BCATS139-10|123_Pa_tig_al|Panthera
86. BCATS159-10|157_Pa_unc|Panthera
87. BCATS166-10|69_Pa_unc|Panthera
88. BCATS138-10|152_Pa_tem|Pardofelis
89. BCATS137-10|85_Pa_tem|Pardofelis
90. BCATS136-10|84_Pa_tem|Pardofelis
91. BCATS168-10|131_Pr_ben|Prionailurus
92. BCATS167-10|130_Pr_ben|Prionailurus
93. BCATS170-10|154_Pr_rub|Prionailurus
94. BCATS169-10|132_Pr_rub|Prionailurus
95. BCATS176-10|136_Pr_viv|Prionailurus
96. BCATS175-10|135_Pr_viv|Prionailurus
97. BCATS174-10|134_Pr_viv|Prionailurus
98. BCATS173-10|133_Pr_viv|Prionailurus
99. BCATS184-10|144_Pu_con|Puma
100. BCATS181-10|86_Pu_con|Puma
101. BCATS180-10|139_Pu_con|Puma
102. BCATS179-10|138_Pu_con|Puma
103. BCATS178-10|137_Pu_con|Puma
104. BCATS182-10|72_Pu_yag|Puma

540 550 560 570 580 590 600 610 620 630 640
Consensus
TCAAACACCCCTATTTGTCTGATCAGTTTTAATCACTGCTGTCCTGCTACTTCTATCACTCCCAGTTTTAGCAGCA---GGAATCACTATGCTACTAACAGA
32. BCATS022-10|93_Fe_lyb|Felis
33. BCATS053-10|95_Le_geo|Leopardus
34. BCATS052-10|70_Le_geo|Leopardus
35. BCATS057-10|75_Le_tig|Leopardus
36. BCATS056-10|71_Le_tig|Leopardus
37. BCATS185-10|217_Ly_lyn_ly|Lynx
38. BCATS065-10|39_Ly_lyn_ly|Lynx
39. BCATS064-10|38_Ly_lyn_ly|Lynx
40. BCATS063-10|37_Ly_lyn_ly|Lynx
41. BCATS060-10|19_Ly_lyn_ly|Lynx
42. BCATS059-10|18_Ly_lyn_ly|Lynx
43. BCATS058-10|146_Ly_lyn|Lynx
44. BCATS071-10|99_Ly_ruf|Lynx
45. BCATS069-10|100_Ly_ruf|Lynx
46. BCATS088-10|89_Ot_man|Otocolobus
47. BCATS086-10|87_Ot_man|Otocolobus
48. BCATS081-10|193_Ot_man|Otocolobus
49. BCATS079-10|102_Ot_man|Otocolobus
50. BCATS186-10|28_Pa_leo_bl|Panthera
51. BCATS106-10|49_Pa_leo|Panthera
52. BCATS104-10|27_Pa_leo_bl|Panthera
53. BCATS103-10|26_Pa_leo_bl|Panthera
54. BCATS115-10|149_Pa_onc|Panthera
55. BCATS113-10|109_Pa_onc|Panthera
56. BCATS189-10|211_Pa_par_ori|Panthera
57. BCATS188-10|163_Pa_par_me|Panthera
58. BCATS187-10|73_Pa_par_ko|Panthera
59. BCATS183-10|122_Pa_par_or|Panthera
60. BCATS135-10|79_Pa_par_or|Panthera
61. BCATS134-10|74_Pa_par_ori|Panthera
62. BCATS128-10|168_Pa_par_ja|Panthera
63. BCATS127-10|162_Pa_par_or|Panthera
64. BCATS126-10|159_Pa_par_or|Panthera
65. BCATS125-10|148_Pa_par_sa|Panthera
66. BCATS124-10|121_Pa_par_or|Panthera
67. BCATS119-10|116_Pa_par_me|Panthera
68. BCATS158-10|68_Pa_tig_al|Panthera
69. BCATS156-10|189_Pa_tig_al|Panthera
70. BCATS155-10|166_Pa_tig|Panthera
71. BCATS154-10|165_Pa_tig_ti|Panthera
72. BCATS153-10|161_Pa_tig_su|Panthera
73. BCATS152-10|156_Pa_tig_al|Panthera
74. BCATS151-10|155_Pa_tig_al|Panthera
75. BCATS150-10|153_Pa_tig_al|Panthera
76. BCATS149-10|150_Pa_tig_al|Panthera
77. BCATS148-10|147_Pa_tig_al|Panthera
78. BCATS147-10|13_Pa_tig_su|Panthera
79. BCATS146-10|12_Pa_tig_su|Panthera
80. BCATS145-10|129_Pa_tig_ti|Panthera
81. BCATS144-10|128_Pa_tig_ti|Panthera
82. BCATS143-10|127_Pa_tig_su|Panthera
83. BCATS142-10|126_Pa_tig_su|Panthera
84. BCATS140-10|124_Pa_tig_al|Panthera
85. BCATS139-10|123_Pa_tig_al|Panthera
86. BCATS159-10|157_Pa_unc|Panthera
87. BCATS166-10|69_Pa_unc|Panthera
88. BCATS138-10|152_Pa_tem|Pardofelis
89. BCATS137-10|85_Pa_tem|Pardofelis
90. BCATS136-10|84_Pa_tem|Pardofelis
91. BCATS168-10|131_Pr_ben|Prionailurus
92. BCATS167-10|130_Pr_ben|Prionailurus
93. BCATS170-10|154_Pr_rub|Prionailurus
94. BCATS169-10|132_Pr_rub|Prionailurus
95. BCATS176-10|136_Pr_viv|Prionailurus
96. BCATS175-10|135_Pr_viv|Prionailurus
97. BCATS174-10|134_Pr_viv|Prionailurus
98. BCATS173-10|133_Pr_viv|Prionailurus
99. BCATS184-10|144_Pu_con|Puma
100. BCATS181-10|86_Pu_con|Puma
101. BCATS180-10|139_Pu_con|Puma
102. BCATS179-10|138_Pu_con|Puma
103. BCATS178-10|137_Pu_con|Puma
104. BCATS182-10|72_Pu_yag|Puma

640
650
660
670
680
690
700
710
720
730
74
Consensus
32. BCATS022-10|93_Fe_lyb|Felis
33. BCATS053-10|95_Le_geo|Leopardus
34. BCATS052-10|70_Le_geo|Leopardus
35. BCATS057-10|75_Le_tig|Leopardus
36. BCATS056-10|71_Le_tig|Leopardus
37. BCATS185-10|217_Ly_lyn_ly|Lynx
38. BCATS065-10|39_Ly_lyn_ly|Lynx
39. BCATS064-10|38_Ly_lyn_ly|Lynx
40. BCATS063-10|37_Ly_lyn_ly|Lynx
41. BCATS060-10|19_Ly_lyn_ly|Lynx
42. BCATS059-10|18_Ly_lyn_ly|Lynx
43. BCATS058-10|146_Ly_lyn|Lynx
44. BCATS071-10|99_Ly_ruf|Lynx
45. BCATS069-10|100_Ly_ruf|Lynx
46. BCATS088-10|89_Ot_man|Otocolobus
47. BCATS086-10|87_Ot_man|Otocolobus
48. BCATS081-10|193_Ot_man|Otocolobus
49. BCATS079-10|102_Ot_man|Otocolobus
50. BCATS186-10|28_Pa_leo_bl|Panthera
51. BCATS106-10|49_Pa_leo|Panthera
52. BCATS104-10|27_Pa_leo_bl|Panthera
53. BCATS103-10|26_Pa_leo_bl|Panthera
54. BCATS115-10|149_Pa_onc|Panthera
55. BCATS113-10|109_Pa_onc|Panthera
56. BCATS189-10|211_Pa_par_ori|Panthera
57. BCATS188-10|163_Pa_par_me|Panthera
58. BCATS187-10|73_Pa_par_ko|Panthera
59. BCATS183-10|122_Pa_par_or|Panthera
60. BCATS135-10|79_Pa_par_or|Panthera
61. BCATS134-10|74_Pa_par_ori|Panthera
62. BCATS128-10|168_Pa_par_ja|Panthera
63. BCATS127-10|162_Pa_par_or|Panthera
64. BCATS126-10|159_Pa_par_or|Panthera
65. BCATS125-10|148_Pa_par_sa|Panthera
66. BCATS124-10|121_Pa_par_or|Panthera
67. BCATS119-10|116_Pa_par_me|Panthera
68. BCATS158-10|68_Pa_tig_al|Panthera
69. BCATS156-10|189_Pa_tig_al|Panthera
70. BCATS155-10|166_Pa_tig|Panthera
71. BCATS154-10|165_Pa_tig_ti|Panthera
72. BCATS153-10|161_Pa_tig_su|Panthera
73. BCATS152-10|156_Pa_tig_al|Panthera
74. BCATS151-10|155_Pa_tig_al|Panthera
75. BCATS150-10|153_Pa_tig_al|Panthera
76. BCATS149-10|150_Pa_tig_al|Panthera
77. BCATS148-10|147_Pa_tig_al|Panthera
78. BCATS147-10|13_Pa_tig_su|Panthera
79. BCATS146-10|12_Pa_tig_su|Panthera
80. BCATS145-10|129_Pa_tig_ti|Panthera
81. BCATS144-10|128_Pa_tig_ti|Panthera
82. BCATS143-10|127_Pa_tig_su|Panthera
83. BCATS142-10|126_Pa_tig_su|Panthera
84. BCATS140-10|124_Pa_tig_al|Panthera
85. BCATS139-10|123_Pa_tig_al|Panthera
86. BCATS159-10|157_Pa_unc|Panthera
87. BCATS166-10|69_Pa_unc|Panthera
88. BCATS138-10|152_Pa_tem|Pardofelis
89. BCATS137-10|85_Pa_tem|Pardofelis
90. BCATS136-10|84_Pa_tem|Pardofelis
91. BCATS168-10|131_Pr_ben|Prionailurus
92. BCATS167-10|130_Pr_ben|Prionailurus
93. BCATS170-10|154_Pr_rub|Prionailurus
94. BCATS169-10|132_Pr_rub|Prionailurus
95. BCATS176-10|136_Pr_viv|Prionailurus
96. BCATS175-10|135_Pr_viv|Prionailurus
97. BCATS174-10|134_Pr_viv|Prionailurus
98. BCATS173-10|133_Pr_viv|Prionailurus
99. BCATS184-10|144_Pu_con|Puma
100. BCATS181-10|86_Pu_con|Puma
101. BCATS180-10|139_Pu_con|Puma
102. BCATS179-10|138_Pu_con|Puma
103. BCATS178-10|137_Pu_con|Puma
104. BCATS182-10|72_Pu_yag|Puma

720 730 740 750 760 770 780 790 800 810
Consensus
----------AGCTCCTGTCACTACCAGTTCTAGCAG
32. BCATS022-10|93_Fe_lyb|Felis
33. BCATS053-10|95_Le_geo|Leopardus
34. BCATS052-10|70_Le_geo|Leopardus
35. BCATS057-10|75_Le_tig|Leopardus
36. BCATS056-10|71_Le_tig|Leopardus
37. BCATS185-10|217_Ly_lyn_ly|Lynx
38. BCATS065-10|39_Ly_lyn_ly|Lynx
39. BCATS064-10|38_Ly_lyn_ly|Lynx
40. BCATS063-10|37_Ly_lyn_ly|Lynx
41. BCATS060-10|19_Ly_lyn_ly|Lynx
42. BCATS059-10|18_Ly_lyn_ly|Lynx
43. BCATS058-10|146_Ly_lyn|Lynx
44. BCATS071-10|99_Ly_ruf|Lynx
45. BCATS069-10|100_Ly_ruf|Lynx
46. BCATS088-10|89_Ot_man|Otocolobus ----------AGCTCCTGTCACTACCAGTTCTAGCAG
47. BCATS086-10|87_Ot_man|Otocolobus ----------AGCTCCTGTCACTACCAGTTCTAGCAG
48. BCATS081-10|193_Ot_man|Otocolobus ----------AGCTCCTGTCACTACCAGTTCTAGCAG
49. BCATS079-10|102_Ot_man|Otocolobus ----------AGCTCCTGTCACTACCAGTTCTAGCAG
50. BCATS186-10|28_Pa_leo_bl|Panthera
51. BCATS106-10|49_Pa_leo|Panthera
52. BCATS104-10|27_Pa_leo_bl|Panthera
53. BCATS103-10|26_Pa_leo_bl|Panthera
54. BCATS115-10|149_Pa_onc|Panthera
55. BCATS113-10|109_Pa_onc|Panthera
56. BCATS189-10|211_Pa_par_ori|Panthera
57. BCATS188-10|163_Pa_par_me|Panthera
58. BCATS187-10|73_Pa_par_ko|Panthera
59. BCATS183-10|122_Pa_par_or|Panthera
60. BCATS135-10|79_Pa_par_or|Panthera
61. BCATS134-10|74_Pa_par_ori|Panthera
62. BCATS128-10|168_Pa_par_ja|Panthera
63. BCATS127-10|162_Pa_par_or|Panthera
64. BCATS126-10|159_Pa_par_or|Panthera
65. BCATS125-10|148_Pa_par_sa|Panthera
66. BCATS124-10|121_Pa_par_or|Panthera
67. BCATS119-10|116_Pa_par_me|Panthera
68. BCATS158-10|68_Pa_tig_al|Panthera
69. BCATS156-10|189_Pa_tig_al|Panthera
70. BCATS155-10|166_Pa_tig|Panthera
71. BCATS154-10|165_Pa_tig_ti|Panthera
72. BCATS153-10|161_Pa_tig_su|Panthera
73. BCATS152-10|156_Pa_tig_al|Panthera
74. BCATS151-10|155_Pa_tig_al|Panthera
75. BCATS150-10|153_Pa_tig_al|Panthera
76. BCATS149-10|150_Pa_tig_al|Panthera
77. BCATS148-10|147_Pa_tig_al|Panthera
78. BCATS147-10|13_Pa_tig_su|Panthera
79. BCATS146-10|12_Pa_tig_su|Panthera
80. BCATS145-10|129_Pa_tig_ti|Panthera
81. BCATS144-10|128_Pa_tig_ti|Panthera
82. BCATS143-10|127_Pa_tig_su|Panthera
83. BCATS142-10|126_Pa_tig_su|Panthera
84. BCATS140-10|124_Pa_tig_al|Panthera
85. BCATS139-10|123_Pa_tig_al|Panthera
86. BCATS159-10|157_Pa_unc|Panthera
87. BCATS166-10|69_Pa_unc|Panthera
88. BCATS138-10|152_Pa_tem|Pardofelis
89. BCATS137-10|85_Pa_tem|Pardofelis
90. BCATS136-10|84_Pa_tem|Pardofelis
91. BCATS168-10|131_Pr_ben|Prionailurus
92. BCATS167-10|130_Pr_ben|Prionailurus
93. BCATS170-10|154_Pr_rub|Prionailurus
94. BCATS169-10|132_Pr_rub|Prionailurus
95. BCATS176-10|136_Pr_viv|Prionailurus
96. BCATS175-10|135_Pr_viv|Prionailurus
97. BCATS174-10|134_Pr_viv|Prionailurus
98. BCATS173-10|133_Pr_viv|Prionailurus
99. BCATS184-10|144_Pu_con|Puma
100. BCATS181-10|86_Pu_con|Puma
101. BCATS180-10|139_Pu_con|Puma
102. BCATS179-10|138_Pu_con|Puma
103. BCATS178-10|137_Pu_con|Puma
104. BCATS182-10|72_Pu_yag|Puma

Appendix 3. Image sources

1. Puma: (http://us.123rf.com/400wm/400/400/isselee/isselee0802/isselee080200241/2597975-puma-17-years--puma-concolor-in-front-of-a-white-background.jpg)
2. Asian Golden cat: (http://en.wikipedia.org/wiki/File:Asian_Golden_cat.jpg)
3. Black-footed cat: (http://farm1.static.flickr.com/116/260095916_838a749a89.jpg)
4. Clouded-leopard: (http://www.myfreewallpapers.net/nature/pages/clouded-leopard.shtml)
5. Lion: (http://wallpapers.free-review.net/wallpapers/15/Big_Lion.jpg)
6. Black-footed cat: (http://farm1.static.flickr.com/116/260095916_838a749a89_b.jpg)
7. Caracal: (http://www.visualphotos.com/photo/1x3740890/caracal_caracal_felis_caracal_augrabies_falls_ba3063.jpg)
8. Eurasian lynx: (http://pixdaus.com/pics/1236252856LLgiwSy.jpg)
9. Domestic cat: (http://image.shutterstock.com/display_pic_with_logo/109102/109102,1196950581,2/stock-photo-young-grey-maine-coon-cat-7584034.jpg)
10. Cheetah: (http://images.picturesdepot.com/photo/f/female_cheetah_wallpaper-29086.jpg)
11. Geoffroy's cat: (http://upload.wikimedia.org/wikipedia/commons/thumb/e/e2/Geoffroy%27s_Cat.jpg/800px-Geoffroy%27s_Cat.jpg)
12. Jaguarundi: (http://upload.wikimedia.org/wikipedia/commons/thumb/8/85/Herpailurus_yagouaroundi_Jaguarundi_ZOO_D%C4%9B%C4%8D%C3%ADn.jpg/800px-Herpailurus_yagouaroundi_Jaguarundi_ZOO_D%C4%9B%C4%8D%C3%ADn.jpg)
13. Iberian lynx: (http://travel.latimes.com/daily-deal-blog/wp-content/uploads/2008/10/iberian_lynx_by_antonio_riv.jpg)
14. Asian leopard cat: (http://upload.wikimedia.org/wikipedia/commons/3/32/Tsushima_Cat_001.jpg)
15. Leopard: (http://www.serengetiexpeditions.com/images/leopard1280x1024.jpg)
16. Pallas cat: (http://upload.wikimedia.org/wikipedia/commons/d/d6/Manoel.jpg)
17. Tigrina: (http://www.themagazine.ca/wp-content/uploads/2011/03/Oncilla.png)
18. Fishing cat: (http://upload.wikimedia.org/wikipedia/commons/archive/5/5c/20070607175227!Prionailurus_viverrinus.jpg)

19. Snow leopard: (http://thundafunda.com/33/animals-pictures-nature/ready-to-pounce-snow-leopard-pictures.jpg)
20. Indian mongoose: (http://upload.wikimedia.org/wikipedia/commons/thumb/4/47/Ruddy_mongoose.jpg/799px-Ruddy_mongoose.jpg)
21. Rusty-spotted cat: (http://www.zoochat.com/gallery/data/543/Rusty_Spotted_Cat_PL_16_10_06.JPG)
22. Desert cat: (http://upload.wikimedia.org/wikipedia/commons/7/79/Sandcat1_CincinnatiZoo.jpg)
23. Serval: (http://www.vectorsite.net/Ybser_2b.jpg)
24. Tiger: (http://fc02.deviantart.net/fs70/f/2011/181/e/5/tiger_and_snow_3_by_jagu77-d3kk8b7.jpg)
25. Jaguar: (http://upload.wikimedia.org/wikipedia/commons/thumb/7/70/Panthera_onca.jpg/800px-Panthera_onca.jpg)
26. European wildcat: (http://medienjagd.test.newsroom.de/wildkatze022010sb088.jpg)
27. Bobcat: (http://images1.wikia.nocookie.net/__cb20071029161722/uncyclopedia/images/thumb/6/61/Bobcat.jpg/765px-Bobcat.jpg)
28. Putative numts: (http://www.wallpaperslibrary.com/Wallpapers/Funny/tiger-rabbit-funny-wallpaper-13.jpg)

7.3. CHAPTER 3: Tracking cats: Problems with placing feline carnivores on $\delta^{18}O$, δD isoscapes

Table S1. Sample list

No.	Museum catalog number	Sampling part	Common name	Sex	Latitude (decimal degrees)	Longitude (decimal degrees)	Elevation (m)	δD (‰ V-SMOW) Mean annual precip	δ18O (‰ V-SMOW) Mean annual precip	δ18O River-water	δD River-water	δD Keratin (‰ V-SMOW)	δ18O Keratin (‰ V-SMOW)	δD (‰ V-SMOW) Mean Sum. precip (June, July, August)	δ18O (‰ V-SMOW) Mean Sum. precip (June, July, August)	Mean annual rel. humidity (%)	δD (‰ V-SMOW) Mean spring precip (March, April, May)	δ18O (‰ V-SMOW) Mean spring precip (March, April, May)
1	232789	hair	bobcat	u	25.826	-81.344	3	-21	-3.50	-0.10	0.55	-112.22	16.41	-22.33	-3.50	70	-13.00	-2.70
2	157063	hair	bobcat	m	34.869	-83.814	1460	-53	-8.10	-7.40	-45.6	-87.37	19.20	-29.00	-4.70	70	-47.33	-7.33
3	276020	hair	bobcat	u	38.902	-81.310	243	-48	-7.50	-7.30	-47.6	-87.37	19.40	-28.33	-4.60	70	-42.33	-6.80
4	298442	hair	bobcat	u	43.998	-74.505	940	-80	-11.90	-9.90	-96.1	-106.85	16.89	-51.00	-8.03	65	-77.67	-11.40
5	88448	hair	bobcat	m	44.628	-65.776	150	-68	-10.20	-8	-57	-94.57	21.70	-45.00	-7.03	80	-63.00	-9.47
6	210545	hair	bobcat	f	30.270	-87.683	4	-26	-4.10	-3.90	-20.3	-97.57	19.62	-20.67	-3.10	80	-18.00	-3.10
7	286410	hair	bobcat	m	36.365	-88.045	120	-39	-6.10	-5.70	-33.1	-87.19	13.60	-18.67	-3.03	70	-30.00	-5.00
8	236419	hair	bobcat	f	35.777	-93.465	670	-49	-7.10	-5.80	-34.5	-85.82	16.96	-28.67	-4.27	65	-43.33	-6.37
9	76459	hair	bobcat	u	42.571	-100.062	800	-77	-10.60	-10.10	-75.1	-65.90	19.36	-60.33	-8.27	60	-85.00	-11.80
10	285332	hair	bobcat	m	44.159	-91.816	213	-64	-9.10	-9.80	-67.9	-100.21	14.70	-44.67	-6.33	70	-66.33	-9.53
11	276360	hair	bobcat	m	44.372	-100.318	440	-79	-10.70	-14.20	-115.5	-107.99	16.43	-62.00	-8.40	60	-87.33	-12.03
12	211368	hair	bobcat	f	46.336	-113.294	1600	-115	-15.20	-17.30	-131.6	-100.92	12.52	-88.33	-11.50	70	-114.67	-15.33
13	214795	hair	bobcat	f	41.001	-107.246	2100	-106	-14.20	-16.40	-123.9	-89.26	13.88	-81.00	-10.57	60	-109.00	-14.70
14	1709	hair	bobcat	f	32.483	-106.724	1200	-67	-9.30	-12.50	-94	-88.51	15.37	-57.67	-7.80	40	-66.67	-9.27

No.	Museum catalog number	Sampling part	Common name	Sex	Latitude (decimal degrees)	Longitude (decimal degrees)	Elevation (m)	δD (‰ V-SMOW) Mean annual precip	δ18O (‰ V-SMOW) Mean annual precip	δ18O River-water	δD River-water	δD Keratin (‰ V-SMOW)	δ18O Keratin (‰ V-SMOW)	δD (‰ V-SMOW) Mean Sum. precip (June, July, August)	δ18O (‰ V-SMOW) Mean Sum. precip (June, July, August)	Mean annual rel. humidity (%)	δD (‰ V-SMOW) Mean spring precip (March, April, May)	δ18O (‰ V-SMOW) Mean spring precip (March, April, May)
15	211376	hair	bobcat	m	45.774	-116.302	480	-98	-12.90	-17.50	-132.7	-81.09	11.16	-76.33	-9.50	60	-90.67	-12.10
16	274903	hair	bobcat	f	47.956	-124.393	90	-86	-11.10	-12.60	-89.7	-86.76	16.75	-75.67	-8.93	85	-83.00	-10.73
17	146256	hair	bobcat	m	40.491	-124.132	50	-80	-10.40	-7.40	-50.4	-95.60	11.58	-65.00	-7.30	70	-76.67	-9.83
18	214967	hair	bobcat	f	31.197	-101.464	820	-50	-6.90	-4.10	-20.5	-57.76	10.37	-41.33	-5.47	55	-44.33	-6.13
19	116282	hair	bobcat	m	27.826	-97.406	2	-27	-3.60	-2.80	-17.4	-70.52	12.35	-24.00	-2.77	80	-16.33	-2.20
20	119799	hair	bobcat	u	30.587	-103.893	1500	-62	-8.60	-4.10	-20.5	-58.10	11.08	-53.67	-7.33	50	-59.33	-8.13
21	211344	hair	bobcat	m	29.023	-99.310	180	-33	-4.50	-2.80	-17.4	-90.64	14.54	-27.67	-3.37	60	-24.00	-3.23
22	188737	hair	bobcat	m	30.752	-99.235	470	-39	-5.50	-3.40	-20.5	-97.09	15.06	-31.67	-4.00	60	-33.00	-4.47
23	135084	hair	bobcat	m	30.300	-94.535	15	-28	-3.90	-2.90	-16.3	-19.34	11.96	-22.33	-2.60	70	-19.67	-2.67
24	188736	hair	bobcat	f	33.657	-97.345	240	-41	-5.80	-3.50	-21.5	-12.90	9.16	-32.00	-4.13	60	-35.00	-4.87
25	014908	hair	bobcat	m	26.122	-98.257	31	-27	-3.70	-1.30	-11.6	-58.13	11.02	-26.00	-3.17	70	-14.00	-2.03
26	4737	hair	bobcat	f	39.305	-111.299	2194	-105	-14.30	-13.30	-105.2	-102.61	13.67	-82.67	-10.60	50	-109.67	-14.87
27	7108	hair	bobcat	f	40.200	-110.067	1550	-98	-13.30	-16.70	-124.4	-65.96	11.70	-76.67	-9.80	50	-99.67	-13.57
28	7106	hair	bobcat	f	40.200	-110.067	1550	-98	-13.30	-16.70	-124.4	-61.10	10.57	-76.67	-9.80	50	-99.67	-13.57
29	1767	hair	bobcat	f	38.334	-112.726	1767	-97	-13.00	-14.60	-107.5	-76.79	11.59	-76.00	-9.53	50	-100.33	-13.50
30	2290	hair	bobcat	m	39.737	-110.871	1890	-102	-13.80	-13.30	-105.2	-67.48	12.49	-80.00	-10.20	50	-105.33	-14.23
31	6531	hair	bobcat	m	38.228	-112.811	1706	-95	-12.90	-14.60	-107.5	-63.18	12.39	-25.00	-9.43	50	-99.33	-13.37

No.	Museum catalog number	Sampling part	Common name	Sex	Latitude (decimal degrees)	Longitude (decimal degrees)	Elevation (m)	δD (‰ V-SMOW) Mean annual precip	δ18O (‰ V-SMOW) Mean annual precip	δ18O River-water	δD River-water	δD Keratin (‰ V-SMOW)	δ18O Keratin (‰ V-SMOW)	δD (‰ V-SMOW) Mean Sum. precip (June, July, August)	δ18O (‰ V-SMOW) Mean Sum. precip (June, July, August)	Mean annual rel. humidity (%)	δD (‰ V-SMOW) Mean spring precip (March, April, May)	δ18O (‰ V-SMOW) Mean spring precip (March, April, May)
32	1885	hair	bobcat	m	41.708	-111.847	1388	-100	-13.50	-14.98	-117.7	-34.85		-76.67	-9.80	50	-100.00	-13.53
33	6503	hair	bobcat	m	41.686	-111.064	2255	-113	-15.20	-14.98	-117.7	-102.24	14.63	-85.00	-11.07	50	-114.00	-15.43
34	6513	hair	bobcat	f	41.561	-111.144	1932	-108	-14.50	-14.98	-117.7	-30.88	11.22	-82.33	-10.60	50	-109.00	-14.73
35	2033	hair	bobcat	m	41.989	-111.413	1820	-107	-14.50	-14.98	-117.7	-69.46	15.17	-81.67	-10.57	50	-108.00	-14.63
36	6506	hair	bobcat	f	38.150	-111.325	2620	-108	-14.60	-15	-114.8	-60.48	9.09	-84.00	-10.83	50	-113.67	-15.33
37	6517	hair	bobcat	m	38.155	-111.487	3400	-119	-16.10	-15	-114.8	-94.56	11.30	-92.00	-12.00	50	-126.67	-17.07
38	6519	hair	bobcat	u	37.425	-113.074	2590	-106	-14.20	-12.30	-92.1	-71.78	10.83	-81.00	-10.27	50	-110.33	-14.87
39	4641	hair	bobcat	m	37.275	-112.638	1700	-92	-12.40	-12.30	-92.1	-63.12	11.17	-72.00	-9.00	50	-95.67	-12.90
40	7107	hair	bobcat	m	37.580	-109.432	1670	-91	-12.50	-13.30	-97.3	-70.73	15.63	-72.67	-9.30	50	-95.00	-12.90
41	6523	hair	bobcat	m	37.938	-112.371	2070	-100	-13.50	-14.60	-107.5	-107.25	15.93	-78.00	-9.87	50	-104.00	-14.03
42	6499	hair	bobcat	f	38.718	-109.551	1463	-92	-12.50	-13.70	-101.00	-31.70	16.04	-72.33	-9.27	50	-93.67	-12.80
43	6525	hair	bobcat	f	38.725	-109.525	1340	-90	-12.30	-13.70	-101.00	-108.39	11.38	-71.33	-9.07	50	-92.00	-12.53
44	27141	hair	bobcat	m	40.181	-111.569	2500	-112	-15.20	-12.80	-103.2	-91.29	12.75	-86.67	-11.17	50	-116.67	-15.70
45	132475	hair	bobcat	m	35.596	-106.125	1930	-85	-11.90	-10.20	-76.3		12.06	-71.00	-9.67	50	-90.67	-12.63
46	146260	hair	puma	u	40.254	-124.133	98	-80	-10.40	-7.40	-50.4	-29.02	12.14	-65.00	-7.27	70	-77.00	-9.90
47	274594	hair	puma	m	40.051	-107.910	1900	-101	-13.60	-16.4	-123.9	-86.76	9.45	-77.67	-10.03	60	-102.67	-13.93
48	265596	hair	puma	u	26.417	-81.420	11	-21	-3.60	-0.1	0.6	-87.04	3.31	-23.00	-3.60	70	-14.33	-2.80

No.	Museum catalog number	Sampling part	Common name	Sex	Latitude (decimal degrees)	Longitude (decimal degrees)	Elevation (m)	δD (‰ V-SMOW) Mean annual precip	δ18O (‰ V-SMOW) Mean annual precip	δ18O River-water	δD River-water	δD Keratin (‰ V-SMOW)	δ18O Keratin (‰ V-SMOW)	δD (‰ V-SMOW) Mean Sum. precip (June, July, August)	δ18O (‰ V-SMOW) Mean Sum. precip (June, July, August)	Mean annual rel. humidity (%)	δD (‰ V-SMOW) Mean spring precip (March, April, May)	δ18O (‰ V-SMOW) Mean spring precip (March, April, May)
49	210433	hair	puma	f	46.135	-115.787	400	-97	-12.80	-17.5	-132.7	-85.31	7.89	-75.33	-9.40	60	-89.67	-12.03
50	228587	hair	puma	f	33.373	-108.903	1500	-76	-10.40	-14.1	-102.8	-71.74	5.74	-64.00	-8.37	45	-80.00	-10.93
51	274078	hair	puma	f	35.648	-105.295	2070	-86	-12.00	-10.2	-76.3	-89.66	13.88	-73.67	-10.00	50	-93.67	-12.97
52	235091	hair	puma	f	35.190	-107.666	2438	-88	-12.20	-9.6	-93.9	-81.94	10.47	-76.00	-10.23	50	-99.67	-13.73
53	261685	hair	puma	m	29.666	-103.362	1160	-54	-7.50	-4.1	-36.7	-60.01	7.86	-46.67	-6.37	50	-49.00	-6.77
54	273040	hair	puma	m	26.971	-99.252	180	-31	-4.20	-1.3	-11.6	-56.36	4.43	-27.67	-3.40	70	-19.67	-2.63
55	272334	hair	puma	m	31.150	-105.497	1600	-67	-9.30	-8.5	-71.1	-95.50	8.88	-58.00	-7.90	40	-65.33	-9.00
56	228468	hair	puma	m	32.937	-94.254	80	-34	-5.00	-3.7	-22.8	-33.22	10.41	-25.00	-3.20	70	-26.67	-3.83
57	261748	hair	puma	m	28.889	-99.097	193	-33	-4.50	-2.8	-17.4	-32.39	16.14	-27.33	-3.33	60	-24.00	-3.17
58	250184	hair	puma	m	48.078	-123.577	600	-94	-12.20	-12.60	-89.7	-62.21	16.84	-81.33	-9.80	85	-92.33	-11.97
59	6559	hair	puma	f	37.827	-112.435	2019	-99	-13.30	-14.60	-107.5	-29.96	6.37	-77.33	-9.77	50	-102.67	-13.87
60	6539	hair	puma	u	37.684	-113.086	1782	-95	-12.80	-12.30	-92.1	-55.06	6.99	-74.00	-9.23	50	-98.67	-13.23
61	6556	hair	puma	f	38.019	-112.237	2200	-102	-13.80	-14.60	-107.5	-55.68	11.11	-79.67	-10.10	50	-70.67	-9.60
62	6561	hair	puma	f	38.416	-112.430	2800	-112	-15.10	-14.60	-107.5	-52.89	14.68	-86.67	-11.13	50	-117.67	-15.87
63	6533	hair	puma	f	37.912	-112.457	2070	-100	-13.50	-14.60	-107.5	-81.91	12.92	-77.67	-9.87	50	-104.00	-14.03
64	6542	hair	puma	m	39.957	-109.263	1600	-98	-13.20	-16.70	-124.4	-44.02	9.36	-75.33	-9.73	55	-99.00	-13.47
65	6555	hair	puma	m	41.818	-113.310	1706	-106	-14.20	-14.98	-117.7	-13.62	15.29	-81.67	-10.37	50	-106.00	-14.33

No.	Museum catalog number	Sampling part	Common name	Sex	Latitude (decimal degrees)	Longitude (decimal degrees)	Elevation (m)	δD (‰ V-SMOW) Mean annual precip	δ18O (‰ V-SMOW) Mean annual precip	δ18O River-water	δD River-water	δD Keratin (‰ V-SMOW)	δ18O Keratin (‰ V-SMOW)	δD (‰ V-SMOW) Mean Sum. precip (June, July, August)	δ18O (‰ V-SMOW) Mean Sum. precip (June, July, August)	Mean annual rel. humidity (%)	δD (‰ V-SMOW) Mean spring precip (March, April, May)	δ18O (‰ V-SMOW) Mean spring precip (March, April, May)
66	4717	hair	puma	m	40.133	-111.018	2400	-110	-15.00	-12.80	-103.2	-52.77	10.40	-85.67	-11.03	50	-114.33	-15.47
67	6543	hair	puma	f	41.818	-113.310	1706	-106	-14.20	-14.98	-117.7	-71.64	2.66	-81.67	-10.37	50	-106.00	-14.33
68	6544	hair	puma	u	37.675	-113.104	1800	-95	-12.80	-12.30	-92.1	-82.17	7.90	-74.00	-9.23	50	-98.67	-13.27
69	7136	hair	puma	f	37.714	-113.031	1900	-97	-13.00	-12.30	-92.1	-73.83	15.38	-75.00	-9.43	50	-100.00	-13.50
70	6545	hair	puma	f	38.567	-112.431	1950	-100	-13.50	-14.60	-107.5	-66.96	20.16	-78.67	-9.93	50	-104.33	-14.07
71	4738	hair	puma	f	38.945	-112.251	1800	-99	-13.40	-13.30	-105.2	-77.50	20.90	-78.00	-9.93	50	-102.67	-13.90
72	6551	hair	puma	f	38.181	-112.306	1900	-98	-13.20	-14.60	-107.5	-66.85	10.51	-77.33	-9.77	50	-102.67	-13.80
73	14970	hair	puma	u	38.973	-112.345	1560	-96	-12.90	-13.30	-105.2	-78.36	17.51	-76.00	-9.60	50	-99.00	-13.40
74	6537	hair	puma	f	38.187	-112.331	2133	-101	-13.70	-14.60	-107.5	-108.98	15.23	-79.67	-10.10	50	-106.00	-14.33
75	6546	hair	puma	m	38.629	-112.123	1640	-96	-12.90	-14.60	-107.5	-101.61	12.25	-76.00	-9.57	50	-99.33	-13.43
76	104561	hair	rabbit	u	33.125	-94.159	79	-35	-5.10	-3.7	-22.8	-54.47	14.21					
77	249782	hair	rabbit	f	47.379	-94.604	406	-82	-11.20	-10.5	-73.8	-101.63	12.08					
78	213352	hair	rabbit	f	48.246	-109.865	1097	-112	-14.90	-16.7	-127.1	-136.66	10.46					
79	11349	hair	rabbit	u	43.024	-98.624	490	-71	-9.90	-10.13	-75.1	-81.41	17.39					
80	486790	hair	rabbit	f	31.193	-101.461	892	-49	-6.90	-4.10	-20.5	-45.74	15.67					
81	24573	hair	rabbit	f	28.341	-99.980	184	-33	-4.60	-4.5	-27.8	-15.98	19.91					
82	108611	hair	rabbit	f	29.684	-101.173	490	-41	-5.80	-4.5	-27.8	-44.76	18.63					

No.	Museum catalog number	Sampling part	Common name	Sex	Latitude (decimal degrees)	Longitude (decimal degrees)	Elevation (m)	δD (‰ V-SMOW) Mean annual precip	δ18O (‰ V-SMOW) Mean annual precip	δ18O River-water	δD River-water	δD Keratin (‰ V-SMOW)	δ18O Keratin (‰ V-SMOW)	δD (‰ V-SMOW) Mean Sum. precip (June, July, August)	δ18O (‰ V-SMOW) Mean Sum. precip (June, July, August)	Mean annual rel. humidity (%)	δD (‰ V-SMOW) Mean spring precip (March, April, May)	δ18O (‰ V-SMOW) Mean spring precip (March, April, May)
83	31665	hair	rabbit	m	27.743	-97.402	2	-27	-3.60	-2.80	-17.4	-30.55	18.85					
84	189168	hair	rabbit	f	33.624	-97.145	230	-40	-5.70	-3.50	-21.5	-52.08	17.64					
85	189173	hair	rabbit	m	30.748	-99.232	470	-39	-5.50	-3.40	-20.5	-52.01	18.25					
86	029023	hair	rabbit	m	26.381	-98.818	53	-28	-3.80	-1.30	-11.6	-23.92	18.62					
87	136554	hair	rabbit	f	30.137	-94.408	15	-28	-3.90	-2.90	-16.3	-54.12	14.43					
88	157806	hair	rabbit	m	32.591	-108.433	1700	-77	-10.50	-14.1	-102.8	-87.74	18.50					
89	TX-2,3,5	Dc, d18Op	White-tailed deer	u	27.826	-97.406	2	-20	-3.3	-2.80	-17.4	13	21.50					
90	FL 1	Dc, d18Op	White-tailed deer	u	30.479	-84.299	47	-20	-3.3	-3.10	-15.7	2	19.00					
91	LA 2	Dc, d18Op	White-tailed deer	u	32.511	-93.753	55	-23	-5.2	-3.7	-22.8	-3	19.10					
92	OK 1,2	Dc, d18Op	White-tailed deer	u	36.183	-95.961	206	-29	-4.4	-4.13	-27.3	8	19.70					
93	TX 1	Dc, d18Op	White-tailed deer	u	31.429	-100.399	585	-29	-4.4	-4.10	-20.5	-6	22.80					
94	MO 4	Dc, d18Op	White-tailed deer	u	37.246	-93.389	386	-30	-5.8	-4.90	-31.2	-10	18.40					
95	OK 10	Dc, d18Op	White-tailed deer	u	36.183	-95.961	206	-36	-5.2	-4.13	-27.3	-1	19.60					
96	WV 1,3	Dc, d18Op	White-tailed deer	u	38.413	-82.434	252	-36	-7.3	-7.30	-47.6	-14	16.50					
97	OK 5	Dc, d18Op	White-tailed deer	u	36.183	-95.961	206	-37	-6.4	-4.13	-27.3	-1	19.30					
98	KS 1	Dc, d18Op	White-tailed deer	u	39.056	-95.689	269	-38	-7.1	-11	-85.5	-11	18.70					
99	OH 3,1	Dc, d18Op	White-tailed deer	u	39.998	-82.892	248	-40	-6.4	-7.30	-47.6	-7	18.30					

No.	Museum catalog number	Sampling part	Common name	Sex	Latitude (decimal degrees)	Longitude (decimal degrees)	Elevation (m)	δD (‰ V-SMOW) Mean annual precip	δ18O (‰ V-SMOW) Mean annual precip	δ18O River-water	δD River-water	δD Keratin (‰ V-SMOW)	δ18O Keratin (‰ V-SMOW)	δD (‰ V-SMOW) Mean Sum. precip (June, July, August)	δ18O (‰ V-SMOW) Mean Sum. precip (June, July, August)	Mean annual rel. humidity (%)	δD (‰ V-SMOW) Mean spring precip (March, April, May)	δ18O (‰ V-SMOW) Mean spring precip (March, April, May)
100	NS 1	Dc, d18Op	White-tailed deer	u	43.827	-66.088	43	-49	-7.7	-11.70	-82.4	-34	15.90					
101	NS 2	Dc, d18Op	White-tailed deer	u	46.135	-60.183	62	-53	-8.1	-11.70	-82.4	-31	15.90					
102	WI 1	Dc, d18Op	White-tailed deer	u	44.513	-88.016	212	-53	-10.2	-10.64	-75.3	-39	14.70					
103	ON 1	Dc, d18Op	White-tailed deer	u	44.1	-77.581	86	-55	-9.9	-8.60	-60.3	-31	15.00					
104	NB 1	Dc, d18Op	White-tailed deer	u	45.954	-66.646	21	-55	-8.7	-11.70	-82.4	-37	14.50					
105	AZ 1	Dc, d18Op	White-tailed deer	u	33.448	-112.073	335	-58	-8.2	-8.80	-65.4	-3	23.00					
106	ON3	Dc, d18Op	White-tailed deer	u	44.288	-78.330	200	-58	-9.3	-8.60	-60.3	-43	13.90					
107	ON 6	Dc, d18Op	White-tailed deer	u	46.491	-80.998	300	-61	-9.8	-8.80	-67.4	-43	13.60					
108	QC 1	Dc, d18Op	White-tailed deer	u	45.682	-74.005	82	-66	-12	-9.90	-96.1	-54	13.90					
109	NE 2	Dc, d18Op	White-tailed deer	u	41.866	-103.665	1200	-70	-12	-13.80	-110.8	-28	16.30					
110	BC 4	Dc, d18Op	White-tailed deer	u	53.243	-131.821	200	-77	-10.6			-50	13.90					
111	OR 1	Dc, d18Op	White-tailed deer	u	40.969	-117.731	400	-87	-14	-14.40	-104.8	-49	17.00					
112	WY 2	Dc, d18Op	White-tailed deer	u	44.769	-106.980	1225	-91	-14.9	-127.38	-16.34	-59	13.60					
113	MT1	Dc, d18Op	White-tailed deer	u	48.212	-106.615	700	-96	-15.5	-14.55	-121.7	-54	14.30					
114	AB 6	Dc, d18Op	White-tailed deer	u	50.042	-110.674	717	-107	-17.4			-81	13.30					
115	SA 1	Dc, d18Op	White-tailed deer	u	52.171	-106.7	500	-110	-16.6			-51	14.00					
116	AB 4,5	Dc, d18Op	White-tailed deer	u	49.631	-112.800	929	-112	-18			-71	10.90					

No.	Museum catalog number	Sampling part	Common name	Sex	Latitude (decimal degrees)	Longitude (decimal degrees)	Elevation (m)	δD (‰ V-SMOW) Mean annual precip	δ18O (‰ V-SMOW) Mean annual precip	δ18O River-water	δD River-water	δD Keratin (‰ V-SMOW)	δ18O Keratin (‰ V-SMOW)	δD (‰ V-SMOW) Mean Sum. precip (June, July, August)	δ18O (‰ V-SMOW) Mean Sum. precip (June, July, August)	Mean annual rel. humidity (%)	δD (‰ V-SMOW) Mean spring precip (March, April, May)	δ18O (‰ V-SMOW) Mean spring precip (March, April, May)
117	AB 1,2	Dc, d18Op	White-tailed deer	u	53.541	-113.494	671	-112	-18			-81	10.60					
118	AB 7	Dc, d18Op	White-tailed deer	u	51.114	-114.020	1084	-116	-18.4			-73	11.30					
119	BC 2	Dc, d18Op	White-tailed deer	u	50.702	-120.444	345	-120	-17.7			-93	10.80					

Table S2. Statistical analysis

Regression equations	Species	Slope	SD (1s)	Intercept	SD (1s)	R^2	P-value	N
$\delta^{18}O_{hair} = f(\delta^{18}O_{river})$	All cats	0.01	0.095	12.920	1.136	0.0002	0.914	74
	All bobcats	0.104	0.091	14.964	1.056	0.03	0.261	44
	All pumas	-0.232	0.181	8.543	2.267	0.055	0.211	30
	All rabbits	0.298	0.156	18.394	1.228	0.248	0.083	13
	All deer	0.588	0.072	22.096	0.806	0.699	< 0.0001	31
	Female bobcats	0.007	0.121	14.018	1.349	0.0002	0.953	22
	Male bobcats	0.152	0.162	14.974	2.120	0.059	0.363	16
	Female pumas	-0.186	0.204	9.190	2.321	0.085	0.385	11
	Male pumas	0.615	0.733	20.517	10.266	0.055	0.418	14
	Female rabbits	0.535	0.188	19.118	1.538	0.618	0.036	7
	Male rabbits	0.009	0.03	18.606	0.219	0.046	0.785	4
$\delta D_{hair} = f(\delta D_{river})$	All cats	0.052	0.073	-68.699	6.633	0.007	0.479	74
	All bobcats	0.042	0.091	-74.343	8.015	0.005	0.65	44
	All pumas	0.129	0.119	-54.855	11.332	0.04	0.291	30
	All rabbits	0.797	0.116	-25.457	6.599	0.81	< 0.0001	13
	All deer	0.856	0.063	20.284	4.383	0.866	< 0.0001	31
	Female bobcats	0.074	0.12	-74.082	10.342	0.019	0.542	22
	Male bobcats	0.114	0.183	-62.123	17.944	0.027	0.544	16
	Female pumas	0.138	0.199	-47.662	17.226	0.051	0.505	11

Regression equations	Species	Slope	SD (1s)	Intercept	SD (1s)	R^2	P-value	N
	Male pumas	-0.181	0.422	-91.547	44.707	0.015	0.675	14
	Female rabbits	0.909	0.176	-23.537	10.346	0.843	0.004	7
	Male rabbits	0.622	0.164	-24.871	8.745	0.878	0.063	4
$\delta D_{hair} = f(\delta^{18}O_{hair})$	All cats	-1.641	0.691	-52.438	9.285	0.074	0.02	73
	All bobcats	-3.457	1.095	-30.451	15.607	0.195	0.003	43
	All pumas	0.072	0.936	-66.977	11.370	0.0002	0.939	30
	All rabbits	8.734	2.282	-204.308	38.210	0.571	0.003	13
	All deer	7.850	0.636	-159.827	10.459	0.84	< 0.0001	31
	Female bobcats	-3.221	1.574	-36.655	22.494	0.181	0.055	21
	Male bobcats	-4.003	2.218	-19.822	29.831	0.189	0.093	16
	Female pumas	2.238	2.309	-82.727	26.800	0.095	0.358	11
	Male pumas	-0.886	0.993	-61.864	12.925	0.062	0.39	14
	Female rabbits	10.889	1.964	-233.724	31.183	0.86	0.003	7
	Male rabbits	54.724	71.022	-1.064.063	1.318.024	0.229	0.522	4
$\delta^{18}O_{hair} = f(\delta^{18}O_{precip})$	All cats	0.02	0.129	13.022	1.494	0	0.88	74
$\delta D_{hair} = f(\delta D_{precip})$	All cats	0.03	0.103	-70.553	8.761	0.001	0.773	74
$\delta D_{hair} = f(\delta D_{mean\ summer\ precip})$	All pumas	0.216	0.231	-51.359	16.394	0.03	0.358	30
$\delta^{18}O_{hair} = f(\delta^{18}O_{mean\ summer\ precip})$	All pumas	-0.597	0.362	6.024	3.269	0.088	0.11	30
$\delta D_{hair} = f(\delta D_{mean\ spring\ precip})$	All pumas	0.143	0.147	-53.948	13.297	0.03	0.34	30
$\delta^{18}O_{hair} = f(\delta^{18}O_{mean\ spring\ precip})$	All pumas	-0.385	0.216	6.773	2.642	0.102	0.086	30

Regression equations	Species	Slope	SD (1s)	Intercept	SD (1s)	R^2	P-value	N
$\delta D_{hair} = f(\delta D_{annual\ precip})$ with rel. humidity (h)	All pumas					0.068	0.387	30
$\delta^{18}O_{hair} = f(\delta^{18}O_{annual\ precip})$ with rel. humidity (h)	All pumas					0.115	0.193	30
$\delta D_{hair} = f(\delta D_{river\ water})$ with rel. humidity (h)	All pumas					0.075	0.35	30
$\delta^{18}O_{hair} = f(\delta^{18}O_{river\ water})$ with rel. humidity (h)	All pumas					0.06	0.436	30
$\delta D_{hair} = f$(rel. humidity (h))	All pumas	0.634	0.444	-100.719	24.549	0.068	0.164	30
$\delta^{18}O_{hair} = f$(rel. humidity (h))	All pumas	-0.022	0.093	12.410	5.131	0.002	0.818	30
$\delta D_{hair} = f(\delta D_{mean\ summer\ precip})$	All bobcats	0.038	0.157	-75.381	9.918	0.001	0.812	44
$\delta^{18}O_{hair} = f(\delta^{18}O_{mean\ summer\ precip})$	All bobcats	0.269	0.157	15.969	1.297	0.066	0.093	44
$\delta D_{hair} = f(\delta D_{mean\ spring\ precip})$	All bobcats	0.035	0.11	-74.901	9.204	0.002	0.751	44
$\delta^{18}O_{hair} = f(\delta^{18}O_{mean\ spring\ precip})$	All bobcats	0.141	0.103	15.358	1.168	0.043	0.176	44
$\delta D_{hair} = f(\delta D_{annual\ precip})$ with rel. humidity (h)	All bobcats					0.09	0.143	44
$\delta^{18}O_{hair} = f(\delta^{18}O_{annual\ precip})$ with rel. humidity (h)	All bobcats					0.207	0.009	44
$\delta D_{hair} = f(\delta D_{river\ water})$ with rel. humidity (h)	All bobcats					0.104	0.105	44
$\delta^{18}O_{hair} = f(\delta^{18}O_{river\ water})$ with rel. humidity (h)	All bobcats					0.213	0.007	44
$\delta D_{hair} = f$(rel. humidity (h))	All bobcats	-0.502	0.339	-47.898	20.370	0.05	0.146	44
$\delta^{18}O_{hair} = f$(rel. humidity (h))	All bobcats	0.127	0.038	6.391	2.305	0.206	0.002	44
$\delta D_{river} = f(\delta^{18}O_{river})$		7.883	0.13	4.370	1.561	0.981	<0.0001	75

7.4. CHAPTER 4: Oxygen isotope composition of North American bobcat and puma bone phosphate: Implications for provenance and climate reconstruction

Appendix 1. Sample list.

No.	Common name	Sample ID	Sex	Sample material	Latitude (decimal degrees)	Longitude (decimal degrees)	Elevation (m)	$\delta^{18}O$ (‰ V-SMOW) Mean annual OIPC	Precip data δ18O (unweighted mean)	MAT (℃)	Average annual rel. humidity (%)	$\delta^{18}O$ Bone phosphate (‰, V-SMOW)	δ18O Keratin (‰ V-SMOW)
1	Puma	10_PU_US_fL_B	u	bone	26.417	-81.420	11	-3.60	-1.40	23.2	72.5	19.26	
2	Puma	102_PU_US_UT_B	m	bone	41.826	-113.329	1800	-14.40	-15.40	7.7	43.5	14.19	
3	Puma	105_PU_US_UT_B	f	bone	38.341	-111.546	2170	-13.40	-10.90	6.5	50.5	17.43	
4	Puma	107_PU_US_UT_B	u	bone	39.192	-109.391	1800	-13.40	-8.80	11.5	48.5	16.49	
5	Puma	109_PU_US_UT_B	m	bone	39.779	-110.443	2000	-14.00	-8.80	7.1	48.5	16.13	
6	Puma	12_PU_US_ID_B	f	bone	46.135	-115.787	400	-12.80	-12.40	8.2	61.0	11.74	
7	Puma	13_PU_US_KS_B	u	bone	39.859	-95.189	300	-7.80	-10.00	12.0	72.0	14.80	
8	Puma	14_PU_US_LA_B	u	bone	32.776	-91.794	30	-4.80	-5.00	18.4	74.5	17.82	
9	Puma	15_PU_US_MT_B	m	bone	46.216	-114.085	1000	-14.10	-18.70	7.7	67.0	12.97	
10	Puma	2_PU_US_CA_B	u	bone	34.873	-119.179	600	-9.10	-4.20	18.5	53.0	17.27	
11	Puma	21_PU_US_NM_B	f	bone	33.373	-108.903	1500	-10.40	-7.80	14.1	44.0	16.94	
12	Puma	23_PU_US_NM_B	f	bone	35.648	-105.295	2070	-12.00	-15.50	10.0	44.5	20.04	
13	Puma	25_PU_US_NM_B	f	bone	35.190	-107.666	2438	-12.20	-8.80	12.7	44.6	18.16	
14	Puma	26_PU_US_NY_B	u	bone	44.113	-73.924	940	-11.90	-12.30	4.5	69.0	12.33	

No.	Common name	Sample ID	Sex	Sample material	Latitude (decimal degrees)	Longitude (decimal degrees)	Elevation (m)	$\delta^{18}O$ (‰ V-SMOW) Mean annual OIPC	Precip data δ18O (unweighted mean)	MAT (℃)	Average annual rel. humidity (%)	$\delta^{18}O$ Bone phosphate (‰, V-SMOW)	δ18O Keratin (‰ V-SMOW)
15	Puma	30_PU_US_PA_B	u	bone	41.324	-78.452	600	-9.60	-10.60	7.5	70.0	13.09	
16	Puma	38_PU_US_TX_B	m	bone	31.150	-105.497	1600	-9.30	-4.40	17.0	42.0	19.55	
17	Puma	39_PU_US_TX_B	m	bone	32.937	-94.254	80	-5.00	-5.00	17.6	65.0		
18	Puma	40_PU_US_TX_B	m	bone	28.889	-99.097	193	-4.50	-4.40	20.7	70.5	18.90	
19	Puma	47_PU_US_WA_B	m	bone	48.078	-123.577	600	-12.20	-9.30	9.8	83.5	12.21	
20	Puma	49_PU_US_WV_B	u	bone	37.925	-80.384	670	-8.10	-8.90	10.9	72.0	15.49	
21	Puma	5_PU_US_CA_B	u	bone	40.254	-124.133	100	-10.40	-6.50	13.2	59.0	15.02	
22	Puma	52_PU_CA_AB_B	u	bone	51.173	-115.571	1460	-16.60	-10.10	3.3	50.0	11.52	
23	Puma	54_PU_ME_BC_B	u	bone	30.819	-115.616	730	-8.20	-4.20	15.0	60.0	19.96	
24	Puma	56_PU_ME_JA_B	f	bone	21.843	-103.783	800	-5.50	-7.00	15.0	60.0	17.46	
25	Puma	58_PU_ME_TA_B	u	bone	25.860	-97.503	10	-3.60	-2.90	21.1	77.0	20.67	
26	Puma	59_PU_ME_VC_B	u	bone	18.424	-95.112	340	-4.60	-2.60	25.0	75.0	16.74	
27	Puma	7_PU_US_CO_B	m	bone	40.051	-107.910	1900	-13.60	-12.30	5.5	48.5	14.88	
28	Puma	81_PU_US_UT_B	f	bone	37.912	-112.457	2130	-13.60	-10.90	7.2	50.5	16.30	
29	Puma	112_PU_US_fL_B	f	bone	25.921	-81.479	1	-3.50	-1.40	22.7	72.5	18.63	
30	Puma	113_PU_US_fL_B	m	bone	26.007	-81.077	1	-3.50	-1.40	22.7	72.5	18.81	
31	Puma	120_PU_US_fL_B	u	bone	26.418	-81.336	4	-3.50	-1.40	22.7	72.5	18.55	

No.	Common name	Sample ID	Sex	Sample material	Latitude (decimal degrees)	Longitude (decimal degrees)	Elevation (m)	$\delta^{18}O$ (‰ V-SMOW) Mean annual OIPC	Precip data δ18O (unweighted mean)	MAT (℃)	Average annual rel. humidity (%)	$\delta^{18}O$ Bone phosphate (‰, V-SMOW)	δ18O Keratin (‰ V-SMOW)
32	Puma	121_PU_US_fL_B	u	bone	26.271	-81.351	1	-3.50	-1.40	22.7	72.5	19.72	
33	Puma	19_PU_US_NM_B	m	bone	31.562	-108.811	1700	-10.10	-6.50	15.5	40.0	21.23	
34	Puma	22_PU_US_NM_B	f	bone	35.254	-107.984	2070	-12.20	-8.80	10.0	44.5	18.97	
35	Puma	3_PU_US_CA_B	m	bone	40.043	-120.754	1220	-12.70	-9.90	10.0	53.0	17.08	
36	Puma	37_PU_US_TX_B	u	bone	29.684	-101.173	490	-5.80	-4.40	20.0	65.0	21.67	
37	Puma	42_PU_US_TX_B	m	bone	28.521	-99.858	184	-4.60	-4.40	21.1	70.5	19.62	
38	Puma	43_PU_US_TX_B	f	bone	30.751	-104.082	1830	-9.30	-7.20	18.3	59.0	20.59	
39	Puma	44_PU_US_UT_B	u	bone	37.366	-113.415	2000	-13.10	-10.90	11.6	50.0	18.13	
40	Puma	45_PU_US_UT_B	m	bone	40.231	-111.664	1370	-13.00	-8.80	8.8	55.0	16.02	
41	Puma	50_PU_US_WY_B	u	bone	44.977	-110.698	2072	-15.70	-16.20	4.4	60.0	14.79	
42	Puma	51_PU_US_WY_B	f	bone	44.547	-110.258	1524	-13.80	-13.80	6.1	62.0	14.41	
43	Puma	8_PU_US_CO_B	m	bone	38.175	-108.418	1970	-13.20	-12.30	7.2	48.0	15.32	
44	Puma	9_PU_US_fL_B	u	bone	28.979	-80.925	2	-4.00	-2.80	22.7	74.5	18.66	
45	Bobcat	100_LY_US_TX_B	f	bone	33.657	-97.345	240	-5.8	-5.00	17.00	70.00	18.67	9.16
46	Bobcat	11_LY_US_VA_B	f	bone	37.354	-80.535	1180	-8.8	-8.90	4.90	65.00	16.24	
47	Bobcat	132_LY_US_UT_B	f	bone	39.305	-111.299	2200	-14.3	-8.80	8.60	55.00	16.60	13.67
48	Bobcat	137_LY_US_UT_B	f	bone	40.200	-110.067	1550	-13.3	-8.80	7.90	50.00	16.80	10.57

No.	Common name	Sample ID	Sex	Sample material	Latitude (decimal degrees)	Longitude (decimal degrees)	Elevation (m)	$\delta^{18}O$ (‰ V-SMOW) Mean annual OIPC	Precip data δ18O (unweighted mean)	MAT (℃)	Average annual rel. humidity (%)	$\delta^{18}O$ Bone phosphate (‰, V-SMOW)	δ18O Keratin (‰ V-SMOW)
49	Bobcat	14_LY_US_WV_B	u	bone	38.902	-81.310	243	-7.5	-7.80	11.50	70.50	15.26	19.40
50	Bobcat	15_LY_US_PA_B	f	bone	40.934	-76.707	314	-9	-10.60	8.50	69.50	15.14	
51	Bobcat	150_LY_US_UT_B	u	bone	37.425	-113.074	2500	-14.1	-10.90	2.00	50.50	16.44	10.83
52	Bobcat	155_LY_US_UT_B	m	bone	37.580	-109.432	1860	-12.9	-8.80	10.60	50.50	19.65	15.63
53	Bobcat	16_LY_US_NY_B	u	bone	43.998	-74.505	940	-11.9	-12.30	4.50	70.50	13.61	16.89
54	Bobcat	161_LY_US_UT_B	f	bone	38.725	-109.525	1340	-12.3	-8.80	12.10	50.50	18.07	11.38
55	Bobcat	171_LY_US_UT_B	u	bone	61.531	-160.302	17	-12.8	-21.25	-1.20	77.50	11.05	
56	Bobcat	18_LY_US_ME_B	f	bone	45.592	-69.983	450	-11.5	-12.30	4.40	70.50	14.51	
57	Bobcat	2_LY_US_fL_B	u	bone	25.826	-81.344	3	-3.5	-1.40	23.70	72.50	19.49	16.41
58	Bobcat	20_LY_US_AL_B	f	bone	30.270	-87.683	4	-4.1	-2.80	19.00	74.50	16.19	19.62
59	Bobcat	22_LY_US_TN_B	m	bone	36.365	-88.045	120	-6.1	-7.20	13.90	72.00	16.28	13.60
60	Bobcat	24_LY_US_IN_B	u	bone	39.028	-86.323	240	-7.2	-7.60	11.90	73.00	14.29	
61	Bobcat	29_LY_US_AR_B	f	bone	35.777	-93.465	670	-7.1	-6.90	12.40	72.50	16.26	16.96
62	Bobcat	3_LY_US_fL_B	f	bone	30.438	-81.631	5	-4,1	-2.80	21.10	72.50	18.08	
63	Bobcat	30_LY_US_AR_B	f	bone	34.529	-90.592	60	-5.4	-4.60	16.40	71.50	16.47	
64	Bobcat	33_LY_US_NE_B	u	bone	42.571	-100.062	800	-10.6	-9.60	9.50	67.00	14.47	19.36
65	Bobcat	35_LY_US_MN_B	m	bone	44.159	-91.816	213	-9.1	-8.30	6.50	75.50	13.91	14.70

No.	Common name	Sample ID	Sex	Sample material	Latitude (decimal degrees)	Longitude (decimal degrees)	Elevation (m)	$\delta^{18}O$ (‰ V-SMOW) Mean annual OIPC	Precip data δ18O (unweighted mean)	MAT (℃)	Average annual rel. humidity (%)	$\delta^{18}O$ Bone phosphate (‰, V-SMOW)	δ18O Keratin (‰ V-SMOW)
66	Bobcat	38_LY_US_SD_B	m	bone	44.372	-100.318	440	-10.7	-9.60	8.50	74.00	13.85	16.43
67	Bobcat	40_LY_US_MT_B	f	bone	46.336	-113.294	1600	-15.2	-18.70	5.40	67.00	12.64	12.52
68	Bobcat	42_LY_US_WY_B	m	bone	41.088	-106.519	2400	-14.7	-16.20	4.70	55.50	15.21	
69	Bobcat	46_LY_US_CO_B	f	bone	41.001	-107.246	2100	-14.2	-12.30	6.20	48.50	14.48	13.88
70	Bobcat	50_LY_US_NM_B	m	bone	35.596	-106.125	1930	-11.9	-11.20	10.20	44.00	18.18	12.06
71	Bobcat	51_LY_US_NM_B	f	bone	32.483	-106.724	1200	-9.3	-7.20	16.40	49.50	18.28	15.37
72	Bobcat	6_LY_US_GA_B	u	bone	32.429	-81.729	60	-4.4	-2.80	18.50	70.50	15.66	
73	Bobcat	61_LY_US_ID_B	m	bone	45.774	-116.302	480	-12.9	-12.40	12.10	61.00	14.55	11.16
74	Bobcat	63_LY_US_WA_B	f	bone	47.956	-124.393	90	-11.1	-9.30	10.20	83.50	14.08	16.75
75	Bobcat	66_LY_US_OR_B	f	bone	42.746	-124.497	18	-10.7	-7.40	11.70	65.50	14.44	
76	Bobcat	68_LY_US_NV_B	m	bone	40.652	-119.355	1200	-12.9	-9.90	10.70	49.50	15.38	
77	Bobcat	70_LY_US_CA_B	m	bone	40.491	-124.132	50	-10.4	-6.50	12.30	59.00	15.63	11.58
78	Bobcat	74_LY_ME_BCS_B	f	bone	22.892	-109.914	140	-5.1	-9.50	23.20	66.30	18.47	
79	Bobcat	75_LY_ME_CI_B	f	bone	29.973	-108.346	2200	-10.5	-6.50	15.00	35.00	16.77	
80	Bobcat	77_LY_ME_JA_B	f	bone	20.340	-102.768	1530	-6.8	-8.00	20.00	55.00	16.74	
81	Bobcat	80_LY_US_TX_B	f	bone	31.197	-101.464	820	-6.9	-4.40	17.30	65.00	18.57	10.37
82	Bobcat	82_LY_US_TX_B	m	bone	27.826	-97.406	2	-3.6	-2.90	22.20	77.50	18.87	12.35

No.	Common name	Sample ID	Sex	Sample material	Latitude (decimal degrees)	Longitude (decimal degrees)	Elevation (m)	$\delta^{18}O$ (‰ V-SMOW) Mean annual OIPC	Precip data δ18O (unweighted mean)	MAT (℃)	Average annual rel. humidity (%)	$\delta^{18}O$ Bone phosphate (‰, V-SMOW)	δ18O Keratin (‰ V-SMOW)
83	Bobcat	85_LY_US_TX_B	u	bone	30.587	-103.893	1500	-8.6	-7.20	16.10	59.00	19.28	11.08
84	Bobcat	86_LY_US_TX_B	m	bone	29.023	-99.310	180	-4.5	-4.40	20.70	70.50	19.17	14.54
85	Bobcat	88_LY_US_TX_B	m	bone	26.122	-98.257	31	-3.7	-2.90	23.20	77.00	18.19	11.02
86	Bobcat	9_LY_US_NC_B	m	bone	34.492	-77.742	20	-5.7	-4.60	17.10	70.50	16.72	
87	Bobcat	90_LY_US_TX_B	m	bone	30.752	-99.235	470	-5.5	-4.40	18.20	65.00	19.90	15.06
88	Bobcat	97_LY_US_TX_B	m	bone	30.300	-94.535	15	-3.9	-2.90	20.10	79.50	17.55	11.96
89	Bobcat	102_LY_US_TX_B	u	bone	29.289	-100.348	337	-5.1	-4.40	20.00	70.00	19.48	
90	Bobcat	167_LY_US_UT_B	u	bone	52.259	-113.786	855	-16.2	-17.70	2.20	75.00	9.06	
91	Bobcat	169_LY_US_UT_B	f	bone	64.838	-147.717	136	-19.4	-21.25	-3.80	75.00	9.46	
92	Bobcat	17_LY_US_NY_B	f	bone	41.391	-73.956	304	-9.3	-11.30	10.00	63.00	15.79	
93	Bobcat	34_LY_US_MN_B	f	bone	45.750	-94.217	324	-10.3	-10.90	6.10	73.00	14.67	
94	Bobcat	37_LY_US_SD_B	m	bone	43.732	-103.614	1620	-13.5	-13.80	7.70	62.00	16.34	
95	Bobcat	44_LY_US_CO_B	u	bone	38.101	-103.125	1180	-10.7	-9.80	10.00	52.00	17.02	
96	Bobcat	45_LY_US_CO_B	u	bone	38.975	-108.459	2136	-12.4	-12.30	7.20	47.50	17.35	
97	Bobcat	53_LY_US_NM_B	f	bone	33.284	-108.877	1400	-10.2	-7.80	11.60	39.00	19.09	
98	Bobcat	59_LY_US_UT_B	f	bone	38.304	-113.072	1500	-12.5	-10.90	11.60	50.00	20.56	
99	Bobcat	60_LY_US_UT_B	f	bone	40.643	-111.281	1970	-14.3	-8.80	6.10	55.00	18.96	

No.	Common name	Sample ID	Sex	Sample material	Latitude (decimal degrees)	Longitude (decimal degrees)	Elevation (m)	$\delta^{18}O$ (‰ V-SMOW) Mean annual OIPC	Precip data δ18O (unweighted mean)	MAT (℃)	Average annual rel. humidity (%)	$\delta^{18}O$ Bone phosphate (‰, V-SMOW)	δ18O Keratin (‰ V-SMOW)
100	Bobcat	7_LY_US_GA_B	m	bone	34.869	-83.814	1460	-8.1	-6.70	13.80	71.00	18.66	19.20
101	Bobcat	73_LY_US_CA_B	u	bone	34.421	-119.697	15	-7.8	-4.20	15.50	70.00	19.55	
102	Bobcat	78_LY_ME_SO_B	m	bone	26.904	-109.694	50	-5.6	-6.00	23.00	55.00	20.69	
103	Bobcat	79_LY_ME_TA_B	f	bone	26.430	-99.144	61	-3.9	-2.90	22.00	65.00	21.94	
104	Bobcat	81_LY_US_TX_B	u	bone	25.908	-97.489	10	-3.6	-2.90	21.00	77.00	17.70	
105	Bobcat	89_LY_US_TX_B	u	bone	29.809	-101.559	390	-5.7	-4.40	19.40	65.00	20.75	
106	Bobcat	91_LY_US_TX_B	u	bone	28.691	-95.969	4	-3.6	-2.90	20.00	77.00	17.86	
107	Bobcat	93_LY_US_TX_B	u	bone	29.990	-100.224	732	-6.1	-4.40	18.30	65.00	19.77	
108	Mule deer	BC2		bone					-17.70		64	10.80	
109	Mule deer	BC4		bone					-10.60		84	13.90	
110	White-tailed deer	ABl		bone					-18.00		75	10.70	
111	White-tailed deer	AB2		bone					-18.00		75	10.40	
112	White-tailed deer	AB4		bone					-18.00		65	10.70	
113	White-tailed deer	AB5		bone					-18.00		65	11.00	
114	White-tailed deer	AB6		bone					-17.40		66	13.30	
115	White-tailed deer	ABlO		bone					-17.40		66	13.10	
116	White-tailed deer	AB7		bone					-18.40		62	11.60	

No.	Common name	Sample ID	Sex	Sample material	Latitude (decimal degrees)	Longitude (decimal degrees)	Elevation (m)	$\delta^{18}O$ (‰ V-SMOW) Mean annual OIPC	Precip data δ18O (unweighted mean)	MAT (℃)	Average annual rel. humidity (%)	$\delta^{18}O$ Bone phosphate (‰, V-SMOW)	δ18O Keratin (‰ V-SMOW)
117	White-tailed deer	AB8		bone					-18.40		62	11.80	
118	White-tailed deer	AB9		bone					-17.40			14.60	
119	White-tailed deer	AB12		bone					-17.40			14.70	
120	White-tailed deer	ABll		bone					-18.40		62	12.60	
121	White-tailed deer	SAl		bone					-16.60		71	14.00	
122	White-tailed deer	ON1		bone					-9.90		81	14.00	
123	White-tailed deer	ON3		bone					-9.30		81	13.90	
124	White-tailed deer	ON6		bone					-9.80		79	13.60	
125	White-tailed deer	ON9		bone					-8.20		81	13.30	
126	White-tailed deer	QCl		bone					-12.00		79	13.90	
127	White-tailed deer	NBl		bone					-8.70		77	14.40	
128	White-tailed deer	NSl		bone					-7.70		83	16.00	
129	White-tailed deer	NS2		bone					-8.10		84	15.90	
130	Mule deer	OR1		bone					-14.00		49	17.00	
131	White-tailed deer	MT1		bone					-15.50		63	14.30	
132	White-tailed deer	WY2		bone					-14.90		60	13.60	
133	White-tailed deer	WY6		bone					-16.60		52	15.20	

No.	Common name	Sample ID	Sex	Sample material	Latitude (decimal degrees)	Longitude (decimal degrees)	Elevation (m)	$\delta^{18}O$ (‰ V-SMOW) Mean annual OIPC	Precip data δ18O (unweighted mean)	MAT (℃)	Average annual rel. humidity (%)	$\delta^{18}O$ Bone phosphate (‰, V-SMOW)	δ18O Keratin (‰ V-SMOW)
134	White-tailed deer	WI1		bone					-10.20		73	14.70	
135	White-tailed deer	OH1		bone					-6.40		70	18.40	
136	White-tailed deer	OH3		bone					-6.40		70	18.00	
137	White-tailed deer	WV2		bone					-7.30		74	16.30	
138	White-tailed deer	WV3		bone					-7.30		74	16.70	
139	White-tailed deer	NE2		bone					-12.00		60	16.30	
140	White-tailed deer	KS1		bone					-7.10		71	18.60	
141	White-tailed deer	MO4		bone					-5.80		70	18.40	
142	White-tailed deer	OK1		bone					-4.40		69	19.90	
143	White-tailed deer	OK2		bone					-4.40		69	19.60	
144	White-tailed deer	OK5		bone					-6.40		69	19.30	
147	White-tailed deer	OK10		bone					-5.20		69	19.60	
148	Mule deer	CA2		bone					-5.80		73	17.60	
149	White-tailed deer	FL1		bone					-3.30		74	19.00	
150	White-tailed deer	AZ1		bone					-8.20		37	23.00	
151	White-tailed deer	TX1		bone					-4.40		63	22.80	
152	White-tailed deer	TX2		bone					-3.30		77	21.80	

No.	Common name	Sample ID	Sex	Sample material	Latitude (decimal degrees)	Longitude (decimal degrees)	Elevation (m)	$\delta^{18}O$ (‰ V-SMOW) Mean annual OIPC	Precip data δ18O (unweighted mean)	MAT (℃)	Average annual rel. humidity (%)	$\delta^{18}O$ Bone phosphate (‰, V-SMOW)	δ18O Keratin (‰ V-SMOW)
153	White-tailed deer	TX3		bone					-3.30		77	21.10	
154	White-tailed deer	TX5		bone					-3.80		77	21.70	
155	White-tailed deer	LA2		bone					-5.20		73	19.10	
156	Cottontail rabbit	1		bone					**-10.50**		85.00	**19.30**	
157	Cottontail rabbit	2		bone					**-10.50**		85.00	**18.90**	
158	Cottontail rabbit	3		bone					**-10.50**		85.00	**18.30**	
159	European rabbit	4		bone					**-8.00**		60.00	**20.10**	
160	European rabbit	5		bone					**-8.00**		75.00	**19.00**	
161	European rabbit	6		bone					**-8.00**		55.00	**20.40**	
162	European rabbit	7		bone					**-7.00**		50.00	**23.40**	
163	European rabbit	8		bone					**-6.00**		45.00	**23.50**	
164	European rabbit	9		bone					**-7.50**		50.00	**21.60**	
165	European rabbit	10		bone					**-7.30**		55.00	**20.90**	
166	European rabbit	11		bone					**-7.50**		50.00	**20.40**	
167	European rabbit	12		bone					**-7.50**		75.00	**17.70**	
168	European rabbit	13		bone					**-7.50**		75.00	**17.40**	
169	European rabbit	14		bone					**-6.70**		75.00	**16.60**	

No.	Common name	Sample ID	Sex	Sample material	Latitude (decimal degrees)	Longitude (decimal degrees)	Elevation (m)	$\delta^{18}O$ (‰ V-SMOW) Mean annual OIPC	Precip data δ18O (unweighted mean)	MAT (℃)	Average annual rel. humidity (%)	$\delta^{18}O$ Bone phosphate (‰, V-SMOW)	δ18O Keratin (‰ V-SMOW)
170	European rabbit	15		bone					**-6.50**		85.00	**15.40**	
171	European rabbit	16		bone					**-6.50**		85.00	**14.40**	
172	European rabbit	17		bone					**-5.50**		65.00	**16.00**	
173	European rabbit	18		bone					**-5.50**		75.00	**16.50**	
174	European rabbit	19		bone					**-5.50**		75.00	**16.70**	
175	European rabbit	20		bone					**-5.50**		75.00	**17.40**	
176	European rabbit	21		bone					**-6.00**		70.00	**17.50**	
177	European rabbit	22		bone					**-6.30**		55.00	**19.60**	
178	European rabbit	23		bone					**-6.30**		50.00	**21.20**	
179	European rabbit	24		bone					**-6.30**		40.00	**24.50**	
180	European rabbit	25		bone					**-5.50**		65.00	**21.20**	
181	European rabbit	26		bone					**-5.00**		50.00	**21.70**	
182	European rabbit	27		bone					**-5.00**		50.00	**22.50**	
183	African Savanna hare	28		bone					**-1.00**		65.00	**18.50**	
184	Abyssinian hare	29		bone					**-1.50**		65.00	**19.50**	
185	Abyssinian hare	30		bone					**-1.50**		65.00	**20.00**	
186	African Savanna	31		bone					**-1.00**		65.00	**20.50**	

No.	Common name	Sample ID	Sex	Sample material	Latitude (decimal degrees)	Longitude (decimal degrees)	Elevation (m)	$\delta^{18}O$ (‰ V-SMOW) Mean annual OIPC	Precip data δ18O (unweighted mean)	MAT (℃)	Average annual rel. humidity (%)	$\delta^{18}O$ Bone phosphate (‰, V-SMOW)	δ18O Keratin (‰ V-SMOW)
	hare												
187	African Savanna hare	32		bone					**-1.00**		65.00	**20.80**	
188	African Savanna hare	33		bone					**-1.00**		75.00	**22.00**	
189	African Savanna hare	34		bone					**-1.00**		65.00	**23.00**	
190	African Savanna hare	35		bone					**-1.00**		65.00	**22.70**	
191	Cape hare	36		bone					**-1.00**		75.00	**24.50**	
192	Abyssinian hare	37		bone					**-1.50**		65.00	**25.60**	
193	Abyssinian hare	38		bone					**-1.00**		75.00	**25.30**	
194	Abyssinian hare	39		bone					**-1.00**		60.00	**26.50**	
195	European rabbit	40		bone					**-7.50**		45.00	**22.30**	
196	European rabbit	41		bone					**-11.00**		85.00	**14.30**	
197	Fox			bone					-5.80			18.00	
198	Fox			bone					-5.80			18.10	
199	Fox			bone					-5.80			17.90	
200	Fox			bone					-5.80			18.00	
201	Fox			bone					-5.80			18.20	

No.	Common name	Sample ID	Sex	Sample material	Latitude (decimal degrees)	Longitude (decimal degrees)	Elevation (m)	$\delta^{18}O$ (‰ V-SMOW) Mean annual OIPC	Precip data δ18O (unweighted mean)	MAT (℃)	Average annual rel. humidity (%)	$\delta^{18}O$ Bone phosphate (‰, V-SMOW)	δ18O Keratin (‰ V-SMOW)
202	Fox			tooth					-5.80			18.00	
203	Fox			tooth					-5.80			17.90	
204	Fox			tooth					-5.80			18.00	
205	Fox			tooth					-5.80			18.20	
206	Fox			tooth					-5.80			18.10	
207	Fox			tooth					-5.80			18.20	
208	Fox			tooth					-5.80			17.80	
209	Fox			tooth					-5.80			18.10	
210	Fox			tooth					-5.80			18.00	
211	Fox			tooth					-5.80			18.00	
212	Fox			tooth					-5.80			18.10	
213	Fox			tooth					-5.80			18.10	
214	Fox			tooth					-5.80			17.90	
215	Fox			tooth					-5.80			18.10	
216	Fox			tooth					-5.80			17.90	
217	Fox			tooth					-5.80			18.00	
218	Fox			tooth					-5.80			18.00	

No.	Common name	Sample ID	Sex	Sample material	Latitude (decimal degrees)	Longitude (decimal degrees)	Elevation (m)	$\delta^{18}O$ (‰ V-SMOW) Mean annual OIPC	Precip data δ18O (unweighted mean)	MAT (℃)	Average annual rel. humidity (%)	$\delta^{18}O$ Bone phosphate (‰, V-SMOW)	δ18O Keratin (‰ V-SMOW)
219	Fox			tooth					-5.80			17.90	
220	Fox			bone					-7.20			15.70	
221	Fox			bone					-7.20			15.60	
222	Fox			bone					-7.20			15.30	
223	Fox			bone					-7.20			15.20	
224	Fox			tooth					-7.20			15.00	
225	Fox			bone					-11.00			10.30	
226	Fox			bone					-11.00			10.80	
227	Fox			bone					-11.00			10.80	
228	Fox			bone					-11.00			10.90	
229	Fox			bone					-8.20			14.90	
230	Fox			bone					-8.20			15.10	
231	Fox			bone					-8.20			14.60	
232	Fox			bone					-8.20			15.00	
233	Fox			bone					-8.20			14.60	
234	Fox			bone					-8.20			14.60	
235	Fox			tooth					-5.50			18.50	

No.	Common name	Sample ID	Sex	Sample material	Latitude (decimal degrees)	Longitude (decimal degrees)	Elevation (m)	$\delta^{18}O$ (‰ V-SMOW) Mean annual OIPC	Precip data δ18O (unweighted mean)	MAT (℃)	Average annual rel. humidity (%)	$\delta^{18}O$ Bone phosphate (‰, V-SMOW)	δ18O Keratin (‰ V-SMOW)
236	Fox			tooth					-5.50			18.30	
237	Fox			tooth					-5.30			18.10	
238	Fox			tooth					-4.70			18.70	
239	Fox			tooth					-5.20			18.30	
240	Fox			tooth					-5.30			18.40	
241	Fox			tooth					-6.40			17.10	
242	Fox			tooth					-6.40			16.80	
243	Fox			tooth					-5.30			18.50	
244	Fox			tooth					-7.00			16.60	
245	Fox			tooth					-5.30			18.10	
246	Fox			tooth					-3.00			21.80	
247	Fox			tooth					-3.00			22.00	
248	Fox			tooth					-4.00			20.10	

Appendix 2. Statistical analysis

	Species	Regression equations	R^2	P - value	n
$\delta^{18}O_{phosphate} = f(\delta^{18}O_{water})$	**All felids**	$\delta^{18}O_p = 20.10(\pm 0.40) + 0.40(\pm 0.04) * \delta^{18}O_w$	0.456	< 0.0001	106
	Bobcats	$\delta^{18}O_p = 20.15(\pm 0.49) + 0.41(\pm 0.05) * \delta^{18}O_w$	0.503	< 0.0001	63
	Pumas	$\delta^{18}O_p = 20.00(\pm 0.67) + 0.38(\pm 0.07) * \delta^{18}O_w$	0.394	< 0.0001	43
	Foxes	$\delta^{18}O_p = 25.85(\pm 0.17) + 1.38(\pm 0.03) * \delta^{18}O_w$	0.983	< 0.0001	52
	Rabbits/Hares	$\delta^{18}O_p = 22.73(\pm 0.86) + 0.47(\pm 0.14) * \delta^{18}O_w$	0.23	0.001	41
	Deers	$\delta^{18}O_p = 21.70(\pm 0.63) + 0.54(\pm 0.05) * \delta^{18}O_w$	0.707	< 0.0001	46
	All mammals	$\delta^{18}O_p = 21.70(\pm 0.17) + 0.68(\pm 0.02) * \delta^{18}O_w$	0.76	< 0.0001	559
Sex effects	**Female bobcats**	$\delta^{18}O_p = 20.32(\pm 0.82) + 0.42(\pm 0.09) * \delta^{18}O_w$	0.501	< 0.0001	27
	Male bobcats	$\delta^{18}O_p = 19.35(\pm 1.00) + 0.29(\pm 0.12) * \delta^{18}O_w$	0.276	0.025	18
	Female pumas	$\delta^{18}O_p = 19.47(\pm 2.10) + 0.23(\pm 0.21) * \delta^{18}O_w$	0.117	0.304	11
	Male pumas	$\delta^{18}O_p = 20.70(\pm 1.09) + 0.45(\pm 0.11) * \delta^{18}O_w$	0.614	0.002	13
$\delta^{18}O_{phosphate} = f(\delta^{18}O_{water})$ with rel. humidity (h)	**All felids**	$\delta^{18}O_p = 26.13(\pm 1.07) + 0.46(\pm 0.04) * \delta^{18}O_w - 0.09(\pm 0.02) * h$	0.595	< 0.0001	106
	Bobcats	$\delta^{18}O_p = 26.75(\pm 1.29) + 0.45(\pm 0.04) * \delta^{18}O_w - 0.10(\pm 0.02) * h$	0.664	< 0.0001	63
	Pumas	$\delta^{18}O_p = 25.78(\pm 2.00) + 0.47(\pm 0.07) * \delta^{18}O_w - 0.08(\pm 0.03) * h$	0.507	< 0.0001	43
	Rabbits/Hares	$\delta^{18}O_p = 30.65(\pm 1.88) + 0.41(\pm 0.11) * \delta^{18}O_w - 0.13(\pm 0.03) * h$	0.502	0.001	41
	Deers	$\delta^{18}O_p = 34.83(\pm 1.48) + 0.67(\pm 0.03) * \delta^{18}O_w - 0.17(\pm 0.02) * h$	0.909	< 0.0001	44
$\delta^{18}O_{phosphate} = f(\text{rel. humidity (h)})$	**Bobcats**	$\delta^{18}O_p = 21.06(\pm 1.92) - 0.07(\pm 0.03) * h$	0.079	0.026	63
	Pumas	$\delta^{18}O_p = 17.55(\pm 2.15) - 0.01(\pm 0.04) * h$	0.002	0.786	43
	Rabbits/Hares	$\delta^{18}O_p = 29.32(\pm 2.10) - 0.14(\pm 0.03) * h$	0.336	< 0.0001	41
	Deer	$\delta^{18}O_p = 18.36(\pm 4.03) - 0.04(\pm 0.06) * h$	0.009	0.546	44

P-values < 0.05 were considered statistically significant.

Appendix 3: Species / Tukey (HSD) / ANCOVA: Analysis of the differences between the categories with a confidence interval of 95%

Contrast		Difference	Standardized Difference	Critical Value	Pr > Diff	Significant	Tukey's d critical value:
Felines	**Other placental mammals**	0.725	3.406	1.964	0.001	Yes	2.777
Bobcat	**Puma**	0.139	0.357	1.983	0.722	No	2.805
Male bobcat	**Female Bobcat**	0.153	0.27	2.018	0.789	No	2.854
Male Puma	**Female Puma**	0.844	0.955	2.080	0.35	No	2.941
Puma	**Deer**	0.218	0.485	1.988	0.629	No	2.811
Bobcat	**Rabbit**	2.206	4.653	1.984	< 0,0001	Yes	2.805
Felines	**Fox**	0.64	1.979	1.975	0.05	Yes	2.794

P-values < 0.05 were considered statistically significant

Appendix 4. Statistical analysis of the intra-individual tissue comparison (hair versus bone phosphate)

	Species	Regression equations	r^2	p-value	n
$\delta^{18}O_{hair} = f(\delta^{18}O_{phosphate})$	**Bobcat**	$\delta^{18}O_h = 19.84(\pm 4.43) - 0.34(\pm 0.26) * \delta^{18}O_p$	0.06	0.203	30
$\delta^{18}O_{phosphate} = f(\delta^{18}O_{water})$	**Bobcat**	$\delta^{18}O_p = 19.76(\pm 0.68) + 0.39(\pm 0.08) * \delta^{18}O_w$	0.46	< 0.0001	30
$\delta^{18}O_{hair} = f(\delta^{18}O_{water})$	**Bobcat**	$\delta^{18}O_h = 14.38(\pm 1.32) + 0.03(\pm 0.16) * \delta^{18}O_w$	0.00	< 0.830	30

P-values < 0.05 were considered statistically significant

ERKLÄRUNG

Ich versichere, dass ich diese Arbeit selbständig verfasst, keine anderen Quellen und Hilfsmittel als die angegebenen benutzt und die Stellen der Arbeit, die anderen Werken dem Wortlaut oder Sinn nach entnommen sind, kenntlich gemacht habe. Diese Arbeit hat in dieser oder ähnlichen Form keiner anderen Prüfungsbehörde vorgelegen.

Bonn, den 05.09.2011